Dissecting substrate recognition by GID Ubiquitin ligases

Dissertation

Zur Erlangung des Grades

Doktor der Naturwissenschaften

Am Fachbereich Biologie

Der Johannes Gutenberg-Universität Mainz

Christian Ochs

geb. am 05.04.1996 in Frankfurt am Main

Mainz, August 2025

Dekan: Prof. Dr. Eckhard Thines

1. Berichterstatter: XXXXXX

2. Berichterstatter: XXXXXX

Tag der mündlichen Prüfung: 29.08.2025

Preface

I hereby declare that I am the sole author and composer of this report and that no other sources, other than those listed, have been used. Furthermore, I declare that I have acknowledged the work of others by providing detailed references of their cited work.

Throughout this study I have received scientific advice and supervision by XXXXXXXXXX and XXXXXXXXXXX at the Institute for Molecular Biology in Mainz. Furthermore, some experiments were conducted by or in collaboration with XXXXXXXXX and XXXXXXXXXXXXXX. Their contributions will be credited accordingly. Furthermore, some experiments were carried out by XXXXXXXXXXXXXX in the context of a Bachelor project, and some were carried out during a six-week International Summer School internship by XXXXXXXXXXXXXX, both under my supervision. They will be credited accordingly as well. Mass spectrometry experiments were carried out by XXXXXXXXXXXXXX of the IMB Proteomics Core Facility. Parts of this study have been published in Kong et al. 2025 and will be cited accordingly.

Mainz, _____

Christian Ochs

Contents

Summary

Protein degradation is an essential process for maintaining the health of the cell, with a variety of different functions in the maintenance of homeostasis, regulation of processes in the cell, the response to environmental stresses, and quality control of the proteome. Perturbation of this system leads to a variety of diseases, including neurodegenerative diseases such as Alzheimer's disease or frontotemporal dementia.

To degrade proteins, the cell uses two main pathways, autophagy and the ubiquitin proteasome system, the latter of which will be the focus of this study. In this pathway, ubiquitin is attached to substrate proteins by the action of E3 ligases. One such E3 ligase of rising importance is the GID/CTLH complex, which was originally found to be involved in the degradation of gluconeogenic enzymes starting with proline via its substrate receptor Gid4. In more recent years, further substrate receptor proteins have been discovered for the GID complex with Gid10 and Gid11, together with the complex's ability to non-canonically recognize substrates via WDR26 in human cells.

Thus far, Gid11 is relatively poorly understood, besides it seeming to recognize N-terminal threonine residues. One of the aims of this study is to better characterize Gid11, analyze its substrate specificities, and identify residues or regions within Gid11 important for substrate recognition. For this purpose, this study the tandem-fluorescent timer approach was used. This study highlights the importance of the third intrinsically disordered region of Gid11, as well as a variety of residues within its binding pocket. Furthermore, it shows that N-termini recognized by Gid11 are usually non-acetylated. Additionally, the Gid11-dependent turnover of two proteins without threonine N-degrons was investigated, leading to the hypothesis that Blm10 is potentially recognized via the fifth intrinsically disordered region of Gid11. A potential example of trans-ubiquitination of Cpa1 via recognition of its complex partner Cpa2 was investigated and disproven.

There are several more proteins such as Hsm3 whose turnover depends on the GID complex, but which do currently not possess a known substrate receptor. Using overexpression of potential substrate receptors to compete for the binding of Gid5, it could be shown that this approach is a viable strategy to find additional, currently unknown Gid5-dependent substrate receptor proteins of the GID complex.

Additional experiments were conducted to investigate the functional conservation of various GID components, both in different yeast species in case of Gid11, and in human cells in the case of core GID components, showing that most human homologs of GID components are non-functional in yeast.

As a side project, the specificity of human ATE1, NTAN1, and NTAQ1 was investigated, highlighting differences between these enzymes and their human counterparts.

Overall, this study provides a characterization of Gid11, its substrate specificities, and identifies several key features necessary for its function. Furthermore, it highlights potential ways to identify further, currently unknown substrate receptors of the GID complex.

Zusammenfassung

Proteinabbau ist ein essenzieller Prozess zur Aufrechterhaltung der Zellgesundheit und erfüllt eine Vielzahl von Funktionen wie die Aufrechterhaltung der Homöostase, die Regulation zellulärer Prozesse, die Antwort auf Umweltstress und die Qualitätskontrolle des Proteoms. Eine Störung dieses Systems führt zu einer Vielzahl von Krankheiten, darunter neurodegenerative Erkrankungen wie Alzheimer oder frontotemporale Demenz.

Zum Proteinabbau nutzt die Zelle zwei Hauptwege: Autophagie und das Ubiquitin-Proteasom-System, wobei Letzteres im Fokus dieser Arbeit steht. In diesem Weg werden Zielproteine durch E3-Ligasen mit Ubiquitin markiert. Eine zunehmend bedeutsame E3-Ligase ist der GID/CTLH-Komplex, der ursprünglich für den Abbau von Glukoneogenese-Enzymen mit N-terminalem Prolin durch den Substratrezeptor Gid4 beschrieben wurde. In den letzten Jahren wurden mit Gid10 und Gid11 weitere Substratrezeptoren entdeckt sowie eine nicht-kanonische Substraterkennung über WDR26 in menschlichen Zellen beschrieben.

Gid11 ist bislang nur unzureichend charakterisiert, abgesehen davon, dass es N-terminale Threoninreste erkennt. Ein Ziel dieser Arbeit ist es, Gid11 näher zu charakterisieren, dessen Substratspezifitäten zu analysieren und wichtige Bereiche oder Aminosäuren für die Substraterkennung zu identifizieren. Hierfür wurde die Tandem-Fluoreszenz-Timer-Methode verwendet. Die Ergebnisse zeigen die Bedeutung der dritten intrinsisch ungeordneten Region von Gid11 sowie diverser Reste in der Bindungstasche. Zudem wird gezeigt, dass N-Termini, die durch Gid11 erkannt werden, in der Regel nicht acetyliert sind. Darüber hinaus wurde der Gid11-abhängige Abbau zweier Proteine ohne Threonin-N-degron untersucht, was zur Hypothese führte, dass Blm10 möglicherweise über die fünfte ungeordnete Region von Gid11 erkannt wird. Ein mögliches Beispiel für trans-Ubiquitinierung von Cpa1 über dessen Komplexpartner Cpa2 konnte widerlegt werden.

Es existieren weitere Proteine, wie Hsm3, deren Abbau vom GID-Komplex abhängt, für die jedoch bisher kein Substratrezeptor bekannt ist. Durch Überexpression potenzieller Substratrezeptoren konnte gezeigt werden, dass diese Methode geeignet ist, bisher unbekannte Gid5-abhängige Substratrezeptoren des GID-Komplexes zu identifizieren.

Weitere Experimente untersuchten die funktionelle Konservierung verschiedener GID-Komponenten sowohl zwischen unterschiedlichen Hefespezies im Fall von Gid11 als auch in menschlichen Zellen bei Kernkomponenten des GID-Komplexes. Dabei zeigte sich, dass die meisten humanen Homologe in Hefe nicht funktional sind.

In einem Nebenprojekt wurde zudem die Spezifität von humanem ATE1, NTAN1 und NTAQ1 untersucht, wobei Unterschiede zwischen diesen Enzymen und ihren Hefehomologen festgestellt wurden.

Insgesamt liefert diese Arbeit eine Charakterisierung von Gid11, seiner Substratspezifität sowie Schlüsselfaktoren, die für seine Funktion notwendig sind. Außerdem werden mögliche Ansätze zur Identifizierung weiterer, bislang unbekannter Substratrezeptoren des GID-Komplexes aufgezeigt.

Introduction

Protein degradation

Protein degradation is an essential process in the cell, serving functions in the quality control, regulation, and homeostasis of the proteome of the cell (Goldberg 1972; McShane and Selbach 2022). This following introduction will give an overview of two mechanisms of protein degradation in the cell, the ubiquitin proteasome system (UPS) and autophagy, followed by an overview of the functions of protein degradation in the cell. Finally, an overview will be given over the ways the UPS recognizes its substrates, and the specific protein complex that will be the focus of this thesis.

Protein degradation via autophagy

Autophagy (Greek for "self-eating") is the process of enveloping cargo in a double-membrane vesicle called the autophagosome (Dikic and Elazar 2018), followed by fusion of the autophagosome with lysosomes, which deliver proteases and further factors involved in the degradation into the organelle (DUVE et al. 1955; Deter et al. 1967; Dikic and Elazar 2018). The generation of the autophagosome involves a large variety of factors at a variety of subcellular locations (Tsukada and Ohsumi 1993; Thumm et al. 1994).

Induction of autophagy begins at the phagosome assembly site (PAS), which is usually located at the endoplasmic reticulum (ER), but can also involve ER-mitochondria and ER-plasma membrane contact sites (Hamasaki et al. 2013; Nascimbeni et al. 2017). As of current understanding, these PAS sites lead to activation of the ULK1 complex and PI3KC3-PI, as well as delivery of ATG9-containing vesicles to the PAS (Karanasios et al. 2013; Manifava et al. 2016; Nishimura et al. 2017). As of now, the best characterized trigger for induction of autophagy is nutrient deprivation, in particular deprivation of amino acids, resulting in inhibition of the mechanistic target of rapamycin (mTOR) complex, particularly mTORC1 (Hosokawa et al. 2009). Nutrient starvation leads to disassociation of ULK1 from mTORC1, followed by autophosphorylation of ULK1 (Jung et al. 2009), leading to its activation. In addition to amino acid deprivation, autophagy can be triggered by an adenosine triphosphate (ATP) to adenosine monophosphate (AMP) imbalance in the cell, usually caused by glucose starvation (Gurumurthy et al. 2010).

The expansion of the nascent phagophore involves a wide variety of factors. However, most prominently involved are proteins of the ubiquitin-like ATG8 family (Tsukada and Ohsumi 1993; Harding et al. 1995; Slobodkin and Elazar 2013; Dikic and Elazar 2018), which are C-terminally processed by ATG4 and deposited on phosphatidylethanolamine (PE) in the phagophore membrane via activation by ATG7 and conjugation to PE via ATG3 (Hamasaki et al. 2013). This promotes phagophore expansion, as well as possibly the sealing of the phagophore membrane (Weidberg et al. 2011). Following sealing of the autophagosome, it undergoes maturation and eventual fusion with autolysosomes via syntaxin 17 (STX17), synaptosomal-associated protein 29 (SNAP29), and vesicle-associated membrane protein 8 (VAMP8) (Diao et al. 2015; Itakura et al. 2012; Dikic and Elazar 2018).

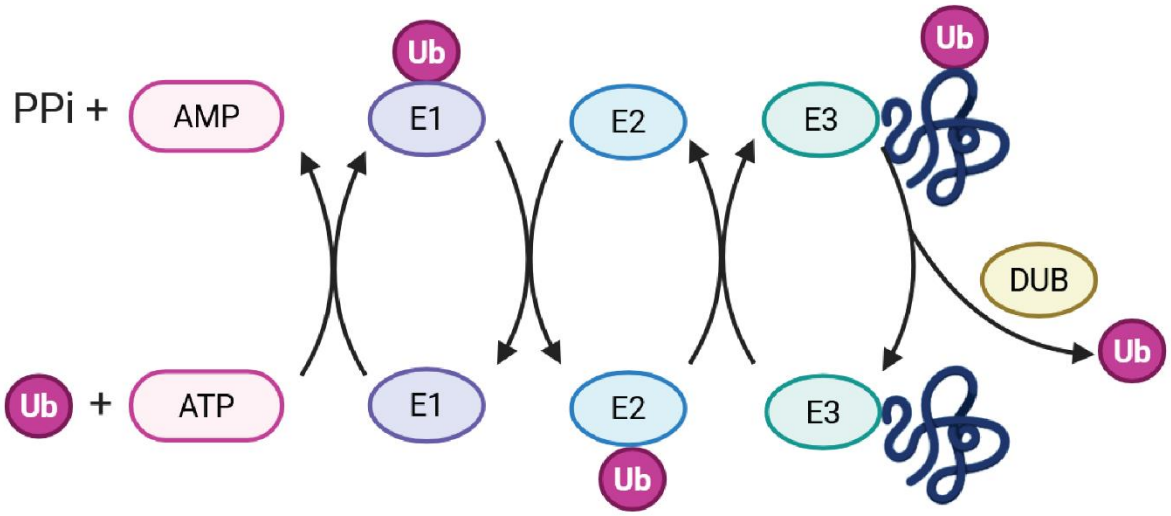

Figure 1: Cartoon representation of the ubiquitination cascade.
Ubiquitin is activated by an E1 ubiquitin activating enzyme and then transferred to a E2 conjugating enzyme. Finally, it is transferred to its substrate by the action of an E3 ubiquitin ligase.. Furthermore, the action of deubiquitinases is shown in removing ubiquitin from proteins. Created with BioRender.

The ubiquitin proteasome system

Protein degradation via autophagy is relatively unspecific, which stands in contrast to the relative specificity observed in the stability of various proteins. However, this was resolved by the discovery of the UPS (Ciehanover et al. 1978; Hershko et al. 1979; McShane and Selbach 2022).

The UPS relies on ubiquitin as a small peptide tag for proteins which should be removed from the cell (Ciehanover et al. 1978). Ubiquitin itself is a 76 amino acid peptide, which can be attached to lysine residues in the target substrate (Weissman 2001; Finley et al. 2012). These proteins are then delivered to the proteasome, a large multiprotein complex which serves as the platform of degradation for the majority of intracellular proteins (Rock et al. 1994; Bard et al. 2018). Proteins can be monoubiquitinated or polyubiquitinated (Wang et al. 2004; Komander and Rape 2012). Furthermore, ubiquitin itself contains seven lysine residues (K6, K11, K27, K29, K33, K48, and K63), in addition to its initiating methionine (Finley et al. 2012). All these residues can serve as attachment points for the formation of ubiquitin chains (Christensen et al. 2007; Maspero et al. 2011; Komander and Rape 2012). Ubiquitin chains can be homotypic, consisting of only one type of ubiquitin linkage, or heterotypic, consisting of several types (Komander and Rape 2012; Finley et al. 2012). Furthermore, ubiquitin chains can be branched, adding further complexity. Out of the different types of ubiquitin chains, K48 and K11-linked chains are the ones usually involved in proteasomal degradation (Xu et al. 2009; Dammer et al. 2011).

The attachment of ubiquitin to a target substrate usually relies on a system called the ubiquitination cascade (Figure 1)(Finley et al. 2012). In this system an E1 ubiquitin activating enzyme (E1) binds ubiquitin under cleavage of ATP to AMP and pyrophosphate, forming a thiol ester bond, providing the energy required for the following steps (Weissman 2001; Finley et al. 2012). In yeast, there is one known E1 enzyme, in human cells two are known (Finley et al. 2012).

In the next step, ubiquitin is transferred to an E2 ubiquitin conjugating enzyme (E2). In human cells, approximately 40 E2s are known (Weissman 2001; Finley et al. 2012). Finally, an E3 ubiquitin ligase (E3) recognizes the target substrate and transfers the ubiquitin molecule to the target. In human cells, approximately 600 E3 enzymes are known to exist (Buetow and Huang 2016; George et al. 2018). Additionally, ubiquitin can be cleaved off proteins through the action of deubiquitinases (DUBs), adding a further layer of complexity (Weissman 2001; Finley et al. 2012; Snyder and Silva 2021; Lange et al. 2022). This structure, with only a few E1s, some more E2s, and many E3s, many of which are still poorly understood, highlights the intricacy of the regulation of the UPS.

Types of E3 ligases

Currently, there are four known main subtypes of E3 ligases (Yang et al. 2021). The largest and earliest studied subfamily is the HECT (homologous to the E6AP carboxyl terminus) family of E3 ligases (Huibregtse et al. 1995). They are characterized by their C-terminal HECT domain while their N-terminus varies, allowing further division into further sub families. HECT E3 ligases bind their corresponding E2 via the HECT domain while the N-terminus is mainly responsible for substrate recognition (Sluimer and Distel 2018). Notably, the Ubiquitin transfer by HECT E3 ligases is a two-step process in which ubiquitin is first transferred to a catalytic cysteine residue within the HECT domain before transferring it to the substrate.

The second major family of E3 ligases is the Really Interesting New Gene (RING) family, characterized by their eponymous RING domain (Freemont et al. 1991). In contrast to HECT E3 ligases, after the E2 has been bound to the RING domain, ubiquitin is transferred directly to the substrate without prior transfer to the E3 ligase proper (Bulatov and Ciulli 2015). RING E3 ligases can be either monomeric or multi-protein complexes. One large family of multi-subunit E3 ligases is the family of Cullin-RING ligases (CRLs), which are characterized by Cullin as the main scaffold between the RING domain and the substrate receptor unit (Nguyen et al. 2017).

A smaller family of E3 ligases is the U-box family of E3 ligases. Their activity is mediated by binding of their E2 to a U-box domain, which is structurally similar to the RING domain (Hatakeyama and Nakayama 2003). U-box E3 ligases have been found to mainly ubiquitinate already mono- or oligoubiquitinated substrates, leading to some researchers dubbing them as “E4s”.

The fourth currently known family of E3 ligases is the “RING-IBR-RING” (RBR) family of E3 ligases, which is characterized by a RING1 domain, followed by a “in between RING” (IBR) domain, which is then followed by a RING2 domain (Aguilera et al. 2000). Similarly to HECT E3 ligases, RBR-ligases transfer ubiquitin in a two-step process in which ubiquitin is first transferred to a catalytic cysteine contained in the RING2 domain before ultimately being transferred to the substrate (Smit and Sixma 2014).

Functions of protein degradation

As briefly mentioned above, the functions of protein degradation can broadly be categorized in the maintenance of homeostasis, quality control, and regulation, with these categories partially overlapping (Goldberg 1972; McShane and Selbach 2022). As mentioned in the

overview on autophagy, one of the best characterized triggers for autophagy is amino acid starvation (Hara et al. 1998; Hosokawa et al. 2009; Dikic and Elazar 2018; McShane and Selbach 2022), leading to the degradation of old proteins to supply amino acids for the synthesis of new ones. However, various other stresses such as oxidative stress, heat stress, or general aging of the cell can also lead to an upregulation of protein degradation in the cell (Dikic 2017; McShane and Selbach 2022). This aspect of protein homeostasis overlaps with general quality control of proteins in the cell, as these types of stresses typically induce damage to proteins in the cell which can lead to the formation of toxic aggregates in the cell (Pandey et al. 2007; Aiken et al. 2011; Suraweera et al. 2012; Dikic 2017; McShane and Selbach 2022).

Besides the clearance of proteins damaged by various stresses, protein quality control also includes the clearance of otherwise aberrant proteins, such as proteins with misincorporated amino acids, misfolded proteins, or proteins attached to stalled ribosomes (Dobson 2003; Chen et al. 2011; Duttler et al. 2013; Harper and Bennett 2016; Joazeiro 2019), the latter of which includes the activity of the ribosome-associated protein quality control in which the E3 ligase Listerin plays a key role (Duttler et al. 2013; Joazeiro 2019; McShane and Selbach 2022). Beyond the ribosome, this quality control mechanism extends into the endoplasmic reticulum, where the Endoplasmic-reticulum-associated protein degradation (ERAD) pathway detects misfolded proteins in a complex process involving successive glycosylation and refolding attempts which, if folding ultimately fails, leads to re-import of the misfolded protein into the cytoplasm and proteasomal degradation, which involves the E3 ligase Hrd1 as well as AAA-ATPase p97/VCP (Cheng et al. 1990; Ward and Kopito 1994; Kaneko et al. 2002; Buchberger et al. 2010; Adams et al. 2019; McShane and Selbach 2022). One further aspect of protein quality control is the detection of “orphaned” proteins which are not bound to their complex partner, usually due to excess production in comparison to said complex partner (Blikstad et al. 1983; Minami et al. 1987; Gunjan and Verreault 2003; Lam et al. 2007; Stiburek et al. 2012; Toyama and Hetzer 2013; Bogenhagen and Haley 2020; Taggart et al. 2020; Soto et al. 2022). Involved in this pathway are Tom1 or its human homolog HUWE1, as well as ubiquitin conjugating enzyme E2 O (UBE2O) which appear to recognise residues that would normally be hidden if the orphaned protein were in its native complex (Gunjan and Verreault 2003; Shemorry et al. 2013; Sung et al. 2016; Yanagitani et al. 2017; McShane and Selbach 2022).

In addition to the two previously mentioned functions, protein degradation can also play a role in the regulation of protein levels in response to outside factors, cell differentiation, or progression in the cell cycle (Harkness et al. 2002; Buccitelli and Selbach 2020; McShane and Selbach 2022). This function often relies on the constant production and simultaneous turnover of a regulatory factor through protein degradation, which is inhibited upon certain environmental signals. Examples for this are the regulation of the hypoxia response via turnover of hypoxia-inducible factor 1 alpha by The von Hippel-Lindau tumour suppressor protein (Semenza and Wang 1992; Ivan and Kaelin 2001; Weidemann and Johnson 2008) or the upregulation of p53 in response to DNA damage via inhibition of its turnover by the E3 ligase MDM2 (Honda et al. 1997; Levine 2020).

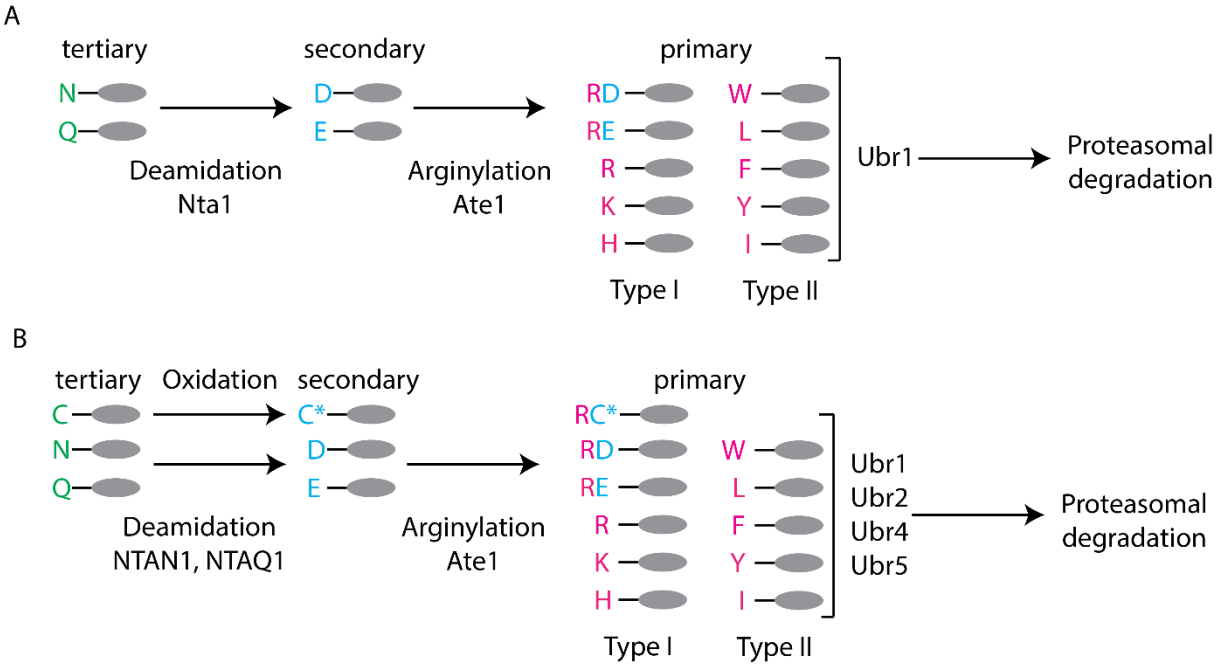

Figure 2: The Arg/N-degron pathway
A: The Arg/N-degron pathway in yeast. Tertiary N- or Q-N-termini are deamidated to form secondary D- or E-N-termini. These secondary termini are then arginlyated by Ate1 to form a primary N-terminus. Primary N-termini are either basic (Type I) or bulky hydrophobic (Type II) and are recognized by Ubr1 and targeted for proteasomal degradation.
B: The Arg/N-degron pathway in mammals. An additional tertiary terminus in mammals in cysteine, which can be oxidized. Furthermore, N- and Q-N-termini are processed by NTAN1 and NTAQ1, respectively. Recognition of primary residues occurs through Ubr2, Ubr4, and Ubr5, respectively.

Degrons

E3 ligases recognize their substrates via degradation signals called degrons (Ravid and Hochstrasser 2008; Mészáros et al. 2017; Varshavsky 2019). Degrons are short linear motives, usually between 2 and 10 amino acids in length, which can be located at the N-terminus, C-terminus, or internal in the primary amino acid sequence (Varshavsky 2019; Zhang et al. 2023; Varshavsky 2024; Zhang et al. 2025). Usually, degrons are transferable, meaning that the introduction of the degron to an otherwise stable protein will lead to destabilization via the E3 recognizing this degron (Chen et al. 2017). Degrons are usually located in disordered regions of proteins, due to their easier accessibility for E3 ligases (Ruan et al. 2020; Hou et al. 2022). As most disordered regions of proteins are located at the termini of a protein (Lobanov et al. 2010), this also leads to a preferred occurrence of degrons at the termini of proteins. Furthermore, protein termini can undergo post-translational modifications, such as N-terminal acetylation or C-terminal amidation, either protecting the degron from recognition by its target E3, or enabling their recognition (Heathcote et al. 2024; Muhar et al. 2025). Both N- and C-terminal degrons can also be generated through proteolytic cleavage of a protein, adding another layer of regulation (Rao et al. 2001; Piatkov et al. 2012a; Piatkov et al. 2012b; Piatkov et al. 2014; Varshavsky 2019). C-terminal degrons are primarily recognized by CRL-type ligases (Koren et al. 2018; Lin et al. 2018). In comparison, internal degrons tend to be hydrophobic, due to their tendency to be buried in the proteins core and to be exposed upon misfolding of the protein, leading to its degradation (Zhang et al. 2023).

As this project focuses on a complex involved in the recognition of N-degrons, a further overview of the different N-degron pathways is given.

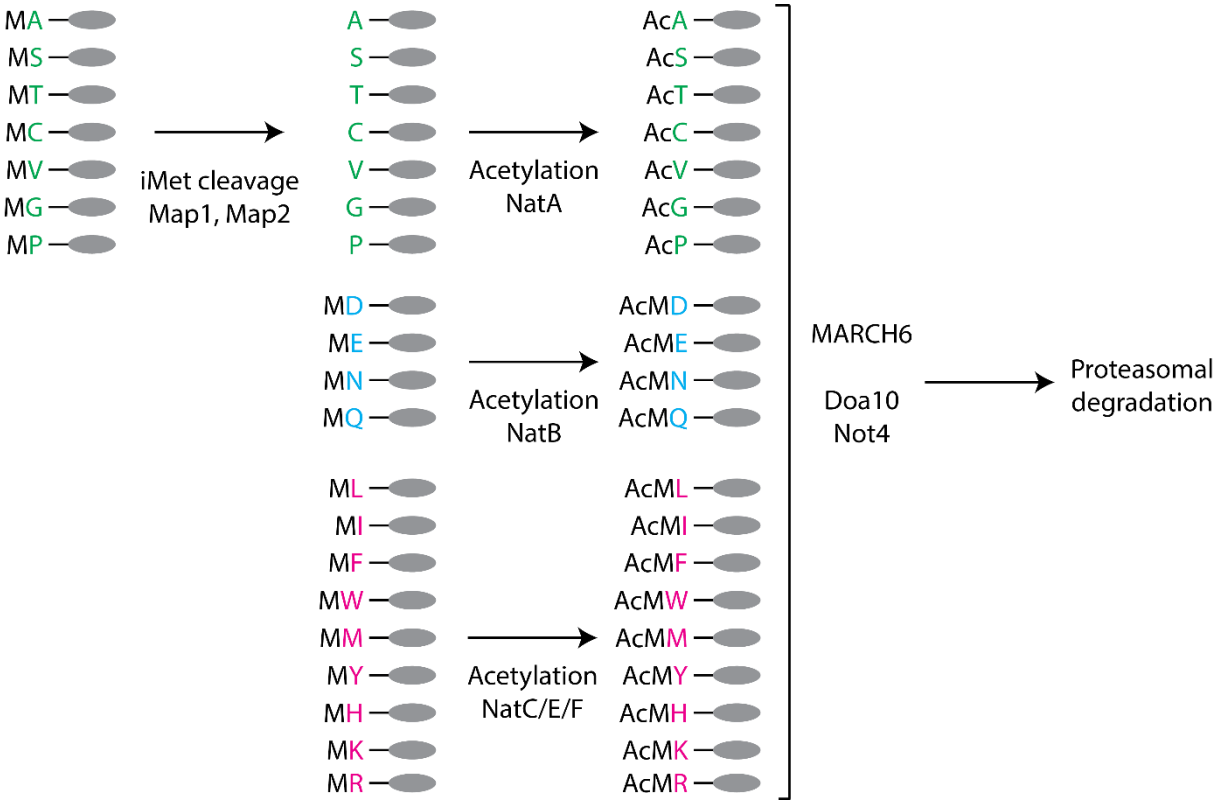

Figure 3: The Ac/N-degron pathway.
If the residue following the initiating methionine has a small radius of gyration (A, S, T, C, V, G, P), it can be cleaved off by the action of methionine aminopeptidases. The exposed residues can be N-terminally acetylated by NatA. Furthermore, N-terminal methionine followed by D, E, N, or Q can be acetylated by NatB. Finally, methionine followed by L, I, F, W, M, Y, H, K or R can be acetylated by NatC, NatE, or NatF. The acetylated N-termini are then recognized by MARCH6 in mammalian cells, or Doa10 and Not4 in yeast and targeted for degradation.

N-degron pathways

In yeast, there are currently three known N-degron pathways: The Arg/N-degron pathway, the Ac/N-degron pathway, and the Pro/N-degron pathway.

The Arg/N-degron pathway

The Arg/N-degron pathway was the first pathway to be discovered (Bachmair et al. 1986).

In this pathway, primary destabilizing residues are recognized by Ubr1 (Figure 2A) (Bartel et al. 1990; Baker and Varshavsky 1995; Varshavsky 2024). Notably, Ubr1 possesses two distinct binding sites for substrates (Pan et al. 2021). Type 1 destabilizing residues in this pathway are the basic amino acids arginine, lysine, and histidine while type 2 destabilizing residues are the hydrophobic amino acids leucine, phenylalanine, tryptophane, tyrosine, isoleucine, or methionine followed by a bulky hydrophobic residue (Bachmair et al. 1986; Varshavsky 2019, 2024). In the context of this degron pathway, these are referred to as primary destabilizing residues. Additionally, methionine followed by a bulky hydrophobic residue has been identified as a primary destabilizing type 2 N-terminus as well (Kim et al. 2014). Secondary destabilizing residues in this pathway are either aspartate or glutamate, which can be arginylated by Ate1 to form a primary destabilizing N-terminus (Ferber and Ciechanover 1987; Kwon et al. 2002; Kim et al. 2022). Additionally, asparagine or glutamine can act as tertiary destabilizing residues through deamidation by the enzyme Nta1 to form their corresponding secondary destabilizing residues (Baker and Varshavsky 1995; Kim et al. 2016; Varshavsky

2024). In mammalian cells, this N-degron pathway exists as well (Figure 2B). However, it possesses more N-recognins with UBR1, UBR2, UBR4, and UBR5 (Ji et al. 2019; Da Jeong et al. 2023; Hehl et al. 2024). Furthermore, processing of tertiary destabilizing residues is carried out by two distinct enzymes, NTAN1 and NTAQ1 (Varshavsky 2019), which are similar in function, but not in sequence (Park et al. 2014; Park et al. 2020). Additionally, N-terminal cysteine can act as a tertiary destabilizing residue in mammalian cells as well by being oxidized and subsequently arginylated (Hu et al. 2005; Lee et al. 2005; Varshavsky 2024).

The Ac/N-degron pathway

N-terminal acetylation is one of the most common protein modifications in the cell, with approximately 80% of proteins in human cells and 60% of proteins in yeast cells undergoing acetylation (Arnesen et al. 2009; Aksnes et al. 2016).

The initiating methionine in front of alanine, serine, threonine, valine or cysteine can be cotranslationally cleaved by the action of the methionine aminopeptidases Map1 and Map2 (Figure 3) (Chang et al. 1990; Li and Chang 1995; Varshavsky 2024). These exposed residues can then be N-terminally acetylated by NatA, which carries out approximately 40% of N-terminal acetylation in the cell (Arnesen et al. 2009; Aksnes et al. 2019). In the case of methionine followed by aspartate, glutamate, glutamine, or asparagine, the N-terminus can be acetylated by NatB (van Damme et al. 2012; Aksnes et al. 2016). Methionine followed by leucin, isoleucine, phenylalanine, tyrosine, lysine, serine, threonine, alanine, or valine can be acetylated by NatC, NatE, or NatF, with only the former two having a homolog in yeast (van Damme et al. 2011b; van Damme et al. 2011a; van Damme et al. 2015; Aksnes et al. 2015; van Damme et al. 2016; Aksnes et al. 2019). Additionally, NatD specifically acetylates histones H2A and H4 (Song et al. 2003) and NatH , which does not have a homolog in yeast, specifically acetylates actin (Drazic et al. 2018). Lastly, chloroplast-specific NatG in plants can acetylate N-termini beginning with methionine, alanine, serine, or threonine (Dinh et al. 2015). These acetylated residues can then be recognized by Not1 or Doa10, leading to ubiquitination of the substrate and its subsequent degradation (Hwang et al. 2010; Shemorry et al. 2013; Nguyen et al. 2019).

Interestingly, the notion that acetylation acts exclusively as a degradation signal has been challenged recently. For example, it has been shown that NatC can acetylate substrates of the UBR4-KCMF1 complex, preventing their recognition (Varland et al. 2023). Similarly, it has been shown in yeast that acetylation of MN-N-termini by NatB or acetylation of N-termini starting with glutamate can lead to their stabilization, rather than their degradation (Kats et al. 2018).

The Pro/N-degron pathway

The final currently known N-degron pathway in yeast is the Pro/N-degron pathway (Figure 4). In this pathway, the initiating methionine preceding a proline residue is cleaved off, followed by recognition by Gid4 or Gid10 (Chen et al. 2017; Melnykov et al. 2019). This pathway particularly targets proteins involved in gluconeogenesis, such as Fbp1, Mdh2, and Icl1 (Chen et al. 2017). Additionally, if the proline is the third residue, it is possible for the second residue to be cleaved by the aminopeptidases Fra1 or Icp55, revealing the destabilizing proline residue (Chen et al. 2021). The E3 ligase involved in this pathway is the GID complex, which is further elaborated on in the following:

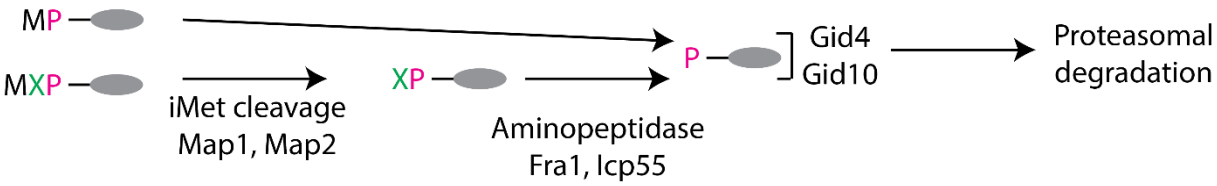

Figure 4: The Pro/N-degron pathway in yeast.
The initiating methionine is cleaved off by the action of Map1 and Map2. If methionine is the third residue and the second residue is S or T, Fra1 and Icp55 can cleave S or T. Exposed proline N-termini are then recognized by Gid4 or Gid10, leading to degradation of their protein.

The GID complex

The main RING-E3 ligase in the Pro/N-degron pathway is the Glucose induced degradation deficient complex (GID-complex) in *Saccharomyces cerevisiae*, also known as the C-terminal to LisH complex (CTLH-complex) in human cells (Chen et al. 2017; Maitland et al. 2022; Varshavsky 2024). This complex is a multi-subunit RING E3 ligase minimally consisting of Gid1, Gid2, Gid5, Gid8, and Gid9 as an anticipatory complex (Figure 5A) (Menssen et al. 2012; Qiao et al. 2020). In this complex Gid2 and Gid9 form the catalytic subunit, responsible for the transfer of ubiquitin from the GID complex's associated E2 Ubc8 to the target substrate (Chrustowicz et al. 2024). Gid1, Gid8, and Gid5 serve structural purposes (Menssen et al. 2012). Notably, the anticipatory complex on its own is not functional until the binding of a substrate receptor unit (Qiao et al. 2020). The first substrate receptor unit to be discovered was Gid4 (Chen et al. 2017). Structurally, Gid4 folds into a ß-barrel and recognizes N-terminal proline degrons (Dong et al. 2018). Its established role is in the degradation of proteins involved in gluconeogenesis, such as Mdh2, Fbp1, and Icl1 (Chen et al. 2017; Varshavsky 2024). Recently, two more substrate receptor units have been discovered. Gid10, which is structurally similar to Gid4 (Shin et al. 2021), and also binds N-terminal proline. Its currently known endogenous substrate is Art2 (Langlois et al. 2022).

The most recently discovered substrate receptor unit is Gid11 (Kong et al. 2021). Structurally, Gid11 is a significantly longer protein that Gid4 and Gid10 and is not predicted to fold into a ß-barrel, but into a seven-bladed ß-propeller (Kong et al. 2025). Recently, it has been found to recognize N-terminal threonine (Kong et al. 2021). However, much of its specificity and the structural basis of its binding are still unknown.

Additionally, the GID complex has been found to be able to form structural higher-order structures (Figure 5B) (Sherpa et al. 2021). First, mediated by Gid7, or its homologs WDR26 or Muskelin in human cells, it can arrange itself in a large ring-like structure, known as a supramolecular chelator assembly. Particularly for larger substrates such as Fbp1 this arrangement has been shown to be necessary to accommodate such substrates. In addition to this, it has been shown in human cells that WDR26 can act as a substrate receptor on its own (Gottemukkala et al. 2024).

Additionally, Gid12, formerly known as Ipf1 (which this protein will be referred to as in this thesis), has been shown to be able to coordinate several higher-order GID complexes into an even larger cage-like assembly with a diameter of about 420 angstroms (Qiao et al. 2022). While the exact regulation or purpose of this assembly still is unknown, it has been shown to

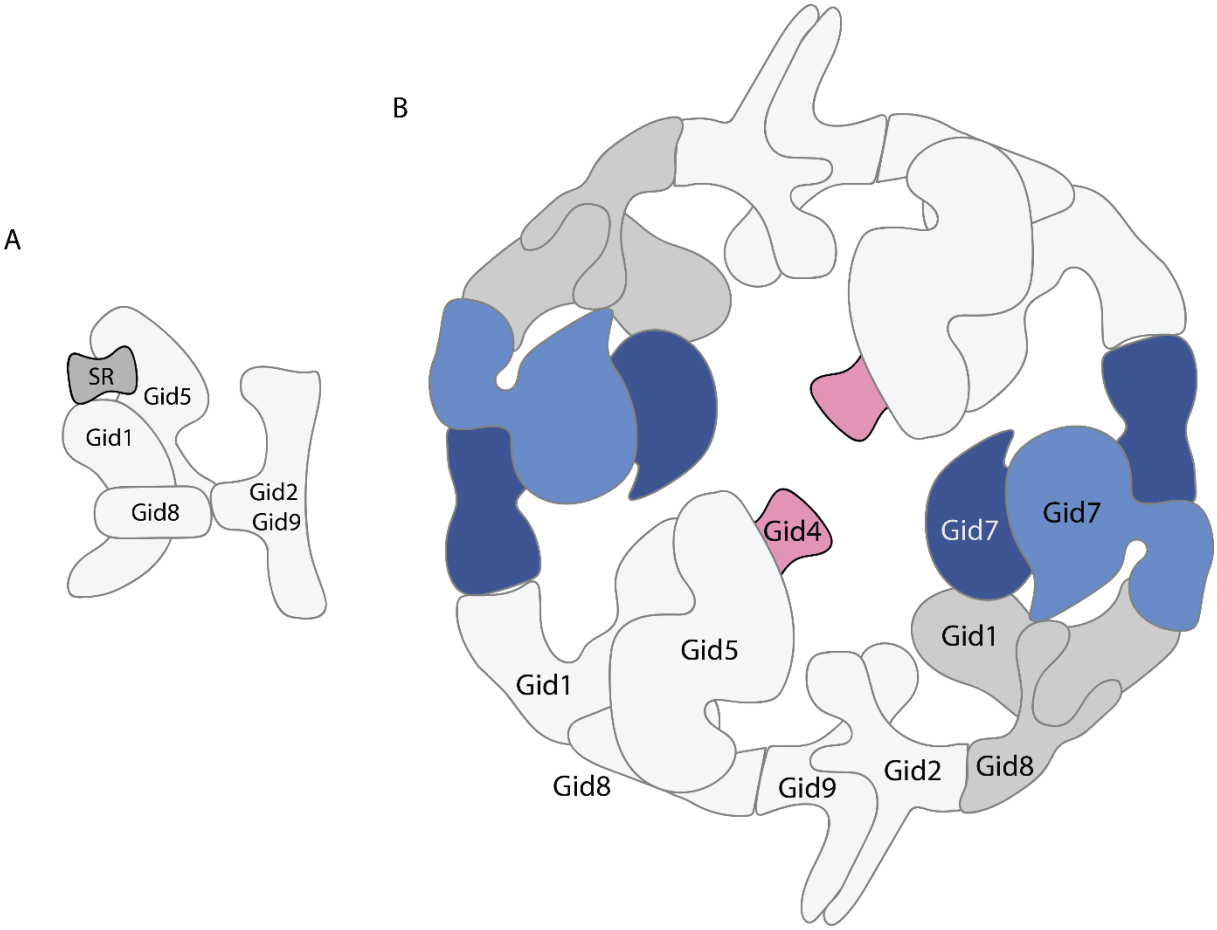

Figure 5: Cartoon representation of the GID complex in yeast.
A: Cartoon representation of the Core GID-complex, consisting of the RING domain subunits Gid2 and Gid9, structural subunits Gid1, Gid5, and Gid8, and a substrate receptor.
B: Cartoon representation of the GID chelator assembly, consisting of four core complexes and mediated by Gid7.

inhibit GID activity, making it likely that it serves as another layer of regulation to the GID complex by sequestering potentially active chelator assemblies.

The GID complex is highly conserved across all eukaryotes, with all core GID components being conserved (Maitland et al. 2022). The human homolog of Gid1 is RanBP9, the ones of Gid2 RMND5A and RMND5B, the one of Ubc8 is UBE2H, the homolog of Gid4 is human GID4, the homolog of Gid5 is ARMC8, Gid7 has two homologs in WDR26 and Muskelin, the homolog of Gid8 is human GID8 or TWA1, and the human homolog of Gid9 is MAEA (Maitland et al. 2022). However, no known homologs exist outside of yeast for Gid10, Gid11, or Ipf1.

The best-studied function of the GID complex is in the degradation of gluconeogenic enzymes in during the transition from ethanol medium to glucose-rich medium (Chiang and Chiang 1998; Santt et al. 2008; Chen et al. 2017). However, with increased recent interest in the GID complex, more functions have been discovered. Among these, is the regulation of the ART-Rsp5 ubiquitin ligase pathway, a component of plasma membrane quality control upon stresses such as heat stress, changes in osmolarity, or nutrient starvation (Langlois et al. 2022). Outside of yeast, the CTLH-complex has been found to be involved together with the E2 Marie Kondo in the clearance of RNA binding proteins during the maternal-to-zygotic transition in *Drosophila melanogaster* (Zavortink et al. 2020). In humans, mutants of WDR26, the homolog of yeast Gid7, are known to cause a neurodevelopmental disorder known as Skraban-

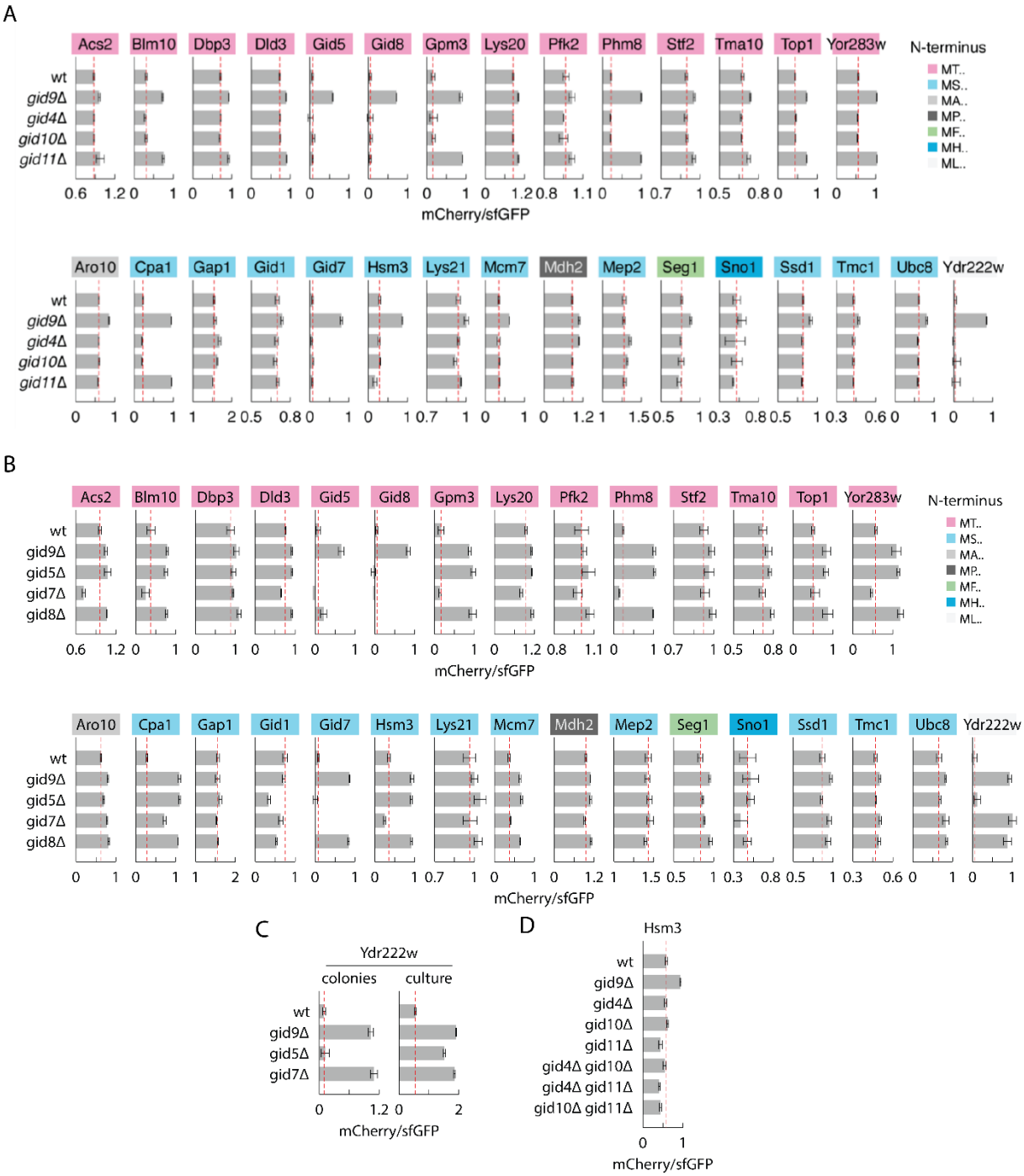

Figure 6: Potential GID substrates identified before this study.
A: Stability of 30 potential GID substrates upon knockout of currently known substrate receptors.
B: Stability of 30 potential GID substrates upon knockout of core components of the GID complex.
C: Dependence of turnover of Ydr222w on Gid5 and Gid7 in colonies and liquid culture.
D: Stability of Hsm3 upon knockout of different combinations of the currently known GID substrate receptors.
A-D: Experiment carried out by XXXXXXXXXXXXX. Error bars show standard deviation between biological replicates (n=4).

Deardorff syndrome (Skraban et al. 2017; Yang et al. 2024). Furthermore, as mentioned above, WDR26 itself can act as a substrate receptor for the metabolic enzyme nicotinamide/nicotinic-acid-mononucleotide-adenylyltransferase 1, regulating prodrug metabolism in human cells (Gottemukkala et al. 2024). Interestingly, this function was found to be regulated by YPEL5, which has a homolog in yeast with Moh1. Further studies in macrophages also showed the CTLH-complex to be involved in the regulation of the host anti-microbial response, with

knockout of CTLH-components leading to increased antimicrobial activity against *Mycobacterium tuberculosis* (Simwela et al. 2024). Altogether, these studies show that the GID complex in yeast or the CTLH complex in higher eukaryotes is involved in a wide variety of functions, highlighting the importance of understanding its functions, components, and recognition of its substrates further.

Kong et al. identified in 2021 30 potential GID substrates, which are shown in (Figure 6A,B). Out of these 30 potential substrates, he generally found proteins with a N-terminal threonine to depend on Gid11 in their turnover, apart from Gid5 and Gid8, which are components of the Gid complex itself (Figure 6A). Additionally, it was found by XXXXXXX that out of these 30 identified potential substrates, Aro10, Cpa1, Ssd1, Tmc1, Ubc8, and Ydr222w depend on Gid7 in their degradation (Figure 6B). Ydr222w is particularly interesting in this regard, as its degradation appears to always depend on Gid7, but it does not appear to depend on Gid5 in colony stability measurements (Figure 6C). When measuring its stability in liquid culture, however, its turnover depends on Gid5. Of additional note is Cpa1, which is the only currently known potential Gid11 substrate whose turnover also depends on Gid7 (Figure 6A,B). Importantly, some potential GID substrates, for example Hsm3, still do not possess any known substrate receptors, despite their turnover depending on GID core components, including Gid5 (Figure 6B,D).

Tandem-fluorescent protein timers

The main tool employed in this study to analyze the stability of proteins is the tandem-fluorescent protein timer (tFT) tag (Khmelinskii et al. 2012). This tag consists of two fluorescent proteins, usually a red and a green fluorescent protein, with two different maturation durations. In the case of the tFT tag used in this study, it consists of superfolder GFP (sfGFP) which matures within minutes after synthesis (Pédelacq et al. 2006) and mCherry, which has a maturation half-time of approximately 40 minutes (Merzlyak et al. 2007). Based on these two different maturation times, one can determine the ratio of mCherry to sfGFP fluorescence. As proteins age, more of the mCherry tags mature, increasing the amount of red fluorescence compared to green fluorescence. Notably, as both fluorescent moieties are contained in the same tag, this ratio is unaffected by the protein's abundance. However, it does not allow for the determination of the age of individual protein molecules and rather provides a readout for the average age of the protein population in the cell. However, it can be employed fully in vivo, allowing for high-throughput measurements in a colony format. Furthermore, by comparing the mCherry to sfGFP ratios between, for example, wild type cells, and a knockout mutant of a potential UPS component of interest, it provides a simple tool for investigating the impact of perturbations in protein degradation.

Materials and Methods

Yeast methods and plasmids

Yeast strains used are listed in Table S 1 and are derived either from BY4741 or BY4742. Plasmids used are listed in Table S 2. Yeast genome manipulations were carried out using PCR-targeting and lithium acetate transformation (Janke et al. 2004; Knop et al. 1999). Unless stated otherwise, all PCRs in this study were carried out using an in-house high-fidelity (HF) polymerase. Used oligonucleotides are listed in Table S 3.

Yeast culture conditions

For general culturing, yeast strains were grown in YP medium containing 2% glucose (10 g/L yeast extract (BD Biosciences), 20 g/L bacto peptone (BD Biosciences), 20 g/L glucose (Merck)) For auxotrophic selection, cells were grown on synthetic complete (SC) medium (6.7 g/L Bacto yeast nitrogen base without amino acids (BD Biosciences), 2 g/L SC amino acid dropout mix, 20 g/L glucose) or SC(MSG) medium (1.7 g/L yeast nitrogen base without amino acids and ammonium sulfate (BD Biosciences), 1 g/L monosodium glutamate (Sigma-Aldrich), 2 g/L amino acid dropout mix, 20 g/L glucose) if antibiotic selection was necessary. For antibiotic selection, the following antibiotics were used in the following concentrations: G418 (Invivogen): 200 mg/L; cloNAT (Werner Biosciences): 100 mg/L; hygromycin B Gold (Invivogen): 200 mg/L for YP-based media and 400 mg/L for SC-based media. To select against the presence of *LYP1* thialysine (Sigma-Aldrich) was added to media at a concentration of 50 mg/L and for selection against the presence of *CAN1* canavanine (Sigma-Aldrich) was added at a concentration of 50 mg/mL. For counter selection against the presence of the URA marker, cells were grown on SC-complete medium containing 0.1% (w/v) 5-fluoroorotic acid (5-FOA) (abcr). To make solid media, 2% Bacto Agar (BD Biosciences) were added. As alternative carbon sources, the following were used: Raffinose (Sigma Aldrich): 20 g/L; Galactose (Serva): 20 g/L; Ethanol (Sigma-Aldrich): 20 mL/L. Cells were grown at 30°C with 220 rpm shaking for liquid media, unless indicated otherwise.

Confirmation of cassette integration using colony PCR

To confirm the integration of DNA cassettes into the yeast genome, overnight cultures of the clone to be tested were set up in 1 mL YPD medium. The following day, 100 µL overnight culture were spun down at 21100 *g* for 1 minute and the supernatant was discarded. The cell pellet was resuspended in 30 µL 0.1% SDS (Sigma-Aldrich) and the cells were lysed at 95°C for 5 minutes. One of the DNA primers for the PCR, “His&Kan_Tag2”, binds 138 base pairs into the cassettes. The other primer was chosen to bind a few hundred base pairs upstream of the cassette integration site. PCR reactions were set up as follows:

Table 1: Reaction mixture for confirmation of cassette integration via colony PCR

Reagent	**Amount**
ddH2O	37 µL
10X HF buffer	5 µL
His&Kan_Tag2 (10 µM)	3 µL
GOI specific primer (10 µM)	3 µL

dNTPs (10 mM)	1 µL
Cell lysate	0.5 µL
HF polymerase	0.5 µL

Table 2: Cycling conditions for confirmation of cassette integration via colony PCR

95°C	5 min	
95°C	30 s	X40
55°C	30 s	X40
72°C	90 s	X40
72°C	7 min	

After the PCR, the reaction mixtures were analysed via agarose gel electrophoresis on 1 % gel. Presence of the PCR product in the tested clone, but not in the parental stain, indicated successful integration of the cassette.

Synthetic genetic array

For investigating libraries of substrates against knockouts of yeast genes, the SGA methodology was used (Baryshnikova et al. 2010). Strains taken from the -Ura Gid-hits library (yMaM330 (MATalpha can1Δ::STE2pr-SpHIS5 lyp1Δ::STE3pr-LEU2 his3Δ1 leu2Δ0 ura3Δ0 leu2Δ0::GAL1pr-I-SCEI-natNT2) ORF-mCherry-SceI-SpCYC1term-ScURA3-SceI-mCherryΔN-sfGFP) were first crossed with the knockout strains of interest on YPD medium, followed by the following selection steps:

- Selection of diploids on SC(MSG)-URA+G418+cloNAT plates, performed twice.
- Sporulation for one week at 23°C on SPO plates (2% potassium acetate (Sigma-Aldrich), 2% Bacto Agar)
- First selection of haploid cells on SC(MSG)-His/Arg/Lys/Ura + canavanine/thialysine plates
- Second selection of haploid cells on SC(MSG)-His/Arg/Lys/Ura + canavanine/thialysine/G418 plates
- Third selection of haploid cells on SC(MSG)-His/Arg/Lys/Ura + canavanine/thialysine/G418/cloNAT plates
- Induction of I-SceI enzyme for reconstitution of the tFT tag on SC-His Raffinose/Galactose plates
- Counterselection against URA-marker on SC-His + 5-FOA plates
- Recovery on SC(MSG)-His/Arg/Lys + canavanine/thialysine plates.

The resulting arrays were pinned on SC-His plates and their fluorescence was measured as described below.

Endogenous mutagenesis using the *delitto perfetto* approach

T2A mutations or N-terminal capping mutations were introduced following the *delitto perfetto* method (Stuckey et al. 2011). CORE cassettes were PCR amplified from pGSKU using P.I and P.IIS primers containing homology arms for the region to be replaced using the following conditions:

Table 3: Reaction mixture for amplification of CORE cassette from pGSKU

Reagent	**Amount**
ddH2O	37 µL
10X HF buffer	5 µL
P.I (10 µM)	3 µL
P.IIS (10 µM)	3 µL
dNTPs (10 mM)	1 µL
pGSKU	0.5 µL (~200 ng)
HF polymerase	0.5 µL

Table 4: Cycling conditions for amplification of CORE cassette from pGSKU

94°C	2 min	
94°C	30 s	X32
57°C	30 s	X32
72°C	5 min	X32
72°C	7 min	

The efficiency of the PCR amplification was confirmed by agarose gel electrophoresis on a 1% agarose gel. In case of weak amplification of the CORE cassette, the PCR was repeated six times. The product of six PCR reactions was combined and precipitated using a 2.5 times volume of 95% ethanol and one tenth volume of 3 M sodium acetate (Sigma-Aldrich) (pH 5.2). The precipitated DNA was spun down at 21100 *g* for ten minutes and the supernatant was discarded. The DNA pellet was washed with 100 µL of 70% ethanol. If the DNA pellet was detached during the washing step, additional centrifugation was carried out for 5 minutes. As much of the ethanol as possible was removed and the pellet was dried under a fume hood for 30 minutes. It was then resuspended in 50 µL DNAse-free water.

5 µL raw PCR product or 5 µL concentrated PCR product were used for the subsequent lithium acetate transformation (Knop et al. 1999). After the transformation, the cells were plated out on YPD+G418 medium and after 48 hours to 72 hours incubation at 30°C they were replica plated onto SC-URA medium and incubated for a further 24 hours to 48 hours.

Colony PCR was carried out as described above to confirm integration of the CORE cassette into the desired locus. However, the primers used were primers URA3.1 and GAL.E and primers binding a few hundred base pairs up- and downstream of the integration site of the CORE cassette. Only strains producing a PCR product for PCR using both URA3.1 and one of the two gene specific primers, as well as the corresponding primer pair using GAL.E, were considered positive for successful integration of the CORE cassette.

For the replacement of the CORE cassette with the desired DNA sequence, DNA oligomers were designed containing the desired mutation as well as 40 base overhangs with the region of interest. Alternatively, for replacements too large for an oligomer, the sequence was ordered as a gBlock (Integrated DNA Technologies), designed the same way. In order to replace the CORE cassette, lithium acetate transformation (Knop et al. 1999) was performed with the following modifications: Overnight cultures were grown in YP+Raffinose medium. The

initial dilution of the cells was done in YP+Raffinose/Galactose medium to induce expression of I-SceI in the CORE cassette and promote recombination. 0.5 µL 100 µM DNA oligomer or 5 µL 10 ng/µL gBlock were used for the transformation. After the transformation, cells were allowed to recover overnight in 1 mL YPD before plating out on SC-complete+5-FOA. After 48 hours to 72 hours incubation of 5-FOA, cells were streaked for single colonies on SC-complete+5-FOA medium.

To confirm replacement of the CORE cassette, colony PCR was carried out using the up- and downstream primers. The PCR product of this colony PCR was gel purified using a QIAquick® Gel Extraction Kit (Qiagen) and sent for Sanger sequencing (Eurofins Genomics) to confirm the replacement of the wild type sequence with the desired mutation.

Plasmid shuffle of *MAP1* variants

To introduce *MAP1* variants into double knockout mutants of *MAP1* and *MAP2*, *MAP2* was first knocked out in the strain carrying the desired tFT-tagged substrate as described above. The resulting strains were transformed with pCPO0069, expressing wild type *MAP1* from a pRS316-based URA^+ plasmid. This was followed by knockout of the endogenous *MAP1* as described above. Next, the resulting strains were transformed with pCPO0070, pCPO0071, or pCPO0072, expressing either wild type *MAP1*, *MAP1 Q365A*, or *Deinococcus radiodurans* MetAP from a pRS315-based LEU^+ plasmid. Selection for the LEU^+ plasmid and against the URA^+ plasmid was carried out on SC-LEU + 5-FOA medium.

Spotting Assay

To evaluate the fitness of yeast strains on selective media, spotting assays were carried out. Pre-cultures of the strains to be investigated were grown in YPD medium to saturation overnight. The next morning, the cells were centrifuged at 2300 *g* for 2 minutes. The supernatant was discarded, and the cell pellet was resuspended in an equal volume of sterile water. The OD600 of the cell suspension was measured and a serial dilution of the cell suspension from an OD600 of 1 to 10^{-4} was carried out. 3 µL of each dilution were then spotted onto YPD and selective medium, respectively. The plates were then incubated at 30°C and pictures were taken after 24 and 48 hours.

Generation of plasmids

Unless stated otherwise, plasmids were assembled via NEBuilder® HiFi DNA Assembly (New England Biolabs). All restriction enzymes used were acquired from New England Biolabs. Gel extractions of DNA fragments were performed using a QIAquick® Gel Extraction Kit (QiagenPreparation of plasmids was performed using a QIAprep® Spin Miniprep Kit (Qiagen) Verification of plasmids was performed either by Sanger Sequencing (Eurofins Genomics) or Oxford Nanopore Whole Plasmid Sequencing (Eurofins Genomics).

For the generation of overexpression plasmids utilizing the *GPD* promoter, pKBJ001, pRS316-GPD, or pRS426-GPD were digested using BamHI and XhoI or HindIII. Yeast genes were PCR amplified from yMaM330 or BY4741 gDNA using primers specific for the gene of interest containing the necessary homology arms for assembly into the vector. Human ATE1 isoform 1 and NTAQ1 were amplified from pAC009 and pAC0010.2, respectively. NTAN1 and human

ATE1 isoform 2 were ordered as gBlocks (Integrated DNA Technologies). Other human genes were amplified from the human ORFeome collection (Rual et al. 2005), if available, or ordered as gBlocks (Integrated DNA Technologies).

pAnB19-XZ plasmids were generated by cutting pAnB19 with EcoRV, followed by NEBuilder® HiFi DNA Assembly to bridge the cut site with the "pAnB19-XZ" oligonucleotide, containing the necessary homology arms and two "NNK" codons. After sequencing of 96 clones, 60 of the 80 desired plasmids could be obtained and the remainder was cloned manually by using a similar oligonucleotide containing the codons for the desired mutations.

pCPO0051 was generated by amplifying the plasmid backbone using primers 313-GID11ter_F and pRS313-GID11pr-HA_R, introducing a SalI cut site and a HA tag. The resulting PCR product was run on a 1% agarose gel and extracted from a gel. It was then digested using SalI and religated using T4 ligase (New England Biolabs). The resulting plasmid was digested using SalI used as the backbone for subsequent cloning of *GID11* variants.

For single codon mutagenesis, or introduction of mutations affecting only a few codons, the desired ORF was amplified as two fragments with overlapping primers introducing a hybridisation site for subsequent NEB HiFi DNA Assembly, as well as the desired mutations. Deletions were achieved similarly by amplifying the regions flanking the desired deletion site.

Immunoblotting of Whole Cell Yeast extracts

3 ODs cells were harvested by centrifugation at 1000 *g* for 2 minutes. Whole cell extracts were prepared by alkaline lysis followed by trichloroacetic acid precipitation (Knop et al. 1999). Cell pellets were resuspended in 150 µL high urea buffer (8 M urea (Sigma-Aldrich), 5% (w/v) SDS, 200 mM Tris-HCl (Sigma-Aldrich) pH 6.8, 0.1 mM EDTA (Sigma-Aldrich), 0.1% (w/v) bromophenol blue (Sigma-Aldrich), 1.5% (w/v) DTT) followed by protein denaturation at 65°C for 15 minutes. After denaturation, the cell extracts were centrifuged at 21100 *g* for 10 minutes and 10 µL extract were used for subsequent gel electrophoresis.

Gel electrophoresis was carried out via SDS-PAGE (LAEMMLI 1970), followed by Western Blotting (Renart et al. 1979) onto nitrocellulose membrane. The blotting process was carried out at 1.3 A, 25 V for 7 minutes using a Trans-Blot® Turbo machine (Bio-Rad). Successful transfer onto the membrane was confirmed using Ponceau staining (Stochaj et al. 2006). Depending on the epitope to be detected, the membranes were then probed using mouse primary antibodies against the HA epitope (dilution 1:2000, clone 12CA5, produced in-house), the myc epitope (dilution 1:2000, clone 9E10, produced in-house), GFP (dilution 1:2000, 11814460001, Roche), ubiquitin (dilution 1:1000, sc-8017, Santa Cruz Biotechnology) or Pgk1 (dilution 1:1000, 459250, Thermo Fisher Scientific) and goat anti-mouse HRP-conjugated secondary antibody (dilution 1:5000, G-21040, Thermo Fisher Scientific). All antibody dilutions were prepared in PBS with 0.1% (v/v) Tween 20 (Carl Roth) and 5% (w/v) milk powder (Carl Roth) added. Visualization was performed using the SuperSignal West Pico PLUS (Thermo Fischer Scientific) and a Chemidoc MP system (Bio-Rad).

Immunoprecipitation of tFT-tagged proteins

For immunoprecipitation of tFT-tagged proteins from cells extracts made from cells grown in ethanol, first overnight cultures of the strain to be lysed were grown in SC-complete and allowed to grow to saturation. This saturated culture was then diluted 3000-fold in fresh SC-complete and allowed to grow for approximately 15 hours, or to an OD600 of approximately 1. The cells were collected by centrifugation at 1000 *g* for 3 minutes, the supernatant was discarded, and the cell pellet was washed with an equal volume of sterile water. The cells were spun down once more at 1000 *g* for 3 minutes, the supernatant was discarded, and the cells were resuspended in an equal volume of SC-complete with 2% ethanol as its carbon source. These cultures were allowed to grow for 6 hours before cell harvesting.

Cell harvest was performed by centrifugation at 1000 *g* for 3 minutes. The supernatant was discarded, and the cell pellet was resuspended in 500 µL water and transferred to a 2 mL microcentrifuge tube. The cells were then spun down at 21100 *g* for 1 minute and the supernatant was discarded. The cell pellet was frozen at -80°C until further use.

For cell lysis, 300 µL lysis buffer (25 mM Tris-HCl pH 8, 150 mM sodium chloride (Sigma-Aldrich), 1 mM EDTA, 0.5% (w/v) sodium deoxycholate (Sigma-Aldrich), 1% (v/v) Triton X-100 (Sigma-Aldrich), 0.1% (w/v) SDS, protease inhibitors (4693159001, Sigma-Aldrich)) were added to the cell pellet, followed by approximately 200 µL acid-washed glass beads (G8772, Sigma-Aldrich). The cells were disrupted by vortexing at maximum speed for 30 seconds, followed by 30 seconds pause at 4°C. This process was carried out eight times in total. The lysates were clarified by centrifugation at 21100 *g* for 10 minutes at 4°C. The supernatant was collected and 25 µL were taken for later immunoblotting.

For immunoprecipitation, 25 µL magnetic anti-GFP nanobody coated agarose bead slurry (Fridy et al. 2014) (produced in-house) were equilibrated with 500 µL ice-cold lysis buffer. The beads were pulled down using a DynaMag™-2 (Invitrogen) magnetic tube rack and the equilibrating buffer was removed. The cleared cell lysates were added to the beads and incubated for 1 hour at 4°C with end-over-end mixing. After protein binding, the magnetic beads were pulled down, the remaining lysate was removed, saving 25 µL for immunoblotting, and the beads were washed four times by resuspending them in 500 µL lysis buffer, followed by pulling them down. After washing, the beads were resuspended in 60 µL elution buffer (25 mM Tris-HCl pH 8, 1% SDS) and incubated at 90°C for 10 minutes with 1500 rpm shaking. Afterwards, the beads were spun down at 20000 *g* for 1 minute at 4°C, followed by pulling them down with the magnet. The supernatant was taken, 10 µL eluate were used for immunoblotting to confirm success of the pull-down, and the remaining 50 µL were sent for mass spectrometry.

Mass spectrometry of whole-cell proteomes

Yeast strains were inoculated in 1 mL SC-complete medium and allowed to grow to saturation overnight. The next day, the cultures were diluted 3000-fold in 100 mL SC-complete medium and grown for approximately 15 hours, or until the OD600 of the culture reached approximately 1. 50 mL of this culture was spun down at 1000 *g* for 3 minutes. The supernatant was discarded; the cell pellet was resuspended in 500 µL water and transferred

to a 2 mL microcentrifuge tube. The supernatant was removed, and the cell pellet was frozen at -80°C until further use. The remaining 50 mL cell suspension was spun down at 1000 *g* for 3 minutes. The supernatant was discarded, and the cell pellet was washed with 50 mL sterile water. The cells were spun down once more at 1000 *g* for 3 minutes and the water was discarded. The cells were resuspended in 50 mL SC-complete medium with 2% ethanol as the carbon source. These cultures were allowed to grow for 24 hours, and 50 ODs cells were harvested in the same way as the previous culture. The cell pellets were frozen until further use.

For cell lysis, 300 µL lysis buffer (25 mM Tris-HCl pH 8, 150 mM sodium chloride (Sigma-Aldrich), 1 mM EDTA, 0.5% (w/v) sodium deoxycholate (Sigma-Aldrich), 1% (v/v) Triton X-100 (Sigma-Aldrich), 0.1% (w/v) SDS, protease inhibitors (4693159001, Sigma-Aldrich)) were added to the cell pellet, followed by approximately 200 µL acid-washed glass beads (G8772, Sigma-Aldrich). The cells were disrupted by vortexing at maximum speed for 30 seconds, followed by 30 seconds pause at 4°C. This process was carried out eight times in total. The lysates were clarified by centrifugation at 21100 *g* for 10 minutes at 4°C. The supernatant was collected, and the concentration was normalized to a concentration of 1 µg/µL before submitting to mass spectrometry.

Mass spectrometric analysis was performed by the proteomics core facility at IMB Mainz as described in Kong et al. 2025. Protein samples were separated on a 4-12% NOVEX NuPAGE gradient SDS gel (Thermo Fisher Scientific) for 10 min at 180 V in 1X MES buffer (Thermo Fisher Scientific). Proteins were fixed and stained with Coomassie G250 brilliant blue (Carl Roth). The gel lanes were cut, and each lane was cut into 1×1 mm pieces. Proteins were reduced in 10 mM DTT (Sigma-Aldrich) for 1 h at 56°C and then alkylated with 50 mM iodoacetamide (Sigma-Aldrich) for 45 min at room temperature. Proteins were digested with mass spectrometry grade trypsin (Serva) overnight at 37°C. Peptides were extracted from the gel by two incubations with 30% ABC/acetonitrile and three subsequent incubations with pure acetonitrile. The acetonitrile was finally evaporated in a concentrator (Eppendorf) and samples were loaded on StageTips (Rappsilber et al. 2003) for desalting and storage. For mass spectrometric analysis on the Q Exactive platform, peptides were separated on a 50 cm self-packed column with a 75 µm inner diameter filled with ReproSil-Pur 120 C18-AQ (Dr. Maisch GmbH) mounted to an EASY HPLC 1000 (Thermo Fisher Scientific) and sprayed online into a Q Exactive Plus mass spectrometer (Thermo Fisher Scientific). A 94 min gradient from 2% to 40% acetonitrile in 0.1% formic acid at a flow of 225 nL/min was used. The mass spectrometer was operated with a top 10 MS/MS data-dependent acquisition scheme per MS full scan.

For mass spectrometric analysis on the Exploris platform, peptides were separated on a 20 cm self-packed column with a 75 µm inner diameter filled with ReproSil-Pur 120 C18-AQ (Dr. Maisch GmbH) mounted to an EASY HPLC 1200 (Thermo Fisher Scientific) and sprayed online into an Exploris 480 mass spectrometer (Thermo Fisher Scientific). A gradient from 2% to 40% acetonitrile in 0.1% formic acid at a flow of 225 nL/min with a duration of 75 min (immunoprecipitation samples) and 105 min (whole cell proteomes) was used. The mass spectrometer was operated with a top 15 (immunoprecipitation samples) and top 20 (whole cell proteomes) MS/MS data-dependent acquisition scheme per MS full scan.

Mass spectrometry raw data were searched using the Andromeda search (Cox et al. 2011) integrated into MaxQuant suite 1.6.5.0 and 1.6.10.43 (Cox and Mann 2008) using the UniProt *Saccharomyces cerevisiae* database (6649 entries). In all analyses, carbamidomethylation at cysteine was set as fixed modification while methionine oxidation and protein N-acetylation were considered as variable modifications. Match between run option was activated. Reverse hits, proteins only identified by site, protein groups based on one unique peptide, and known contaminants were removed. The LFQ (label-free quantitation) values were $\log_2$-transformed and the median across replicates was calculated. This enrichment was plotted against -$\log_{10}$-transformed p-values (Welch t-test).

Mass spectrometry to identify *in vivo* N-terminal acetylation

Mass spectrometric analysis was performed by the proteomics core facility at IMB Mainz.

In vitro protein acetylation and enzymatic digestion

tFT-tagged immunoprecipitates eluted from the beads were reduced with DTT, followed by alkylation by iodoacetamide, quenching by DTT, and purification using the SP3 approach (Hughes et al. 2019). Thereafter, the purified proteins were eluted twice in 50 µL of 3 M guanidinium chloride, 250 mM MOPS pH 7.9, at 37°C with orbital shaking for 10 min. *In vitro* protein acetylation reaction was then initiated by adding D6-acetic anhydride (175641, Sigma-Aldrich) to 50 mM followed by incubation at 37°C with orbital shaking for 30 min. The reaction was repeated once. Afterwards, unreacted D6-acetic anhydride was quenched by adding ammonium bicarbonate buffer. This step also diluted the concentration of guanidinium chloride to 1 M. Following incubation at 37°C with orbital shaking for 10 min, proteins were digested by trypsin (2 µg per sample) at 37°C overnight. The resultant peptide solution was acidified with formic acid and purified by solid phase extraction in C18 StageTips (AttractSPE Bio - C18, Affinisep) (Rappsilber et al. 2003).

Liquid chromatography tandem mass spectrometry

Peptides were separated via an in-house packed 45 cm analytical column (inner diameter 75 µm; ReproSil-Pur 120 C18-AQ 1.9-µm silica particles, Dr. Maisch GmbH) on a Vanquish Neo UHPLC system (Thermo Fisher Scientific). The online reversed-phase chromatography separation was conducted through a 70 min non-linear gradient of 1.6-32% acetonitrile in 0.1% formic acid at a nanoflow rate of 300 nL/min. The eluted peptides were sprayed directly by electrospray ionization into an Orbitrap Astral mass spectrometer (Thermo Fisher Scientific). Mass spectrometry was conducted in data-dependent acquisition mode using a top50 method with one full scan in the Orbitrap analyzer (scan range 325 to 1300 m/z, resolution 120000, target value 3×10^6, maximum injection time 25 ms) followed by 50 fragment scans in the Astral analyzer via higher energy collision dissociation (HCD; normalized collision energy 26%, scan range 150 to 2000 m/z, target value 1×10^4, maximum injection time 10 ms, isolation window 1.4 m/z). Precursor ions of unassigned, +1 or higher than +6 charge state were rejected. Additionally, precursor ions already isolated for fragmentation were dynamically excluded for 15 s.

Mass spectrometry data processing

Mass spectrometry raw data files were processed using MaxQuant software (version 2.1.3.0) (Cox and Mann 2008). MS/MS mass spectra were searched using Andromeda search engine (Cox et al. 2011) against a target-decoy database containing the forward and reverse protein sequences of UniProt *Saccharomyces cerevisiae* reference proteome (6089 entries, release 2022_03), the N-terminal variants of the Gpm3 protein and a default list of common contaminants. Trypsin/P specificity was chosen. A maximum of 2 missed cleavages was tolerated. Cysteine carbamidomethylation was set as fixed modification. Methionine oxidation, protein N-terminal acetylation, D3-acetylation at lysine, serine, threonine and tyrosine residues as well as the protein N-terminus were assigned as variable modifications. Up to 6 modifications per peptide were allowed. The minimum peptide length was set to 7 amino acids. The "second peptides" option was switched on. The "match between runs" function was turned off. False discovery rate (FDR) was set to 1% at both peptide and protein levels. To compare the levels with or without *in vivo* acetylation at the N-terminus of the reporter protein, all detected N-terminal peptide sequences of the reporter protein were extracted from the MaxQuant output modificationSpecificPeptides.txt file. Among these peptide sequences, the ones that contained an N-terminal wild type acetylation modification were considered as *in vivo* Nt-acetylation. The remaining ones that were detected with N-terminal D3-acetylation or no acetylation at the N-terminus were considered as without *in vivo* Nt-acetylation. The intensities of these peptides were then summed separately for the ones with or without *in vivo* Nt-acetylation.

Fluorescence measurement of tFT-tagged strains

Fluorescence measurements of tFT-tagged strains were carried out as described before (Kong et al. 2023). Yeast strains were arranged in a 1536-colony format with four biological replicates per strain to be tested. Each biological replicate was spotted in four technical replicates, with additionally 8 technical replicates of a non-fluorescent background strain and 4 technical replicates of a reference strain expressing a stable tFT construct. These arrays were grown for 24 hours at 30°C on SC-complete medium or, if necessary, SC-dropout medium for maintenance of plasmids, supplemented with 200 mg/L adenine to reduce yeast autofluorescence.

Fluorescence measurements were carried out in a microplate reader (Spark, Tecan), equipped with a monochromator and a custom-fitted temperature control chamber. Fluorescence intensities were measured as follows: mCherry was measured with an excitation wavelength of 586 nm with an excitation bandwidth of 10 nm, and an emission wavelength of 612 nm with an emission bandwidth of 10 nm. sfGFP was measured with an excitation wavelength of 488 nm and an excitation bandwidth of 10 nm, and an emission wavelength of 510 nm with an emission bandwidth of 10 nm. The optimal gain was automatically determined. For each sample strain, the background fluorescence of the surrounding background was subtracted, followed by normalization to the reference strain to account for local fluorescence differences on the plate. Finally, the mCherry/sfGFP ratio was determined for each cluster of technical replicates using the normalized fluorescence values.

Structural modeling using AlphaFold

AlphaFold2 models were retrieved from the AlphaFold Protein Structure Database (Jumper et al. 2021; Varadi et al. 2024) (https://alphafold.ebi.ac.uk/). Multiple sequence alignments of Gid11 homologs were generated using Clustal Omega (Sievers and Higgins 2021; Madeira et al. 2024) and visualized using Jalview (Waterhouse et al. 2009).

For AlphaFold3 modeling (Abramson et al. 2024), the sequences of the proteins to be modelled were retrieved from the Saccharomyces Genome Database (Engel et al. 2025) (https://www.yeastgenome.org/). Models were either generated using the online AlphaFold3 server (Abramson et al. 2024) (https://alphafoldserver.com) or or an internal Nextflow-based pipeline (https://github.com/imbforge/fold2go) using the AlphaFold3 model weights released by Abramson et al. In general, models were run 20 times each, with the confidence of each model evaluated using the ipTM and pTM scores provided in the output. The model with the highest confidence was chosen. If two models received the same confidence score, the first model to be submitted was chosen arbitrarily.

Visualization of models was done using UCSF ChimeraX 1.8, developed by the Resource for Biocomputing, Visualization, and Informatics at the University of California, San Francisco, with support from National Institutes of Health R01-GM129325 and the Office of Cyber Infrastructure and Computational Biology, National Institute of Allergy and Infectious Diseases (Goddard et al. 2018; Pettersen et al. 2021; Meng et al. 2023).

Results

Some of the experiments presented in the following section have been published as a preprint on bioRxiv (Kong et al. 2025) and will be cited accordingly. Furthermore, certain experiments were conducted by XXXXXXXXX, XXXXXXXXXXXXXX, XXXXXXXXXXXXXX, or XXXXXXXXXXXXXX, and are included here to provide context for the results. Specifically, XXXXXXXXXXXXXX contributed experiments during a six-week International Summer School internship, and XXXXXXXXXXXXXX during their Bachelor's thesis project, both under my supervision. These contributions are credited where appropriate.

Characterization of the Gid11 substrate receptor

The role of Moh1 and Ipf1 in GID^{Gid11} activity

Moh1 and Ipf1 were both shown to interact with the GID complex before (Qiao et al. 2022). However, as of writing this thesis, their roles in the function of the GID complex are still unclear. There is, however, the possibility that they are involved in Gid11-dependent turnover of proteins. This possibility was explored in the following experiments.

To determine whether Moh1 and Ipf1 facilitate the turnover of potential GID substrates, crossing was performed in which strains containing tFT-tagged, previously identified proteins with GID-dependent turnover were crossed with query strains containing knockout mutations for either *MOH1*, *IPF1*, *GID9*, and *GID5*. After crossing, sporulation, and selection for daughter cells containing both the tFT-tagged substrate and the knockout, stability of the substrates was measured via the tFT timer (Figure 7).

Knockout of *IPF1* did not stabilize any of the substrates, however, it had a slight destabilizing effect on some substrates like Gpm3-tFT (Kong et al. 2025) or Ssd1-tFT. This is in line with previously published work on Ipf1 which showed Ipf1 to sterically inhibit Gid activity for the GID^{Gid4} complex (Qiao et al. 2022). It is possible that Ipf1 has a general inhibitory function on Gid activity.

Knockout of *MOH1* did not affect most of the substrates (Kong et al. 2025). Notably, it did stabilize Ssd1-tFT and Ymr086w-tFt. However, it did not stabilize any of the currently known Gid11 substrates. Based on this, it appears that Moh1 is not required for activity of the GID^{Gid11} complex. However, it does raise an interesting possibility in that it might act as a substrate receptor, or as a new, still unknown recruitment platform for another substrate receptor involved in the degradation of Ssd1 and/or Ymr086W. Interestingly, this substrate receptor would likely act in a Gid5 independent, but Gid7 dependent manner. Together with the previously shown knockout experiments, it could be postulated that one of these potential substrate receptor proteins is Mho1. However as of now, the function of Mho1 is largely unknown besides a role in the formation of pseudohyphae in yeast strains which are capable

Figure 7: Stability of potential GID substrates upon knockout of MOH1 and IPF1.
Query strains expressing tFT-tagged potential GID substrates were crossed with strains carrying MOH1 or IPF1 knockout alleles. After sporulation and selection steps, stability was determined using fluorescence measurements. Error bars indicate the standard deviation between biological replicates (n=3).

of forming such structures (Schlatter et al. 2012). Further elucidation of the role of Mho1 was deemed outside of the scope of this project and not further pursued. However, it might prove an interesting beginning point in the search for new substrate receptors in the future.

To further investigate whether overexpression of Moh1 affects GID dependent turnover, *MOH1* and *IPF1* were overexpressed from the *GPD* promoter off a pRS413-based plasmid in strains expressing tFT-tagged Mdh2, Phm8, Gpm3, or Yor283w (Figure 8A). Overexpression of *MOH1* did not affect the stability of any of the tested substrates while overexpression of *IPF1* led to a stabilization of all tested substrates (Kong et al. 2025). Additionally, overexpression of *MOH1* was carried out against the Gid7-dependent putative substrates Cpa1-tFT, Seg1-tFT, Ssd1-tFT, and Ubc8-tFT in wild type and *gid9Δ* background, giving the same result as the previous experiment (Figure 8B). This is consistent with the effects seen in the previous crossing, as well as the previously mentioned regulatory role of Ipf1 for the GID^{Gid4} complex (Qiao et al. 2022), further strengthening the idea that Ipf1 has a general inhibitory function on the GID complex.

Definition of the Gid11 degron

Based on previous work it seemed likely that Gid11 recognized N-terminal threonine residues (Kong et al. 2021). Beyond that, however, not much is clear about the precise nature of the degron recognized by Gid11. The following experiments aim to elucidate this further.

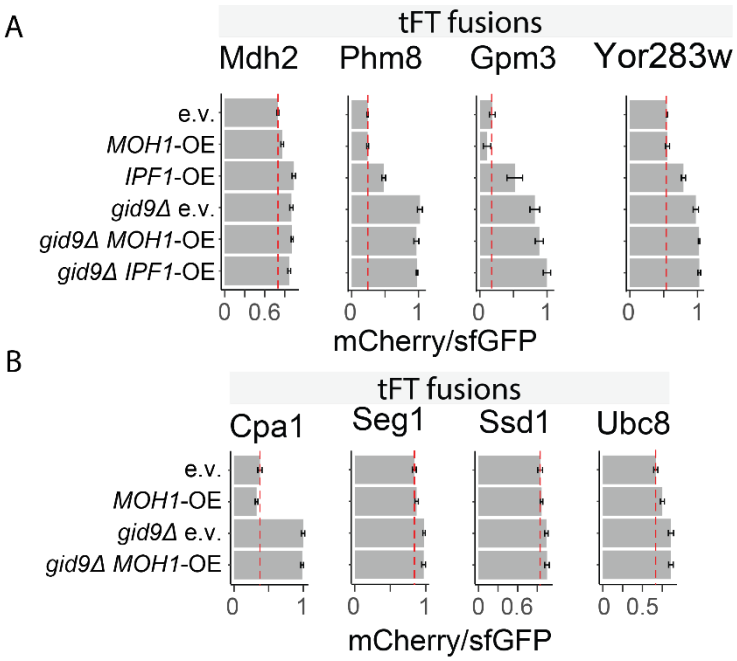

Figure 8: Overexpression experiments of MOH1 and IPF1
A: Stability, as determined by fluorescence, of tFT-tagged Mdh2, Phm8, Gpm3, and Yor283w upon overexpression of MOH1 or IPF1, both in wild type and gid9Δ background.
B: Stability, as determined by fluorescence, of tFT-tagged Cpa1, Seg1, Ssd1, and Ubc8 upon overexpression of MOH1, both in wild type and gid9Δ background.
A-B: Error bars indicate standard deviation between biological replicates (n=4). e.v.: Empty vector.

T2A mutants of Gpm3 and Yor283w

If the N-threonine degron is a bona fide degron, then replacement of this threonine should completely abolish recognition of the substrate by Gid11. To confirm this, using the delitto perfetto approach, strains were generated in which the N-terminal threonine of Gpm3-tFT or Yor283w-tFT has been replaced with an alanine (Storici and Resnick 2006). Compared to the experiments previously carried out by Kong et al., the mutation has been introduced endogenously, allowing for quantification of protein abundance after the mutation has been introduced. Gid11 has been shown to be induced upon transition to ethanol medium, and Gid11 substrates have been shown to accumulate in this condition upon *GID11* knockout. For this reason, the glucose to ethanol transition was also chosen for the following immunoblots. Immunoblots involving Gpm3 were carried out by XXXXXXXXXX. Immunoblotting after shifting the cells to ethanol showed the degradation of both substrates to be impaired upon replacement of the N-terminal threonine (Figure 9A) (Kong et al. 2025). Additionally, probing either against ubiquitin for Gpm3 or myc-tagged, overexpressed ubiquitin in the case of Yor283w showed their ubiquitination to be impaired as well when the N-terminal threonine was replaced (Figure 9B) (Kong et al. 2025). This confirms the importance of the N-terminal threonine for the Gid11-dependent turnover of these two substrates.

Replacement of non-hydrophobic third residue in Gid11 substrates

Notably, five of the ten currently known Gid11 substrates possess a bulky, hydrophobic residue (isoleucine or valine) in their third position (Figure 10A). The remaining five substrates either possess an alanine or a basic residue in their third position. Additionally, MPS profiling experiments carried out by XXXXXXXXXX (Kong et al. 2025) indicated that Gid11 prefers bulky,

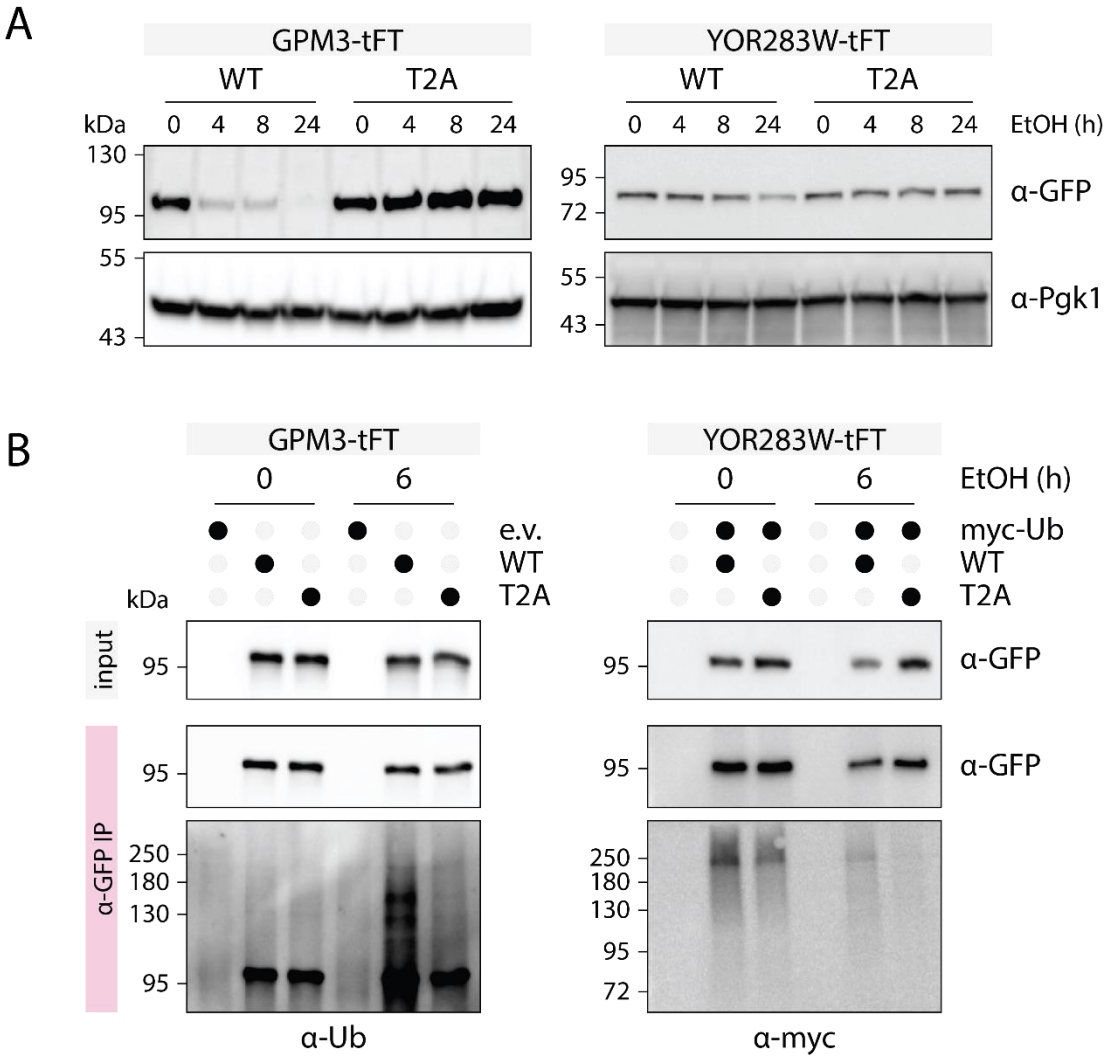

Figure 9: Mutation of N-terminal threonine impairs Gid11-dependent turnover.
A: Immunoblots showing changes in abundance of Gpm3 and Yor283w upon shift from glucose to ethanol medium, as well as the impact of T2A mutation.
B: Immunoblots showing the impact of T2A mutation on the ubiquitination of Gpm3 and Yor283w.
A-B: Blots involving Gpm3 were made by XXXXXXXXXXXXX.

hydrophobic residues in the third position. This raised the question of whether it is possible to improve turnover of apparently suboptimal substrates by replacing their third residue with bulky hydrophobic ones.

To test this, the third residue of Dbp3, Dld3, Lys20, Stf2, or Yor283w was replaced by valine by XXXXXXXXXXXXX. These tFT-tagged constructs were expressed from their endogenous promoter off a pRS313-based plasmid, or from the *GPD* promoter off a pRS413-based plasmid for Yor283w and their stability was determined via fluorescence measurements in colonies.

Replacement of the third residue with valine destabilized substrates in tFT measurements, with the notable exception of Yor283w (Figure 10B) (Kong et al. 2025). Here, the K3V mutant was stabilized compared to the wild type protein. However, all X3V mutants were still recognized by Gid11, as indicated by their stabilization upon knockout of *Gid11*. This reinforces the preference of Gid11 for bulky, hydrophobic residues in the third position of the substrate N-terminus.

A

protein	N-terminus
Acs2	MTIKEH
Dbp3	MTKEEI
Dld3	MTAAHP
Gpm3	MTVTDT
Lys20	MTAAKP
Pfk2	MTVTTP
Phm8	MTIAKD
Stf2	MTRTNK
Top1	MTIADA
Yor283w	MTKEVP

B

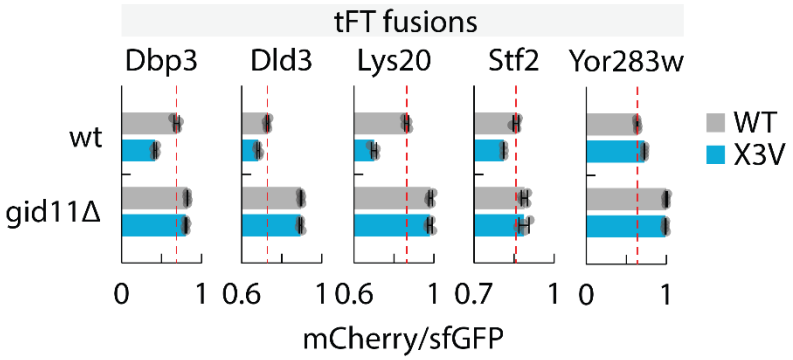

Figure 10: Impact of X3V mutations on Gid11 substrates without hydrophobic third residue.
A: N-terminal sequences of Gid11 substrates with confirmed N-threonine degrons. Highlighted are hydrophobic residues in the third position.
B: Stability, as determined by fluorescence, of tFT-tagged Dbp3, Dld3, Ly20, Stf2, and Yor283w upon replacement of their third residue with valine. Error bars indicate the standard deviation between biological replicates (n=4).

N-terminal processing of the Gid11 degron

Proteins beginning with MT are N-terminally processed. This processing involves the cleavage of the initiating methionine, followed by potential N-terminal acetylation carried out by NatA (Li and Chang 1995; Arnesen et al. 2009; Aksnes et al. 2019; Varshavsky 2024). Since these are also the N-termini recognized by Gid11, it is possible that the degrons recognized by Gid11 also undergo this processing. If they do, however, and if these processing steps are potentially even required for recognition by Gid11 was unknown at the time.

N-terminal processing by methionine aminopeptidases

As mentioned above, the first step of N-terminal processing in yeast is the cleavage of the initiating methionine, leaving the N-terminal threonine exposed. This process is carried out by Map1 and Map2 in yeast (Li and Chang 1995; Varshavsky 2024).

To analyze whether processing by Map1 or Map2 is required for recognition of N-termini by Gid11, an SGA was carried out in which *MAP1* or *MAP2* knockout strains were crossed with strains expression a variety of tFT-tagged GID dependent substrates. After the requisite selection steps, the mCherry/sfGFP ratio of those cells was measured. Here, it turned out that knockout of either *MAP1* or *MAP2* alone did not significantly affect the stability of any of the measured GID substrates (Figure 11). However, this was not entirely surprising, as Map1 and Map2 have partially redundant activity, meaning that knockout of one might possibly be compensated by the other and vice versa and double knockout of both genes is lethal to the cell (Li and Chang 1995). Nonetheless, this experiment did raise the possibility that N-terminal cleavage of the initiating methionine is not required. However, it also raised the possibility that the N-termini of Gid11 substrates are not substrates of Map1 or Map2 at all.

To further clarify and distinguish between these possibilities, a plasmid shuffle experiment was performed. In this plasmid shuffle experiment the endogenous yeast MetAPs were replaced with a variant of Map1 bearing a Q365A mutation and the MetAP from *Deinococcus radiodurans*, both of which were previously reported to have a vastly diminished affinity for MT- N-termini (Bonissone et al. 2013; Walker and Bradshaw 1999) (Figure 12A). Thus, we expected the introduction of these two variants to stabilize Gid11 substrates if the cleavage of the initiating methionine is required for substrate recognition. The desired *MAP1* variants

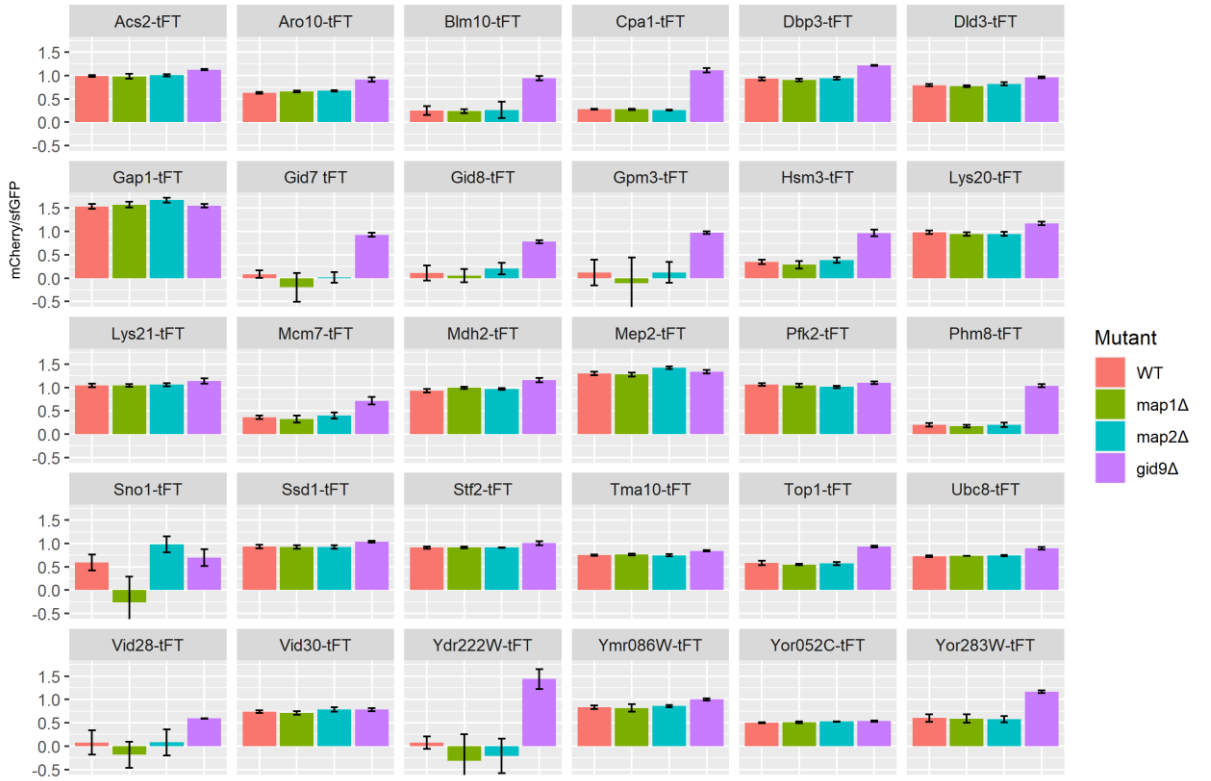

Figure 11: Stability of potential GID substrates upon knockout of MAP1 and MAP2.
Query strains expressing tFT-tagged potential GID substrates were crossed with strains carrying MAP1 or MAP2 knockout alleles. After sporulation and selection steps, stability was determined using fluorescence measurements. Error bars indicate the standard deviation between biological replicates (n=3).

were introduced on a pRS315-based plasmid into *map1Δmap2Δ* strains expressing the tFT-tagged Mdh2, Phm8, Gpm3, or Yor283w. The stability of these proteins was then measured using fluorescence measurements in colonies. This measurement revealed that none of the MetAP variants had any significant impact on the stability of any of the measured substrates (Figure 12B). One possible interpretation of this result is that cleavage of the methionine is indeed not necessary for recognition of Gid11 dependent degrons. However, it is also possible that the diminished activity of the Map1 variants used in this experiment is sufficient to cleave the initiating methionine from N-degrons recognized by Gid11. In this case, no stabilization would be observed either.

In an orthogonal experiment, XXXXXXXXX capped three Gid11 dependent substrates, Phm8, Gpm3, and Yor283w with an N-terminal ubiquitin (Kong et al. 2025). This ubiquitin is N-terminally cleaved off, leaving the desired N-terminus (Varshavsky 2005), in this case one either with or without the initiating methionine. In this experiment, inclusion or exclusion of the initiating methionine did not show any effect on the turnover of Gid11 dependent substrates, showing that the initiating methionine is not part of the Gid11 degron (Figure 12C).

N-terminal acetylation of the Gid11 degron

After cleavage of the initiating methionine, the N-terminus of Gid11 substrates can further be processed. In the case of N-terminal threonines, this is mostly done by NatA (Polevoda and Sherman 2001; Arnesen et al. 2009; Aksnes et al. 2019). However, it was still unclear whether N-terminal acetylation was required, possible, or counterproductive to recognition of N-terminal degrons by Gid11. For this purpose, XXXXXXXXXXXXXX attempted to knock out

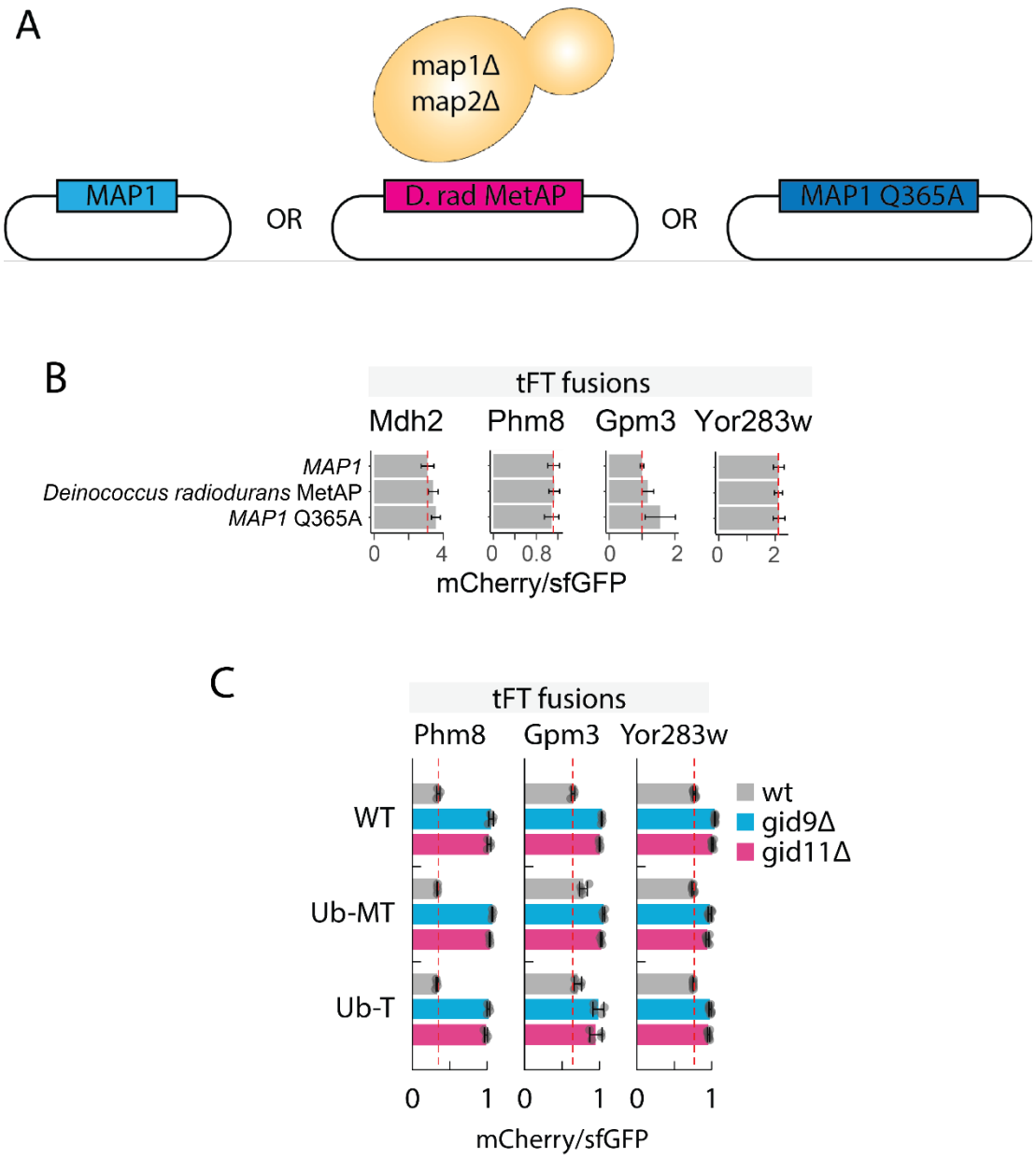

Figure 12: N-terminal processing of GID substrates by methionine aminopeptidases.
A: Schematic representation of the final strains obtained by plasmid shuffle. D.rad: Deinococcus radiodurans
B: Stability, as determined by fluorescence measurements, of GID dependent substrates upon complementation of MAP1 MAP2 double knockout with MAP1 variants.
C: Stability, as determined by fluorescence measurements, of Gid11 dependent substrates upon generation of N-termini with or without the initiating methionine using the ubiquitin fusion technique. Experiment carried out by XXXXXXXXXXXXX.
B-C: Error bars indicate the standard deviation between biological replicates (n=4).

NAA10. However, these cells showed a strong growth defect. Fluorescence measurement of Gid11 substrates in these cells showed stabilization of proteins with Gid11 dependent turnover. However, immunoblotting of HA-Gid11 upon switching growth medium to SC-ethanol showed that knockout of *NAA10* led to strong expression of HA-Gid11 even prior to the switch from glucose to ethanol medium (Figure 13A). This led us to believe that knockout of any NatA components leads to a general dysregulation of Gid11, rather than affecting recognition of its substrates directly, in line with the currently known phenotypes caused by *NAA10* knockout (Whiteway and Szostak 1985; Polevoda et al. 1999; Gautschi et al. 2003; Deutschbauer et al. 2005; Kats et al. 2022).

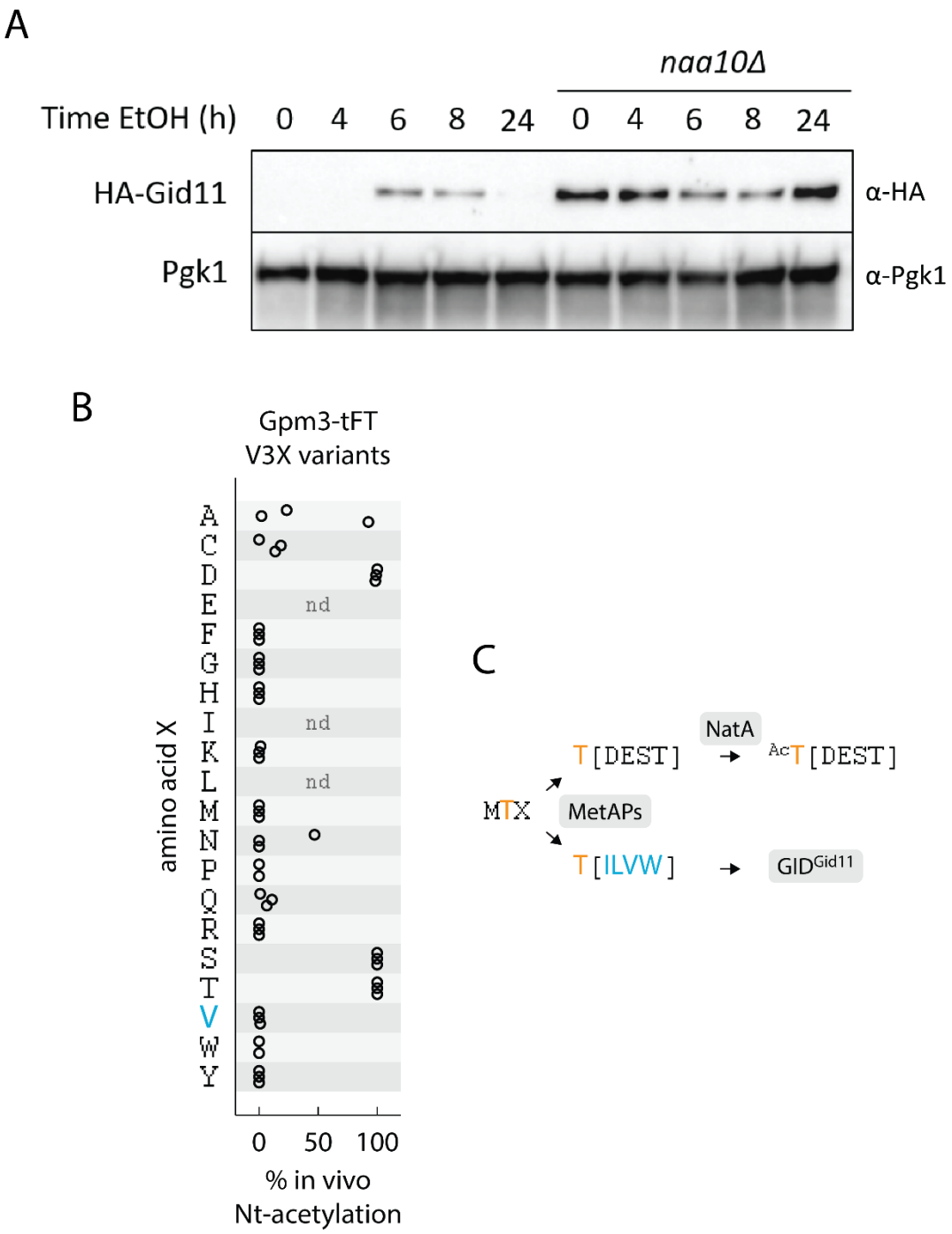

Figure 13: Involvement of NatA in Gid11-dependent turnover
A: Immunoblot probing against HA-tagged Gid11 in wild type or naa10Δ mutants upon shift from glucose to ethanol medium.
B: In vivo acetylation percentages of immunoprecipitated Gpm3-tFT V3X variants, as determined by mass spectrometry. Experiment carried out in collaboration with XXXXXXXXXXXXX and the IMB Proteomics Core Facility.
C: Model of N-terminal processing of MTX-N-termini.

To approach the question of N-terminal acetylation of Gid11 substrates from a different angle, we measured acetylation levels of Gpm3-tFT upon introduction of different residues in the third position of the N-terminus. For this reason, XXXXXXXXXXXXX and I immunoprecipitated Gpm3-tFT V3X variants and submitted them to mass spectrometry to identify the extent to which these constructs are N-terminally acetylated. After *in vitro* acetylation with deuterated acetic anhydride, the proteins were analyzed by mass spectrometry (Figure 13B). This showed

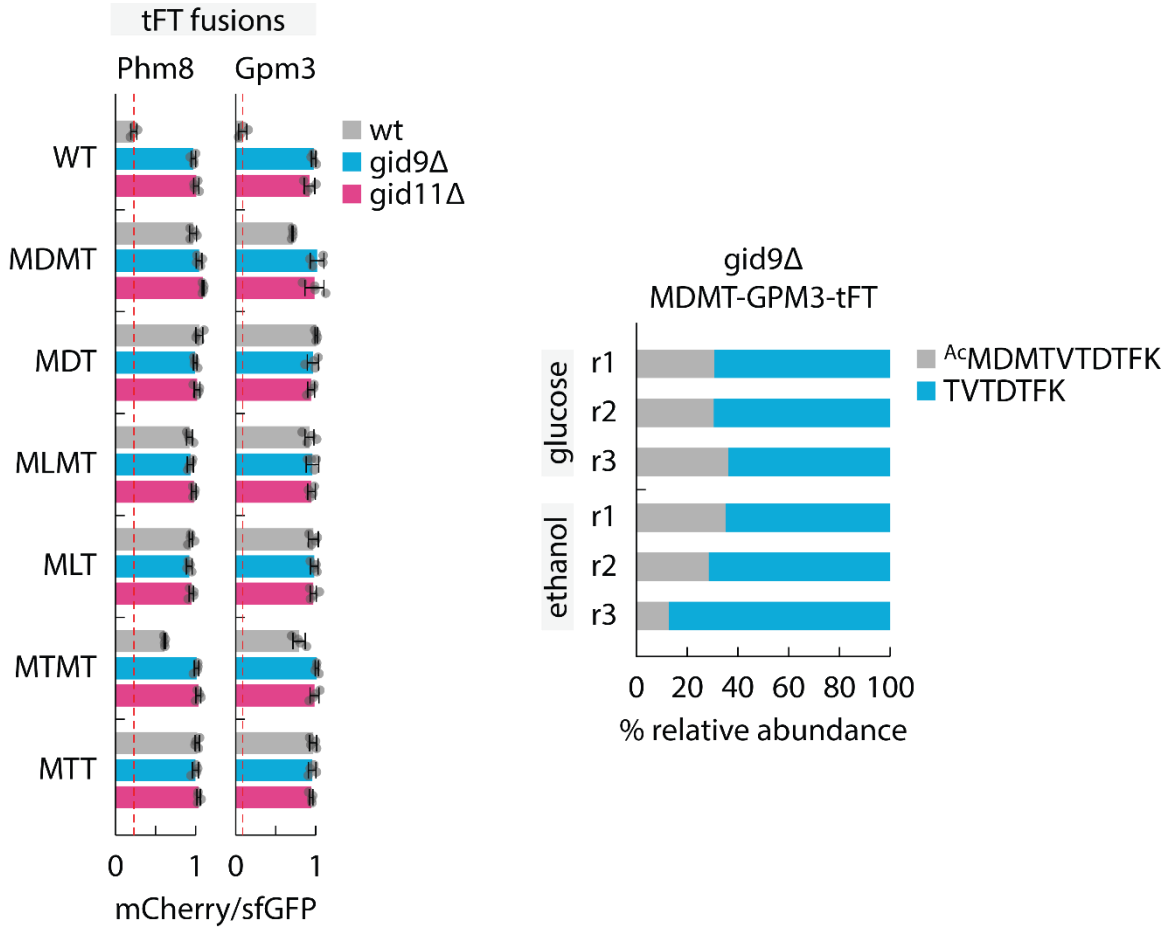

Figure 14: Impact of N-terminal capping on Gid11-dependent turnover.
A: Stability, as determined by fluorescence measurements, of tFT-tagged Phm8 or Gpm3 upon N-terminal capping. Error bars indicate the standard deviation between biological replicates (n=4).
B: Immunoprecipitation followed by mass spectrometry shows MDMT-Gpm3-tFT strains to contain a large population of wild type Gpm3-tFT. r: biological replicate number.

that N-termini containing either hydrophobic or basic residues in the third position were generally not acetylated *in vivo*. In contrast to that, an acidic or polar residue in the third position of the N-terminus appeared to promote N-terminal acetylation of Gpm3 (Kong et al. 2025). Considering that all currently known Gid11 substrates either contain a hydrophobic or basic residue in the third position, it appears that Gid11 substrates specifically avoid N-terminal acetylation due to their sequence context (Figure 13C). This is consistent with data by the Arnesen lab, who found a similar pattern in the context of the Arg/N-degron pathway involving cysteine oxidation by ADO1 in human cells (Heathcote et al. 2024).

N-terminal capping of Gid11 substrates

To determine if degrons recognized by Gid11 are required to be at the extreme N-terminus, the N-terminus of two Gid11 dependent substrates, Phm8 and Gpm3, was capped with a methionine, followed by threonine (MT), aspartate (MD), or leucine (ML). Furthermore, the original initiation methionine was either included or excluded in the capping. These residues for capping were chosen, as the MT-terminus mimics the original N-terminus of Phm8 and Gpm3 and thus, can potentially undergo cleavage of the initiating methionine, followed by N-terminal acetylation by NatA. In contrast, the MD- and ML- N-termini typically do not undergo cleavage of the initiating methionine. However, they are substrates of NatB and NatC,

respectively (Polevoda and Sherman 2001; van Damme et al. 2012; Aksnes et al. 2019). If degrons recognized by Gid11 are indeed at the extreme N-terminus, this should lead to stabilization of these substrates and abolishment of the Gid11 dependence of their turnover.

In general, capping of both Phm8 and Gpm3 largely abolished their degradation (Figure 14A)(Kong et al. 2025). Furthermore, the capped variants were not further stabilized by knockout of either *GID9* or *GID11*, indicating that they are not recognized by Gid11 anymore. Notably, there were three exceptions to this: Both MTMT-Gpm3-tFT and MTMT-Phm8-tFT were turned over in a Gid11-dependent manner, albeit less efficiently. The same appeared to be true for MDMT-Gpm3. For the MTMT variants of Phm8 and Gpm3 we recognized that the second methionine of the MTM-N-terminus might be hydrophobic enough to allow recognition by Gid11, explaining their slight turnover by Gid11. However, this could not explain the turnover of MDMT-Gpm3. To further investigate possible reasons for its turnover, MDMT-Gpm3-tFT was immunoprecipitated using anti-GFP antibodies. The immunoprecipitated MDMT-Gpm3-tFT was submitted for mass-spectrometry to investigate the precise N-termini of this construct present in the cell. Analysis of the N-terminus of submitted MDMT-Gpm3 revealed a subpopulation of wild type Gpm3 (Figure 14B) (Kong et al. 2025). As this would be turned over as normal, and since the tFT timer does not distinguish between the wild type and capped variants, this explains the apparent phenotype.

Structural basis for Gid11 activity

Role of Gid11 IDRs in activity

Overall, Gid11 possesses five IDRs (Figure 15A, B) (Kong et al. 2025), with the largest spanning approximately 150 amino acids. It was hypothesized that these IDRs render purification efforts of Gid11 difficult, leading to aggregation and precipitation of the protein. Thus, the question was raised whether it is possible to remove these IDRs, and if the resulting protein would still be functional. For this purpose, five variants of Gid11 were generated by XXXXXXXXXXXXX, referred to as IDR1Δ to IDR5Δ, respectively. Notably, deletion of any of the IDRs, apart from the IDR3Δ did not appear to affect turnover of Phm8-tFT or Cpa1-tFT (Figure 15C) (Kong et al. 2025). Even more strikingly, a variant of Gid11 lacking all IDRs expect for the third one, was still functional, albeit at a slightly lower level than the wild type variant (Figure 15C) (Kong et al. 2025).

To show that the IDR deletion variants can bind to the GID complex, and to rule out misfolding of the nonfunctional IDR3Δ variant by extension, the ability of all variants to stabilize Hsm3 was tested. This is based on the same assumptions as the overexpression assay described above. Notably, the ability of the tested variants to stabilize Hsm3 did not appear to correlate with the ability to turn over Phm8. In particular, the IDR5Δ variant and the variant lacking four IDRs stabilized Hsm3-tFT only to a very slight extent, same as the IDR3Δ variant (Figure 15D) (Kong et al. 2025).

To test if the difference in activity of the IDR deletion variants correlates with their abundance in the cell, immunoblotting was performed, six hours after shifting cells expressing the variants to medium containing ethanol as the primary carbon source. However, the signal detected in the immunoblots did not appear to correlate with the activity levels seen in the fluorescence

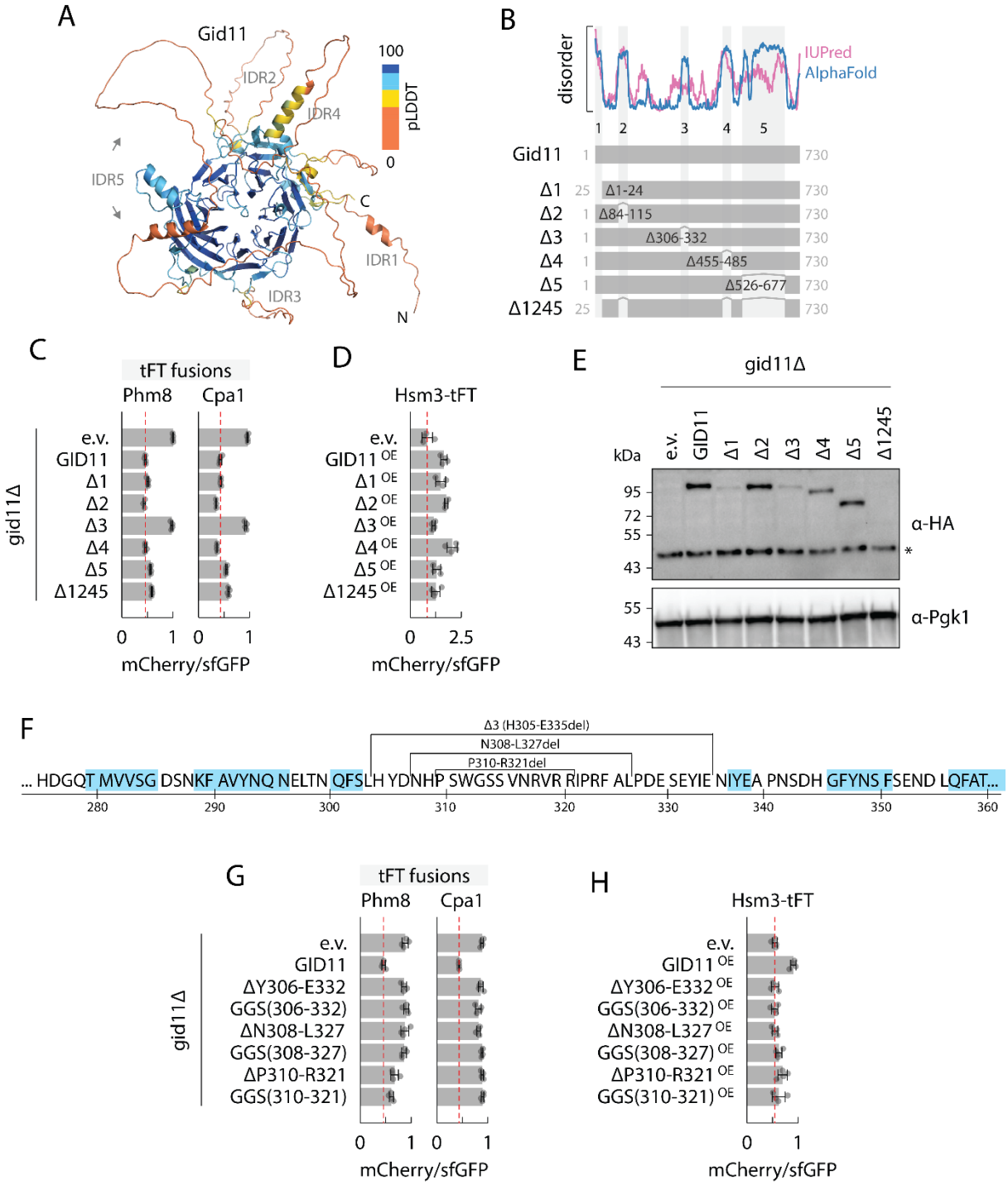

Figure 15: Investigation of the impact of deletion of IDRs on Gid11 activity.
A: AlphaFold3 (Abramson et al. 2024) model of Gid11, with IDRs highlighted. Colored by pLDDT score.
B: Cartoon showing which regions of Gid11 were deleted, based on AlphaFold3 (Abramson et al. 2024) and IUPred (Erdős et al. 2021) predictions.
C: Stability, as determined by fluorescence measurements, of tFT-tagged Phm8 and Cpa1 upon deletion of Gid11 IDRs.
D: Stability, as determined by fluorescence measurements, of tFT-tagged of Hsm3 upon overexpression of Gid11 IDR deletion variants.
*E: Immunoblot to determine abundance of Gid11 IDR deletion variants upon 6 hour shift to ethanol medium. *: Unspecific band*
F: Sequence of Gid11 IDR 3 and surrounding areas. Areas predicted to form ß-sheets by AlphaFold3 (Abramson et al. 2024) are highlighted in blue. Regions deleted in G and H are highlighted.
G: Stability, as determined by fluorescence measurements, of tFT-tagged Phm8 and Cpa1 upon deletion of certain sections of IDR3 or replacement with a GGS linker.
H: Stability, as determined by fluorescence measurements, of tFT-tagged Hsm3 upon overexpression of various IDR3 variants.

measurements (Figure 15E) (Kong et al. 2025). Strikingly, the variant containing only the third

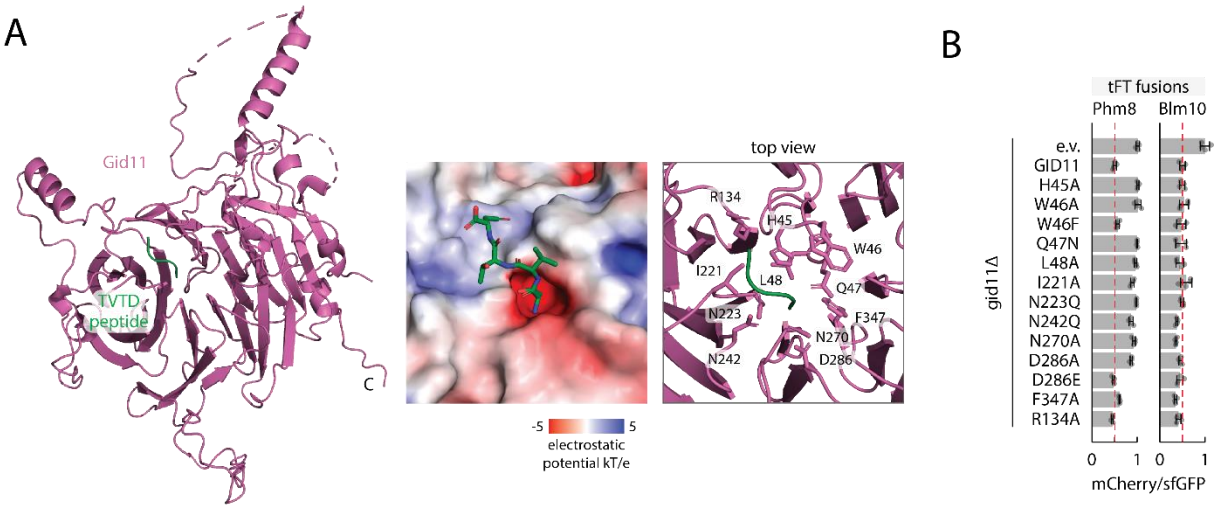

Figure 16: Defining the binding pocket of Gid11.
A: AlphaFold3 (Abramson et al. 2024) prediction of Gid11 structure together with the TVTD peptide representing the Gpm3 N-terminus. Middle image shows surface charges of the predicted binding interface, and the right image highlights predicted amino acid contacts (<4 angstroms).
B: Stability, as determined by fluorescence measurements, of tFT-tagged Phm8 and Blm10 upon mutation of Gid11 residues previously predicted by AlphaFold3 (Abramson et al. 2024) to form contacts with degron N-termini. Error bars indicate the standard deviation between biological replicates (n=4)

IDR could not be detected in the immunoblot, presumably due to low abundance, yet it is seen as functional in the fluorescence measurements.

As the third IDR is located between two parts of a ß-strand, we suspected that its deletion might lead to misfolding of Gid11. Thus, to provide a flexible linker without any possible critical residues, we generated a mutant in which the third IDR was replaced with a GGS linker of equal length. However, this mutant was also non-functional in fluorescence measurements (Figure 15G) (Kong et al. 2025).

Strikingly, when performing multiple sequence alignments of Gid11, the third IDR is only conserved in Gid11 homologs previously identified to be able to complement knockout of GID11 against Phm8-tFT. Based on these alignments, shorter truncations of the third IDR were performed (Figure 15F). Interestingly, deletion of the region spanning asparagine 308 to leucine 327 still yielded a non-functional protein (Figure 15G). However, deletion of proline 310 to arginine 321 yielded a functional protein and was able to slightly stabilize Hsm3 upon overexpression (Figure 15H). This narrows down the residues responsible for activity against Phm8 to be either in the region spanning residues 308-309 or residues 322-327.

Prediction of residues critical for Gid11 activity using AlphaFold3

As Gid11 currently cannot be purified, that rules out techniques such as crystallography, Cryo-ER, or NMR to resolve its structure. However, due to advances in protein structure modelling with AlphaFold2 (Jumper et al. 2021) and more recently AlphaFold3 (Abramson et al. 2024), we decided to use these tools to model binding of threonine N-degrons to Gid11 (Figure 16A). This revealed a negatively charged pocket on the surface of Gid11. Furthermore, AlphaFold3 predicts the negatively charged α-amino group of the N-terminal threonine to be coordinated with this pocket. Consistent with this, when carrying out the modeling with N-terminally acetylated peptides, the confidence of the model is consistently lower, and the position of the acetylated peptide is slightly changed, even though AlphaFold3 still places the acetylated

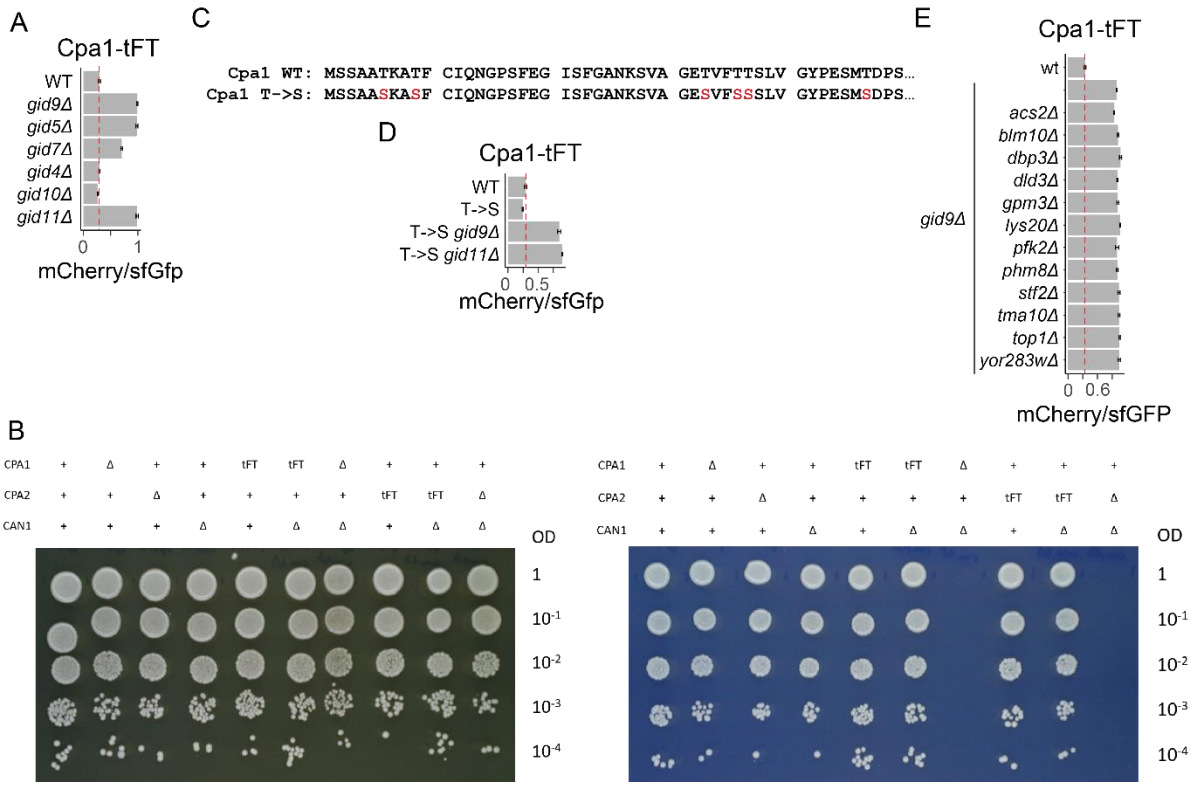

Figure 17: Investigating Gid11-dependent degradation of Cpa1.
A: Stability, as determined by fluorescence measurements, of tFT-tagged Cpa1 upon knockout of various GID components.
B: Spotting assay to confirm synthetic lethality of knockout of CPA1 or CPA2 together with CAN1, as well as functionality of tFT-tagged Cpa1 and Cpa2. Left: YPD, right: SC-complete.
C: N-terminus of Cpa1, highlighting the amino acid residues mutated in the T->S mutant.
D: Stability, as determined by fluorescence measurements, of tFT-tagged Cpa1 upon mutation of threonine residues in its N-terminus.
E: Stability, as determined by fluorescence measurements, of tFT-tagged Cpa1 upon knockout of currently known Gid11 substrates in a gid9Δ background.
A,D,E: Error bars indicate standard deviation between biological replicates (n=4)

peptides roughly in the same pocket. Searching for contacts between the N-terminal degron and residues within Gid11 showed histidine 45, tryptophane 46, glutamine 47, leucine 48, isoleucine 221, glutamines 223, 242, and 270, glutamate 286, and phenylalanine 347 as potential interacting residues. Mutation of these residues, carried out by XXXXXXXXXXXXX, confirmed all of these residues with the exception of phenylalanine 347 to be involved in the recognition and subsequent degradation of Phm8 (Figure 16B) (Kong et al. 2025).

Non-canonical putative Gid11 substrates

Among the previously identified potential Gid11 dependent substrates, Cpa1 and Blm10 are special in that Cpa1 does not bear a N-terminal threonine and the N-terminal threonine of Blm10 has been shown to not be required for its Gid11 dependent turnover (Kong et al. 2021). Nonetheless, knockout of *GID11* leads to a marked stabilization of these proteins, shown both in previous proteomic experiments, and in the tFT fluorescence assay (Kong et al. 2025). Strikingly, Cpa1 is also currently the only protein known whose turnover depends both on Gid11 and Gid7 (Figure 17A).

Performing knockout experiments with Cpa1 and its complex partner Cpa2 (Thoden et al. 1999) showed to our surprise that the resulting strains were unable to grow on SC-complete medium. However, the strains expressing tFT-tagged substrates usually used in our

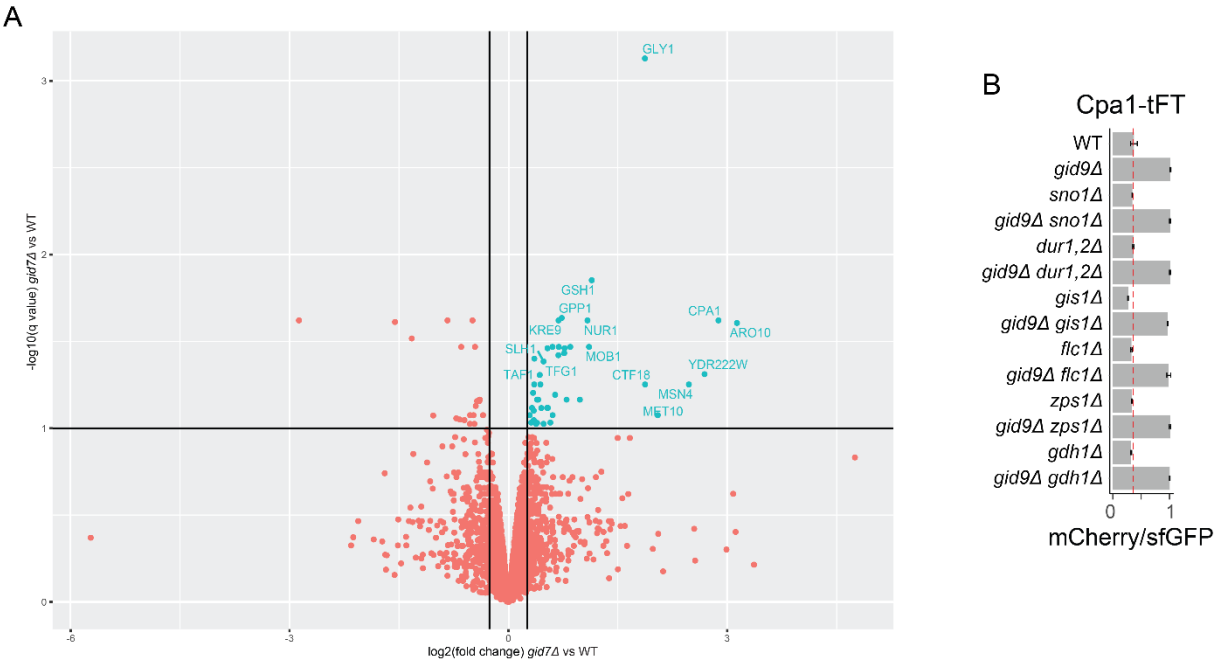

Figure 18: Search for further proteins with Gid11 and Gid7 dependent turnover.
A: Whole proteome mass spectrometry data of gid7Δ or WT cells upon shift to ethanol medium for 24 hours. An abundance change of 20% and a q-value of 0.1 were chosen as cut-offs.
B: Stability, as determined by fluorescence measurements, of tFT-tagged Cpa1 upon knockout of proteins identified to have Gid11 and Gid7-dependent turnover upon cross-referencing the data with A with data obtained by XXXXXXXXXXXXX in gid11Δ cells. Error bars indicate the standard deviation between biological replicates (n=4).

experiments are derived from yMaM330, a strain which contains a variety of markers required for crossing experiments. Among these, a *CAN1* knockout in this strain stood out, as Can1 is responsible for arginine uptake (Broach et al. 1979). As the complex of Cpa1 and Cpa2 is involved in the synthesis of arginine (Price et al. 1978; Thoden et al. 1999), we hypothesized that the double knockout of *CPA1* or *CPA2* together with knockout of *CAN1* impairs the arginine metabolism in yeast to a point where growth on a chemically defined medium would not be possible anymore. To test this, a spotting assay was performed, in which single knockout as well as double knockouts of *CPA1* or *CPA2* and *CAN1* were grown on YPD as well as SC-complete medium (Figure 17B). Assuming our hypothesis about the synthetic lethality of these genes was true, we also saw this as an opportunity to show that Cpa1-tFT and Cpa2-tFT were functional. For this reason, *CPA1* and *CPA2* were tFT-tagged in a BY4741 *can1Δ* strain and spotted as well (Figure 17B). All tested strains grew unimpaired on YPD medium. On SC-complete medium, however, the *cpa1Δcan1Δ* and *cpa2Δcan1Δ* strains were unable to grow at all, showing that double knockout of either *CPA1* or *CPA2* together with *CAN1* is indeed synthetically lethal on SC-medium. Notably, the strains in which either Cpa1 or Cpa2 is tFT-tagged grew unimpaired in a *can1Δ* background, demonstrating that Cpa1-tFT and Cpa2-tFT are functional.

To understand whether one of the threonine residues within the N-terminus of Cpa1 is required for its Gid11 dependent turnover, for example after being exposed by proteolytic cleavage, a variant of Cpa1 was created in which all threonine residues within the first 50 amino acids of Cpa1 were replaced with serine (Figure 17C). However, this replacement did not significantly affect stability of Cpa1, and possibly even slightly destabilized it (Figure 17D).

Furthermore, the turnover of this Cpa1 variant was still dependent on both Gid9 and Gid11, indicating that its recognition by the GID complex had not been affected.

Next, to rule out that stabilization of Cpa1 upon knockout of *GID11* is an indirect effect caused by the stabilization of another Gid11 dependent substrate, an experiment was carried out in which the stability of Cpa1-tFt was measured in a *gid9Δ* background, with additional knockout of the currently known Gid11 dependent substrates. The logic behind this experiment was that if stabilization of a Gid11 dependent substrate leads to stabilization of Cpa1, then its knockout should reverse the phenotype caused by knockout of *GID9*. However, additional knockout of any of the currently known potential Gid11 substrates on top of knockout of *GID9* did not destabilize Cpa1, ruling out that at least stabilization of these proteins leads to a decrease in Cpa1 turnover (Figure 17E).

As mentioned before, Cpa1 is currently the only known potential Gid11 substrate which also depends on Gid7 for its turnover. Thus, it was hypothesized that any potential factor which destabilizes Cpa1 upon its turnover would exhibit Gid7 and Gid11 dependent turnover upon shift to ethanol. As a proteomics data set of the yeast proteome in ethanol medium upon knockout of *GID11* already existed, whole proteome proteomics were carried out for *gid7Δ* cells after a 24-hour shift to SC-complete medium containing 2% ethanol (Figure 18A). This dataset was cross-referenced with the already existent *GID11* knockout dataset, using a 20% increase in protein abundance upon knockout of either *GID11* or *GID7* and a q-value of 0.1 as cut-offs. Using these parameters, ten proteins were found to be enriched in both datasets, aside from Cpa1 itself. These proteins are: Sno1, Pdc2, Dur1,2, Gis1, Idi1, Syf1, Flc1, Zps1, Taf1, and Gdh1. Interestingly, Kong et al. showed in 2021 that Sno1 is stabilized upon knockout of *UBC8* and that Dur1,2 is stabilized upon knockout of *GID2* or *UBC8*. However, that work also showed Gdh1 to be destabilized upon knockout of *GID2*. Notably, the N-termini of Dur1,2 and Idi1 are broadly in line with the currently known target specificity of Gid11. However, out of this dataset, *IDI1*, *SYF1*, and *TAF1* are essential genes, making knockout impossible. However, temperature-sensitive mutants are available for them (Forster et al. 2022; Li et al. 2011; Stirling et al. 2011), possibly allowing to investigate their potential role in Cpa1-turnover this way. For the remaining proteins found in this dataset, the same experiment as before was carried out, investigating whether their knockout can rescue the phenotype seen in a *gid9Δ* mutant. However, for none of the investigated genes, their knockout led to a rescue of Cpa1 turnover (Figure 18B), meaning none of them are likely to be factors to be involved in the stabilization of Cpa1-tFt upon knockout of GID components. According to the literature, it should be possible to C-terminally tag all of the proteins found in this experiment (Gameiro et al. 2025), meaning that tFT-based stability measurements should be possible with them to verify the results found in the proteomic analysis.

Cpa1 usually exists in a complex with Cpa2, which carries an N-terminal threonine. Thus, a possible hypothesis to explain the dependence of its turnover on Gid11 is that the N-terminus of Cpa2 is recognized by Gid11, leading to subsequent ubiquitination of Cpa1. While this kind of mechanism has been hypothesized before, it has not been proven to exist in living cells, yet. Alphafold3 (Abramson et al. 2024) predictions of the Cpa1-Cpa2 complex predict the Cpa2 N-terminus to be exposed, lending credibility to this idea (Figure 19A).

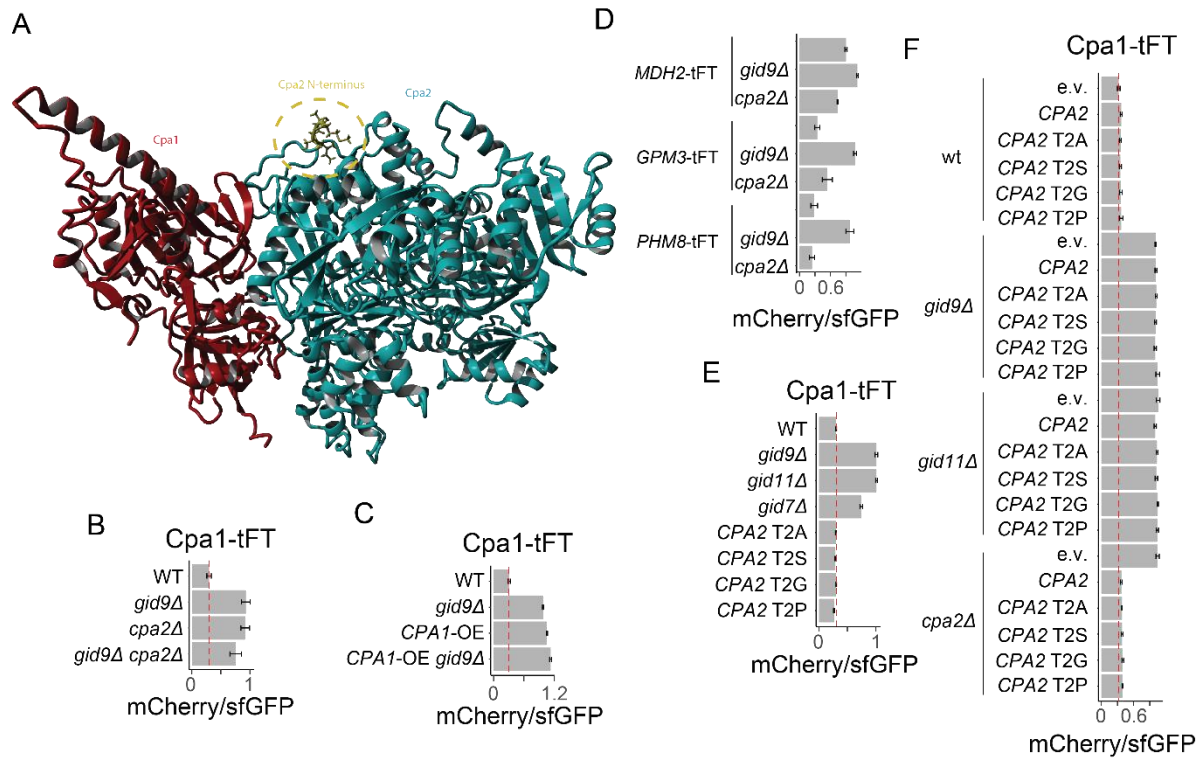

Figure 19: Cpa1 turnover does not depend on Cpa2's N-terminal threonine.
A: AlphaFold2 (Jumper et al. 2021) model of the Cpa1 (red)-Cpa2 (cyan) complex. The Cpa2 N-terminus is highlighted in yellow.
B: Stability, as determined by fluorescence measurements, of tFT-tagged Cpa1 upon knockout of CPA2 in WT or gid9Δ background.
C: Stability, as determined by fluorescence measurements, of tFT-tagged Cpa1 upon endogenous overexpression of CPA1 in WT or gid9Δ background.
D: Stability, as determined by fluorescence measurements, of tFT-tagged Mdh2, Gpm3, or Phm8 upon knockout of CPA2
E: Stability, as determined by fluorescence measurements, of tFT-tagged Cpa1 upon endogenous mutation of the Cpa2 N-terminal threonine.
F: Stability, as determined by fluorescence measurements, of tFT-tagged Cpa1 upon complementation of CPA2 knockout with endogenously expressed CPA2 variants.
B-F: Error bars indicate the standard deviation between biological replicates (n=4).

After confirming the synthetic lethality of the *CPA1* or *CPA2* double knockout with *CAN1* and verifying the functionality of tFT-tagged Cpa1 and Cpa2, the stability of Cpa1-tFT under Cpa2-knockout was measured. Consistent with the hypothesis, knockout of *CPA2* led to a stabilization of Cpa1-tFT to the same extent as knockout of *GID9* (Figure 19B). Furthermore, knocking out both *CPA2* and *GID9* did not produce an additive effect in stabilization, making it appear as if they stabilize Cpa1-tFT through the same pathway. Furthermore, overexpressed Cpa1-tFT becomes stable and is only stabilized to a minor extent upon knockout of *GID9* (Figure 19C), consistent with the idea that it requires binding partner or complex partner for degradation, which would be saturated upon overexpression of *CPA1*.

To rule out that knockout of *CPA2* stabilizes GID-substrates in general, the stability of Mdh2-tFt, Gpm3-tFT, and Phm8-tFT was determined in *CPA2* knockout strains. Knockout of *CPA2* generally did not affect GID-substrates, leading only to minor stabilization of Gpm3-tFT (Figure 19D). Thus, it can be ruled out that knockout of *CPA2* generally stabilizes GID substrates.

To prove that the N-terminal threonine of Cpa2 is required for turnover for Cpa1-tFT, two experiments were conducted in which the N-terminal threonine of Cpa2 was replaced with

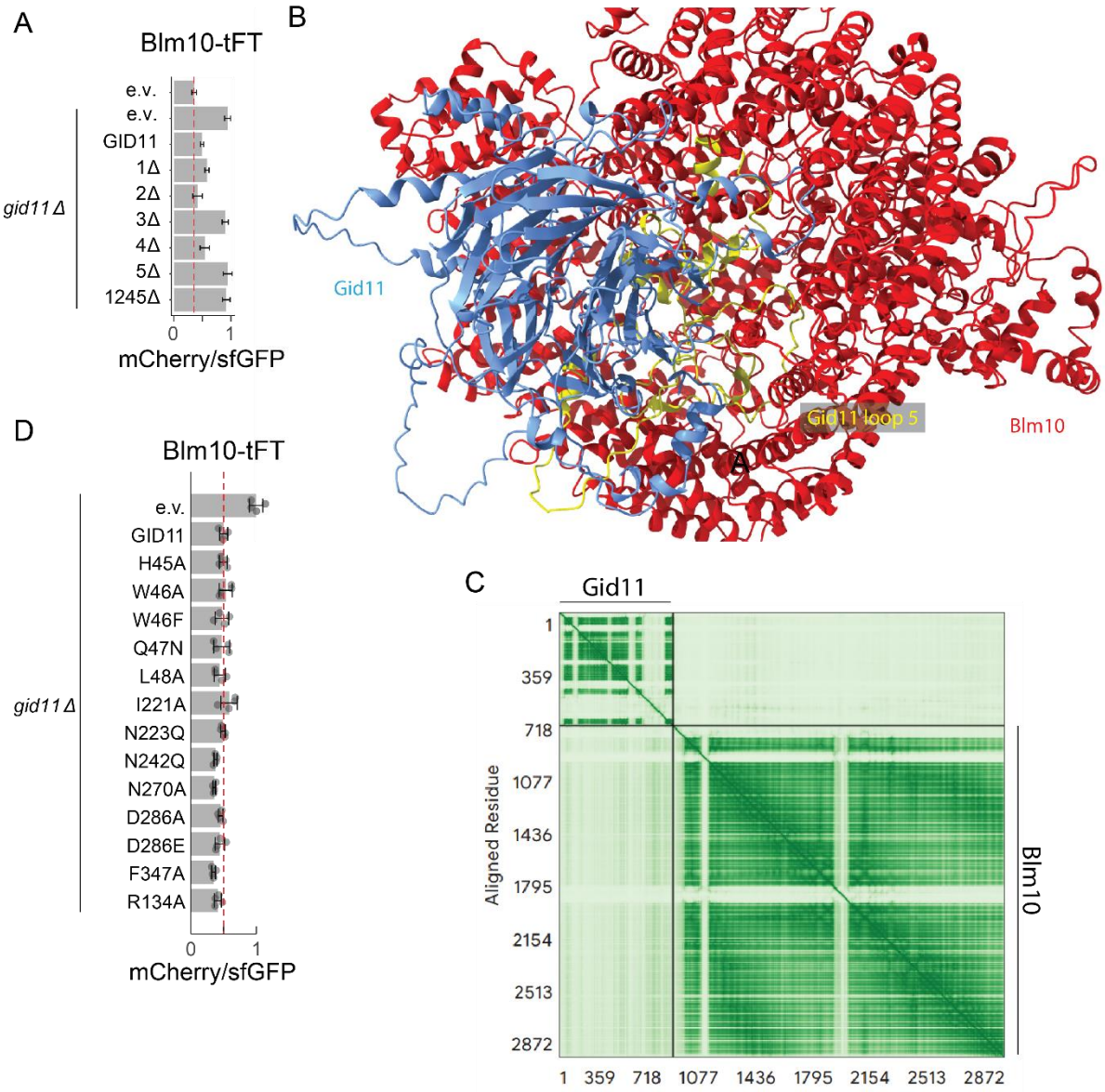

Figure 20: Potential mechanisms for recognition of Blm10 by Gid11.
A: Stability, as determined by fluorescence measurements, of tFT-tagged Blm10 upon deletion of Gid11 IDRs.
B: AlphaFold3 (Abramson et al. 2024) model of Blm10 (red) to Gid11 (blue). Gid11 IDR5 is highlighted in yellow.
C: PAE matrix of the model in B.
D: Stability, as determined by fluorescence measurements, of tFT-tagged Blm10 upon mutation of Gid11 residues previously predicted by AlphaFold3 (Abramson et al. 2024) to form contacts with degron N-termini.
A,D: Error bars indicate the standard deviation between biological replicates (n=4).

alanine, serine, glycine, or proline. In the first experiment, the N-terminal mutations were introduced endogenously into the *CPA2* locus. In the second experiment, the ability of these variants to complement a knockout of *CPA2* if expressed from a plasmid was evaluated. However, replacement of the N-terminal threonine endogenously did not affect Cpa1-tFT stability, and all variants were able to complement *CPA2* knockout (Figure 19E,F). Thus, it can be concluded that, if Cpa2 truly plays a role in the degradation of Cpa1-tFt, this is not due to its N-terminal threonine. Furthermore, it is possible that the observed stabilization of Cpa1-tft upon knockout of *CPA2* is not due to impairment of recognition by the GID complex, but due to general upregulation of Cpa1 due to an impairment in arginine synthesis.

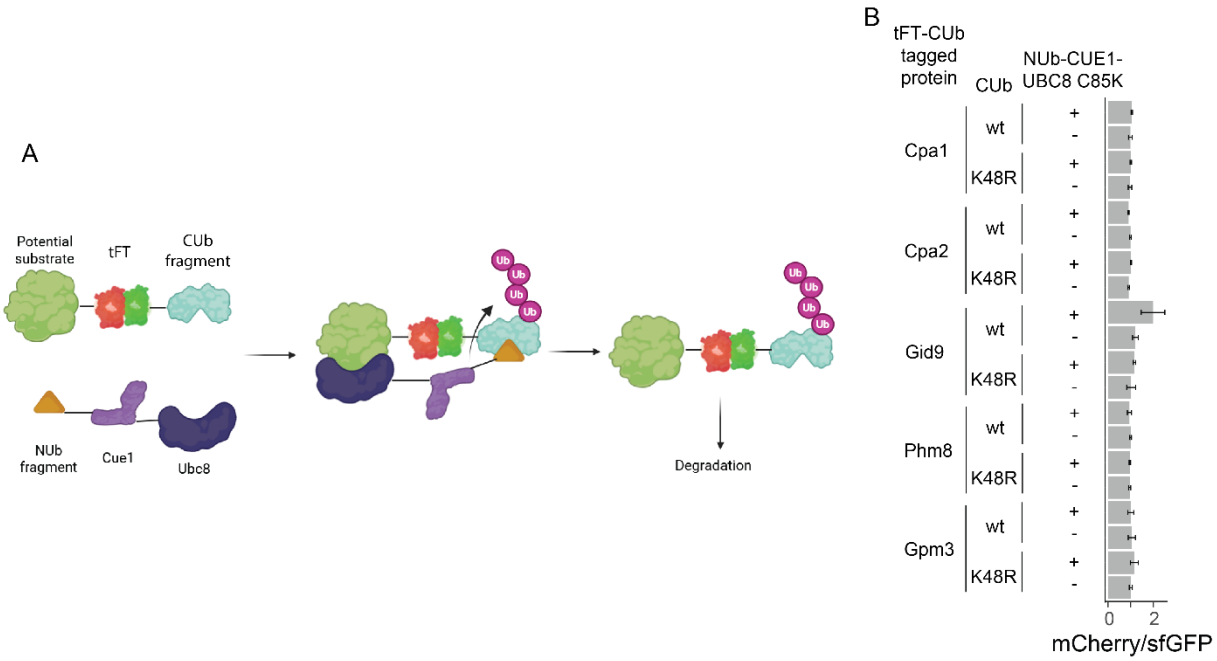

Figure 21: Adapting the Ubiquiton system to detect interactions between E3 ligases and substrates.
A: Cartoon representation of the approach: A component of the UPS, in this case Ubc8 is N-terminally tagged with the N-terminal ubiquitin fragment, as well as Cue1. A potential substrate or interactor of the UPS component is then tagged with the tFT-tag, followed by the C-terminal ubiquitin fragment. Interaction between the UPS component and the potential substrate allows the ubiquitin fragments to reassemble and serve as a chain elongation site for Cue1, targeting the substrate for degradation.
B: First proof-of-concept experiment, showing the stability, as determined by fluorescence, of Cpa1, Cpa2, Gid9, Phm8, and Gpm3 tagged with the tFT-tag followed by the C-terminal ubiquitin fragment upon expression of Ubc8 N-terminally tagged with the N-terminal ubiquitin fragment and Cue1. Error bars indicate the standard deviation between biological replicates (n=4).

In contrast to Cpa1, Blm10 bears a N-terminal threonine. However, replacement of the threonine with either an alanine or a glycine residue does not appear to affect its turnover by Gid11 (Kong et al. 2021). Interestingly, during the experiments with the Gid11 IDR deletion mutants, deletion of loop 5 abolished turnover of Blm10 by Gid11 (Figure 20A). At this point, Blm10 is the only known protein to be affected by deletion of loop 5 of Gid11. Alphafold3 modeling (Abramson et al. 2024) of Blm10 with Gid11 predicted loop 5 of Gid11 to be nestled deep within the central cavity of Blm10, possibly explaining the recognition of Blm10 by Gid11 via loop 5 (Figure 20B,C). Notably, structural predictions of Gid11 in complex with other GID components, such as those in Kong et al. 2025 predict loop 5 of Gid11 to be relatively exposed, making it feasible that loop 5 serves a function in binding potential substrates such as Blm10.

Interestingly, when mutating the residues shown to be part of the Phm8 binding pocket earlier, it does not affect turnover of Blm10 (Figure 20D), as shown by XXXXXXXXXXXXX (Kong et al. 2025).

It is yet unknown whether Cpa1 and Blm10 are bona fide substrates of the GID^{Gid11}-complex. To verify this interaction, multiple approaches could be employed. While the simplest one would be to perform a pull-down of Gid11 and attempt to identify these substrates, we elected to attempt to adapt the Ubiquiton system (Renz et al. 2024) by combining it with the tFT-tag commonly used in our laboratory. The reasoning was that, if feasible, this system could later be used to “reprogram” E3 ligases or E2 conjugating enzymes normally not involved in protein degradation, with the protein stability readout provided by the tFT tag being a simple

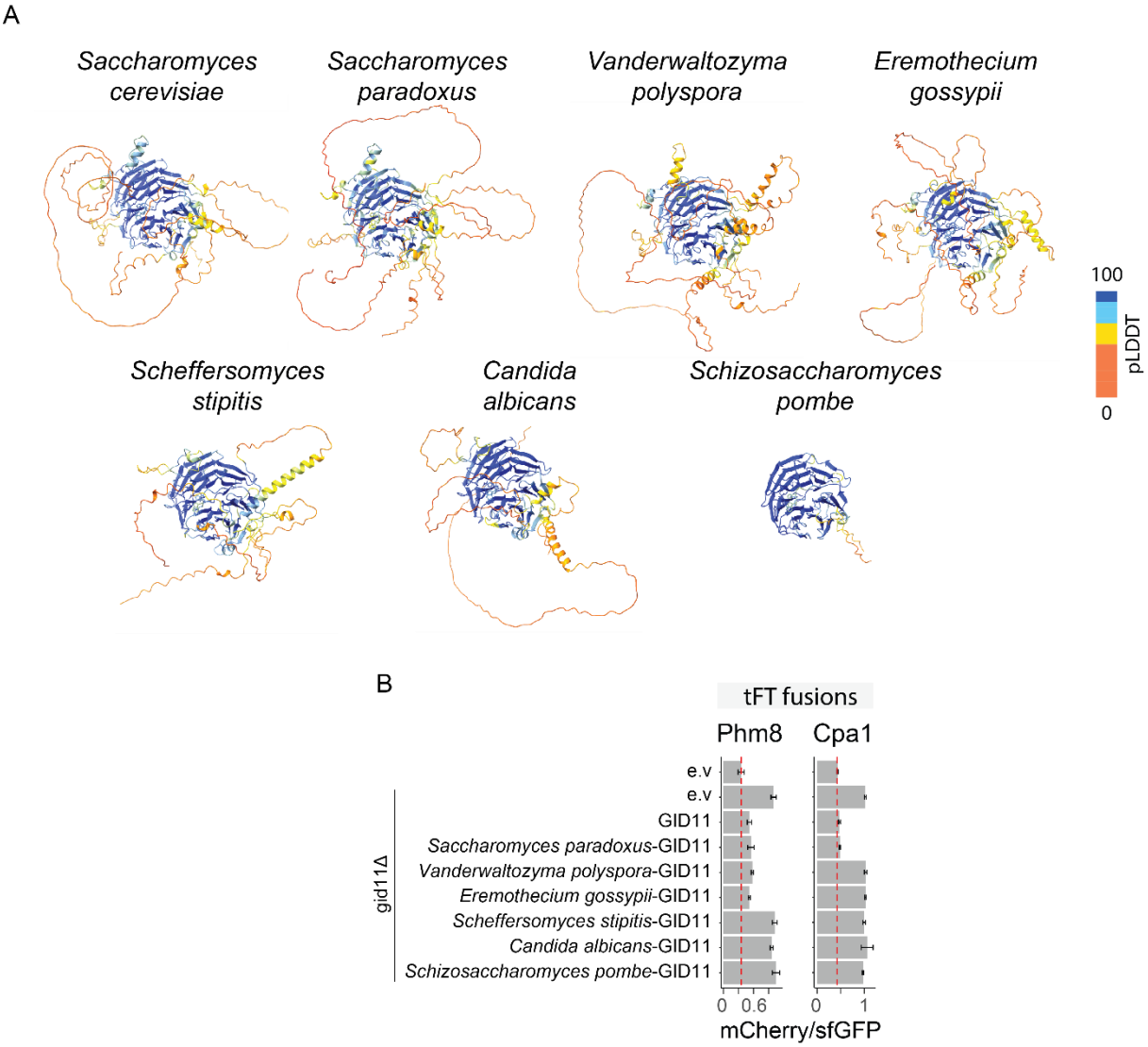

Figure 22: Functional conservation of Gid11 activity.
A: AlphaFold3 (Abramson et al. 2024) models of Gid11 and its homologs from different yeast species, colored by pLDDT score.
B: Stability, as determined by fluorescence measurements, of tFT-tagged Phm8 and Cpa1 upon complementation of GID11 knockout with Gid11 variants from different yeast species. Error bars indicate the standard deviation between biological replicates (n=4)

readout to use in a high-throughput manner (Figure 21A). In a first proof of concept experiment, a catalytically inactive variant of Ubc8, the C85K mutation, was N-terminally fused with Cue1, an E3 ligase creating K48-linked ubiquitin chains, as well as the N-terminal ubiquitin fragment. This construct was expressed from a pRS413-based plasmid off the GPD promoter, with simultaneous overexpression of Ubc7, the E2 conjugating enzyme associated with Cue1, from the same plasmid. Cpa1, Cpa2, Gid9, Phm8, and Gpm3 were endogenously tagged with the tFT timer followed either by the C-terminal ubiquitin fragment or a K48R variant which is unable to form K48-linked chains. Fluorescence measurements of these strains showed that neither of the tested substrates were destabilized upon expression of the NUb-Cue1-Ubc8 construct (Figure 21B). Even though this first experiment was unsuccessful, more optimizations can be done to potentially make it functional. However, these optimizations were deemed outside the scope of this project. Nonetheless, the question remains whether Cpa1 and Blm10 are bona fide substrates of Gid11. Further approaches that could verify such

an interaction would include proximity-based labeling techniques such as Ub-POD (Mukhopadhyay et al. 2024), in which the E3 of interest, in this case a subunit of the GID complex, is tagged with BirA, which then biotinylates any proteins in the vicinity.

Conservation of Gid11 activity

Gid11 is conserved across different species of yeast all the way to *Schizosaccharomyces pombe*. However, with increasing evolutionary distance from *S. cerevisiae*, structure predictions of Gid11 homologs (Abramson et al. 2024) showed these proteins to be increasingly compact (Figure 22A, Figure S 1), with fewer intrinsically disordered regions (IDRs). This raised the question whether these homologs would still be able to recognize Gid11 substrates in *S. cerevisiae*. For this purpose, a suite of plasmids was created by XXXXXXXXX, encoding different homologs of Gid11 (Figure 22B). Against these homologs, one canonical Gid11 substrate, Phm8, and one putative substrate, Cpa1, were measured. For Phm8, all Gid11 homologs stemming from members of the *Saccharomycetaceae* family were able to complement knockout of *GID11*. Interestingly, when measuring activity of these Gid11 homologs against Cpa1, only the homolog from *Saccharomyces paradoxus*, which differs from *Saccharomyces cerevisiae* Gid11 only in a few amino acids, was able to complement knockout of *GID11*. This demonstrates a separation of function, as recognition of Phm8 must be taken over by regions conserved in Gid11 homologs from *Vanderwaltozyma polyspora* or *Eremothecium gossypii*. In contrast, turnover of Cpa1 must depend on a region only conserved in Gid11 homologs very closely related to the one from *Saccharomyces cerevisiae*.

Replacement of Gid components with human homologs

Since the GID complex is conserved through all eukaryotes (Maitland et al. 2022), the question arose whether the human homologs of components of the GID complex are still functional in yeast. Especially concerning the search for new GID/CTLH-substrate receptors, being able to screen for their function in yeast might prove a useful tool. To investigate this, in a first exploratory experiment, human *GID4* was expressed from the *GPD* promoter from a pRS413-based plasmid in cells expressing tFT-tagged Hsm3, Mdh2, or Phm8. However, in none of these strains, expression of human *GID4* led to a stabilization of the substrates, or a potential destabilization in the case of Mdh2-tFT (Figure 23A). However, this could have happened for a variety of reasons. Human Gid4 still possesses the C-terminal motif required for binding to Gid5. Thus, a potential explanation is that the C-terminus of human Gid4 is positioned in such a way that binding to Gid5, and the rest of the complex, is sterically disfavored. Alternatively, expression of human *GID4* in yeast cells might lead to misfolding of the resulting protein. Despite the initial negative result, the choice was made to continue this line of experiments as a bachelor's project carried out by XXXXXXXXXXXXXX (Haschke 2023). She generated plasmids which allowed for the expression of yeast *GID4* with the last ten or twelve amino acids of the resulting protein replaced with their human counterpart. Alternatively, she also generated plasmids from which human *GID4* could be expressed with the last ten or fifteen amino acids of the resulting protein replaced with their human counterpart. Notably, replacement of the yeast C-terminus with the human C-terminus still allowed for binding of Gid4 to the Gid complex, while the replacement of the human C-terminus did not rescue

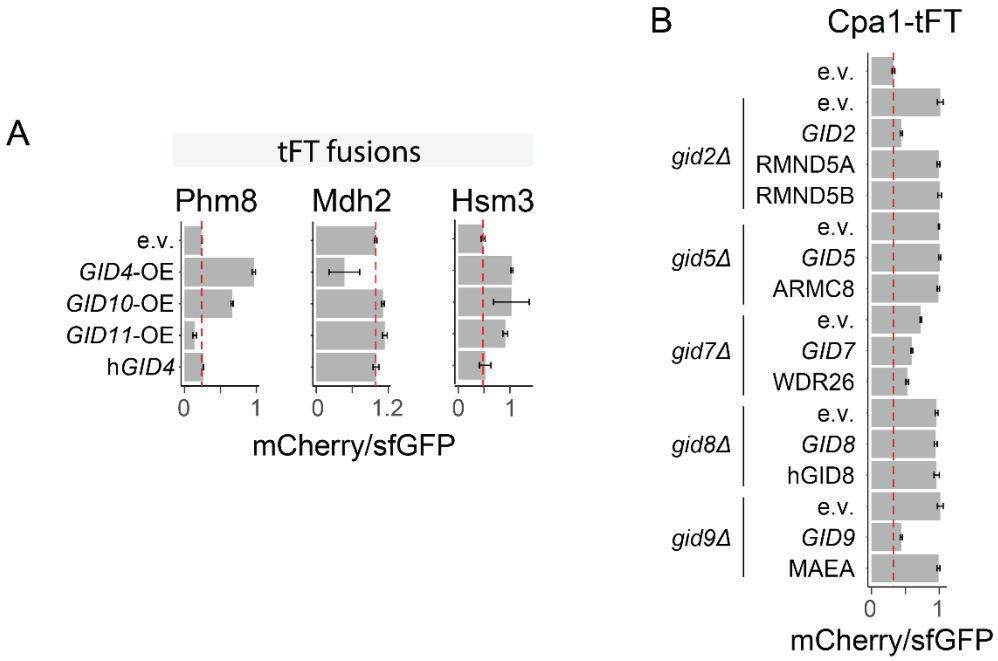

Figure 23: Conservation of GID functionality from human to yeast.
A: Stability, as determined by fluorescence measurements, of tFT-tagged Phm8, Mdh2, or Hsm3 upon overexpression of GID4, GID10, and GID11 or additional expression of human GID4.
B: Stability, as determined by fluorescence measurements, of tFT-tagged Cpa1 upon replacement of yeast GID components with their respective human homologs.
A-B: Error bars indicate the standard deviation between biological replicates (n=4)

function. While this did not shed any light on whether the non-functionality of human Gid4 is due to steric reasons or misfolding, it did show that the human Gid4 C-terminus is capable of binding to Gid5.

As an extension of this experiment, the question was raised whether further human homologs of GID components can complement a knockout of their yeast counterparts. For that purpose, over the course of a Bachelor project carried out by XXXXXXXXXXXXX, pRS413-based plasmids were generated, in which homologs of GID components were expressed from the GPD promoter. The homologs selected were as follows: *RMND5A* and *RMND5B* for *GID2*, *ARMC8* for *GID5*, *WDR26* for *GID7*, human *GID8* for *GID8*, and *MAEA* for *GID9*. Muskelin was not chosen for *GID7*, because its status as a homolog was not certain at the time. Cpa1-tFt was chosen as a model substrate for this experiment, because its turnover is dependent on all GID components tested in this experiment. Complementation of the knockout of the corresponding GID components showed that complementation with *WDR26* was able to rescue the phenotype of *GID7* knockout, showing that it is indeed functional in yeast (Figure 23B). The other human Gid homologs were unable to complement the knockout of their corresponding yeast homolog. While there are numerous possible reasons for that, the most likely reason is that over the evolutionary timespan between the yeast and human homologs, the binding surfaces changed enough that most human GID homologs are not able to interact with their yeast counterparts anymore or, if they do, they are unable to coordinate the remaining components into the assembly required for function. Of course, misfolding or a deficiency in expression of these proteins cannot be ruled out either. However, due to a lack of antibodies available for these proteins, their expression could not be quantified. Furthermore, it must be noted that complementation with yeast *GID5* and *GID8* failed as well,

potentially due to expression from the GPD promoter, which might lead to misregulation of their expression.

Search for new GID substrate receptors

Currently, there are three known substrate receptors for the GID complex in yeast: Gid4, Gid10, and Gid11 (Varshavsky 2024). However, there are a variety of proteins for which XXXXXXXXXXXXXX could show that turnover depends on the GID complex, but which currently do not possess a known substrate receptor. These proteins are: Aro10, Hsm3, Lys21, Mcm7, Seg1, Ssd1, Tmc1, and Ydr222W. All these show stabilization upon knockout of core components of the GID complex (Figure 6B), but not upon knockout of either *GID4*, *GID10*, or *GID11* (Figure 6A). For that reason, it is very likely that they are recognized through a currently unknown substrate receptor.

Out of the aforementioned potential substrates, the degradation of Hsm3, Lys21, and Mcm7 also depends on Gid5 (Figure 6B), with the role of Gid5 for Ydr222w turnover seemingly changing based on the growth conditions of the cells. In colonies or under growth in medium containing ethanol, Gid5 does not appear to be required for the turnover for Ydr222w. However, in liquid medium containing glucose, its degradation seems to be Gid5-dependent (Figure 6C). The turnover of Aro10, Seg1, and Ssd1 on the other hand appears to be completely independent of Gid5 and instead depends on Gid7 (Figure 6B). How these substrates engage the GID complex is currently completely unknown. However, it has been shown in human cells that WDR26, the homolog of Gid7 can act as a substrate receptor as well, making it possible that it serves a similar role, potentially involving further Gid7-dependent substrate receptors, in yeast (Gottemukkala et al. 2024).

Manual verification of previous genome-wide knockout screens

The most straightforward way to search for factors involved in the degradation of a protein in yeast is to perform a genome-wide knockout screen. For this purpose, XXXXXXXXXXXXXX selected Hsm3, Mcm7, Ssd1, and Ydr222w as potential GID substrates to be investigated further. He then introduced the tFT-tagged genes for these proteins into the knockout library by crossing, followed by stability measurement via fluorescence.

In this previous knockout screen he identified the following proteins as potential new substrate receptors: Nit3, Ylr365w, Ylr407w, Ydr344c, Rcr1, Bem4, Ubp15, Irc13, Bub3, and Ygl149w for Hsm3; Vps9, Ymr141c, and Cdc26 for Mcm7; Doa1 for Ydr222w; and Ubc12, Tma10, Mho1, and Moh1 for Ssd1 (Figure 24A-D).

However, the results from these screens were excessively noisy. Furthermore, a positive result in the knockout screen can be due to a variety of factors, particularly artifacts introduced during the crossing and selection steps. For that reason, it was deemed necessary to manually confirm the knockouts.

To confirm the results from that knockout screen, manual knockouts of the candidate genes were performed, both in a wild type and *gid9Δ* background. The latter to rule out the

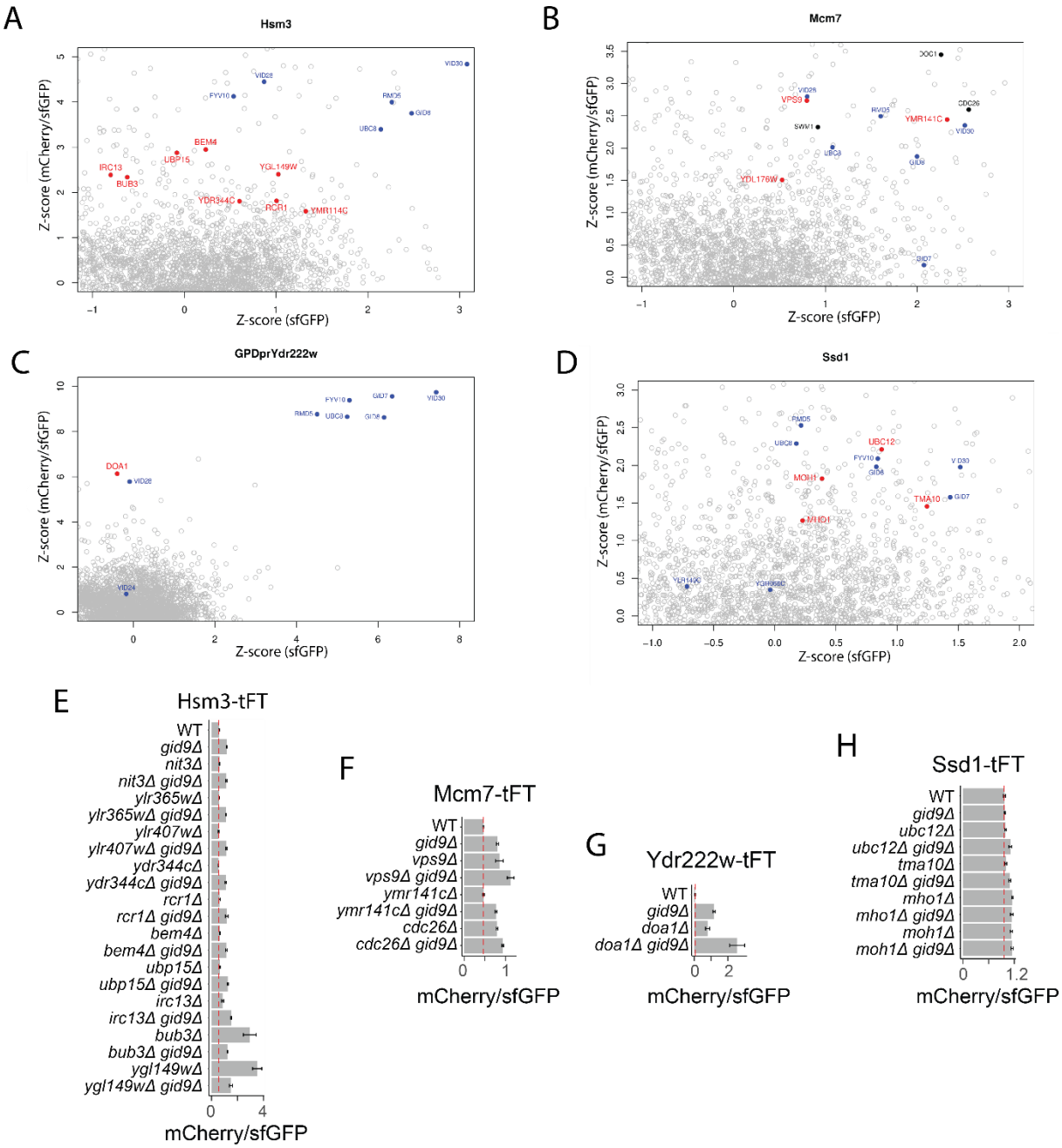

Figure 24: Knockout screens to attempt and find new GID substrate receptors.
A-D: Knockout screens performed by XXXXXXXXXXXXXX to find new substrate receptors, obtained by crossing query strains expressing the tFT-tagged protein of interest with a yeast knockout library. Known GID components are highlighted in blue, potential hits are highlighted in red.
E-H: Stability, as determined by fluorescence measurements, of tFT-tagged Hsm3, Mcm7, Ydr222w, and Ssd1 upon knockout of potential hits from the screens in A-D in WT and gid9Δ background. Error bars indicate the standard deviation between biological replicates (n=4).

involvement of the candidate protein in a different pathway, as in this case the effects of the double knockout should be additive.

For Hsm3-tFt as a substrate, knockout of none of the candidate proteins led to stabilization to the same extent as *GID9* knockout. That said, knockout of *BUB3* and *YGL149C* led to stabilization (Figure 24E). However, this phenotype could not be recapitulated in a *gid9Δ* background and is likely an artifact or due to pipetting error.

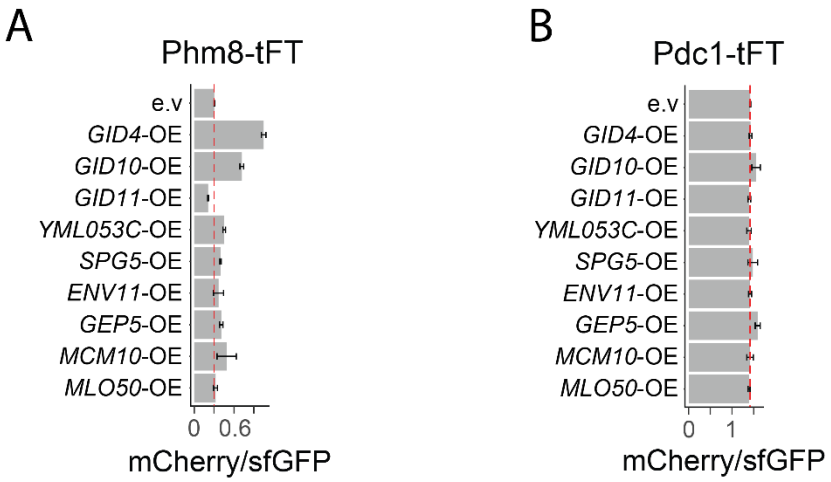

Figure 25: Overexpression as a tool to identify potential Gid5 dependent GID substrate receptors.
A: Stability, as determined by fluorescence measurements, of tFT-tagged Phm8 upon overexpression of known and putative GID substrate receptors.
B: Stability, as determined by fluorescence measurements, of tFT-tagged Pdc1 upon overexpression of known and putative GID substrate receptors.
A-B: Error bars indicate the standard deviation between biological replicates (n=4).

For Mcm7-tFT as a substrate, knockout of both *VPS9* and *CDC26* led to a marked stabilization of Mcm7-tFT in the wild type background (Figure 24F). However, the double knockout with *GID9* led to an additional stabilization, indicating that both Vps9 and Cdc26 act in a separate pathway from the GID complex. Cdc26 is a subunit of the APC/C complex, indicating that degradation of Mcm7-tFt might, at least partly, depend on that pathway as well.

Knockout of *DOA1* stabilized Ydr222w-tFT (Figure 24G). However, as the stabilization phenotype is additive with knockout of *GID9*, it was deemed likely to be active in a different pathway and thus not pursued further.

For Ssd1-tFt knockout of both *MHO1* and *MOH1* led to a stabilization of the substrate to a similar extent as knockout of *GID9* (Figure 24H). Additionally, knockout of *GID9* did not lead to additional stabilization of the substrate, further lending credibility to the idea that Mho1 and Moh1 might be bona fide substrate receptors. Notably, it has been shown before that degradation of Ssd1-tFT does not depend on Gid5, but on Gid7 (Figure 6B). Thus, Mho1 and Moh1 might possibly be involved in substrate recognition through a new, currently unknown substrate receptor unit.

Search for new substrate receptors utilizing competition for Gid5 binding

As GID substrate receptors are hypothesized to engage the GID complex by binding to Gid5 via their C-terminal Φ[D/E]ΦX motif (Kong et al. 2021), we hypothesized that substrate receptors should compete for this binding site if overexpressed. In turn, this should lead to stabilization of substrates depending on the other substrate receptors. For this purpose, the three known substrate receptors Gid4, Gid10, and Gid11 were overexpressed, alongside six further proteins which were selected due to the existence of the motif in their C-terminus. As a model substrate, a Gid11 substrate, Phm8, tagged with the tFT, was selected. As an additional control, the overexpression was also carried out against Pdc1-tFT, which should not be affected by overexpression of Gid substrate receptors.

Overexpression of Gid4 or Gid10 led to a marked increase in Phm8-tFT stability, while overexpression of Gid11 led to destabilization of the substrate. Notably, overexpression of the six selected potential substrate receptors only led to slight stabilization of Phm8, but none to the extent seen upon overexpression of Gid4 or Gid10 (Figure 25A). Pdc1 on the other hand was only slightly stabilized by overexpression of Gid10 and Gep5, showing that the stabilization caused by Gid substrate receptor overexpression is not a general effect, for example due to proteotoxic effects caused by the overexpression (Figure 25B).

Overall, this experiment confirms that overexpression of GID substrate receptors bearing the C-terminal Φ[D/E]ΦX motif leads to competition at the Gid5 binding site, which could be confirmed by overexpressing the known substrate receptors. This concept could be expanded in the future to perform a genome-wide overexpression screen to identify potential Gid5 dependent GID substrate receptors.

Exploration of the specificity of human ATE1, NTAN1, and NTAQ1 in yeast

As mentioned in the introduction, in the Arg/N-degron pathway tertiary N or Q residues on the N-terminus can be processed to form secondary D or E residues by Nta1 in yeast or NTAN1 and NTAQ1 in humans (Baker and Varshavsky 1995; Kim et al. 2016; Varshavsky 2024). These residues can then further be arginylated by Ate1 to form primary destabilizing residues for the Arg/N-degron pathway (Ferber and Ciechanover 1987; Kwon et al. 2002; Kim et al. 2022). At the time a colleague, Andrea Coti was investigating the Arg/N-degron pathway in human cells. In the context of her project, the question was raised whether it would be possible to investigate the substrate specificity of NTAN1, NTAQ1, and ATE1 in yeast cells, especially as N-termini ending with E or Q were surprisingly stable in her experiment in human cells compared to previous experiments performed in yeast (Kats et al. 2018). For this purpose, an array of plasmids was generated, consisting of 80 plasmids based on pAnB19, expressing the mCherry/sfGFP tFT-tag with an N-terminal peptide sequence exposing either N-terminal DZ, EZ, NZ, or QZ, where Z is any of the 20 amino acids (Figure 26A). This construct is N-terminally capped with Ubiquitin, which would be co-translationally cleaved off, exposing the desired N-terminus (Varshavsky 2005). This array was generated by cutting pAnB19 with EcoRV and performing NEB HiFi-Assembly with degenerate oligonucleotides containing both the necessary homology arms, the codon for the desired N-terminal amino acid, followed by an NNK codon. Using this technique, 60 of the 80 desired plasmids could be generated. The remaining 20 plasmids were cloned manually using the same technique but using oligonucleotides coding for the desired N-terminus. On the other hand, yeast *ATE1*, human *ATE1* in two different isoforms, yeast *NTA1,* and huma *NTAN1* and *NTAQ1* were expressed from the *GPD* promoter from a pRS426-based plasmid (Figure 26A).

To simplify the crossing process required for this experiment, the decision was made to measure the stability of these constructs in diploids which would result from crossing a BY4741-based *nta1Δate1Δ* strain containing the 80 XZ-plasmids and a BY4742-based strain containing the plasmids expressing either *ATE1* or *NTA1* variant in a corresponding *ate1Δ* or *nta1Δ* background. This would result in diploids which are endogenously homozygous knocked

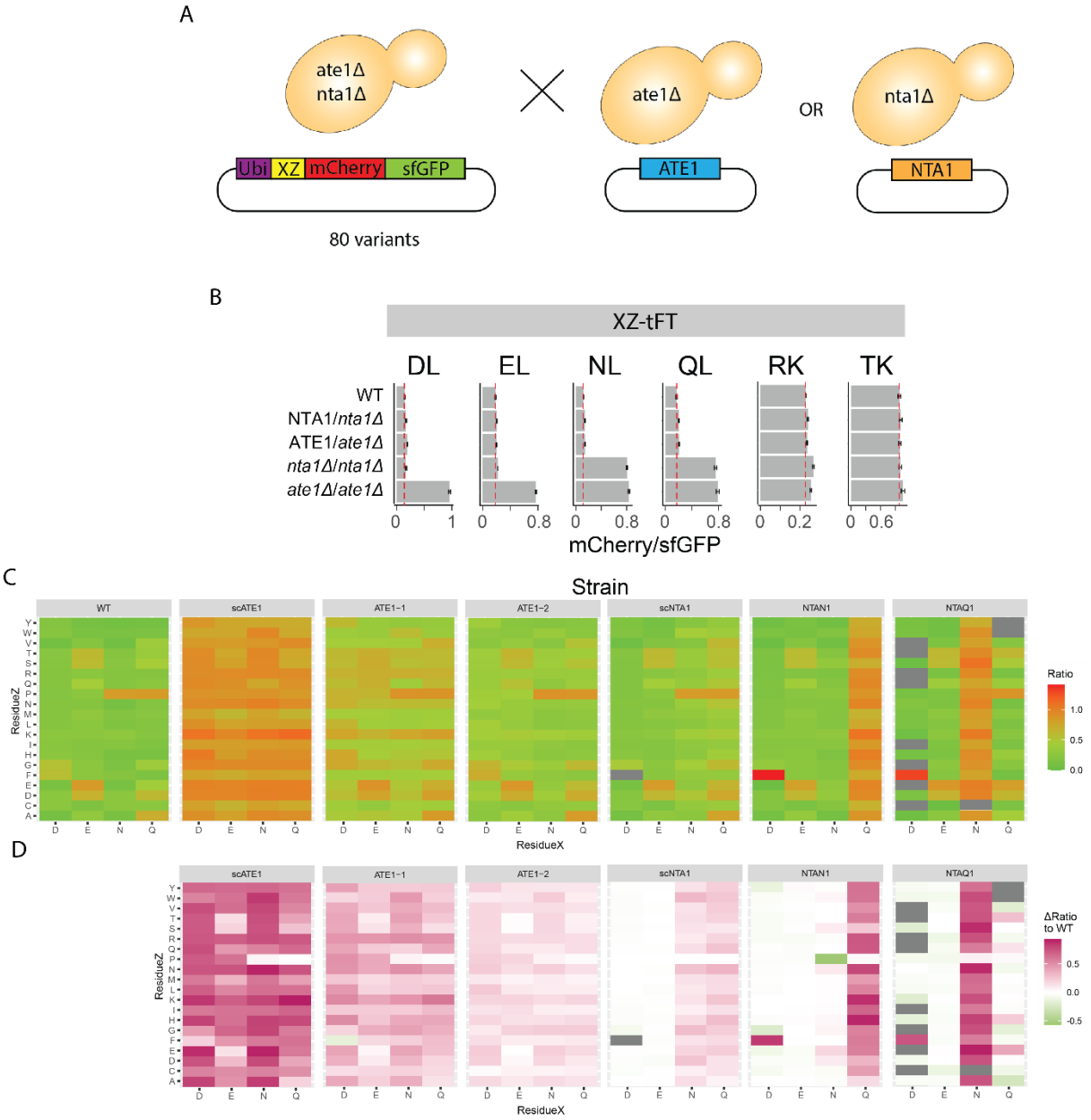

Figure 26: Comparison of the activity of Nta1 and Ate1 with their human homologs.
A: Schematic representation of the experiment: ate1Δnta1Δ cells expressing 80 XZ-tFT variants are crossed to ate1Δ or nta1Δ strains complemented with an ATE1 or NTA1 variant, respectively.
B: Stability, as determined by fluorescence measurement, of six selected constructs in diploid strains heterozygous or homozygous for knockout of ATE1 or NTA1. Error bars indicate the standard deviation between biological replicates (n=4).
C: Absolute mCherry/sfGFP ratios in strains expressing 80 XZ-constructs in yeast strains complemented with the indicated ATE1 or NTA1 variant
D: Difference between complemented yeast strains and the corresponding wild type expressing 80 XZ-constructs.

out for either *ATE1* or *NTA1*, but complemented by the pRS426-based plasmid, and heterozygous for the knockout of the other enzyme.

To see if this approach is viable, it was first necessary to see if a heterozygous knockout of *ATE1* or *NTA1* would still allow enough enzyme to be expressed to function as the wild type. For this experiment, BY4741-based *ate1Δ* or *nta1Δ* strains expressing the constructs N-terminally ending with DL, EL, NL, or QL, as well at TK or RK were crossed with the corresponding BY4742-based wild type, *ate1Δ*, or *nta1Δ* strain to generate homozygous or

heterozygous knockout strains. The fluorescent constructs were chosen as their N-termini were previously shown to be unstable in yeast (Kats et al. 2018) with the TK and RK constructs serving as an unstable and a stable control respectively, which should not be affected by knockout of *ATE1* or *NTA1*. Fluorescence measurements of the diploids resulting from these crosses showed that indeed heterozygous expression of either *ATE1* or *NTA1* led to the same level of destabilization of the constructs as homozygous expression (Figure 26B). This means that heterozygous expression is sufficient to process tertiary or secondary residues.

With this control experiment done, the final crossing was performed. BY4741-based *ate1Δnta1Δ* strains containing the XZ-plasmids were crossed with BY4742-based *ate1Δ* or *nta1Δ* strains containing the pRS426-based plasmids coding for the corresponding Ate1 or Nta1 variants. Fluorescence measurements of the resulting diploids showed that expression of yeast *ATE1* from the pRS426-based plasmid could not complement the knockout completely (Figure 26C,D). This could be due to a variety of reasons, but the most likely one is that expression from the *GPD* promoter does interfere with the regulation of *ATE1*. For this reason, the results for the complementation of *ate1Δ* were disregarded. Expression of *NTA1* or its human homologs from the *GPD* promoter led to a growth defect in the cells, hinting at a certain level of toxicity caused by overexpression of *NTA1*. This made it necessary to discard some data, particularly for the complementation with NTAQ1. Nonetheless, the complementation of *NTA1* knockout with a plasmid was able to almost completely save the phenotype caused by the knockout. Complementation of the knockout with either NTAN1 or NTAQ1 only rescued the knockout phenotype for constructs starting with N or Q respectively, demonstrating how over the course of the evolutionary process these two paralogues specialized more towards certain N-termini. More notably, NTAN1 appears to have a stronger preference for NP-N-termini when compared to its yeast counterpart. On the other hand, NTAQ1 appears to disfavor QE, QH, QQ, and QT-N-termini when compared to the yeast homolog.

Discussion

Characterization of the Gid11 substrate receptor

Impact of N-terminal acetylation on Gid11 substrate recognition

Overall, the characterization of the degron bound by Gid11 paints a very clear picture of a preference for N-terminal threonine residues, which are unacetylated. This could be shown in our MPS profiling (Kong et al. 2025) and mass spectrometry experiments. It appears that Gid11 substrates have evolved to have a bulky hydrophobic or basic residue in their third position, allowing them to avoid acetylation by NatA (Figure 13B,C). Interestingly, a study by Heathcote et al. published in 2024 showed a similar pattern to the one observed in our acetylation studies. In that study Heathcote et al. investigated protein turnover in the Arg/N-degron pathway involving tertiary cysteine residues. They found that in cells, cysteine residues followed by hydrophobic or basic residues were turned over readily by ADO, while cysteine residues followed by acidic or polar residues were poor ADO substrates *in vivo*. Heathcote et al. traced this back to the activity of NatA. They found N-terminal cysteine followed by polar or acidic amino acids to be readily N-terminally acetylated, while cysteine followed by a basic or hydrophobic amino acid was a poor NatA substrate. While that study was conducted in human cells, compared to the yeast studies conducted here, they still match with the acetylation data obtained in this project, where we found that threonine followed by basic or bulky hydrophobic residues was not acetylated *in vivo*, while threonine followed by acidic or polar amino acids was almost entirely acetylated. Interestingly, this also matches well with molecular simulation data recently released by Kong et al., where the molecular simulations predicted non-acetylated, protonated Gpm3 N-termini to bind to the negatively charged Gid11 binding pocket of Gid11, while acetylated, or unprotonated Gpm3 N-termini were not predicted to bind to the Gid11 binding pocket. This raises the possibility that, at least in the case of substrate binding to Gid11, N-terminal acetylation abolishes substrate binding to Gid11 by blocking protonation of the N-terminus, thus removing its positive charge. This mechanism of acetylation shielding degrons and blocking degradation of their substrates has been found several times now (Mueller et al. 2021; Linster et al. 2022; Varland et al. 2023; Heathcote et al. 2024; Kong et al. 2025), raising the question whether this is a general function of N-terminal acetylation and whether degradation via the Ac/N-degron pathway is the exception rather than the rule.

Structural basis for binding of Gid11 substrates

Regarding the structural basis of substrate binding to Gid11, the binding pocket for canonical substrates beginning with threonine could be defined quite well, down to a single amino acid level (Figure 16B). However, the loop deletion and conservation experiments keep raising questions. Normally, IDRs are known to be involved in facilitating interactions between proteins or to act as recognition sites, besides a mere function as a functional linker between protein domains (Chakrabarti and Chakravarty 2022). Thus, it is surprising that a relatively large portion of Gid11 can be deleted without significantly affecting its functionality regarding

its canonical substrates (Figure 15C). AlphaFold3 models suggest loop 3, which is the only loop shown to influence canonical Gid11 substrates might interact with regions of Gid1. However, mutations of the corresponding interacting regions in Gid1 did not have an impact on Gid11 dependent turnover (Kong et al. 2025), making it questionable whether this is truly the reason for the abolishment of Gid11 activity upon deletion of the third IDR. Furthermore, it is remarkable that in the Gid11 conservation experiments, the Gid11 homologs that are still functional are those which also still possess their loop 3, while those which do not are non-functional against canonical Gid11 substrates (Figure 22, Figure S 1). This raises the possibility that IDR 3 of Gid11 serves a function required for recognition of substrates, which became unnecessary for its function in other yeast species as they diverged from *Saccharomyces cerevisiae*. In that context, experiments with replacement of the *Saccharomyces cerevisiae* IDR3 region with those of other yeast species might give further insight. However, the alignment of the Gid11 sequences shows that these yeast species not only lack IDR3, but also parts of the beta sheet regions surrounding it. For that reason, great care would need to be taken to ensure these replacements do not lead to misfolding, and corresponding controls, such as Western Blotting, immunoprecipitation experiments, and overexpression experiments against tFT-tagged Hsm3 would need to be done.

To further explore the importance of certain residues within Gid11, more methods can be employed, for example saturation mutagenesis of Gid11 (Siloto and Weselake 2012) followed by MPS profiling to identify variants of Gid11 which are non-functional or have impaired functionality (Reinbold et al. 2023).

Turnover of non-canonical Gid11 substrates

Cpa1 is special compared to other proteins whose turnover depends on Gid11 as its N-terminus does not bear a N-terminal threonine. Nonetheless, upon knockout of *GID11*, it is strongly stabilized in the cell (Kong et al. 2021).

As Cpa1 forms a complex with Cpa2 (Price et al. 1978) and Cpa2 does bear a N-terminal threonine, this led to the hypothesis that Cpa2 is recognized by Gid11 and Cpa1 is ubiquitinated *in trans* by the GID complex. Johnson et al. found in 1990 that ß-Galactosidase tetramers consisting of a mixture of wild type subunits and subunits with their lysine residues replaced by arginine would still lead to ubiquitination of the lysine-rich subunits, even if these do not bear a N-degron. However, these tetramers are functionally still homotetramers, with some subunits bearing mutations. However, for protein complexes consisting of two entirely subunits, ubiquitination *in trans* has not been shown before. For this reason, this hypothesis for recognition of Cpa1 was particularly attractive.

While it could not be shown that the Cpa1/2 complex is recognized by Gid11 via the N-terminal threonine of Cpa2 (Figure 19E,F), the loop deletion mutants of Gid11 still shed some light on a separation of function between the recognition of “canonical” Gid11 substrates such as Phm8, and potential “non-canonical” substrates such as Cpa1. In particular, the fact that the smallest deletion of loop 3 allowed Gid11 to lead to turnover of Phm8 but not Cpa1 (Figure 15G) warrants further investigation. Of note is that only Gid11 from *Saccharomyces paradoxus* was able to facilitate turnover of Cpa1, while Phm8 could be turned over by a wider range of Gid11 homologs (Figure 22B). One potential explanation is that Cpa1, while affected quite

strongly in its turnover via Gid11, is not a particularly robust substrate and because of that, small perturbations of Gid11 function can already lead to complete or almost complete stabilization of Cpa1. The fact that Cpa1 is also Gid7 dependent in its turnover is of note. One potential explanation for this behavior is that that Cpa1 requires specific steric circumstances to be recognized and ubiquitinated by the GID^{Gid11}-complex. In this scenario, small perturbations in Gid11 function or positioning could be amplified over the scale of the entire Chelator-Gid11 complex, meaning that the residues in Cpa1 required for its ubiquitination cannot be placed in the correct position anymore.

Similarly to Cpa1, Blm10 has been shown not to be a canonical Gid11 substrates. Even though it bears a N-terminal threonine, mutation of that threonine does not affect its turnover (Kong et al. 2021). However, the loop deletion mutations showed that loop 5 is required for turnover of Blm10 (Figure 20D). This is particularly noteworthy as Blm10 is currently the only known potential Gid11 substrate whose turnover depends on this loop. However, it is currently unclear if Blm10 is a bona fide substrate of Gid11. As Blm10 is a binder of the core regulatory particle of the proteasome (Schmidt et al. 2005), it is possible that its real function is in recruitment of the GID complex, or Gid11 itself to the proteasome and stabilization of Blm10 upon knockout of *GID11* is a side effect of Blm10 being unable to recruit Gid11.

The biggest challenge with both Cpa1 and Blm10 is that currently, there is no evidence that either protein interacts directly with Gid11. Previous attempts to show an interaction between Gid11 and its substrates in a yeast two-hybrid assay failed. Attempts to purify Gid11 for methods such as crystallography or Isothermal Titration Calorimetry also have failed thus far. Because of this, the proof of interaction between Gid11 and these two potential substrates must be done *in vivo*. As mentioned above, there have been attempts to modify the ubiquitin system for this purpose (Renz et al. 2024), but further optimizations, especially regarding the relative positioning and spacing of the components of the system, would need to be made (Figure 21). One very simple way interaction between Gid11 and these putative substrates could be shown is via immunoprecipitation, for example of HA-tagged Gid11, followed by mass spectrometry. However, interactions between E3 ligases and their substrates are usually relatively transient (Iconomou and Saunders 2016), making them poorly suited for immunoprecipitation experiments. Nonetheless, with a sufficiently large amount of protein this might be feasible. Alternatively, approaches such as protein crosslinking could be used to artificially stabilize the interaction between Gid11 and its substrates (Piersimoni et al. 2022), allowing for immunoprecipitation followed by mass spectrometry. Another potential way to detect the interaction between Gid11 and its putative substrates is via proximity-based labeling. Recently, three approaches have been published to do so: Ub-POD (Mukhopadhyay et al. 2024), BioE3 (Barroso-Gomila et al. 2023), and E-STUB (Huang et al. 2024). In essence, these three approaches work very similarly by first labeling an E3 ligase of interest, in this case Gid11 or any other components of the GID complex with BirA, a biotin ligase from *Escherichia coli* (Cronan 1989). After incubation of the cells with biotin, a pull-down of biotinylated proteins is performed using streptavidin (Weber et al. 1989) followed by mass spectrometry to identify enriched proteins in the biotinylated fraction. For the mere purpose detecting interactions between Gid11 and Cpa1 and Blm10, this experiment could be simplified and

instead of mass spectrometry, detection of Cpa1 or Blm10 specifically could be performed using immunoblotting.

Were an interaction between these non-canonical putative substrates and Gid11 to be found, this would most likely show that Gid11 possesses more than one binding site for substrates. As mentioned before, AlphaFold modeling of Gid11 with Blm10 does show loop 5 of Gid11 to interact with Blm10, and deletion of this loop leads to a marked stabilization of Blm10 in the cell. Such a scenario would not be unheard of, either. For example, the N-recognin of the Arg/N-degron pathway, Ubr1, is known to recognize different N-degrons via several different substrate binding sites on its surface (Tasaki et al. 2009; Matta-Camacho et al. 2010; Varshavsky 2024).

Similarly, as explained above for canonical Gid11 substrates, performing saturation mutagenesis of Gid11 followed by cell sorting based on Cpa1 stability could provide more information on the recognition of these non-canonical substrates, especially if one would be able to identify residues which affect only non-canonical substrates, but not canonical ones.

Overall, these putative substrates offer a lot of opportunities and open questions still to be explored, even though that is outside the scope of this thesis.

Search for new GID substrate receptors

Using overexpression of known GID substrate receptors, it could be shown that it is possible to use competition for the Gid5 binding pocket as a tool for finding new Gid5 dependent substrate receptor proteins (Figure 25). Particularly for proteins like Hsm3, where it is known that they are degraded in a Gid5 dependent manner, but for which there is no currently known substrate receptor, this can prove a useful tool. While this small-scale experiment worked as a proof of concept, the next step is to expand this to a genome-wide overexpression screen. For this purpose, there are several valid approaches. Genome-wide overexpression libraries such as the MoBY 1.0 or MoBY 2.0 (Ho et al. 2009; Ho 2011) or the MORF (Gelperin et al. 2005) libraries could be used. However, particularly with libraries using 2µ-based plasmids, one needs to be cautious of proteotoxic effects due to high overexpression of these genes. Another possible avenue for such an overexpression screen is a replacement of the endogenous promoter of the gene of interest with a strong promoter such as the *GPD*, *TEF*, or *GAL1* promoter (Peng et al. 2015). The generation of such a library could be carried out relatively easily using approaches such as the N-SWAT approach (Yofe et al. 2016). However with this approach, the selection of the promoter becomes even more important, as an endogenous approach only provides one copy of the gene, while plasmid-based approaches provide a copy number of 2 to 5 for CEN-based plasmids, while 2µ-based plasmids can reach copy numbers upwards of 30 copies (Karim et al. 2013). To find the ideal combination of plasmid or endogenous expression together with the ideal promoter, further experiments would need to be carried out. After this initial optimization stage, the final readout could be performed in an SGA format in which a query strain expressing Phm8-tFT or Hsm3-tFT for example, is crossed with the overexpression library. After sporulation and selection for spores carrying both the overexpression and the tFT-tagged substrate, substrate stability could then be determined by fluorescence.

An alternative approach for finding potential substrate receptors could be *in silico* modeling using AlphaFold3 (Abramson et al. 2024). In this approach one could model Gid5 together with several, for example three or four, proteins from the yeast proteome at a time. In this approach, one would then evaluate which proteins are predicted by AlphaFold3 to bind to the established binding groove in Gid5. Especially if each protein is represented in several randomized collections of proteins, one could evaluate which proteins are predicted to interact with Gid5 more than random chance would dictate. However, this approach would be quite intensive in computational resources, necessitating the use of a high-powered computation cluster.

In the case of Hsm3, there is also the possibility that Hsm3 itself binds to Gid5 to facilitate its own degradation. Its C-terminus is "ADCR", which roughly fits the established motif for Gid5 dependent substrate receptors, or an acidic residue surrounded by two hydrophobic residues, followed by any amino acid. However, as all substrates used in this project are C-terminally tagged, the bulky tFT tag would likely interfere with such a binding mode. Nonetheless, direct binding of Hsm3 cannot be ruled out until experiments are carried out to do so. One simple experiment for this would be to delete a portion of the C-terminus of Hsm3. If Hsm3 truly binds directly to Hsm3, this should stabilize Hsm3 compared to the wild type version.

Finally, the question remains regarding substrates like Ssd1 or Ymr086w which exhibit Gid5 independent, but Gid7 dependent turnover (Figure 6B). In human cells, WDR26 was found to act as a substrate receptor for NMNAT1 (Gottemukkala et al. 2024), with the human homolog of Moh1, YPEL5, acting in a regulatory function. As *MOH1* has been found to stabilize Ssd1 and Ymr086w upon knockout (Figure 7), it is not too far-fetched to believe that Moh1 is part of a Gid7-based substrate recognition platform, potentially also involving Mho1, as knockout of *MHO1* has been found to stabilize Ssd1 as well. It is reasonable to hypothesize that over the course of evolution, Moh1 has lost its ability to act as a substrate recognition platform, instead acting as a regulatory subunit. Mho1 is currently a very poorly understood protein. Its only known function is in invasive growth in yeast strains capable of pseudohyphal growth, as well as a synthetic lethality of *MHO1* knockout together with *PLC1* knockout (Schlatter et al. 2012). However, this is broadly in line with what is currently known about Ssd1, which is known to be a translational repressor involved in cell wall maintenance and cell morphogenesis (Wanless et al. 2014; Miles et al. 2019; Bayne et al. 2022). However, none of the strains currently used in this lab are capable of pseudohyphal growth. This means it might be necessary to establish the function of Moh1, Mho1, and their relationship with Ssd1 in a different yeast strain, for example the yeast strain Σ1278b, which is a strain commonly used in the study of pseudohyphal growth (André 2018). Overall, this line of potential inquiry provides plenty of open questions and opportunities for the discovery of a potential new Gid7-dependent substrate receptor platform, especially with regards of the evolution of Moh1 to YPEL5, and its shift of function from a potential substrate receptor platform to a regulatory element of the CTLH-complex in human cells.

The phenotypes seen for knockout and overexpression of *IPF1* are broadly in line with what would be expected based on results by Qiao et al. published in 2022 (Figure 7, Figure 8). However, it is of note that that study was only performed with the GID^{Gid4}-complex. In the experiments conducted in this project, knockout of *IPF1* also affected Gid11 substrates and

even some substrates such as Ssd1 where currently no substrate receptor is known. This makes it likely that the function of Ipf1 in regulating and sequestering the GID complex is not specific to the GID^{Gid4}-complex, but a general function regardless of the substrate receptor.

Exploration of the specificity of NTAN1 and NTAQ1

The initial inspiration for this experiment was the observed difference in stability between N-termini beginning with N and Q between experiments carried out in yeast by Kats et al. and stability profiling experiments performed by Andrea in our lab. While the results obtained in this study point towards some specific differences in specificity between NTAN1 and NTAQ1 and their yeast homolog Nta1 (Figure 26B, C), these do not explain the general difference in stability that was observed. However, Andrea found that N and Q residues tend to be N-terminally acetylated in human cells, in line with currently unpublished data by the Arnesen lab (Coti 2024). Further research will need to be carried out to investigate which N-acetyltransferases are responsible for this, a task which is currently being carried out by Tatiana Aksinina, a PhD student in our lab.

Concluding remarks

The aim of this study was to elucidate protein turnover by the GID complex in yeast. This was achieved mainly through characterization of Gid11, the nature of substrates turned over by it, and elucidation of the binding pocket and intrinsically disordered regions in the protein. Additionally, some light was shed on non-canonical Gid11 substrates in the form of Cpa1 and Blm10, where it could be shown that degradation of Cpa1 does not depend on the N-terminal threonine of its complex partner Cpa2, and that degradation of Blm10 relies on the fifth IDR of Gid11 rather than any residues within the Gid11 binding pocket.

Additionally, regarding the search for new GID substrate receptors, it could be shown that overexpression of potential GID substrate receptors is a viable method to identify new Gid5 dependent receptors. Furthermore, stabilization of Ssd1 upon knockout of Gid7, Moh1, and Mho1 raises the possibility of a new mode of substrate binding, analogous to the one shown by WDR26 in human cells.

Overall, this study shed some light on the GID complex, while raising further avenues for its future investigation.

Appendix I

Supplementary

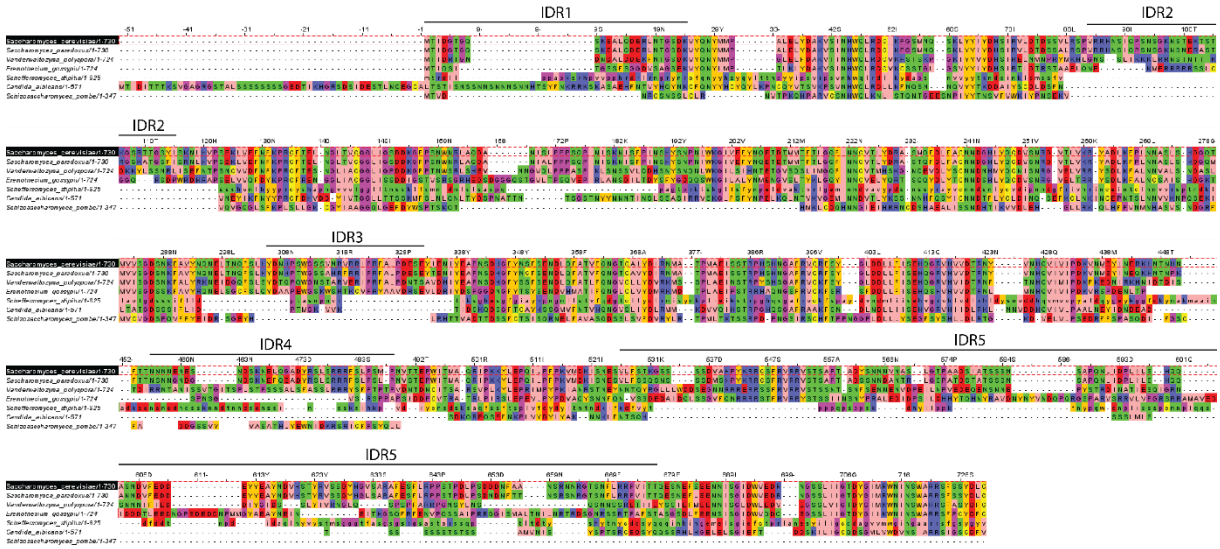

Figure S 1: Clustal Omega (Sievers and Higgins 2021; Madeira et al. 2024) alignment of Gid11 homologs in different yeast species. The IDRs predicted in the Saccharomyces cerevisiae homolog of Gid11 are highlighted.

Table S 1: Yeast strains used in this study.

Strain	Genotype	Reference
AK1252-1	yMaM330 (MATalpha can1Δ::STE2pr-SpHIS5 lyp1Δ::STE3pr-LEU2 his3Δ1 leu2Δ0 ura3Δ0 leu2Δ0::GAL1pr-I-SCEI-natNT2) HSM3-mCherry-sfGFP gid9Δ::kanMX	Kong et al. 2021
AK1253-1	yMaM330 (MATalpha can1Δ::STE2pr-SpHIS5 lyp1Δ::STE3pr-LEU2 his3Δ1 leu2Δ0 ura3Δ0 leu2Δ0::GAL1pr-I-SCEI-natNT2) HSM3-mCherry-sfGFP gid4Δ::kanMX	Kong et al. 2021
AK1258-1	yMaM330 (MATalpha can1Δ::STE2pr-SpHIS5 lyp1Δ::STE3pr-LEU2 his3Δ1 leu2Δ0 ura3Δ0 leu2Δ0::GAL1pr-I-SCEI-natNT2) GPM3-mCherry-sfGFP gid9Δ::kanMX	Kong et al. 2021
AK1261	YMaM330 CPA1-mCherry-sfGFP gid5Δ::kanMX6	Kong et al. 2021
AK1262-3	yMaM1080 (yMaM330 CPA1-mCherry-sfGFP) gid7Δ::kanMX	Kong et al. 2021
AK1264-1	yMaM330 (MATalpha can1Δ::STE2pr-SpHIS5 lyp1Δ::STE3pr-LEU2 his3Δ1 leu2Δ0 ura3Δ0 leu2Δ0::GAL1pr-I-SCEI-natNT2) CPA1-mCherry-sfGFP gid9Δ::kanMX	Kong et al. 2021
AK1269-1	yMaM330 (MATalpha can1Δ::STE2pr-SpHIS5 lyp1Δ::STE3pr-LEU2 his3Δ1 leu2Δ0 ura3Δ0 leu2Δ0::GAL1pr-I-SCEI-natNT2) PHM8-mCherry-sfGFP gid9Δ::kanMX	Kong et al. 2021
AK1274-2	yMaM330 (MATalpha can1Δ::STE2pr-SpHIS5 lyp1Δ::STE3pr-LEU2 his3Δ1 leu2Δ0 ura3Δ0 leu2Δ0::GAL1pr-I-SCEI-natNT2) BLM10-mCherry-sfGFP gid9Δ::kanMX	Kong et al. 2021

AK1280-1	yMaM330 (MATalpha can1Δ::STE2pr-SpHIS5 lyp1Δ::STE3pr-LEU2 his3Δ1 leu2Δ0 ura3Δ0 leu2Δ0::GAL1pr-I-SCEI-natNT2) MDH2-mCherry-sfGFP gid9Δ::kanMX	Kong et al. 2021
AK1285-1	yMaM330 (MATalpha can1Δ::STE2pr-SpHIS5 lyp1Δ::STE3pr-LEU2 his3Δ1 leu2Δ0 ura3Δ0 leu2Δ0::GAL1pr-I-SCEI-natNT2) YOR283W-mCherry-sfGFP gid9Δ::kanMX	Kong et al. 2021
AK1288	YMaM330 YDR222W-mCherry-sfGFP gid5Δ::kanMX6	Kong et al. 2021
AK1291-2	yMaM330 (MATalpha can1Δ::STE2pr-SpHIS5 lyp1Δ::STE3pr-LEU2 his3Δ1 leu2Δ0 ura3Δ0 leu2Δ0::GAL1pr-I-SCEI-natNT2) YDR222W-mCherry-sfGFP gid9Δ::kanMX	Anton Khmelinskii/Knop lab
BY4741	MATa his3Δ1 leu2Δ0 met15Δ0 ura3Δ0	Brachmann et al. 1998
BY4742	MATalpha his3Δ1 leu2Δ0 lys2Δ0 ura3Δ0	Brachmann et al. 1998
Hap YKO_mQC	BY4741 MATa orfΔ::kanMX	Winzeler et al. 1999
-Ura Gid hits library	yMaM330 (MATalpha can1Δ::STE2pr-SpHIS5 lyp1Δ::STE3pr-LEU2 his3Δ1 leu2Δ0 ura3Δ0 leu2Δ0::GAL1pr-I-SCEI-natNT2) ORF-mCherry-SceI-SpCYC1term-ScURA3-SceI-mCherryΔN-sfGFP	Kong et al. 2025
yAH0001-1	yCPO0053 (MATalpha can1Δ::STE2pr-SpHIS5 lyp1Δ::STE3pr-LEU2 his3Δ1 leu2Δ0 ura3Δ0 leu2Δ0::GAL1pr-I-SCEI-natNT2 CPA1-mCherry-sfGFP) gid2Δ::KanMX	Haschke 2023
yAH0002	yMaM330 + p413-GPD	Haschke 2023
yAH0003-1	yCPO0053 (MATalpha can1Δ::STE2pr-SpHIS5 lyp1Δ::STE3pr-LEU2 his3Δ1 leu2Δ0 ura3Δ0 leu2Δ0::GAL1pr-I-SCEI-natNT2 CPA1-mCherry-sfGFP) gid8Δ::KanMX	Haschke 2023
yCPO0001	MATalpha can1Δ::STE2pr-SpHIS5 lyp1Δ::STE3pr-LEU2 his3Δ1 leu2Δ0 ura3Δ0 leu2Δ0::GAL1pr-I-SCEI-natNT2 HSM3-mCherry-sfGFP gid9Δ::kanMX	This study
yCPO0002	MATalpha can1Δ::STE2pr-SpHIS5 lyp1Δ::STE3pr-LEU2 his3Δ1 leu2Δ0 ura3Δ0 leu2Δ0::GAL1pr-I-SCEI-natNT2 MCM7-mCherry-sfGFP gid9Δ::kanMX	This study
yCPO0003	MATalpha can1Δ::STE2pr-SpHIS5 lyp1Δ::STE3pr-LEU2 his3Δ1 leu2Δ0 ura3Δ0 leu2Δ0::GAL1pr-I-SCEI-natNT2 SSD1-mCherry-sfGFP gid9Δ::kanMX	This study
yCPO0004	MATalpha can1Δ::STE2pr-SpHIS5 lyp1Δ::STE3pr-LEU2 his3Δ1 leu2Δ0 ura3Δ0 leu2Δ0::GAL1pr-I-SCEI-natNT2 HSM3-mCherry-sfGFP	This study
yCPO0005	MATalpha can1Δ::STE2pr-SpHIS5 lyp1Δ::STE3pr-LEU2 his3Δ1 leu2Δ0 ura3Δ0 leu2Δ0::GAL1pr-I-SCEI-natNT2 MCM7-mCherry-sfGFP	This study
yCPO0006	MATalpha can1Δ::STE2pr-SpHIS5 lyp1Δ::STE3pr-LEU2 his3Δ1 leu2Δ0 ura3Δ0 leu2Δ0::GAL1pr-I-SCEI-natNT2 SSD1-mCherry-sfGFP	This study
yCPO0007	MATalpha can1Δ::STE2pr-SpHIS5 lyp1Δ::STE3pr-LEU2 his3Δ1 leu2Δ0 ura3Δ0 leu2Δ0::GAL1pr-I-SCEI-natNT2 HSM3-mCherry-sfGFP nit3Δ::hphNT	This study
yCPO0008	MATalpha can1Δ::STE2pr-SpHIS5 lyp1Δ::STE3pr-LEU2 his3Δ1 leu2Δ0 ura3Δ0 leu2Δ0::GAL1pr-I-SCEI-natNT2 HSM3-mCherry-sfGFP gid9Δ::KanMX nit3Δ::hphNT	This study

yCPO0009	MATalpha can1Δ::STE2pr-SpHIS5 lyp1Δ::STE3pr-LEU2 his3Δ1 leu2Δ0 ura3Δ0 leu2Δ0::GAL1pr-I-SCEI-natNT2 HSM3-mCherry-sfGFP ylr365wΔ::hphNT	This study
yCPO0010	MATalpha can1Δ::STE2pr-SpHIS5 lyp1Δ::STE3pr-LEU2 his3Δ1 leu2Δ0 ura3Δ0 leu2Δ0::GAL1pr-I-SCEI-natNT2 HSM3-mCherry-sfGFP gid9Δ::KanMX ylr365wΔ::hphNT	This study
yCPO0011	MATalpha can1Δ::STE2pr-SpHIS5 lyp1Δ::STE3pr-LEU2 his3Δ1 leu2Δ0 ura3Δ0 leu2Δ0::GAL1pr-I-SCEI-natNT2 HSM3-mCherry-sfGFP ylr407w::hphNT	This study
yCPO0012	MATalpha can1Δ::STE2pr-SpHIS5 lyp1Δ::STE3pr-LEU2 his3Δ1 leu2Δ0 ura3Δ0 leu2Δ0::GAL1pr-I-SCEI-natNT2 HSM3-mCherry-sfGFP gid9Δ::KanMX ylr407wΔ::hphNT	This study
yCPO0013	MATalpha can1Δ::STE2pr-SpHIS5 lyp1Δ::STE3pr-LEU2 his3Δ1 leu2Δ0 ura3Δ0 leu2Δ0::GAL1pr-I-SCEI-natNT2 HSM3-mCherry-sfGFP ydr344cΔ::hphNT	This study
yCPO0014	MATalpha can1Δ::STE2pr-SpHIS5 lyp1Δ::STE3pr-LEU2 his3Δ1 leu2Δ0 ura3Δ0 leu2Δ0::GAL1pr-I-SCEI-natNT2 HSM3-mCherry-sfGFP gid9Δ::KanMX ydr344cΔ::hphNT	This study
yCPO0015	MATalpha can1Δ::STE2pr-SpHIS5 lyp1Δ::STE3pr-LEU2 his3Δ1 leu2Δ0 ura3Δ0 leu2Δ0::GAL1pr-I-SCEI-natNT2 HSM3-mCherry-sfGFP rcr1Δ::hphNT	This study
yCPO0016	MATalpha can1Δ::STE2pr-SpHIS5 lyp1Δ::STE3pr-LEU2 his3Δ1 leu2Δ0 ura3Δ0 leu2Δ0::GAL1pr-I-SCEI-natNT2 HSM3-mCherry-sfGFP gid9Δ::KanMX rcr1Δ::hphNT	This study
yCPO0017	MATalpha can1Δ::STE2pr-SpHIS5 lyp1Δ::STE3pr-LEU2 his3Δ1 leu2Δ0 ura3Δ0 leu2Δ0::GAL1pr-I-SCEI-natNT2 HSM3-mCherry-sfGFP bem4Δ::hphNT	This study
yCPO0018	MATalpha can1Δ::STE2pr-SpHIS5 lyp1Δ::STE3pr-LEU2 his3Δ1 leu2Δ0 ura3Δ0 leu2Δ0::GAL1pr-I-SCEI-natNT2 HSM3-mCherry-sfGFP gid9Δ::KanMX bem4Δ::hphNT	This study
yCPO0019	MATalpha can1Δ::STE2pr-SpHIS5 lyp1Δ::STE3pr-LEU2 his3Δ1 leu2Δ0 ura3Δ0 leu2Δ0::GAL1pr-I-SCEI-natNT2 HSM3-mCherry-sfGFP ubp15Δ::hphNT	This study
yCPO0020	MATalpha can1Δ::STE2pr-SpHIS5 lyp1Δ::STE3pr-LEU2 his3Δ1 leu2Δ0 ura3Δ0 leu2Δ0::GAL1pr-I-SCEI-natNT2 HSM3-mCherry-sfGFP gid9Δ::KanMX ubp15Δ::hphNT	This study
yCPO0021	MATalpha can1Δ::STE2pr-SpHIS5 lyp1Δ::STE3pr-LEU2 his3Δ1 leu2Δ0 ura3Δ0 leu2Δ0::GAL1pr-I-SCEI-natNT2 HSM3-mCherry-sfGFP irc13Δ::hphNT	This study
yCPO0022	MATalpha can1Δ::STE2pr-SpHIS5 lyp1Δ::STE3pr-LEU2 his3Δ1 leu2Δ0 ura3Δ0 leu2Δ0::GAL1pr-I-SCEI-natNT2 HSM3-mCherry-sfGFP gid9Δ::KanMX irc13Δ::hphNT	This study
yCPO0023	MATalpha can1Δ::STE2pr-SpHIS5 lyp1Δ::STE3pr-LEU2 his3Δ1 leu2Δ0 ura3Δ0 leu2Δ0::GAL1pr-I-SCEI-natNT2 HSM3-mCherry-sfGFP bub3Δ::hphNT	This study
yCPO0024	MATalpha can1Δ::STE2pr-SpHIS5 lyp1Δ::STE3pr-LEU2 his3Δ1 leu2Δ0 ura3Δ0 leu2Δ0::GAL1pr-I-SCEI-natNT2 HSM3-mCherry-sfGFP gid9Δ::KanMX bub3Δ::hphNT	This study
yCPO0025	MATalpha can1Δ::STE2pr-SpHIS5 lyp1Δ::STE3pr-LEU2 his3Δ1 leu2Δ0 ura3Δ0 leu2Δ0::GAL1pr-I-SCEI-natNT2 HSM3-mCherry-sfGFP gid9Δ::KanMX ygl149wΔ::hphNT	This study
yCPO0026	MATalpha can1Δ::STE2pr-SpHIS5 lyp1Δ::STE3pr-LEU2 his3Δ1 leu2Δ0 ura3Δ0 leu2Δ0::GAL1pr-I-SCEI-natNT2 MCM7-mCherry-sfGFP vps9Δ::hphNT	This study
yCPO0027	MATalpha can1Δ::STE2pr-SpHIS5 lyp1Δ::STE3pr-LEU2 his3Δ1 leu2Δ0 ura3Δ0 leu2Δ0::GAL1pr-I-SCEI-	This study

	natNT2 MCM7-mCherry-sfGFP gid9Δ::KanMX vps9Δ::hphNT	
yCPO0028	MATalpha can1Δ::STE2pr-SpHIS5 lyp1Δ::STE3pr-LEU2 his3Δ1 leu2Δ0 ura3Δ0 leu2Δ0::GAL1pr-I-SCEI-natNT2 MCM7-mCherry-sfGFP ymr141cΔ::hphNT	This study
yCPO0029	MATalpha can1Δ::STE2pr-SpHIS5 lyp1Δ::STE3pr-LEU2 his3Δ1 leu2Δ0 ura3Δ0 leu2Δ0::GAL1pr-I-SCEI-natNT2 MCM7-mCherry-sfGFP gid9Δ::KanMX ymr141cΔ::hphNT	This study
yCPO0030	MATalpha can1Δ::STE2pr-SpHIS5 lyp1Δ::STE3pr-LEU2 his3Δ1 leu2Δ0 ura3Δ0 leu2Δ0::GAL1pr-I-SCEI-natNT2 MCM7-mCherry-sfGFP cdc26Δ::hphNT	This study
yCPO0031	MATalpha can1Δ::STE2pr-SpHIS5 lyp1Δ::STE3pr-LEU2 his3Δ1 leu2Δ0 ura3Δ0 leu2Δ0::GAL1pr-I-SCEI-natNT2 MCM7-mCherry-sfGFP gid9Δ::KanMX cdc26Δ::hphNT	This study
yCPO0032	MATalpha can1Δ::STE2pr-SpHIS5 lyp1Δ::STE3pr-LEU2 his3Δ1 leu2Δ0 ura3Δ0 leu2Δ0::GAL1pr-I-SCEI-natNT2 SSD1-mCherry-sfGFP ubc12Δ::hphNT	This study
yCPO0033	MATalpha can1Δ::STE2pr-SpHIS5 lyp1Δ::STE3pr-LEU2 his3Δ1 leu2Δ0 ura3Δ0 leu2Δ0::GAL1pr-I-SCEI-natNT2 SSD1-mCherry-sfGFP tma10Δ::hphNT	This study
yCPO0034	MATalpha can1Δ::STE2pr-SpHIS5 lyp1Δ::STE3pr-LEU2 his3Δ1 leu2Δ0 ura3Δ0 leu2Δ0::GAL1pr-I-SCEI-natNT2 SSD1-mCherry-sfGFP gid9Δ::KanMX tma10Δ::hphNT	This study
yCPO0035	MATalpha can1Δ::STE2pr-SpHIS5 lyp1Δ::STE3pr-LEU2 his3Δ1 leu2Δ0 ura3Δ0 leu2Δ0::GAL1pr-I-SCEI-natNT2 SSD1-mCherry-sfGFP mho1Δ::hphNT	This study
yCPO0036	MATalpha can1Δ::STE2pr-SpHIS5 lyp1Δ::STE3pr-LEU2 his3Δ1 leu2Δ0 ura3Δ0 leu2Δ0::GAL1pr-I-SCEI-natNT2 SSD1-mCherry-sfGFP gid9Δ::KanMX mho1Δ::hphNT	This study
yCPO0040	MATalpha can1Δ::STE2pr-SpHIS5 lyp1Δ::STE3pr-LEU2 his3Δ1 leu2Δ0 ura3Δ0 leu2Δ0::GAL1pr-I-SCEI-natNT2 SSD1-mCherry-sfGFP moh1Δ::hphNT	This study
yCPO0041	MATalpha can1Δ::STE2pr-SpHIS5 lyp1Δ::STE3pr-LEU2 his3Δ1 leu2Δ0 ura3Δ0 leu2Δ0::GAL1pr-I-SCEI-natNT2 SSD1-mCherry-sfGFP gid9Δ::KanMX moh1Δ::hphNT	This study
yCPO0042	MATalpha can1Δ::STE2pr-SpHIS5 lyp1Δ::STE3pr-LEU2 his3Δ1 leu2Δ0 ura3Δ0 leu2Δ0::GAL1pr-I-SCEI-natNT2 YDR222W-mCherry-sfGFP doa1Δ::hphNT	This study
yCPO0043	yMaM330 (MATalpha can1Δ::STE2pr-SpHIS5 lyp1Δ::STE3pr-LEU2 his3Δ1 leu2Δ0 ura3Δ0 leu2Δ0::GAL1pr-I-SCEI-natNT2) YDR222W-mCherry-sfGFP gid9Δ::kanMX doa1Δ::hphNT	This study
yCPO0044	MATalpha can1Δ::STE2pr-SpHIS5 lyp1Δ::STE3pr-LEU2 his3Δ1 leu2Δ0 ura3Δ0 leu2Δ0::GAL1pr-I-SCEI-natNT2 SSD1-mCherry-sfGFP gid9Δ::KanMX ubc12Δ::hphNT	This study
yCPO0045	MATalpha can1Δ::STE2pr-SpHIS5 lyp1Δ::STE3pr-LEU2 his3Δ1 leu2Δ0 ura3Δ0 leu2Δ0::GAL1pr-I-SCEI-natNT2 HSM3-mCherry-sfGFP ygl149wΔ::hphNT	This study
yCPO0052	MATalpha can1Δ::STE2pr-SpHIS5 lyp1Δ::STE3pr-LEU2 his3Δ1 leu2Δ0 ura3Δ0 leu2Δ0::GAL1pr-I-SCEI-natNT2 PHM8-mCherry-sfGFP	This study

yCPO0053	MATalpha can1Δ::STE2pr-SpHIS5 lyp1Δ::STE3pr-LEU2 his3Δ1 leu2Δ0 ura3Δ0 leu2Δ0::GAL1pr-I-SCEI-natNT2 CPA1-mCherry-sfGFP	This study
yCPO0054	MATalpha can1Δ::STE2pr-SpHIS5 lyp1Δ::STE3pr-LEU2 his3Δ1 leu2Δ0 ura3Δ0 leu2Δ0::GAL1pr-I-SCEI-natNT2 SSD1-mCherry-sfGFP gid9Δ::kanMX	This study
yCPO0055	yKEK261 (BY4741 map1Δ::kanMX) + pRS316-MAP1pr-MAP1-MAP1ter	This study
yCPO0056-1	BY4741 (MATa his3Δ1 leu2Δ0 met15Δ0 ura3Δ0) nta1Δ::KanMX	This study
yCPO0057-1	BY4742 (MATalpha his3Δ1 leu2Δ0 lys2Δ0 ura3Δ0) nta1Δ::NatNT2	This study
yCPO0058-1	BY4742 (MATalpha his3Δ1 leu2Δ0 lys2Δ0 ura3Δ0) ate1Δ::NatNT2	This study
yCPO0059-1	yKEK261 (BY4741 map1Δ::kanMX) map2Δ::hphNT + pRS316-MAP1pr-MAP1-MAP1ter	This study
yCPO0060	BY4741 nta1Δ::KanMX ate1Δ::hphNT	This study
yCPO0063-1	yCPO0053 (MATalpha can1Δ::STE2pr-SpHIS5 lyp1Δ::STE3pr-LEU2 his3Δ1 leu2Δ0 ura3Δ0 leu2Δ0::GAL1pr-I-SCEI-natNT2 CPA1-mCherry-sfGFP) cpa1Δ::(GAL1-I-SCEI KanMX KlURA3)	This study
yCPO0064-1	BY4741 PFK2 T2A	This study
yCPO0065-1	yCPO0053 (MATalpha can1Δ::STE2pr-SpHIS5 lyp1Δ::STE3pr-LEU2 his3Δ1 leu2Δ0 ura3Δ0 leu2Δ0::GAL1pr-I-SCEI-natNT2 CPA1-mCherry-sfGFP) CPA1 T6S, T9S, T33S, T36S, T37S, T47S	This study
yCPO0066-1	yKEK261 (BY4741 map1Δ::kanMX) map2Δ::hphNT	This study
yCPO0067-1	yCPO0055 (BY4741 map1Δ::kanMX + pRS316-MAP1pr-MAP1-MAP1ter) map2Δ::hphNT	This study
yCPO0068-1	MATalpha can1Δ::STE2pr-SpHIS5 lyp1Δ::STE3pr-LEU2 his3Δ1 leu2Δ0 ura3Δ0 leu2Δ0::GAL1pr-I-SCEI-natNT2 SSD1-mCherry-sfGFP gid9Δ::KanMX	This study
yCPO0069	BY4741 nta1Δ::KanMX ate1Δ::hphNT + pAnB19-DE	This study
yCPO0070	BY4741 nta1Δ::KanMX ate1Δ::hphNT + pAnB19-DH	This study
yCPO0071	BY4741 nta1Δ::KanMX ate1Δ::hphNT + pAnB19-DR	This study
yCPO0072	BY4741 nta1Δ::KanMX ate1Δ::hphNT + pAnB19-DP	This study
yCPO0073	BY4741 nta1Δ::KanMX ate1Δ::hphNT + pAnB19-EE	This study
yCPO0074	BY4741 nta1Δ::KanMX ate1Δ::hphNT + pAnB19-EH	This study
yCPO0075	BY4741 nta1Δ::KanMX ate1Δ::hphNT + pAnB19-EK	This study
yCPO0076	BY4741 nta1Δ::KanMX ate1Δ::hphNT + pAnB19-ET	This study
yCPO0077	BY4741 nta1Δ::KanMX ate1Δ::hphNT + pAnB19-NP	This study
yCPO0078	BY4741 nta1Δ::KanMX ate1Δ::hphNT + pAnB19-NR	This study
yCPO0079	BY4741 nta1Δ::KanMX ate1Δ::hphNT + pAnB19-QA	This study
yCPO0080	BY4741 nta1Δ::KanMX ate1Δ::hphNT + pAnB19-QH	This study
yCPO0081	BY4741 nta1Δ::KanMX ate1Δ::hphNT + pAnB19-QK	This study
yCPO0082-1	BY4741 (reconstituted from yCPO0062-1)	This study
yCPO0083	BY4741 + pAnB19-DE	This study
yCPO0084	BY4741 + pAnB19-DH	This study
yCPO0085	BY4741 + pAnB19-DR	This study
yCPO0086	BY4741 + pAnB19-DP	This study
yCPO0087	BY4741 + pAnB19-EE	This study

yCPO0088	BY4741 + pAnB19-EH	This study
yCPO0089	BY4741 + pAnB19-EK	This study
yCPO0090	BY4741 + pAnB19-ET	This study
yCPO0091	BY4741 + pAnB19-NP	This study
yCPO0092	BY4741 + pAnB19-NR	This study
yCPO0093	BY4741 + pAnB19-QA	This study
yCPO0094	BY4741 + pAnB19-QH	This study
yCPO0095	BY4741 + pAnB19-QK	This study
yCPO0096-1	BY4742 map2Δ::hphNT	This study
yCPO0097	BY4741 (MATa his3Δ1 leu2Δ0 lys2Δ0 ura3Δ0) ate1Δ::hphNT	This study
yCPO0098-1	BY4741 (reconstituted from yCPO0061-1)	This study
yCPO0099-1	yCPO0053 (MATalpha can1Δ::STE2pr-SpHIS5 lyp1Δ::STE3pr-LEU2 his3Δ1 leu2Δ0 ura3Δ0 leu2Δ0::GAL1pr-I-SCEI-natNT2 CPA1-mCherry-sfGFP) (Reconstituted from yCPO0063)	This study
yCPO0101	MATalpha can1Δ::STE2pr-SpHIS5 lyp1Δ::STE3pr-LEU2 his3Δ1 leu2Δ0 ura3Δ0 leu2Δ0::GAL1pr-I-SCEI-natNT2 SSD1-mCherry-sfGFP gid9Δ::KanMX mho1Δ::hphNT	This study
yCPO0102-1	BY4741 gpm3Δ::(GAL1-I-SCEI KanMX KlURA3)	This study
yCPO0103-1	BY4741 GPM3 T2A	This study
yCPO0104-1	BY4741 (reconstituted from yCPO0102-2)	This study
yCPO0105-1	yCPO0099-1 (MATalpha can1Δ::STE2pr-SpHIS5 lyp1Δ::STE3pr-LEU2 his3Δ1 leu2Δ0 ura3Δ0 leu2Δ0::GAL1pr-I-SCEI-natNT2 CPA1-mCherry-sfGFP) gid9Δ::KanMX	This study
yCPO0106-1	yCPO0065-1 (MATalpha can1Δ::STE2pr-SpHIS5 lyp1Δ::STE3pr-LEU2 his3Δ1 leu2Δ0 ura3Δ0 leu2Δ0::GAL1pr-I-SCEI-natNT2 CPA1-mCherry-sfGFP CPA1 T6S, T9S, T33S, T36S, T37S, T47S) gid9Δ::KanMX	This study
yCPO0108-1	yCPO0099-1 (MATalpha can1Δ::STE2pr-SpHIS5 lyp1Δ::STE3pr-LEU2 his3Δ1 leu2Δ0 ura3Δ0 leu2Δ0::GAL1pr-I-SCEI-natNT2 CPA1-mCherry-sfGFP) gid11Δ::KanMX	This study
yCPO0110-1	yCPO0052 (MATalpha can1Δ::STE2pr-SpHIS5 lyp1Δ::STE3pr-LEU2 his3Δ1 leu2Δ0 ura3Δ0 leu2Δ0::GAL1pr-I-SCEI-natNT2 PHM8-mCherry-sfGFP) map2Δ::hphNT	This study
yCPO0111-1	yMaM1091 (MATalpha can1Δ::STE2pr-SpHIS5 lyp1Δ::STE3pr-LEU2 his3Δ1 leu2Δ0 ura3Δ0 leu2Δ0::GAL1pr-I-SCEI-natNT2 MDH2-mCherry-sfGFP) map2Δ::hphNT	This study
yCPO0114	BY4741 + pAnB19-NL	This study
yCPO0115	BY4741 + pAnB19-QL	This study
yCPO0116	BY4741 + pAnB19-DL	This study
yCPO0117	BY4741 + pAnB19-EL	This study
yCPO0118	BY4741 + pAnB19-RK	This study
yCPO0119	BY4741 + pAnB19-TK	This study
yCPO0120	BY4741 nta1Δ::KanMX + pAnB19-NL	This study
yCPO0121	BY4741 nta1Δ::KanMX + pAnB19-QL	This study

yCPO0122	BY4741 nta1Δ::KanMX + pAnB19-DL	This study
yCPO0123	BY4741 nta1Δ::KanMX + pAnB19-EL	This study
yCPO0124	BY4741 nta1Δ::KanMX + pAnB19-RK	This study
yCPO0125	BY4741 nta1Δ::KanMX + pAnB19-TK	This study
yCPO0126	BY4741 ate1Δ::hphNT + pAnB19-NL	This study
yCPO0127	BY4741 ate1Δ::hphNT + pAnB19-QL	This study
yCPO0128	BY4741 ate1Δ::hphNT + pAnB19-DL	This study
yCPO0129	BY4741 ate1Δ::hphNT + pAnB19-EL	This study
yCPO0130	BY4741 ate1Δ::hphNT + pAnB19-RK	This study
yCPO0131	BY4741 ate1Δ::hphNT + pAnB19-TK	This study
yCPO0133	BY4741 nta1Δ::KanMX ate1Δ::hphNT + pAnB19-NA	This study
yCPO0134	BY4741 nta1Δ::KanMX ate1Δ::hphNT + pAnB19-NC	This study
yCPO0135	BY4741 nta1Δ::KanMX ate1Δ::hphNT + pAnB19-ND	This study
yCPO0136	BY4741 nta1Δ::KanMX ate1Δ::hphNT + pAnB19-NE	This study
yCPO0137	BY4741 nta1Δ::KanMX ate1Δ::hphNT + pAnB19-NF	This study
yCPO0138	BY4741 nta1Δ::KanMX ate1Δ::hphNT + pAnB19-NG	This study
yCPO0139	BY4741 nta1Δ::KanMX ate1Δ::hphNT + pAnB19-NH	This study
yCPO0140	BY4741 nta1Δ::KanMX ate1Δ::hphNT + pAnB19-NI	This study
yCPO0141	BY4741 nta1Δ::KanMX ate1Δ::hphNT + pAnB19-NK	This study
yCPO0142	BY4741 nta1Δ::KanMX ate1Δ::hphNT + pAnB19-NL	This study
yCPO0143	BY4741 nta1Δ::KanMX ate1Δ::hphNT + pAnB19-NM	This study
yCPO0144	BY4741 nta1Δ::KanMX ate1Δ::hphNT + pAnB19-NN	This study
yCPO0145	BY4741 nta1Δ::KanMX ate1Δ::hphNT + pAnB19-NP	This study
yCPO0146	BY4741 nta1Δ::KanMX ate1Δ::hphNT + pAnB19-NQ	This study
yCPO0147	BY4741 nta1Δ::KanMX ate1Δ::hphNT + pAnB19-NR	This study
yCPO0148	BY4741 nta1Δ::KanMX ate1Δ::hphNT + pAnB19-NS	This study
yCPO0149	BY4741 nta1Δ::KanMX ate1Δ::hphNT + pAnB19-NT	This study
yCPO0150	BY4741 nta1Δ::KanMX ate1Δ::hphNT + pAnB19-NV	This study
yCPO0151	BY4741 nta1Δ::KanMX ate1Δ::hphNT + pAnB19-NW	This study
yCPO0152	BY4741 nta1Δ::KanMX ate1Δ::hphNT + pAnB19-NY	This study
yCPO0153	BY4741 nta1Δ::KanMX ate1Δ::hphNT + pAnB19-QA	This study
yCPO0154	BY4741 nta1Δ::KanMX ate1Δ::hphNT + pAnB19-QC	This study
yCPO0155	BY4741 nta1Δ::KanMX ate1Δ::hphNT + pAnB19-QD	This study
yCPO0156	BY4741 nta1Δ::KanMX ate1Δ::hphNT + pAnB19-QE	This study
yCPO0157	BY4741 nta1Δ::KanMX ate1Δ::hphNT + pAnB19-QF	This study
yCPO0158	BY4741 nta1Δ::KanMX ate1Δ::hphNT + pAnB19-QG	This study
yCPO0159	BY4741 nta1Δ::KanMX ate1Δ::hphNT + pAnB19-QH	This study
yCPO0160	BY4741 nta1Δ::KanMX ate1Δ::hphNT + pAnB19-QI	This study
yCPO0161	BY4741 nta1Δ::KanMX ate1Δ::hphNT + pAnB19-QK	This study
yCPO0162	BY4741 nta1Δ::KanMX ate1Δ::hphNT + pAnB19-QL	This study
yCPO0163	BY4741 nta1Δ::KanMX ate1Δ::hphNT + pAnB19-QM	This study
yCPO0164	BY4741 nta1Δ::KanMX ate1Δ::hphNT + pAnB19-QN	This study
yCPO0165	BY4741 nta1Δ::KanMX ate1Δ::hphNT + pAnB19-QP	This study
yCPO0166	BY4741 nta1Δ::KanMX ate1Δ::hphNT + pAnB19-QQ	This study
yCPO0167	BY4741 nta1Δ::KanMX ate1Δ::hphNT + pAnB19-QR	This study

yCPO0168	BY4741 nta1Δ::KanMX ate1Δ::hphNT + pAnB19-QS	This study
yCPO0169	BY4741 nta1Δ::KanMX ate1Δ::hphNT + pAnB19-QT	This study
yCPO0170	BY4741 nta1Δ::KanMX ate1Δ::hphNT + pAnB19-QV	This study
yCPO0171	BY4741 nta1Δ::KanMX ate1Δ::hphNT + pAnB19-QW	This study
yCPO0172	BY4741 nta1Δ::KanMX ate1Δ::hphNT + pAnB19-QY	This study
yCPO0173	BY4741 nta1Δ::KanMX ate1Δ::hphNT + pAnB19-DA	This study
yCPO0174	BY4741 nta1Δ::KanMX ate1Δ::hphNT + pAnB19-DC	This study
yCPO0175	BY4741 nta1Δ::KanMX ate1Δ::hphNT + pAnB19-DD	This study
yCPO0176	BY4741 nta1Δ::KanMX ate1Δ::hphNT + pAnB19-DE	This study
yCPO0177	BY4741 nta1Δ::KanMX ate1Δ::hphNT + pAnB19-DF	This study
yCPO0178	BY4741 nta1Δ::KanMX ate1Δ::hphNT + pAnB19-DG	This study
yCPO0179	BY4741 nta1Δ::KanMX ate1Δ::hphNT + pAnB19-DH	This study
yCPO0180	BY4741 nta1Δ::KanMX ate1Δ::hphNT + pAnB19-DI	This study
yCPO0181	BY4741 nta1Δ::KanMX ate1Δ::hphNT + pAnB19-DK	This study
yCPO0182	BY4741 nta1Δ::KanMX ate1Δ::hphNT + pAnB19-DL	This study
yCPO0183	BY4741 nta1Δ::KanMX ate1Δ::hphNT + pAnB19-DM	This study
yCPO0184	BY4741 nta1Δ::KanMX ate1Δ::hphNT + pAnB19-DN	This study
yCPO0185	BY4741 nta1Δ::KanMX ate1Δ::hphNT + pAnB19-DP	This study
yCPO0186	BY4741 nta1Δ::KanMX ate1Δ::hphNT + pAnB19-DQ	This study
yCPO0187	BY4741 nta1Δ::KanMX ate1Δ::hphNT + pAnB19-DR	This study
yCPO0188	BY4741 nta1Δ::KanMX ate1Δ::hphNT + pAnB19-DS	This study
yCPO0189	BY4741 nta1Δ::KanMX ate1Δ::hphNT + pAnB19-DT	This study
yCPO0190	BY4741 nta1Δ::KanMX ate1Δ::hphNT + pAnB19-DV	This study
yCPO0191	BY4741 nta1Δ::KanMX ate1Δ::hphNT + pAnB19-DW	This study
yCPO0192	BY4741 nta1Δ::KanMX ate1Δ::hphNT + pAnB19-DY	This study
yCPO0193	BY4741 nta1Δ::KanMX ate1Δ::hphNT + pAnB19-EA	This study
yCPO0194	BY4741 nta1Δ::KanMX ate1Δ::hphNT + pAnB19-EC	This study
yCPO0195	BY4741 nta1Δ::KanMX ate1Δ::hphNT + pAnB19-ED	This study
yCPO0196	BY4741 nta1Δ::KanMX ate1Δ::hphNT + pAnB19-EE	This study
yCPO0197	BY4741 nta1Δ::KanMX ate1Δ::hphNT + pAnB19-EF	This study
yCPO0198	BY4741 nta1Δ::KanMX ate1Δ::hphNT + pAnB19-EG	This study
yCPO0199	BY4741 nta1Δ::KanMX ate1Δ::hphNT + pAnB19-EH	This study
yCPO0200	BY4741 nta1Δ::KanMX ate1Δ::hphNT + pAnB19-EI	This study
yCPO0201	BY4741 nta1Δ::KanMX ate1Δ::hphNT + pAnB19-EK	This study
yCPO0202	BY4741 nta1Δ::KanMX ate1Δ::hphNT + pAnB19-EL	This study
yCPO0203	BY4741 nta1Δ::KanMX ate1Δ::hphNT + pAnB19-EM	This study
yCPO0204	BY4741 nta1Δ::KanMX ate1Δ::hphNT + pAnB19-EN	This study
yCPO0205	BY4741 nta1Δ::KanMX ate1Δ::hphNT + pAnB19-EP	This study
yCPO0206	BY4741 nta1Δ::KanMX ate1Δ::hphNT + pAnB19-EQ	This study
yCPO0207	BY4741 nta1Δ::KanMX ate1Δ::hphNT + pAnB19-ER	This study
yCPO0208	BY4741 nta1Δ::KanMX ate1Δ::hphNT + pAnB19-ES	This study
yCPO0209	BY4741 nta1Δ::KanMX ate1Δ::hphNT + pAnB19-ET	This study
yCPO0210	BY4741 nta1Δ::KanMX ate1Δ::hphNT + pAnB19-EV	This study
yCPO0211	BY4741 nta1Δ::KanMX ate1Δ::hphNT + pAnB19-EW	This study
yCPO0212	BY4741 nta1Δ::KanMX ate1Δ::hphNT + pAnB19-EY	This study

yCPO0221-1	yCPO0053 (MATalpha can1Δ::STE2pr-SpHIS5 lyp1Δ::STE3pr-LEU2 his3Δ1 leu2Δ0 ura3Δ0 leu2Δ0::GAL1pr-I-SCEI-natNT2 CPA1-mCherry-sfGFP) gid11Δ::KanMX	This study
yCPO0222-1	yCPO0099-1 (MATalpha can1Δ::STE2pr-SpHIS5 lyp1Δ::STE3pr-LEU2 his3Δ1 leu2Δ0 ura3Δ0 leu2Δ0::GAL1pr-I-SCEI-natNT2 CPA1-mCherry-sfGFP) gid11Δ::KanMX	This study
yCPO0223-1	yCPO0099-2 (MATalpha can1Δ::STE2pr-SpHIS5 lyp1Δ::STE3pr-LEU2 his3Δ1 leu2Δ0 ura3Δ0 leu2Δ0::GAL1pr-I-SCEI-natNT2 CPA1-mCherry-sfGFP) gid11Δ::KanMX	This study
yCPO0225	MATalpha can1Δ::STE2pr-SpHIS5 lyp1Δ::STE3pr-LEU2 his3Δ1 leu2Δ0 ura3Δ0 leu2Δ0::GAL1pr-I-SCEI-natNT2 SEG1-mCherry-sfGFP	This study
yCPO0226	MATalpha can1Δ::STE2pr-SpHIS5 lyp1Δ::STE3pr-LEU2 his3Δ1 leu2Δ0 ura3Δ0 leu2Δ0::GAL1pr-I-SCEI-natNT2 CPA1-mCherry-sfGFP gid9Δ::KanMX blm10Δ::hphNT	This study
yCPO0227-1	MATalpha can1Δ::STE2pr-SpHIS5 lyp1Δ::STE3pr-LEU2 his3Δ1 leu2Δ0 ura3Δ0 leu2Δ0::GAL1pr-I-SCEI-natNT2 CPA1-mCherry-sfGFP gid9Δ::KanMX dbp3Δ::hphNT	This study
yCPO0228-1	MATalpha can1Δ::STE2pr-SpHIS5 lyp1Δ::STE3pr-LEU2 his3Δ1 leu2Δ0 ura3Δ0 leu2Δ0::GAL1pr-I-SCEI-natNT2 CPA1-mCherry-sfGFP gid9Δ::KanMX dld3Δ::hphNT	This study
yCPO0229-1	MATalpha can1Δ::STE2pr-SpHIS5 lyp1Δ::STE3pr-LEU2 his3Δ1 leu2Δ0 ura3Δ0 leu2Δ0::GAL1pr-I-SCEI-natNT2 CPA1-mCherry-sfGFP gid9Δ::KanMX gpm3Δ::hphNT	This study
yCPO0230-1	MATalpha can1Δ::STE2pr-SpHIS5 lyp1Δ::STE3pr-LEU2 his3Δ1 leu2Δ0 ura3Δ0 leu2Δ0::GAL1pr-I-SCEI-natNT2 CPA1-mCherry-sfGFP gid9Δ::KanMX lys20Δ::hphNT	This study
yCPO0231-1	MATalpha can1Δ::STE2pr-SpHIS5 lyp1Δ::STE3pr-LEU2 his3Δ1 leu2Δ0 ura3Δ0 leu2Δ0::GAL1pr-I-SCEI-natNT2 CPA1-mCherry-sfGFP gid9Δ::KanMX phm8Δ::hphNT	This study
yCPO0232-1	MATalpha can1Δ::STE2pr-SpHIS5 lyp1Δ::STE3pr-LEU2 his3Δ1 leu2Δ0 ura3Δ0 leu2Δ0::GAL1pr-I-SCEI-natNT2 CPA1-mCherry-sfGFP gid9Δ::KanMX stf2Δ::hphNT	This study
yCPO0233-1	MATalpha can1Δ::STE2pr-SpHIS5 lyp1Δ::STE3pr-LEU2 his3Δ1 leu2Δ0 ura3Δ0 leu2Δ0::GAL1pr-I-SCEI-natNT2 CPA1-mCherry-sfGFP gid9Δ::KanMX tma10Δ::hphNT	This study
yCPO0234-1	MATalpha can1Δ::STE2pr-SpHIS5 lyp1Δ::STE3pr-LEU2 his3Δ1 leu2Δ0 ura3Δ0 leu2Δ0::GAL1pr-I-SCEI-natNT2 CPA1-mCherry-sfGFP gid9Δ::KanMX top1Δ::hphNT	This study
yCPO0235-1	MATalpha can1Δ::STE2pr-SpHIS5 lyp1Δ::STE3pr-LEU2 his3Δ1 leu2Δ0 ura3Δ0 leu2Δ0::GAL1pr-I-SCEI-natNT2 CPA1-mCherry-sfGFP gid9Δ::KanMX yor283wΔ::hphNT	This study
yCPO0236-1	MATalpha can1Δ::STE2pr-SpHIS5 lyp1Δ::STE3pr-LEU2 his3Δ1 leu2Δ0 ura3Δ0 leu2Δ0::GAL1pr-I-SCEI-natNT2 SEG1-mCherry-sfGFP gid9Δ::KanMX	This study
yCPO0237-1	MATalpha can1Δ::STE2pr-SpHIS5 lyp1Δ::STE3pr-LEU2 his3Δ1 leu2Δ0 ura3Δ0 leu2Δ0::GAL1pr-I-SCEI-natNT2 YDR222W-mCherry-sfGFP gid9Δ::KanMX	This study
yCPO0238	MATalpha can1Δ::STE2pr-SpHIS5 lyp1Δ::STE3pr-LEU2 his3Δ1 leu2Δ0 ura3Δ0 leu2Δ0::GAL1pr-I-SCEI-natNT2 CPA1-mCherry-sfGFP gid9Δ::KanMX acs2Δ::hphNT	This study
yCPO0239-1	MATalpha can1Δ::STE2pr-SpHIS5 lyp1Δ::STE3pr-LEU2 his3Δ1 leu2Δ0 ura3Δ0 leu2Δ0::GAL1pr-I-SCEI-natNT2 CPA1-mCherry-sfGFP gid9Δ::KanMX pfk2Δ::hphNT	This study

yCPO0242	MATalpha can1Δ::STE2pr-SpHIS5 lyp1Δ::STE3pr-LEU2 his3Δ1 leu2Δ0 ura3Δ0 leu2Δ0::GAL1pr-I-SCEI-natNT2 YDR222W-mCherry-sfGFP pRS413-GPD	This study
yCPO0243	MATalpha can1Δ::STE2pr-SpHIS5 lyp1Δ::STE3pr-LEU2 his3Δ1 leu2Δ0 ura3Δ0 leu2Δ0::GAL1pr-I-SCEI-natNT2 YDR222W-mCherry-sfGFP pRS413-GPDpr-MOH1-CYCter	This study
yCPO0244	MATalpha can1Δ::STE2pr-SpHIS5 lyp1Δ::STE3pr-LEU2 his3Δ1 leu2Δ0 ura3Δ0 leu2Δ0::GAL1pr-I-SCEI-natNT2 YDR222W-mCherry-sfGFP gid9Δ::KanMX pRS413-GPD	This study
yCPO0245	MATalpha can1Δ::STE2pr-SpHIS5 lyp1Δ::STE3pr-LEU2 his3Δ1 leu2Δ0 ura3Δ0 leu2Δ0::GAL1pr-I-SCEI-natNT2 YDR222W-mCherry-sfGFP gid9Δ::KanMX pRS413-GPDpr-MOH1-CYCter	This study
yCPO0246	MATalpha can1Δ::STE2pr-SpHIS5 lyp1Δ::STE3pr-LEU2 his3Δ1 leu2Δ0 ura3Δ0 leu2Δ0::GAL1pr-I-SCEI-natNT2 SEG1-mCherry-sfGFP pRS413-GPD	This study
yCPO0247	MATalpha can1Δ::STE2pr-SpHIS5 lyp1Δ::STE3pr-LEU2 his3Δ1 leu2Δ0 ura3Δ0 leu2Δ0::GAL1pr-I-SCEI-natNT2 SEG1-mCherry-sfGFP pRS413-GPDpr-MOH1-CYCter	This study
yCPO0248	MATalpha can1Δ::STE2pr-SpHIS5 lyp1Δ::STE3pr-LEU2 his3Δ1 leu2Δ0 ura3Δ0 leu2Δ0::GAL1pr-I-SCEI-natNT2 SEG1-mCherry-sfGFP gid9Δ::KanMX pRS413-GPD	This study
yCPO0249	MATalpha can1Δ::STE2pr-SpHIS5 lyp1Δ::STE3pr-LEU2 his3Δ1 leu2Δ0 ura3Δ0 leu2Δ0::GAL1pr-I-SCEI-natNT2 SEG1-mCherry-sfGFP gid9Δ::KanMX pRS413-GPDpr-MOH1-CYCter	This study
yCPO0250	MATalpha can1Δ::STE2pr-SpHIS5 lyp1Δ::STE3pr-LEU2 his3Δ1 leu2Δ0 ura3Δ0 leu2Δ0::GAL1pr-I-SCEI-natNT2 CPA1-mCherry-sfGFP pRS413-GPD	This study
yCPO0251	MATalpha can1Δ::STE2pr-SpHIS5 lyp1Δ::STE3pr-LEU2 his3Δ1 leu2Δ0 ura3Δ0 leu2Δ0::GAL1pr-I-SCEI-natNT2 CPA1-mCherry-sfGFP pRS413-GPDpr-MOH1-CYCter	This study
yCPO0252	MATalpha can1Δ::STE2pr-SpHIS5 lyp1Δ::STE3pr-LEU2 his3Δ1 leu2Δ0 ura3Δ0 leu2Δ0::GAL1pr-I-SCEI-natNT2 CPA1-mCherry-sfGFP gid9Δ::KanMX pRS413-GPD	This study
yCPO0253	MATalpha can1Δ::STE2pr-SpHIS5 lyp1Δ::STE3pr-LEU2 his3Δ1 leu2Δ0 ura3Δ0 leu2Δ0::GAL1pr-I-SCEI-natNT2 CPA1-mCherry-sfGFP gid9Δ::KanMX pRS413-GPDpr-MOH1-CYCter	This study
yCPO0254	MATalpha can1Δ::STE2pr-SpHIS5 lyp1Δ::STE3pr-LEU2 his3Δ1 leu2Δ0 ura3Δ0 leu2Δ0::GAL1pr-I-SCEI-natNT2 SSD1-mCherry-sfGFP pRS413-GPD	This study
yCPO0255	MATalpha can1Δ::STE2pr-SpHIS5 lyp1Δ::STE3pr-LEU2 his3Δ1 leu2Δ0 ura3Δ0 leu2Δ0::GAL1pr-I-SCEI-natNT2 SSD1-mCherry-sfGFP pRS413-GPDpr-MOH1-CYCter	This study
yCPO0256	MATalpha can1Δ::STE2pr-SpHIS5 lyp1Δ::STE3pr-LEU2 his3Δ1 leu2Δ0 ura3Δ0 leu2Δ0::GAL1pr-I-SCEI-natNT2 SSD1-mCherry-sfGFP gid9Δ::KanMX pRS413-GPD	This study
yCPO0257	MATalpha can1Δ::STE2pr-SpHIS5 lyp1Δ::STE3pr-LEU2 his3Δ1 leu2Δ0 ura3Δ0 leu2Δ0::GAL1pr-I-SCEI-natNT2 SSD1-mCherry-sfGFP gid9Δ::KanMX pRS413-GPDpr-MOH1-CYCter	This study
yCPO0258	MATalpha can1Δ::STE2pr-SpHIS5 lyp1Δ::STE3pr-LEU2 his3Δ1 leu2Δ0 ura3Δ0 leu2Δ0::GAL1pr-I-SCEI-natNT2 UBC8-mCherry-sfGFP pRS413-GPD	This study

yCPO0259	MATalpha can1Δ::STE2pr-SpHIS5 lyp1Δ::STE3pr-LEU2 his3Δ1 leu2Δ0 ura3Δ0 leu2Δ0::GAL1pr-I-SCEI-natNT2 UBC8-mCherry-sfGFP pRS413-GPDpr-MOH1-CYCter	This study
yCPO0260	MATalpha can1Δ::STE2pr-SpHIS5 lyp1Δ::STE3pr-LEU2 his3Δ1 leu2Δ0 ura3Δ0 leu2Δ0::GAL1pr-I-SCEI-natNT2 UBC8-mCherry-sfGFP gid9Δ::KanMX pRS413-GPD	This study
yCPO0261	MATalpha can1Δ::STE2pr-SpHIS5 lyp1Δ::STE3pr-LEU2 his3Δ1 leu2Δ0 ura3Δ0 leu2Δ0::GAL1pr-I-SCEI-natNT2 UBC8-mCherry-sfGFP gid9Δ::KanMX pRS413-GPDpr-MOH1-CYCter	This study
yCPO0262	MATalpha can1Δ::STE2pr-SpHIS5 lyp1Δ::STE3pr-LEU2 his3Δ1 leu2Δ0 ura3Δ0 leu2Δ0::GAL1pr-I-SCEI-natNT2 MDH2-mCherry-sfGFP pRS413-GPD	This study
yCPO0263	MATalpha can1Δ::STE2pr-SpHIS5 lyp1Δ::STE3pr-LEU2 his3Δ1 leu2Δ0 ura3Δ0 leu2Δ0::GAL1pr-I-SCEI-natNT2 MDH2-mCherry-sfGFP pRS413-GPDpr-MOH1-CYCter	This study
yCPO0264	MATalpha can1Δ::STE2pr-SpHIS5 lyp1Δ::STE3pr-LEU2 his3Δ1 leu2Δ0 ura3Δ0 leu2Δ0::GAL1pr-I-SCEI-natNT2 MDH2-mCherry-sfGFP pRS413-GPDpr-IPF1-CYCter	This study
yCPO0265	MATalpha can1Δ::STE2pr-SpHIS5 lyp1Δ::STE3pr-LEU2 his3Δ1 leu2Δ0 ura3Δ0 leu2Δ0::GAL1pr-I-SCEI-natNT2 MDH2-mCherry-sfGFP gid9Δ::kanMX pRS413GPD	This study
yCPO0266	MATalpha can1Δ::STE2pr-SpHIS5 lyp1Δ::STE3pr-LEU2 his3Δ1 leu2Δ0 ura3Δ0 leu2Δ0::GAL1pr-I-SCEI-natNT2 MDH2-mCherry-sfGFP gid9Δ::kanMX pRS413-GPDpr-MOH1-CYCter	This study
yCPO0267	MATalpha can1Δ::STE2pr-SpHIS5 lyp1Δ::STE3pr-LEU2 his3Δ1 leu2Δ0 ura3Δ0 leu2Δ0::GAL1pr-I-SCEI-natNT2 MDH2-mCherry-sfGFP gid9Δ::kanMX pRS413-GPDpr-IPF1-CYCter	This study
yCPO0268	MATalpha can1Δ::STE2pr-SpHIS5 lyp1Δ::STE3pr-LEU2 his3Δ1 leu2Δ0 ura3Δ0 leu2Δ0::GAL1pr-I-SCEI-natNT2 PHM8-mCherry-sfGFP pRS413-GPD	This study
yCPO0269	MATalpha can1Δ::STE2pr-SpHIS5 lyp1Δ::STE3pr-LEU2 his3Δ1 leu2Δ0 ura3Δ0 leu2Δ0::GAL1pr-I-SCEI-natNT2 PHM8-mCherry-sfGFP pRS413-GPDpr-MOH1-CYCter	This study
yCPO0270	MATalpha can1Δ::STE2pr-SpHIS5 lyp1Δ::STE3pr-LEU2 his3Δ1 leu2Δ0 ura3Δ0 leu2Δ0::GAL1pr-I-SCEI-natNT2 PHM8-mCherry-sfGFP pRS413-GPDpr-IPF1-CYCter	This study
yCPO0271	MATalpha can1Δ::STE2pr-SpHIS5 lyp1Δ::STE3pr-LEU2 his3Δ1 leu2Δ0 ura3Δ0 leu2Δ0::GAL1pr-I-SCEI-natNT2 PHM8-mCherry-sfGFP gid9Δ::kanMX pRS413GPD	This study
yCPO0272	MATalpha can1Δ::STE2pr-SpHIS5 lyp1Δ::STE3pr-LEU2 his3Δ1 leu2Δ0 ura3Δ0 leu2Δ0::GAL1pr-I-SCEI-natNT2 PHM8-mCherry-sfGFP gid9Δ::kanMX pRS413-GPDpr-MOH1-CYCter	This study
yCPO0273	MATalpha can1Δ::STE2pr-SpHIS5 lyp1Δ::STE3pr-LEU2 his3Δ1 leu2Δ0 ura3Δ0 leu2Δ0::GAL1pr-I-SCEI-natNT2 PHM8-mCherry-sfGFP gid9Δ::kanMX pRS413-GPDpr-IPF1-CYCter	This study

yCPO0274	MATalpha can1Δ::STE2pr-SpHIS5 lyp1Δ::STE3pr-LEU2 his3Δ1 leu2Δ0 ura3Δ0 leu2Δ0::GAL1pr-I-SCEI-natNT2 GPM3-mCherry-sfGFP pRS413-GPD	This study
yCPO0275	MATalpha can1Δ::STE2pr-SpHIS5 lyp1Δ::STE3pr-LEU2 his3Δ1 leu2Δ0 ura3Δ0 leu2Δ0::GAL1pr-I-SCEI-natNT2 GPM3-mCherry-sfGFP pRS413-GPDpr-MOH1-CYCter	This study
yCPO0276	MATalpha can1Δ::STE2pr-SpHIS5 lyp1Δ::STE3pr-LEU2 his3Δ1 leu2Δ0 ura3Δ0 leu2Δ0::GAL1pr-I-SCEI-natNT2 GPM3-mCherry-sfGFP pRS413-GPDpr-IPF1-CYCter	This study
yCPO0277	MATalpha can1Δ::STE2pr-SpHIS5 lyp1Δ::STE3pr-LEU2 his3Δ1 leu2Δ0 ura3Δ0 leu2Δ0::GAL1pr-I-SCEI-natNT2 GPM3-mCherry-sfGFP gid9Δ::kanMX pRS413GPD	This study
yCPO0278	MATalpha can1Δ::STE2pr-SpHIS5 lyp1Δ::STE3pr-LEU2 his3Δ1 leu2Δ0 ura3Δ0 leu2Δ0::GAL1pr-I-SCEI-natNT2 GPM3-mCherry-sfGFP gid9Δ::kanMX pRS413-GPDpr-MOH1-CYCter	This study
yCPO0279	MATalpha can1Δ::STE2pr-SpHIS5 lyp1Δ::STE3pr-LEU2 his3Δ1 leu2Δ0 ura3Δ0 leu2Δ0::GAL1pr-I-SCEI-natNT2 GPM3-mCherry-sfGFP gid9Δ::kanMX pRS413-GPDpr-IPF1-CYCter	This study
yCPO0280	MATalpha can1Δ::STE2pr-SpHIS5 lyp1Δ::STE3pr-LEU2 his3Δ1 leu2Δ0 ura3Δ0 leu2Δ0::GAL1pr-I-SCEI-natNT2 YOR283W-mCherry-sfGFP pRS413-GPD	This study
yCPO0281	MATalpha can1Δ::STE2pr-SpHIS5 lyp1Δ::STE3pr-LEU2 his3Δ1 leu2Δ0 ura3Δ0 leu2Δ0::GAL1pr-I-SCEI-natNT2 YOR283W-mCherry-sfGFP pRS413-GPDpr-MOH1-CYCter	This study
yCPO0282	MATalpha can1Δ::STE2pr-SpHIS5 lyp1Δ::STE3pr-LEU2 his3Δ1 leu2Δ0 ura3Δ0 leu2Δ0::GAL1pr-I-SCEI-natNT2 YOR283W-mCherry-sfGFP pRS413-GPDpr-IPF1-CYCter	This study
yCPO0283	MATalpha can1Δ::STE2pr-SpHIS5 lyp1Δ::STE3pr-LEU2 his3Δ1 leu2Δ0 ura3Δ0 leu2Δ0::GAL1pr-I-SCEI-natNT2 YOR283W-mCherry-sfGFP gid9Δ::kanMX pRS413GPD	This study
yCPO0284	MATalpha can1Δ::STE2pr-SpHIS5 lyp1Δ::STE3pr-LEU2 his3Δ1 leu2Δ0 ura3Δ0 leu2Δ0::GAL1pr-I-SCEI-natNT2 YOR283W-mCherry-sfGFP gid9Δ::kanMX pRS413-GPDpr-MOH1-CYCter	This study
yCPO0285	MATalpha can1Δ::STE2pr-SpHIS5 lyp1Δ::STE3pr-LEU2 his3Δ1 leu2Δ0 ura3Δ0 leu2Δ0::GAL1pr-I-SCEI-natNT2 YOR283W-mCherry-sfGFP gid9Δ::kanMX pRS413-GPDpr-IPF1-CYCter	This study
yCPO0286-1	BY4741 map2Δ::KanMX map1Δ::hphNT MDH2-mCherry-sfGFP-natNT2 pRS316-MAP1pr-MAP1-MAP1ter	This study
yCPO0287	BY4741 map2Δ::KanMX map1Δ::hphNT PHM8-mCherry-sfGFP-natNT2 pRS316-MAP1pr-MAP1-MAP1ter	This study
yCPO0288-1	BY4741 map2Δ::KanMX map1Δ::hphNT GPM3-mCherry-sfGFP-natNT2 pRS316-MAP1pr-MAP1-MAP1ter	This study

yCPO0289	BY4741 map2Δ::KanMX map1Δ::hphNT YOR283W-mCherry-sfGFP-natNT2 pRS316-MAP1pr-MAP1-MAP1ter	This study
yCPO0290	BY4741 pRS315	This study
yCPO0291	BY4741 map2Δ::KanMX map1Δ::hphNT MDH2-mCherry-sfGFP-natNT2 pRS315-MAP1pr-MAP1-MAP1ter	This study
yCPO0292	BY4741 map2Δ::KanMX map1Δ::hphNT MDH2-mCherry-sfGFP-natNT2 pRS315-MAP1pr-D.radMetAP	This study
yCPO0293	BY4741 map2Δ::KanMX map1Δ::hphNT MDH2-mCherry-sfGFP-natNT2 pRS315-MAP1pr-MAP1 Q365A-MAP1ter	This study
yCPO0294	BY4741 map2Δ::KanMX map1Δ::hphNT PHM8-mCherry-sfGFP-natNT2 pRS315-MAP1pr-MAP1-MAP1ter	This study
yCPO0295	BY4741 map2Δ::KanMX map1Δ::hphNT PHM8-mCherry-sfGFP-natNT2 pRS315-MAP1pr-D.radMetAP	This study
yCPO0296	BY4741 map2Δ::KanMX map1Δ::hphNT PHM8-mCherry-sfGFP-natNT2 pRS315-MAP1pr-MAP1 Q365A-MAP1ter	This study
yCPO0297	BY4741 map2Δ::KanMX map1Δ::hphNT GPM3-mCherry-sfGFP-natNT2 pRS315-MAP1pr-MAP1-MAP1ter	This study
yCPO0298	BY4741 map2Δ::KanMX map1Δ::hphNT GPM3-mCherry-sfGFP-natNT2 pRS315-MAP1pr-D.radMetAP	This study
yCPO0299	BY4741 map2Δ::KanMX map1Δ::hphNT GPM3-mCherry-sfGFP-natNT2 pRS315-MAP1pr-MAP1 Q365A-MAP1ter	This study
yCPO0300	BY4741 map2Δ::KanMX map1Δ::hphNT YOR283W-mCherry-sfGFP-natNT2 pRS315-MAP1pr-MAP1-MAP1ter	This study
yCPO0301	BY4741 map2Δ::KanMX map1Δ::hphNT YOR283W-mCherry-sfGFP-natNT2 pRS315-MAP1pr-D.radMetAP	This study
yCPO0302	BY4741 map2Δ::KanMX map1Δ::hphNT YOR283W-mCherry-sfGFP-natNT2 pRS315-MAP1pr-MAP1 Q365A-MAP1ter	This study
yCPO0303-1	yMaM330 (MATalpha can1Δ::STE2pr-SpHIS5 lyp1Δ::STE3pr-LEU2 his3Δ1 leu2Δ0 ura3Δ0 leu2Δ0::GAL1pr-I-SCEI-natNT2) CPA1-mCherry-sfGFP cpa2Δ::KanMX	This study
yCPO0312-1	yMaM330 (MATalpha can1Δ::STE2pr-SpHIS5 lyp1Δ::STE3pr-LEU2 his3Δ1 leu2Δ0 ura3Δ0 leu2Δ0::GAL1pr-I-SCEI-natNT2) CPA1-mCherry-sfGFP gid9Δ::kanMX cpa2Δ::hphNT	This study
yCPO0313-1	BY4741 MDH2-mCherry-sfGFP KanMX	This study
yCPO0314-1	BY4741 PHM8-mCherry-sfGFP KanMX	This study
yCPO0315	yMaM1079 (MATalpha can1Δ::STE2pr-SpHIS5 lyp1Δ::STE3pr-LEU2 his3Δ1 leu2Δ0 ura3Δ0 leu2Δ0::GAL1pr-I-SCEI-natNT2 GPM3-mCherry-sfGFP) gpm3Δ::(GAL1pr-I-SCEI KanMX KlURA3)	This study
yCPO0322	yMaM1080 (MATalpha can1Δ::STE2pr-SpHIS5 lyp1Δ::STE3pr-LEU2 his3Δ1 leu2Δ0 ura3Δ0 leu2Δ0::GAL1pr-I-SCEI-natNT2 CPA1-mCherry-sfGFP) cpa2Δ::(GAL1pr-I-SCEI KanMX KlURA3)	This study
yCPO0323-1	yMaM1082 (MATalpha can1Δ::STE2pr-SpHIS5 lyp1Δ::STE3pr-LEU2 his3Δ1 leu2Δ0 ura3Δ0	This study

	leu2Δ0::GAL1pr-I-SCEI-natNT2 PHM8-mCherry-sfGFP) phm8Δ::(GAL1pr-I-SCEI KanMX KlURA3)	
yCPO0342-1	yMaM1080 (MATalpha can1Δ::STE2pr-SpHIS5 lyp1Δ::STE3pr-LEU2 his3Δ1 leu2Δ0 ura3Δ0 leu2Δ0::GAL1pr-I-SCEI-natNT2 CPA1-mCherry-sfGFP) CPA2 T2A	This study
yCPO0343-1	yMaM1080 (MATalpha can1Δ::STE2pr-SpHIS5 lyp1Δ::STE3pr-LEU2 his3Δ1 leu2Δ0 ura3Δ0 leu2Δ0::GAL1pr-I-SCEI-natNT2 CPA1-mCherry-sfGFP) CPA2 T2S	This study
yCPO0344-1	yMaM1080 (MATalpha can1Δ::STE2pr-SpHIS5 lyp1Δ::STE3pr-LEU2 his3Δ1 leu2Δ0 ura3Δ0 leu2Δ0::GAL1pr-I-SCEI-natNT2 CPA1-mCherry-sfGFP) CPA2 T2G	This study
yCPO0345-1	yMaM1080 (MATalpha can1Δ::STE2pr-SpHIS5 lyp1Δ::STE3pr-LEU2 his3Δ1 leu2Δ0 ura3Δ0 leu2Δ0::GAL1pr-I-SCEI-natNT2 CPA1-mCherry-sfGFP) CPA2 T2P	This study
yCPO0346-1	MATalpha can1Δ::STE2pr-SpHIS5 lyp1Δ::STE3pr-LEU2 his3Δ1 leu2Δ0 ura3Δ0 leu2Δ0::GAL1pr-I-SCEI-natNT2 MT-PHM8 1delM-mCherry-sfGFP	Kong et al. 2025
yCPO0347-1	MATalpha can1Δ::STE2pr-SpHIS5 lyp1Δ::STE3pr-LEU2 his3Δ1 leu2Δ0 ura3Δ0 leu2Δ0::GAL1pr-I-SCEI-natNT2 MT-PHM8-mCherry-sfGFP	Kong et al. 2025
yCPO0348-1	MATalpha can1Δ::STE2pr-SpHIS5 lyp1Δ::STE3pr-LEU2 his3Δ1 leu2Δ0 ura3Δ0 leu2Δ0::GAL1pr-I-SCEI-natNT2 MD-PHM8 1delM-mCherry-sfGFP	Kong et al. 2025
yCPO0349-1	MATalpha can1Δ::STE2pr-SpHIS5 lyp1Δ::STE3pr-LEU2 his3Δ1 leu2Δ0 ura3Δ0 leu2Δ0::GAL1pr-I-SCEI-natNT2 MD-PHM8-mCherry-sfGFP	Kong et al. 2025
yCPO0350	MATalpha can1Δ::STE2pr-SpHIS5 lyp1Δ::STE3pr-LEU2 his3Δ1 leu2Δ0 ura3Δ0 leu2Δ0::GAL1pr-I-SCEI-natNT2 ML-PHM8 1delM-mCherry-sfGFP	Kong et al. 2025
yCPO0351-1	MATalpha can1Δ::STE2pr-SpHIS5 lyp1Δ::STE3pr-LEU2 his3Δ1 leu2Δ0 ura3Δ0 leu2Δ0::GAL1pr-I-SCEI-natNT2 ML-PHM8-mCherry-sfGFP	Kong et al. 2025
yCPO0352	yMaM1080 (MATalpha can1Δ::STE2pr-SpHIS5 lyp1Δ::STE3pr-LEU2 his3Δ1 leu2Δ0 ura3Δ0 leu2Δ0::GAL1pr-I-SCEI-natNT2 CPA1-mCherry-sfGFP) pRS413-GPD pRS416-TEF	This study
yCPO0353	yMaM1080 (MATalpha can1Δ::STE2pr-SpHIS5 lyp1Δ::STE3pr-LEU2 his3Δ1 leu2Δ0 ura3Δ0 leu2Δ0::GAL1pr-I-SCEI-natNT2 CPA1-mCherry-sfGFP) pRS413-GPD pRS416-GPDpr-CPA2-CYCter	This study
yCPO0354	MATalpha can1Δ::STE2pr-SpHIS5 lyp1Δ::STE3pr-LEU2 his3Δ1 leu2Δ0 ura3Δ0 leu2Δ0::GAL1pr-I-SCEI-natNT2 CPA1-mCherry-sfGFP gid9Δ::kanMX pRS413-GPD pRS416-TEF	This study
yCPO0355	MATalpha can1Δ::STE2pr-SpHIS5 lyp1Δ::STE3pr-LEU2 his3Δ1 leu2Δ0 ura3Δ0 leu2Δ0::GAL1pr-I-SCEI-natNT2 CPA1-mCherry-sfGFP gid9Δ::kanMX pRS413-GPD pRS416-GPDpr-CPA2-CYCter	This study
yCPO0356	MATalpha can1Δ::STE2pr-SpHIS5 lyp1Δ::STE3pr-LEU2 his3Δ1 leu2Δ0 ura3Δ0 leu2Δ0::GAL1pr-I-SCEI-natNT2 CPA1-mCherry-sfGFP gid11Δ::kanMX pRS413-GPD pRS416-TEF	This study

yCPO0357	MATalpha can1Δ::STE2pr-SpHIS5 lyp1Δ::STE3pr-LEU2 his3Δ1 leu2Δ0 ura3Δ0 leu2Δ0::GAL1pr-I-SCEI-natNT2 CPA1-mCherry-sfGFP gid11Δ::kanMX pRS413-GPD pRS416-GPDpr-CPA2-CYCter	This study
yCPO0358	BY4741 p413-GPD p416-TEF	This study
yCPO0359	BY4741 p413-GPDpr-CPA1-mCherry-sfGFP p416-TEF	This study
yCPO0360	BY4741 p413-GPDpr-CPA1-mCherry-sfGFP p416-GPDpr-CPA2-CYCter	This study
yCPO0361	BY4741 gid9Δ::KanMX p413-GPDpr-CPA1-mCherry-sfGFP p416-TEF	This study
yCPO0362	BY4741 gid9Δ::KanMX p413-GPDpr-CPA1-mCherry-sfGFP p416-GPDpr-CPA2-CYCter	This study
yCPO0363	BY4741 gid11Δ::KanMX p413-GPDpr-CPA1-mCherry-sfGFP p416-TEF	This study
yCPO0364	BY4741 gid11Δ::KanMX p413-GPDpr-CPA1-mCherry-sfGFP p416-GPDpr-CPA2-CYCter	This study
yCPO0365-1	MATalpha can1Δ::STE2pr-SpHIS5 lyp1Δ::STE3pr-LEU2 his3Δ1 leu2Δ0 ura3Δ0 leu2Δ0::GAL1pr-I-SCEI-natNT2 MT-PHM8 1delM-mCherry-sfGFP gid9Δ::KanMX	Kong et al. 2025
yCPO0366-1	MATalpha can1Δ::STE2pr-SpHIS5 lyp1Δ::STE3pr-LEU2 his3Δ1 leu2Δ0 ura3Δ0 leu2Δ0::GAL1pr-I-SCEI-natNT2 MT-PHM8 1delM-mCherry-sfGFP gid11Δ::KanMX	Kong et al. 2025
yCPO0367-1	MATalpha can1Δ::STE2pr-SpHIS5 lyp1Δ::STE3pr-LEU2 his3Δ1 leu2Δ0 ura3Δ0 leu2Δ0::GAL1pr-I-SCEI-natNT2 MT-PHM8-mCherry-sfGFP gid9Δ::KanMX	Kong et al. 2025
yCPO0368-1	MATalpha can1Δ::STE2pr-SpHIS5 lyp1Δ::STE3pr-LEU2 his3Δ1 leu2Δ0 ura3Δ0 leu2Δ0::GAL1pr-I-SCEI-natNT2 MT-PHM8-mCherry-sfGFP gid11Δ::KanMX	Kong et al. 2025
yCPO0369-1	MATalpha can1Δ::STE2pr-SpHIS5 lyp1Δ::STE3pr-LEU2 his3Δ1 leu2Δ0 ura3Δ0 leu2Δ0::GAL1pr-I-SCEI-natNT2 MD-PHM8 1delM-mCherry-sfGFP gid9Δ::KanMX	Kong et al. 2025
yCPO0370-1	MATalpha can1Δ::STE2pr-SpHIS5 lyp1Δ::STE3pr-LEU2 his3Δ1 leu2Δ0 ura3Δ0 leu2Δ0::GAL1pr-I-SCEI-natNT2 MD-PHM8 1delM-mCherry-sfGFP gid11Δ::KanMX	Kong et al. 2025
yCPO0371-1	MATalpha can1Δ::STE2pr-SpHIS5 lyp1Δ::STE3pr-LEU2 his3Δ1 leu2Δ0 ura3Δ0 leu2Δ0::GAL1pr-I-SCEI-natNT2 MD-PHM8-mCherry-sfGFP gid9Δ::KanMX	Kong et al. 2025
yCPO0372-1	MATalpha can1Δ::STE2pr-SpHIS5 lyp1Δ::STE3pr-LEU2 his3Δ1 leu2Δ0 ura3Δ0 leu2Δ0::GAL1pr-I-SCEI-natNT2 MD-PHM8-mCherry-sfGFP gid11Δ::KanMX	Kong et al. 2025
yCPO0373-1	MATalpha can1Δ::STE2pr-SpHIS5 lyp1Δ::STE3pr-LEU2 his3Δ1 leu2Δ0 ura3Δ0 leu2Δ0::GAL1pr-I-SCEI-natNT2 ML-PHM8 1delM-mCherry-sfGFP gid9Δ::KanMX	Kong et al. 2025
yCPO0374-1	MATalpha can1Δ::STE2pr-SpHIS5 lyp1Δ::STE3pr-LEU2 his3Δ1 leu2Δ0 ura3Δ0 leu2Δ0::GAL1pr-I-SCEI-natNT2 ML-PHM8 1delM-mCherry-sfGFP gid11Δ::KanMX	Kong et al. 2025
yCPO0375-1	MATalpha can1Δ::STE2pr-SpHIS5 lyp1Δ::STE3pr-LEU2 his3Δ1 leu2Δ0 ura3Δ0 leu2Δ0::GAL1pr-I-SCEI-natNT2 ML-PHM8-mCherry-sfGFP gid9Δ::KanMX	Kong et al. 2025
yCPO0376-1	MATalpha can1Δ::STE2pr-SpHIS5 lyp1Δ::STE3pr-LEU2 his3Δ1 leu2Δ0 ura3Δ0 leu2Δ0::GAL1pr-I-SCEI-natNT2 ML-PHM8-mCherry-sfGFP gid11Δ::KanMX	Kong et al. 2025
yCPO0377-1	yMaM330 (MATalpha can1Δ::STE2pr-SpHIS5 lyp1Δ::STE3pr-LEU2 his3Δ1 leu2Δ0 ura3Δ0 leu2Δ0::GAL1pr-I-SCEI-natNT2) MDH2-mCherry-sfGFP cpa2Δ::KanMX	This study

yCPO0378-1	yMaM330 (MATalpha can1Δ::STE2pr-SpHIS5 lyp1Δ::STE3pr-LEU2 his3Δ1 leu2Δ0 ura3Δ0 leu2Δ0::GAL1pr-I-SCEI-natNT2) GPM3-mCherry-sfGFP cpa2Δ::KanMX	This study
yCPO0379-1	yMaM330 (MATalpha can1Δ::STE2pr-SpHIS5 lyp1Δ::STE3pr-LEU2 his3Δ1 leu2Δ0 ura3Δ0 leu2Δ0::GAL1pr-I-SCEI-natNT2) PHM8-mCherry-sfGFP cpa2Δ::KanMX	This study
yCPO0380-1	BY4741 CPA1-mCherry-sfGFP hphNT	This study
yCPO0381-1	BY4741 CPA2-mCherry-sfGFP hphNT	This study
yCPO0382-1	BY4741 CPA1-mCherry-sfGFP hphNT gid9Δ::KanMX	This study
yCPO0383-1	BY4741 CPA1-mCherry-sfGFP hphNT gid4Δ::KanMX	This study
yCPO0384-1	BY4741 CPA1-mCherry-sfGFP hphNT gid10Δ::KanMX	This study
yCPO0385-1	BY4741 CPA1-mCherry-sfGFP hphNT gid11Δ::KanMX	This study
yCPO0386-1	BY4741 CPA1-mCherry-sfGFP hphNT cpa2Δ::KanMX	This study
yCPO0387-1	BY4741 CPA1-mCherry-sfGFP hphNT gid7Δ::KanMX	This study
yCPO0388-1	BY4741 CPA1-mCherry-sfGFP hphNT gid5Δ::KanMX	This study
yCPO0389-1	BY4741 CPA2-mCherry-sfGFP hphNT gid9Δ::KanMX	This study
yCPO0390-1	BY4741 CPA2-mCherry-sfGFP hphNT gid4Δ::KanMX	This study
yCPO0391-1	BY4741 CPA2-mCherry-sfGFP hphNT gid10Δ::KanMX	This study
yCPO0392-1	BY4741 CPA2-mCherry-sfGFP hphNT gid11Δ::KanMX	This study
yCPO0393-1	BY4741 CPA2-mCherry-sfGFP hphNT gid7Δ::KanMX	This study
yCPO0394-1	BY4741 CPA2-mCherry-sfGFP hphNT gid5Δ::KanMX	This study
yCPO0395-1	yMaM1079 (MATalpha can1Δ::STE2pr-SpHIS5 lyp1Δ::STE3pr-LEU2 his3Δ1 leu2Δ0 ura3Δ0 leu2Δ0::GAL1pr-I-SCEI-natNT2 GPM3-mCherry-sfGFP) gpm3Δ::(GAL1pr-I-SCEI KanMX KlURA3)	This study
yCPO0396-1	MATalpha can1Δ::STE2pr-SpHIS5 lyp1Δ::STE3pr-LEU2 his3Δ1 leu2Δ0 ura3Δ0 leu2Δ0::GAL1pr-I-SCEI-natNT2 MT-GPM3 1delM-mCherry-sfGFP	Kong et al. 2025
yCPO0397-1	MATalpha can1Δ::STE2pr-SpHIS5 lyp1Δ::STE3pr-LEU2 his3Δ1 leu2Δ0 ura3Δ0 leu2Δ0::GAL1pr-I-SCEI-natNT2 MT-GPM3-mCherry-sfGFP	Kong et al. 2025
yCPO0398-1	MATalpha can1Δ::STE2pr-SpHIS5 lyp1Δ::STE3pr-LEU2 his3Δ1 leu2Δ0 ura3Δ0 leu2Δ0::GAL1pr-I-SCEI-natNT2 MD-GPM3 1delM-mCherry-sfGFP	Kong et al. 2025
yCPO0399-1	MATalpha can1Δ::STE2pr-SpHIS5 lyp1Δ::STE3pr-LEU2 his3Δ1 leu2Δ0 ura3Δ0 leu2Δ0::GAL1pr-I-SCEI-natNT2 MD-GPM3-mCherry-sfGFP	Kong et al. 2025
yCPO0400-1	MATalpha can1Δ::STE2pr-SpHIS5 lyp1Δ::STE3pr-LEU2 his3Δ1 leu2Δ0 ura3Δ0 leu2Δ0::GAL1pr-I-SCEI-natNT2 ML-GPM3 1delM-mCherry-sfGFP	Kong et al. 2025
yCPO0401-1	MATalpha can1Δ::STE2pr-SpHIS5 lyp1Δ::STE3pr-LEU2 his3Δ1 leu2Δ0 ura3Δ0 leu2Δ0::GAL1pr-I-SCEI-natNT2 ML-GPM3-mCherry-sfGFP	Kong et al. 2025
yCPO0402-1	MATalpha can1Δ::STE2pr-SpHIS5 lyp1Δ::STE3pr-LEU2 his3Δ1 leu2Δ0 ura3Δ0 leu2Δ0::GAL1pr-I-SCEI-natNT2 MT-GPM3 1delM-mCherry-sfGFP gid9Δ::KanMX	Kong et al. 2025
yCPO0403-1	MATalpha can1Δ::STE2pr-SpHIS5 lyp1Δ::STE3pr-LEU2 his3Δ1 leu2Δ0 ura3Δ0 leu2Δ0::GAL1pr-I-SCEI-natNT2 MT-GPM3 1delM-mCherry-sfGFP gid11Δ::KanMX	Kong et al. 2025

yCPO0404-1	MATalpha can1Δ::STE2pr-SpHIS5 lyp1Δ::STE3pr-LEU2 his3Δ1 leu2Δ0 ura3Δ0 leu2Δ0::GAL1pr-I-SCEI-natNT2 MT-GPM3-mCherry-sfGFP gid9Δ::KanMX	Kong et al. 2025
yCPO0405-1	MATalpha can1Δ::STE2pr-SpHIS5 lyp1Δ::STE3pr-LEU2 his3Δ1 leu2Δ0 ura3Δ0 leu2Δ0::GAL1pr-I-SCEI-natNT2 MT-GPM3-mCherry-sfGFP gid11Δ::KanMX	Kong et al. 2025
yCPO0406-1	MATalpha can1Δ::STE2pr-SpHIS5 lyp1Δ::STE3pr-LEU2 his3Δ1 leu2Δ0 ura3Δ0 leu2Δ0::GAL1pr-I-SCEI-natNT2 MD-GPM3 1delM-mCherry-sfGFP gid9Δ::KanMX	Kong et al. 2025
yCPO0407-1	MATalpha can1Δ::STE2pr-SpHIS5 lyp1Δ::STE3pr-LEU2 his3Δ1 leu2Δ0 ura3Δ0 leu2Δ0::GAL1pr-I-SCEI-natNT2 MD-GPM3 1delM-mCherry-sfGFP gid11Δ::KanMX	Kong et al. 2025
yCPO0408-1	MATalpha can1Δ::STE2pr-SpHIS5 lyp1Δ::STE3pr-LEU2 his3Δ1 leu2Δ0 ura3Δ0 leu2Δ0::GAL1pr-I-SCEI-natNT2 MD-GPM3-mCherry-sfGFP gid9Δ::KanMX	Kong et al. 2025
yCPO0409-1	MATalpha can1Δ::STE2pr-SpHIS5 lyp1Δ::STE3pr-LEU2 his3Δ1 leu2Δ0 ura3Δ0 leu2Δ0::GAL1pr-I-SCEI-natNT2 MD-GPM3-mCherry-sfGFP gid11Δ::KanMX	Kong et al. 2025
yCPO0410-1	MATalpha can1Δ::STE2pr-SpHIS5 lyp1Δ::STE3pr-LEU2 his3Δ1 leu2Δ0 ura3Δ0 leu2Δ0::GAL1pr-I-SCEI-natNT2 ML-GPM3 1delM-mCherry-sfGFP gid9Δ::KanMX	Kong et al. 2025
yCPO0411-1	MATalpha can1Δ::STE2pr-SpHIS5 lyp1Δ::STE3pr-LEU2 his3Δ1 leu2Δ0 ura3Δ0 leu2Δ0::GAL1pr-I-SCEI-natNT2 ML-GPM3 1delM-mCherry-sfGFP gid11Δ::KanMX	Kong et al. 2025
yCPO0412-1	MATalpha can1Δ::STE2pr-SpHIS5 lyp1Δ::STE3pr-LEU2 his3Δ1 leu2Δ0 ura3Δ0 leu2Δ0::GAL1pr-I-SCEI-natNT2 ML-GPM3-mCherry-sfGFP gid9Δ::KanMX	Kong et al. 2025
yCPO0413-1	MATalpha can1Δ::STE2pr-SpHIS5 lyp1Δ::STE3pr-LEU2 his3Δ1 leu2Δ0 ura3Δ0 leu2Δ0::GAL1pr-I-SCEI-natNT2 ML-GPM3-mCherry-sfGFP gid11Δ::KanMX	Kong et al. 2025
yCPO0414-1	BY4741 can1Δ::KanMX	This study
yCPO0415-1	BY4741 CPA1-mCherry-sfGFP hphNT can1Δ::KanMX	This study
yCPO0416-1	BY4741 CPA2-mCherry-sfGFP hphNT can1Δ::KanMX	This study
yCPO0417-1	BY4741 cpa1Δ::hphNT	This study
yCPO0418-1	BY4741 cpa2Δ::hphNT	This study
yCPO0419-1	BY4741 can1Δ::KanMX cpa1Δ::hphNT	This study
yCPO0420-1	BY4741 can1Δ::KanMX cpa2Δ::hphNT	This study
yCPO0421-1	yMaM1094 (MATalpha can1Δ::STE2pr-SpHIS5 lyp1Δ::STE3pr-LEU2 his3Δ1 leu2Δ0 ura3Δ0 leu2Δ0::GAL1pr-I-SCEI-natNT2 YOR283W-mCherry-sfGFP) yor283wΔ::(GAL1pr-I-SCEI KanMX KlURA3)	This study
yCPO0422-1	MATalpha can1Δ::STE2pr-SpHIS5 lyp1Δ::STE3pr-LEU2 his3Δ1 leu2Δ0 ura3Δ0 leu2Δ0::GAL1pr-I-SCEI-natNT2 YOR283W T2A-mCherry-sfGFP	This study
yCPO0423-1	BY4741 CPA1-mCherry-sfGFP-GGGGS-CUb hphNT	This study
yCPO0424-1	BY4741 CPA2-mCherry-sfGFP-GGGGS-CUb hphNT	This study
yCPO0425-1	BY4741 GID9-mCherry-sfGFP-GGGGS-CUb hphNT	This study
yCPO0426-1	BY4741 PHM8-mCherry-sfGFP-GGGGS-CUb hphNT	This study
yCPO0427-1	BY4741 GPM3-mCherry-sfGFP-GGGGS-CUb hphNT	This study
yCPO0428-1	BY4741 CPA1-mCherry-sfGFP-GGGGS-CUb K48R hphNT	This study
yCPO0429-1	BY4741 CPA2-mCherry-sfGFP-GGGGS-CUb K48R hphNT	This study

yCPO0430-1	BY4741 GID9-mCherry-sfGFP-GGGGS-CUb K48R hphNT	This study
yCPO0431-1	BY4741 PHM8-mCherry-sfGFP-GGGGS-CUb K48R hphNT	This study
yCPO0432-1	BY4741 GPM3-mCherry-sfGFP-GGGGS-CUb K48R hphNT	This study
yCPO0433	BY4741 CPA1-mCherry-sfGFP-GGGGS-CUb hphNT ubc8Δ::KanMX	This study
yCPO0434-1	BY4741 CPA2-mCherry-sfGFP-GGGGS-CUb hphNT ubc8Δ::KanMX	This study
yCPO0435-1	BY4741 GID9-mCherry-sfGFP-GGGGS-CUb hphNT ubc8Δ::KanMX	This study
yCPO0436-1	BY4741 PHM8-mCherry-sfGFP-GGGGS-CUb hphNT ubc8Δ::KanMX	This study
yCPO0437-1	BY4741 GPM3-mCherry-sfGFP-GGGGS-CUb hphNT ubc8Δ::KanMX	This study
yCPO0438-1	BY4741 CPA1-mCherry-sfGFP-GGGGS-CUb K48R hphNT ubc8Δ::KanMX	This study
yCPO0439-1	BY4741 CPA2-mCherry-sfGFP-GGGGS-CUb K48R hphNT ubc8Δ::KanMX	This study
yCPO0440-1	BY4741 GID9-mCherry-sfGFP-GGGGS-CUb K48R hphNT ubc8Δ::KanMX	This study
yCPO0441	BY4741 PHM8-mCherry-sfGFP-GGGGS-CUb K48R hphNT ubc8Δ::KanMX	This study
yCPO0442-1	BY4741 GPM3-mCherry-sfGFP-GGGGS-CUb K48R hphNT ubc8Δ::KanMX	This study
yCPO0443-1	MATalpha can1Δ::STE2pr-SpHIS5 lyp1Δ::STE3pr-LEU2 his3Δ1 leu2Δ0 ura3Δ0 leu2Δ0::GAL1pr-I-SCEI-natNT2 HA-GID11 naa10Δ::KanMX	This study
yCPO0454	MATalpha can1Δ::STE2pr-SpHIS5 lyp1Δ::STE3pr-LEU2 his3Δ1 leu2Δ0 ura3Δ0 leu2Δ0::GAL1pr-I-SCEI-natNT2 CPA1-mCherry-sfGFP sno1Δ::hphNT	This study
yCPO0455	MATalpha can1Δ::STE2pr-SpHIS5 lyp1Δ::STE3pr-LEU2 his3Δ1 leu2Δ0 ura3Δ0 leu2Δ0::GAL1pr-I-SCEI-natNT2 CPA1-mCherry-sfGFP dur1,2Δ::hphNT	This study
yCPO0456	MATalpha can1Δ::STE2pr-SpHIS5 lyp1Δ::STE3pr-LEU2 his3Δ1 leu2Δ0 ura3Δ0 leu2Δ0::GAL1pr-I-SCEI-natNT2 CPA1-mCherry-sfGFP gis1Δ::hphNT	This study
yCPO0457	MATalpha can1Δ::STE2pr-SpHIS5 lyp1Δ::STE3pr-LEU2 his3Δ1 leu2Δ0 ura3Δ0 leu2Δ0::GAL1pr-I-SCEI-natNT2 CPA1-mCherry-sfGFP idi1Δ::hphNT	This study
yCPO0458	MATalpha can1Δ::STE2pr-SpHIS5 lyp1Δ::STE3pr-LEU2 his3Δ1 leu2Δ0 ura3Δ0 leu2Δ0::GAL1pr-I-SCEI-natNT2 CPA1-mCherry-sfGFP syf1Δ::hphNT	This study
yCPO0460	MATalpha can1Δ::STE2pr-SpHIS5 lyp1Δ::STE3pr-LEU2 his3Δ1 leu2Δ0 ura3Δ0 leu2Δ0::GAL1pr-I-SCEI-natNT2 CPA1-mCherry-sfGFP flc1Δ::hphNT	This study
yCPO0461	MATalpha can1Δ::STE2pr-SpHIS5 lyp1Δ::STE3pr-LEU2 his3Δ1 leu2Δ0 ura3Δ0 leu2Δ0::GAL1pr-I-SCEI-natNT2 CPA1-mCherry-sfGFP zps1Δ::hphNT	This study
yCPO0462	MATalpha can1Δ::STE2pr-SpHIS5 lyp1Δ::STE3pr-LEU2 his3Δ1 leu2Δ0 ura3Δ0 leu2Δ0::GAL1pr-I-SCEI-natNT2 CPA1-mCherry-sfGFP gdh1Δ::hphNT	This study
yCPO0463	MATalpha can1Δ::STE2pr-SpHIS5 lyp1Δ::STE3pr-LEU2 his3Δ1 leu2Δ0 ura3Δ0 leu2Δ0::GAL1pr-I-SCEI-natNT2 CPA1-mCherry-sfGFP gid9Δ::KanMX sno1Δ::hphNT	This study

yCPO0464	MATalpha can1Δ::STE2pr-SpHIS5 lyp1Δ::STE3pr-LEU2 his3Δ1 leu2Δ0 ura3Δ0 leu2Δ0::GAL1pr-I-SCEI-natNT2 CPA1-mCherry-sfGFP gid9Δ::KanMX dur1,2Δ::hphNT	This study
yCPO0465	MATalpha can1Δ::STE2pr-SpHIS5 lyp1Δ::STE3pr-LEU2 his3Δ1 leu2Δ0 ura3Δ0 leu2Δ0::GAL1pr-I-SCEI-natNT2 CPA1-mCherry-sfGFP gid9Δ::KanMX gis1Δ::hphNT	This study
yCPO0466	MATalpha can1Δ::STE2pr-SpHIS5 lyp1Δ::STE3pr-LEU2 his3Δ1 leu2Δ0 ura3Δ0 leu2Δ0::GAL1pr-I-SCEI-natNT2 CPA1-mCherry-sfGFP gid9Δ::KanMX syf1Δ::hphNT	This study
yCPO0467	MATalpha can1Δ::STE2pr-SpHIS5 lyp1Δ::STE3pr-LEU2 his3Δ1 leu2Δ0 ura3Δ0 leu2Δ0::GAL1pr-I-SCEI-natNT2 CPA1-mCherry-sfGFP gid9Δ::KanMX flc1Δ::hphNT	This study
yCPO0468	MATalpha can1Δ::STE2pr-SpHIS5 lyp1Δ::STE3pr-LEU2 his3Δ1 leu2Δ0 ura3Δ0 leu2Δ0::GAL1pr-I-SCEI-natNT2 CPA1-mCherry-sfGFP gid9Δ::KanMX zps1Δ::hphNT	This study
yCPO0469	MATalpha can1Δ::STE2pr-SpHIS5 lyp1Δ::STE3pr-LEU2 his3Δ1 leu2Δ0 ura3Δ0 leu2Δ0::GAL1pr-I-SCEI-natNT2 CPA1-mCherry-sfGFP gid9Δ::KanMX gdh1Δ::hphNT	This study
yCPO0478	MATalpha can1Δ::STE2pr-SpHIS5 lyp1Δ::STE3pr-LEU2 his3Δ1 leu2Δ0 ura3Δ0 leu2Δ0::GAL1pr-I-SCEI-natNT2 CPA1-mCherry-sfGFP gid9Δ::KanMX idi1Δ::hphNT	This study
yCPO109-1	yCPO0065-1 (MATalpha can1Δ::STE2pr-SpHIS5 lyp1Δ::STE3pr-LEU2 his3Δ1 leu2Δ0 ura3Δ0 leu2Δ0::GAL1pr-I-SCEI-natNT2 CPA1-mCherry-sfGFP CPA1 T6S, T9S, T33S, T36S, T37S, T47S) gid11Δ::KanMX	This study
yCPO213	BY4742 ate1Δ::NatNT2 + p426-GPDpr-scATE1	This study
yCPO214	BY4742 ate1Δ::NatNT2 + p426-GPDpr-ATE1isoform1	This study
yCPO215	BY4742 ate1Δ::NatNT2 + p426-GPDpr-ATE1isoform2	This study
yCPO216	BY4742 nta1Δ::NatNT2 + p426-GPDpr-scNTA1	This study
yCPO217	BY4742 nta1Δ::NatNT2 + p426-GPDpr-NTAN1	This study
yCPO218	BY4742 nta1Δ::NatNT2 + p426-GPDpr-NTAQ1	This study
yCPO224	MATalpha can1Δ::STE2pr-SpHIS5 lyp1Δ::STE3pr-LEU2 his3Δ1 leu2Δ0 ura3Δ0 leu2Δ0::GAL1pr-I-SCEI-natNT2 YDR222W-mCherry-sfGFP	This study
yCPO240	yKEK262 (BY4741 map2Δ::KanMX) pRS316-MAP1pr-MAP1-MAP1ter	This study
yCPO241-1	BY4741 map2Δ::KanMX map1Δ::hphNT pRS316-MAP1pr-MAP1-MAP1ter	This study
yJJF0001	yMaM1028 (MATalpha can1Δ::STE2pr-SpHIS5 lyp1Δ::STE3pr-LEU2 his3Δ1 leu2Δ0::GAL1pr-NLS-I-SCEI-natNT2 ura3Δ0) PDC1-mCherry-sfGFP	Jia-Jun Fung/Khmelinskii lab
yJK0001	yKEK087 (MATalpha can1Δ::STE2pr-SpHIS5 lyp1Δ::STE3pr-LEU2 his3Δ1 leu2Δ0 ura3Δ0 leu2Δ0::GAL1pr-I-SCEI-natNT2 PHM8-mCherry-sfGFP gid11Δ::kanMX) pRS313-GID11pr-HA-GID11-GID11ter	This study
yJK0002	yKEK087 (MATalpha can1Δ::STE2pr-SpHIS5 lyp1Δ::STE3pr-LEU2 his3Δ1 leu2Δ0 ura3Δ0 leu2Δ0::GAL1pr-I-SCEI-natNT2 PHM8-mCherry-sfGFP gid11Δ::kanMX) pRS313-GID11pr-HA-AsGo GID11 L697_C724delinsLIIGTDYGIMRWNINSWARRSFSSYDLC -GID11ter	This study
yJK0003	yKEK087 (MATalpha can1Δ::STE2pr-SpHIS5 lyp1Δ::STE3pr-LEU2 his3Δ1 leu2Δ0 ura3Δ0 leu2Δ0::GAL1pr-I-SCEI-natNT2 PHM8-mCherry-sfGFP	This study

	gid11Δ::kanMX) pRS313-GID11pr-HA-CaAl GID11 I543_V571delinsLIIGTDYGIMRWNINSWARRSFSSYDLC-GID11ter	
yJK0004	yKEK087 (MATalpha can1Δ::STE2pr-SpHIS5 lyp1Δ::STE3pr-LEU2 his3Δ1 leu2Δ0 ura3Δ0 leu2Δ0::GAL1pr-I-SCEI-natNT2 PHM8-mCherry-sfGFP gid11Δ::kanMX) pRS313-GID11pr-HA-SaPa GID11-GID11ter	This study
yJK0005	yKEK087 (MATalpha can1Δ::STE2pr-SpHIS5 lyp1Δ::STE3pr-LEU2 his3Δ1 leu2Δ0 ura3Δ0 leu2Δ0::GAL1pr-I-SCEI-natNT2 PHM8-mCherry-sfGFP gid11Δ::kanMX) pRS313-GID11pr-HA-ScPo GID11 V320_L347delinsLIIGTDYGIMRWNINSWARRSFSSYDLC-GID11ter	This study
yJK0006	yKEK087 (MATalpha can1Δ::STE2pr-SpHIS5 lyp1Δ::STE3pr-LEU2 his3Δ1 leu2Δ0 ura3Δ0 leu2Δ0::GAL1pr-I-SCEI-natNT2 PHM8-mCherry-sfGFP gid11Δ::kanMX) pRS313-GID11pr-HA-ScSt GID11 I625_V653delinsLIIGTDYGIMRWNINSWARRSFSSYDLC-GID11ter	This study
yJK0007	yKEK087 (MATalpha can1Δ::STE2pr-SpHIS5 lyp1Δ::STE3pr-LEU2 his3Δ1 leu2Δ0 ura3Δ0 leu2Δ0::GAL1pr-I-SCEI-natNT2 PHM8-mCherry-sfGFP gid11Δ::kanMX) pRS313-GID11pr-HA-VaPo GID11 I697_C724delinsLIIGTDYGIMRWNINSWARRSFSSYDLC-GID11ter	This study
yJK0008	yKEK086 (MATalpha can1Δ::STE2pr-SpHIS5 lyp1Δ::STE3pr-LEU2 his3Δ1 leu2Δ0 ura3Δ0 leu2Δ0::GAL1pr-I-SCEI-natNT2 CPA1-mCherry-sfGFP gid11Δ::kanMX) pRS313-GID11pr-HA-GID11-GID11ter	This study
yJK0009	yKEK086 (MATalpha can1Δ::STE2pr-SpHIS5 lyp1Δ::STE3pr-LEU2 his3Δ1 leu2Δ0 ura3Δ0 leu2Δ0::GAL1pr-I-SCEI-natNT2 CPA1-mCherry-sfGFP gid11Δ::kanMX) pRS313-GID11pr-HA-AsGo GID11 L697_C724delinsLIIGTDYGIMRWNINSWARRSFSSYDLC-GID11ter	This study
yJK0010	yKEK086 (MATalpha can1Δ::STE2pr-SpHIS5 lyp1Δ::STE3pr-LEU2 his3Δ1 leu2Δ0 ura3Δ0 leu2Δ0::GAL1pr-I-SCEI-natNT2 CPA1-mCherry-sfGFP gid11Δ::kanMX) pRS313-GID11pr-HA-CaAl GID11 I543_V571delinsLIIGTDYGIMRWNINSWARRSFSSYDLC-GID11ter	This study
yJK0011	yKEK086 (MATalpha can1Δ::STE2pr-SpHIS5 lyp1Δ::STE3pr-LEU2 his3Δ1 leu2Δ0 ura3Δ0 leu2Δ0::GAL1pr-I-SCEI-natNT2 CPA1-mCherry-sfGFP gid11Δ::kanMX) pRS313-GID11pr-HA-SaPa GID11-GID11ter	This study
yJK0012	yKEK086 (MATalpha can1Δ::STE2pr-SpHIS5 lyp1Δ::STE3pr-LEU2 his3Δ1 leu2Δ0 ura3Δ0 leu2Δ0::GAL1pr-I-SCEI-natNT2 CPA1-mCherry-sfGFP gid11Δ::kanMX) pRS313-GID11pr-HA-ScPo GID11 V320_L347delinsLIIGTDYGIMRWNINSWARRSFSSYDLC-GID11ter	This study
yJK0013	yKEK086 (MATalpha can1Δ::STE2pr-SpHIS5 lyp1Δ::STE3pr-LEU2 his3Δ1 leu2Δ0 ura3Δ0 leu2Δ0::GAL1pr-I-SCEI-natNT2 CPA1-mCherry-sfGFP gid11Δ::kanMX) pRS313-GID11pr-HA-ScSt GID11	This study

	I625_V653delinsLIIGTDYGIMRWNINSWARRSFSSYDLC-GID11ter	
yJK0014	yKEK086 (MATalpha can1Δ::STE2pr-SpHIS5 lyp1Δ::STE3pr-LEU2 his3Δ1 leu2Δ0 ura3Δ0 leu2Δ0::GAL1pr-I-SCEI-natNT2 CPA1-mCherry-sfGFP gid11Δ::kanMX) pRS313-GID11pr-HA-VaPo GID11 I697_C724delinsLIIGTDYGIMRWNINSWARRSFSSYDLC-GID11ter	This study
yJK0015	yKEK087 (MATalpha can1Δ::STE2pr-SpHIS5 lyp1Δ::STE3pr-LEU2 his3Δ1 leu2Δ0 ura3Δ0 leu2Δ0::GAL1pr-I-SCEI-natNT2 PHM8-mCherry-sfGFP gid11Δ::kanMX) pRS313-GID11pr-HA-GID11 M1_K24del-GID11ter	This study
yJK0016	yKEK087 (MATalpha can1Δ::STE2pr-SpHIS5 lyp1Δ::STE3pr-LEU2 his3Δ1 leu2Δ0 ura3Δ0 leu2Δ0::GAL1pr-I-SCEI-natNT2 PHM8-mCherry-sfGFP gid11Δ::kanMX) pRS313-GID11pr-HA-GID11 V84_I115del-GID11ter	This study
yJK0017	yKEK087 (MATalpha can1Δ::STE2pr-SpHIS5 lyp1Δ::STE3pr-LEU2 his3Δ1 leu2Δ0 ura3Δ0 leu2Δ0::GAL1pr-I-SCEI-natNT2 PHM8-mCherry-sfGFP gid11Δ::kanMX) pRS313-GID11pr-HA-GID11 Y306_E332del-GID11ter	This study
yJK0018	yKEK087 (MATalpha can1Δ::STE2pr-SpHIS5 lyp1Δ::STE3pr-LEU2 his3Δ1 leu2Δ0 ura3Δ0 leu2Δ0::GAL1pr-I-SCEI-natNT2 PHM8-mCherry-sfGFP gid11Δ::kanMX) pRS313-GID11pr-HA-GID11 N455_P485del-GID11ter	This study
yJK0019	yKEK087 (MATalpha can1Δ::STE2pr-SpHIS5 lyp1Δ::STE3pr-LEU2 his3Δ1 leu2Δ0 ura3Δ0 leu2Δ0::GAL1pr-I-SCEI-natNT2 PHM8-mCherry-sfGFP gid11Δ::kanMX) pRS313-GID11pr-HA-GID11 V526_T677del-GID11ter	This study
yJK0020	yKEK086 (MATalpha can1Δ::STE2pr-SpHIS5 lyp1Δ::STE3pr-LEU2 his3Δ1 leu2Δ0 ura3Δ0 leu2Δ0::GAL1pr-I-SCEI-natNT2 CPA1-mCherry-sfGFP gid11Δ::kanMX) pRS313-GID11pr-HA-GID11 M1_K24del-GID11ter	This study
yJK0021	yKEK086 (MATalpha can1Δ::STE2pr-SpHIS5 lyp1Δ::STE3pr-LEU2 his3Δ1 leu2Δ0 ura3Δ0 leu2Δ0::GAL1pr-I-SCEI-natNT2 CPA1-mCherry-sfGFP gid11Δ::kanMX) pRS313-GID11pr-HA-GID11 V84_I115del-GID11ter	This study
yJK0022	yKEK086 (MATalpha can1Δ::STE2pr-SpHIS5 lyp1Δ::STE3pr-LEU2 his3Δ1 leu2Δ0 ura3Δ0 leu2Δ0::GAL1pr-I-SCEI-natNT2 CPA1-mCherry-sfGFP gid11Δ::kanMX) pRS313-GID11pr-HA-GID11 Y306_E332del-GID11ter	This study
yJK0023	yKEK086 (MATalpha can1Δ::STE2pr-SpHIS5 lyp1Δ::STE3pr-LEU2 his3Δ1 leu2Δ0 ura3Δ0 leu2Δ0::GAL1pr-I-SCEI-natNT2 CPA1-mCherry-sfGFP gid11Δ::kanMX) pRS313-GID11pr-HA-GID11 N455_P485del-GID11ter	This study
yJK0024	yKEK086 (MATalpha can1Δ::STE2pr-SpHIS5 lyp1Δ::STE3pr-LEU2 his3Δ1 leu2Δ0 ura3Δ0 leu2Δ0::GAL1pr-I-SCEI-natNT2 CPA1-mCherry-sfGFP	This study

	gid11Δ::kanMX) pRS313-GID11pr-HA-GID11 V526_T677del-GID11ter	
yKEK067	yMaM1074 (MATalpha can1Δ::STE2pr-SpHIS5 lyp1Δ::STE3pr-LEU2 his3Δ1 leu2Δ0 ura3Δ0 leu2Δ0::GAL1pr-I-SCEI-natNT2 HSM3-mCherry-sfGFP) gid10Δ::kanMX	Ka-Yiu Kong/Khmelinskii lab
yKEK069	yMaM1080 (MATalpha can1Δ::STE2pr-SpHIS5 lyp1Δ::STE3pr-LEU2 his3Δ1 leu2Δ0 ura3Δ0 leu2Δ0::GAL1pr-I-SCEI-natNT2 CPA1-mCherry-sfGFP) gid10Δ::kanMX	Ka-Yiu Kong/Khmelinskii lab
yKEK084	yMaM1074 (MATalpha can1Δ::STE2pr-SpHIS5 lyp1Δ::STE3pr-LEU2 his3Δ1 leu2Δ0 ura3Δ0 leu2Δ0::GAL1pr-I-SCEI-natNT2 HSM3-mCherry-sfGFP) gid11Δ::kanMX	Ka-Yiu Kong/Khmelinskii lab
yKEK086	yMaM1080 (MATalpha can1Δ::STE2pr-SpHIS5 lyp1Δ::STE3pr-LEU2 his3Δ1 leu2Δ0 ura3Δ0 leu2Δ0::GAL1pr-I-SCEI-natNT2 CPA1-mCherry-sfGFP) gid11Δ::kanMX	Kong et al. 2025
yKEK087	yMaM1082 (MATalpha can1Δ::STE2pr-SpHIS5 lyp1Δ::STE3pr-LEU2 his3Δ1 leu2Δ0 ura3Δ0 leu2Δ0::GAL1pr-I-SCEI-natNT2 PHM8-mCherry-sfGFP) gid11Δ::kanMX	Kong et al. 2025
yKEK088	yMaM1090 (MATalpha can1Δ::STE2pr-SpHIS5 lyp1Δ::STE3pr-LEU2 his3Δ1 leu2Δ0 ura3Δ0 leu2Δ0::GAL1pr-I-SCEI-natNT2 BLM10-mCherry-sfGFP) gid11Δ::kanMX	Ka-Yiu Kong/Khmelinskii lab
yKEK111	yMaM1100 (MATalpha can1Δ::STE2pr-SpHIS5 lyp1Δ::STE3pr-LEU2 his3Δ1 leu2Δ0 ura3Δ0 leu2Δ0::GAL1pr-I-SCEI-natNT2 UBC8-mCherry-sfGFP) gid9Δ::hphNT1	Ka-Yiu Kong/Khmelinskii lab
yKEK141	yKEK067 (MATalpha can1Δ::STE2pr-SpHIS5 lyp1Δ::STE3pr-LEU2 his3Δ1 leu2Δ0 ura3Δ0 leu2Δ0::GAL1pr-I-SCEI-natNT2 HSM3-mCherry-sfGFP gid10Δ::kanMX) gid4Δ::hphNT1	Ka-Yiu Kong/Khmelinskii lab
yKEK142	AK1253-1 (MATalpha can1Δ::STE2pr-SpHIS5 lyp1Δ::STE3pr-LEU2 his3Δ1 leu2Δ0 ura3Δ0 leu2Δ0::GAL1pr-I-SCEI-natNT2 HSM3-mCherry-sfGFP gid4Δ::kanMX) gid11Δ::hphNT1	Ka-Yiu Kong/Khmelinskii lab
yKEK143	yKEK084 (MATalpha can1Δ::STE2pr-SpHIS5 lyp1Δ::STE3pr-LEU2 his3Δ1 leu2Δ0 ura3Δ0 leu2Δ0::GAL1pr-I-SCEI-natNT2 HSM3-mCherry-sfGFP gid11Δ::kanMX) gid10Δ::hphNT1	Ka-Yiu Kong/Khmelinskii lab
yKEK176	BY4741 gid9Δ::kanMX	Ka-Yiu Kong/Khmelinskii lab
yKEK179	BY4741 gid11Δ::kanMX	Kong et al., 2021
yKEK213	yMaM1102 (MATalpha can1Δ::STE2pr-SpHIS5 lyp1Δ::STE3pr-LEU2 his3Δ1 leu2Δ0 ura3Δ0 leu2Δ0::GAL1pr-I-SCEI-natNT2 YDR222W-mCherry-sfGFP) gid7Δ::kanMX	Ka-Yiu Kong/Khmelinskii lab
yKEK261	BY4741 map1Δ::kanMX	Ka-Yiu Kong/Khmelinskii lab
yKEK262	BY4741 map2Δ::kanMX	Ka-Yiu Kong/Khmelinskii lab
yKEK263	BY4741 moh1Δ::kanMX	Kong et al. 2025
yKEK264	BY4741 ipf1Δ::kanMX	Kong et al. 2025
yLZY0037-1	BY4741 gid5Δ::KanMX	Kong et al. 2025

yMaM1074	yMaM330 (MATalpha can1Δ::STE2pr-SpHIS5 lyp1Δ::STE3pr-LEU2 his3Δ1 leu2Δ0 ura3Δ0 leu2Δ0::GAL1pr-I-SCEI-natNT2) HSM3-mCherry-sfGFP	Kong et al., 2021
yMaM1079	yMaM330 (MATalpha can1Δ::STE2pr-SpHIS5 lyp1Δ::STE3pr-LEU2 his3Δ1 leu2Δ0 ura3Δ0 leu2Δ0::GAL1pr-I-SCEI-natNT2) GPM3-mCherry-sfGFP	Kong et al., 2021
yMaM1080	yMaM330 (MATalpha can1Δ::STE2pr-SpHIS5 lyp1Δ::STE3pr-LEU2 his3Δ1 leu2Δ0 ura3Δ0 leu2Δ0::GAL1pr-I-SCEI-natNT2) CPA1-mCherry-sfGFP	Kong et al., 2021
yMaM1082	yMaM330 (MATalpha can1Δ::STE2pr-SpHIS5 lyp1Δ::STE3pr-LEU2 his3Δ1 leu2Δ0 ura3Δ0 leu2Δ0::GAL1pr-I-SCEI-natNT2) PHM8-mCherry-sfGFP	Kong et al., 2021
yMaM1090	yMaM330 (MATalpha can1Δ::STE2pr-SpHIS5 lyp1Δ::STE3pr-LEU2 his3Δ1 leu2Δ0 ura3Δ0 leu2Δ0::GAL1pr-I-SCEI-natNT2) BLM10-mCherry-sfGFP	Kong et al., 2021
yMaM1091	yMaM330 (MATalpha can1Δ::STE2pr-SpHIS5 lyp1Δ::STE3pr-LEU2 his3Δ1 leu2Δ0 ura3Δ0 leu2Δ0::GAL1pr-I-SCEI-natNT2) MDH2-mCherry-sfGFP	Kong et al., 2021
yMaM1094	yMaM330 (MATalpha can1Δ::STE2pr-SpHIS5 lyp1Δ::STE3pr-LEU2 his3Δ1 leu2Δ0 ura3Δ0 leu2Δ0::GAL1pr-I-SCEI-natNT2) YOR283W-mCherry-sfGFP	Kong et al., 2021
yMaM1100	yMaM330 (MATalpha can1Δ::STE2pr-SpHIS5 lyp1Δ::STE3pr-LEU2 his3Δ1 leu2Δ0 ura3Δ0 leu2Δ0::GAL1pr-I-SCEI-natNT2) UBC8-mCherry-sfGFP	Matthias Meurer/Knop lab
yMaM1102	yMaM330 (MATalpha can1Δ::STE2pr-SpHIS5 lyp1Δ::STE3pr-LEU2 his3Δ1 leu2Δ0 ura3Δ0 leu2Δ0::GAL1pr-I-SCEI-natNT2) YDR222W-mCherry-sfGFP	Matthias Meurer/Knop lab
yMaM1145	yMaM330 (MATalpha can1Δ::STE2pr-SpHIS5 lyp1Δ::STE3pr-LEU2 his3Δ1 leu2Δ0 ura3Δ0 leu2Δ0::GAL1pr-I-SCEI-natNT2) CPA1-mCherry-sfGFP gid4Δ::kanMX	Matthias Meurer/Knop lab
yMaM330	Y8205 (MATalpha can1Δ::STE2pr-SpHIS5 lyp1Δ::STE3pr-LEU2 his3Δ1 leu2Δ0 ura3Δ0) leu2Δ0::GAL1pr-I-SCEI-natNT2	Khmelinskii and Knop 2014

Table S 2: List of plasmids used in this study.

Plasmid	**Description**	**Reference**
humanORFeome collection 7.1	pDONR223-ORF	Rual et al. 2005
humanORFeome collection 8.1	pDONR223-ORF	Rual et al. 2005
p413GPD	p413GPD AmpR, CEN ARS HIS3	Sikorski and Hieter 1989
p426GPD	p426GPD AmpR, 2µ URA3	Sikorski and Hieter 1989
pAC0010.2-6	pET-3C-GST-His-ATE1	Coti 2024
pAC009-1	pET-3C-GST-His-NTAQ1	Coti 2024
pAH001-1	p413-GPDpr-RMND5A-CYC1ter	Haschke 2023
pAH002-1	p413-GPDpr-GID2-CYCter	Haschke 2023
pAH003	p413-GPDpr-ARMC8-CYCter	Haschke 2023
pAH004	p413-GPDpr-hGID8-CYCter	Haschke 2023

pAH005	p413-GPDpr-RMND5B-CYCter	Haschke 2023
pAH006	p413-GPDpr-GID8-CYCter	Haschke 2023
pAH007-1	p413-GPDpr-RANBP9-CYCter	Haschke 2023
pAH008-1	p413-GPDpr-MAEA-CYCter	Haschke 2023
pAH009	p413-GPDpr-RANBP10-CYCter	Haschke 2023
pAH010	p413-GPDpr-WDR26-CYCter	Haschke 2023
pAH011-1	p413-GPDpr-GID1-CYCter	Haschke 2023
pAH012-1	p413-GPDpr-GID9-CYCter	Haschke 2023
pAH013-1	p413-GPDpr-hGID4 1-870-scGID4 1057-1089-CYCter	Haschke 2023
pAH014-1	p413-GPDpr-scGID4 1-1056-hGID4 871-903-CYCter	Haschke 2023
pAH015-1	p413-GPDpr-hGID4 1-867-scGID4 1042-1089-CYCter	Haschke 2023
pAH016-1	p413-GPDpr-scGID4 1-1041-hGID4 868-903-CYCter	Haschke 2023
pAnB19	pRS413-GPDpr-Ubi-EcoRV-STOP-eK-mCherry-sfGFP	Kats et al. 2018
pAnB19-DC-1	pRS413-pGPD-Ubi-DC-eK-mCherry-sfGFP (GATTGT)	This study
pAnB19-DD-1	pRS413-pGPD-Ubi-DD-eK-mCherry-sfGFP (GATGAT)	This study
pAnB19-DE	pRS413-pGPD-Ubi-DE-eK-mCherry-sfGFP (GACGAG)	Kats et al. 2018
pAnB19-DH	pRS413-pGPD-Ubi-DH-eK-mCherry-sfGFP (GACCAC)	Kats et al. 2018
pAnB19-DI-1	pRS413-pGPD-Ubi-DI-eK-mCherry-sfGFP (GATATT)	This study
pAnB19-DP	pRS413-pGPD-Ubi-DP-eK-mCherry-sfGFP (CACCCA)	Kats et al. 2018
pAnB19-DR	pRS413-pGPD-Ubi-DR-eK-mCherry-sfGFP (GACAGA)	Kats et al. 2018
pAnB19-DT-1	pRS413-pGPD-Ubi-DT-eK-mCherry-sfGFP (GATACT)	This study
pAnB19-ED-1	pRS413-pGPD-Ubi-ED-eK-mCherry-sfGFP (GAAGAT)	This study
pAnB19-EE	pRS413-pGPD-Ubi-EE-eK-mCherry-sfGFP (GAGGAG)	Kats et al. 2018
pAnB19-EH	pRS413-pGPD-Ubi-EH-eK-mCherry-sfGFP (GAACAC)	Kats et al. 2018
pAnB19-EK	pRS413-pGPD-Ubi-EK-eK-mCherry-sfGFP (GAGAAG)	Kats et al. 2018
pAnB19-EN-1	pRS413-pGPD-Ubi-EN-eK-mCherry-sfGFP (GAAAAT)	This study
pAnB19-EQ-1	pRS413-pGPD-Ubi-EQ-eK-mCherry-sfGFP (GAACAA)	This study
pAnB19-ET	pRS413-pGPD-Ubi-ET-eK-mCherry-sfGFP (GAAACC)	Kats et al. 2018
pAnB19-NC-1	pRS413-pGPD-Ubi-NC-eK-mCherry-sfGFP (AATTGT)	This study
pAnB19-ND	pRS413-pGPD-Ubi-ND-eK-mCherry-sfGFP (AATGAT)	This study
pAnB19-NI-1	pRS413-pGPD-Ubi-NI-eK-mCherry-sfGFP (AATATT)	This study
pAnB19-NK-1	pRS413-pGPD-Ubi-NK-eK-mCherry-sfGFP (AATAAA)	This study
pAnB19-NN	pRS413-pGPD-Ubi-NN-eK-mCherry-sfGFP (AATAAT)	This study
pAnB19-NP	pRS413-pGPD-Ubi-NP-eK-mCherry-sfGFP (AACCCA)	Kats et al. 2018
pAnB19-NR	pRS413-pGPD-Ubi-NR-eK-mCherry-sfGFP (AACAGA)	Kats et al. 2018
pAnB19-NS	pRS413-pGPD-Ubi-NS-eK-mCherry-sfGFP (AATTCT)	This study
pAnB19-NT	pRS413-pGPD-Ubi-NT-eK-mCherry-sfGFP (AATACT)	This study
pAnB19-NY-1	pRS413-pGPD-Ubi-NY-eK-mCherry-sfGFP (AATTAT)	This study
pAnB19-QA	pRS413-pGPD-Ubi-QA-eK-mCherry-sfGFP (CAAGCG)	Kats et al. 2018
pAnB19-QD-1	pRS413-pGPD-Ubi-QD-eK-mCherry-sfGFP (CAAGAT)	This study
pAnB19-QH	pRS413-pGPD-Ubi-QH-eK-mCherry-sfGFP (CAACAC)	Kats et al. 2018
pAnB19-QK	pRS413-pGPD-Ubi-QK-eK-mCherry-sfGFP (CAGAAG)	Kats et al. 2018
pAnB19-QN-1	pRS413-pGPD-Ubi-QN-eK-mCherry-sfGFP (CAAAAT)	This study
pAnB19-QS	pRS413-pGPD-Ubi-QS-eK-mCherry-sfGFP (CAATCT)	This study
pAnB19-QW	pRS413-pGPD-Ubi-QW-eK-mCherry-sfGFP (CAATGG)	This study

pAnB19-QY	pRS413-pGPD-Ubi-QY-eK-mCherry-sfGFP (CAATAT)	This study
pAnB19-XZ	pRS413-pGPD-Ubi-XZ-eK-mCherry-sfGFP (NNKNNK)	This study
pCD040-1	pRS313_GID11pr-GID11(Y306-E332 GGS)-GID11ter	Kong et al. 2025
pCD041-1	pRS313_GID11pr-GID11(N308-L327 GGS)-GID11ter	Kong et al. 2025
pCPO0009	pRS316-ATE1pr-ATE1isoform1-ATE1ter	This study
pCPO0010	pRS316-ATE1pr-ATE1isoform2-ATE1ter	This study
pCPO001-1	p426-GPD-ATE1	This study
pCPO0011-1	pRS316-GPDpr-ATE1-CYCter	This study
pCPO0012-1	pRS316-GPDpr-ATE1isoform1-CYCter	This study
pCPO0013-1	pRS316-GPDpr-ATE1isoform2-CYCter	This study
pCPO0014-1	pRS316-GPDpr-NTA1-CYCter	This study
pCPO0015-1	pRS316-GPDpr-NTAN1-CYCter	This study
pCPO0016-1	pRS316-GPDpr-NTAQ1-CYCter	This study
pCPO0017	pRS413-GPDpr-MOH1-CYCter	This study
pCPO0018	pRS413-GPDpr-IPF1-CYCter	This study
pCPO002-1	p426-GPD-NTA1	This study
pCPO0022	pRS413-GPDpr-PHM8-GGGS-mCherry-sfGFP	This study
pCPO0027-1	pRS413-GPDpr-CPA2-CYCter	This study
pCPO0028-1	pRS415-GPDpr-CPA2-CYCter	This study
pCPO0029-1	pRS416-GPDpr-CPA2-CYCter	This study
pCPO003-1	p426-GPD-NTAQ1	This study
pCPO0031-1	pRS313-CPA2pr-CPA2 T2A-CPA2ter	This study
pCPO0032-1	pRS313-CPA2pr-CPA2 T2S-CPA2ter	This study
pCPO0033-1	pRS313-CPA2pr-CPA2 T2G-CPA2ter	This study
pCPO0034-1	pRS313-CPA2pr-CPA2 T2P-CPA2ter	This study
pCPO0035-1	pRS313-CPA2pr-CPA2-CPA2ter	This study
pCPO0041	pRS413-GPD-CPA1-CUb-URA3-CYCter	This study
pCPO004-1	p426-GPD-hATE1isoform2	This study
pCPO0042-1	pRS413-GPD-GPM3-CUb-URA3-CYCter	This study
pCPO0043-1	pRS413-GPD-MDH2-CUb-URA3-CYCter	This study
pCPO0044-1	pRS413-GPD-PHM8-CUb-URA3-CYCter	This study
pCPO0045-1	pRS415-GPD-NUb-CPA2-CYCter	This study
pCPO0046-1	pRS415-GPD-NUb-GID4-CYCter	This study
pCPO0047-1	pRS415-GPD-NUb-GID11-CYCter	This study
pCPO0048	Ylp128-ADH-NUbo-CUE1-mCherry-VSV	Renz et al. 2024
pCPO0049-1	pRS413-GPD-CPA2-CUb-URA3-CYCter	This study
pCPO0050-1	pRS413-GPD-GID5-CUb-URA3-CYCter	This study
pCPO005-1	p426-GPD-hATE1isoform1	This study
pCPO0051-2	pRS313-GID11pr-HA-SalI-GID11ter	This study
pCPO0052-1	pRS413-GPDpr-NUb-CUE1-UBC8 C85K-CYCter	This study
pCPO0053-1	pRS415-GPD-UBC7-CYCter	This study
pCPO0054-1	pFA6a mCherry-sfGFP-GGGGS-CUb hphNT1	This study
pCPO0055-1	pFA6a mCherry-sfGFP-GGGGS-CUb K48R hphNT1	This study
pCPO0056-1	pRS413 GPDpr-UBC7-CYCter GPDpr-NUb-CUE1-UBC8 C85K-CYCter	This study

pCPO0057-1	pRS313-GID11pr-HA-GID11 M1V24del V84I115del N455P485del V526P485del-CYCter	Kong et al. 2025
pCPO0058	pRS413-GPDpr-GPM3 V3E-GGGS-mCherry-sfGFP	Kong et al. 2025
pCPO0059-1	pRS413-GPDpr-GPM3 V3F-GGGS-mCherry-sfGFP	Kong et al. 2025
pCPO0060-1	pRS413-GPDpr-GPM3 V3I-GGGS-mCherry-sfGFP	Kong et al. 2025
pCPO006-1	p426-GPD-NTAN1	This study
pCPO0061-1	pRS413-GPDpr-GPM3 V3L-GGGS-mCherry-sfGFP	Kong et al. 2025
pCPO0062-1	pRS413-GPDpr-GPM3 V3S-GGGS-mCherry-sfGFP	Kong et al. 2025
pCPO0063	pRS313-GID11pr-HA-GID11 H305_E335delinsGGSGGSGGSGGSGGSGGSGGSGGSGGSG-GID11ter	Kong et al. 2025
pCPO0064	pRS313-GID11pr-HA-GID11 M1-L304-AflII-GID11N336-STOP731	This study
pCPO0065	pRS413-GPDpr-MOH1-CYCter	Kong et al. 2025
pCPO0066	pRS413-GPDpr-IPF1-CYCter	Kong et al. 2025
pCPO0067-1	pRS313-DBP3pr-DBP3 K3V-mCherry-sfGFP-DBP3ter	Kong et al. 2025
pCPO0068-1	pRS313-DBP3pr-DBP3-mCherry-sfGFP-DBP3ter	Kong et al. 2025
pCPO0069	pRS316-MAP1pr-MAP1-MAP1ter	This study
pCPO0070	pRS315-MAP1pr-MAP1-MAP1ter	This study
pCPO0071	pRS315-MAP1pr-MAP1 Q365A-MAP1ter	This study
pCPO0072	pRS315-MAP1pr-Deinococcus radiodurans MetAP-MAP1ter	This study
pCPO0073	pRS313-GID11pr-HA-GID11 P310-R321-GID11ter	Kong et al. 2025
pCPO0074	pRS313-GID11pr-HA-GID11 P308-L327-GID11ter	Kong et al. 2025
pFA6a-hphNT1	pFA6a-hphNT1	Janke et al. 2004
pFA6a-kanMX	pFA6a-kanMX	Janke et al. 2004
pJK0001-1	pRS313-GID11pr-HA-GID11-GID11ter	Kong et al. 2025
pJK0002-1	pRS313-GID11pr-HA-AsGo GID11 L697_C724delinsLIIGTDYGIMRWNINSWARRSFSSYDLC-GID11ter	This study
pJK0003-1	pRS313-GID11pr-HA-CaAl GID11 I543_V571delinsLIIGTDYGIMRWNINSWARRSFSSYDLC-GID11ter	This study
pJK0004-1	pRS313-GID11pr-HA-SaPa GID11-GID11ter	This study
pJK0005-1	pRS313-GID11pr-HA-ScPo GID11 V320_L347delinsLIIGTDYGIMRWNINSWARRSFSSYDLC-GID11ter	This study
pJK0006-1	pRS313-GID11pr-HA-ScSt GID11 I625_V653delinsLIIGTDYGIMRWNINSWARRSFSSYDLC-GID11ter	This study
pJK0007-1	pRS313-GID11pr-HA-VaPo GID11 I697_C724delinsLIIGTDYGIMRWNINSWARRSFSSYDLC-GID11ter	This study
pJK0008-1	pRS313-GID11pr-HA-GID11 M1_K24del-GID11ter	Kong et al. 2025
pJK0009	pRS313-GID11pr-HA-GID11 V84_I115del-GID11ter	Kong et al. 2025
pJK0010	pRS313-GID11pr-HA-GID11 Y306_E332del-GID11ter	Kong et al. 2025
pJK0011	pRS313-GID11pr-HA-GID11 N455_P485del-GID11ter	Kong et al. 2025
pJK0012-1	pRS313-GID11pr-HA-GID11 V526_T677del-GID11ter	Kong et al. 2025
pJK0013-1	pRS313-LYS20pr-LYS20 A3V-mCherry-sfGFP-LYS20ter	Kong et al. 2025
pJK0014-1	pRS313-STF2pr-STF2 R3V-mCherry-sfGFP-STF2ter	Kong et al. 2025

pJK0015	pRS413-GPDpr-YOR283W K3V-mCherry-sfGFP-CYCter	Kong et al. 2025
pJK0016-1	pRS313-DLD3pr-DLD3 A3V-mCherry-sfGFP-DLD3ter	Kong et al. 2025
pKBJ001-1	pRS413-GPDpr-Ubi-EcoRV-STOP-eK-mCherry-sfGFP-CYC1term	This study
pKEK028	pRS413-GPDpr-CPA1-mCherry-sfGFP	This study
pKEK043	pRS413-GPDpr-YOR283W-mCherry-sfGFP	Kong et al. 2021
pKEK078	pRS413-GPDpr-GID11	This study
pKEK198	pRS413-GPDpr-GID4	This study
pKEK199	pRS413-GPDpr-GID10	This study
pKEK348	pRS313-DLD3pr-DLD3-mCherry-sfGFP-DLD3ter	Kong et al. 2025
pKEK351	pRS313-LYS20pr-LYS20-mCherry-sfGFP-LYS20ter	Kong et al. 2025
pKEK363	pRS313-STF2pr-STF2-mCherry-sfGFP-STF2ter	Kong et al. 2025
pKEK392	pRS413-GPDpr-YML053C	This study
pKEK393	pRS413-GPDpr-SPG5	This study
pKEK400	pRS413-GPDpr-Myc-Ub-CYC1ter	This study
pKEK452	pRS313-GID11pr-GID11-GID11ter	This study
pKEK529	pRS413-GPDpr-ENV11	This study
pKEK531	pRS413-GPDpr-GEP5	This study
pKEK533	pRS413-GPDpr-MCM10	This study
pKEK535	pRS413-GPDpr-MLO50	This study
pMaM60	pFA6a-mCherry-sfGFP-hphNT1	Khmelinskii et al. 2012
pRS315	pRS315 pBluescript, LEU2 CEN6 ARS	Sikorski and Hieter 1989
pRS316	pRS316 pBluescript, URA3 CEN6 ARS	Sikorski and Hieter 1989

Table S 3: List of oligonucleotides used in this study.

Oligonucleotide name	**Sequence**
313_CPA1pr_F	TTGGAGCTCCACCGCGGTGGCGGCCGCTCTAGAACTAGTGGATCCttgaaatatttt
313_CPA2pr_F	TTGGAGCTCCACCGCGGTGGCGGCCGCTCTAGAACTAGTGGATCCAAGAATGGCAACATTGT TATTATTGTGAAAAATGAG
313-GID11pr-HA_R	agtGTCGACAGCGTAATCTGGAACATCGTATGGGTACATtctttaacacgtatacttttgtaacttattgctgtt tttc
313-GID11ter_F	tacGTCGACacttcagccatacatatattgtgattttaattcacc
316_ATE1pr_F	TTGGAGCTCCACCGCGGTGGCGGCCGCTCTAGAACTAGTGGATCCAACTGTGGATCACTGG TAGTTACTTCA
316_GPDpr_F	TTGGAGCTCCACCGCGGTGGCGGCCGCTCTAGAACTAGTGGATCCAGTTTATCATTATCAATA CTGCCATTTCAAAGAAT
316_NTA1pr_F	TTGGAGCTCCACCGCGGTGGCGGCCGCTCTAGAACTAGTGGATCCGCCGTCGTGGTGACG
316_NTA1ter_R	CCTCACTAAAGGGAACAAAAGCTGGGTACCGGGCCCCCCCTCGAGAAGTAGTCTATTAAAAA CTCTACGGCGAGG
416-GPDpr_F	GCGCAATTAACCCTCACTAAAGGGAACAAAAGCTGGAGCTCAGTTTATCATTA
426GPD_BamHI_ATE1-1_F	AAACACCAGAACTTAGTTTCGACGGATTCTAGAACTAGTGGATCCATGGCTTTCTGGGCGG
426GPD_BamHI_ATE1-2_F	AAACACCAGAACTTAGTTTCGACGGATTCTAGAACTAGTGGATCCATGGCTTTCTGGGCGG
426GPD_BamHI_NTAN1_F	AAACACCAGAACTTAGTTTCGACGGATTCTAGAACTAGTGGATCCatgccgctgctcg

426GPD_BamHI_NTAQ1_F	AAACACCAGAACTTAGTTTCGACGGATTCTAGAACTAGTGGATCCAtggaaggtaatggcccc
426GPD_BamHI_scATE1_F	AAACACCAGAACTTAGTTTCGACGGATTCTAGAACTAGTGGATCCATGTCCGATAGATTCGTTATTTGGGC
426GPD_BamHI_yNTA1_F	AAACACCAGAACTTAGTTTCGACGGATTCTAGAACTAGTGGATCCATGCTAATAGACGCAATTCATGGTGC
426GPD_Hind3_ATE1_R	ACATAACTAATTACATGACTCGAGGTCGACGGTATCGATAAGCTTTCAGTTTCTGAACAGCAGCATCCG
426GPD_Hind3_ATE1-1_R	GAGGGCGTGAATGTAAGCGTGACATAACTAATTACATGACTCGAGTCAGTTTCTGAACAGCAGCATCCGC
426GPD_Hind3_ATE1-2_R	GAGGGCGTGAATGTAAGCGTGACATAACTAATTACATGACTCGAGTCAGTTTCTGAACAGCAGCATCCGC
426GPD_HindIII_NTAN1_R	ACATAACTAATTACATGACTCGAGGTCGACGGTATCGATAAGCTTacttcctggagaagagatcttttccc
426GPD_HindIII_NTAQ1_R	ACATAACTAATTACATGACTCGAGGTCGACGGTATCGATAAGCTTgcagtttttactgccaaaccgatg
426GPD_HindIII_yATE1_R	ACATAACTAATTACATGACTCGAGGTCGACGGTATCGATAAGCTTTCACATTTGCTCACTATATAAAATGACGGCT
426GPD_HindIII_yNTA_R	ACATAACTAATTACATGACTCGAGGTCGACGGTATCGATAAGCTTTCACCTAAACACTTCAAATTGGACCTCAC
ACS2_-152_F	CACCGCACGTTTAGCCTGATC
ACS2_S1	ATTGTTATACACAAACAGAATACAGGAAAGTAAATCAATACAATAATAAAATATGcgtacgctgcaggtcgac
ACS2_S2	AAACAGAAAAGGAGCGAAATTTTATCTCATTACGAAATTTTTCTCATTTAAGTTAatcgatgaattcgagctcg
ARMC8_171_F	GCAAGAAACCTCAAGCACAGAGC
ARMC8_230_R	GCAAGACTTCCCAACACCACTG
ARMC8_694_F	AGGGATAAGCCTATTGAGATGCAGC
ARMC8_XhoI_pKBJ001_R	gagggcgtgaatgtaagcgtgacataactaattacatgactcgagTTAGGTTGACGTCACTCCCTGC
ATE1_F_-324	GCCATGTCTGGATGGTGCTG
ATE1_S1	TTGTTACAAAAGACAAGATAGTCTCAAGATACAACTGAGAAGAAGCACAATTATGcgtacgctgcaggtcgac
ATE1_S2	TGCTAAAAAATGTTATACATTAGGATTGTTATTAGAATAGTGTGTTGAAGGCTCAatcgatgaattcgagctcg
ATE1-1_ATE1ter_F	TGCTGCTGTTCAGAAACTGAGCCTTCAACACACTATTCTAATAACAATCC
ATE1-1_ATE1ter_R	TAGAATAGTGTGTTGAAGGCTCAGTTTCTGAACAGCAGCA
ATE1-2_ATE1ter_R	TAGAATAGTGTGTTGAAGGCTCAGTTTCTGAACAGCAGCA
ATE1-2_ATEter_F	TGCTGCTGTTCAGAAACTGAGCCTTCAACACACTATTCTAATAACAATCC
ATE1iso1_1270_F	CCTTCTGATTTGCTGTGCCCTG
ATE1iso1_25_F	CCCAGCGTCGTGGACTATTTC
ATE1iso1_655_F	AAACTAATGCAGCAGAACCCAGC
ATE1iso1_CYCter_F	TGCTGCTGTTCAGAAACTGAtcatgtaattagttatgtcacgcttacattcac
ATE1iso1_CYCter_R	tgacataactaattacatgaTCAGTTTCTGAACAGCAGCATCCG
ATE1iso2_1270_F	CCTTCTGATTTGCTGTGCCCTG
ATE1iso2_25_F	CCCAGCGTCGTGGACTATTTC
ATE1iso2_655_F	AAACTAATGCAGCAGAACCCAGC
ATE1iso2_CYCter_F	TGCTGCTGTTCAGAAACTGAtcatgtaattagttatgtcacgcttacattcac

ATE1iso2_CYCter_R	tgacataactaattacatgaTCAGTTTCTGAACAGCAGCATCCG
ATE1pr_ATE1-1_F	AACTGAGAAGAAGCACAATTATGGCTTTCTGGGCGGG
ATE1pr_ATE1-2_F	AACTGAGAAGAAGCACAATTATGGCTTTCTGGGCGGG
ATE1pr_ATE1-2_R	CCCCCCGCCCAGAAAGCCATAATTGTGCTTCTTCTCAGTTGTATCTTGAGAC
ATE1pr-ATE1-1_R	CCCCCCGCCCAGAAAGCCATAATTGTGCTTCTTCTCAGTTGTATCTTGAGAC
ATE1ter_316_R	CCTCACTAAAGGGAACAAAAGCTGGGTACCGGGCCCCCCCTCGAGTGCACAGTTAAAGTCAGTGCACCA
BEM4_F_+225	CTTCAAATAGTGAATCCCTTCC
BEM4_LS1	GTCACTCGCGAACTAAAACTAACCGCGAATAACAAATCACCTCATCTATATTTCAGCCCCAAAAGATTGTGGTTTCAAGTGAAAATAACTGTCCTACTAAcgtacgctgcaggtcgac
BEM4_LS2	TTAATCCAACAATATTCAAGATTTAATATTTATATATATATATATATATATACATGCAGAGGGAACGTTTTCTCCCCTCGTAGGTAAGGCGATTACGTGTatcgatgaattcgagctcg
BLM10_-185_F	TCTTACCAGTGGAGAAGTACACG
BLM10_S1	TCATTGTTCGTTAGCTAGCTTTGCACATTAATTTTTCGATTTGTTACCGCCAATGcgtacgctgcaggtcgac
BLM10_S2	TAGATGTACATATATGTCTAGATATGTGCTTAATATCCTATACTAATATGAATCAatcgatgaattcgagctcg
BUB3_F_+247	AAACGCGCTAAGATACGACC
BUB3_LS1	TGCATGTCCGAGAATACAAAAAATAGTGAACGAAAAAAATATCACATCGCGAAAGAAAAGCTATCTGATATCTGCAACACGAAAACACAACAGTCGCGGCcgtacgctgcaggtcgac
BUB3_LS2	TTTCTTTATTCCTTAAAGGAGGAGAAGCGAAGAGAGAGCGATGAATCTGAATTTTTTTTCTGGAATGTTCTATCATACTACACGAATCTTCACGAAGATAatcgatgaattcgagctcg
CAN1_-229_F	GAAAGAAGAGTGGTTGCGAACAGAG
CAN1-S1	TTCTTCAGACTTCTTAACTCCTGTAAAAACAAAAAAAAAAAAAGGCATAGCAATGcgtacgctgcaggtcgac
CAN1-S2	TGAGAATGCGAAATGGCGTGGAAATGTGATCAAAGGTAATAAAACGTCATATCTAatcgatgaattcgagctcg
CDC26_F_+204	GCTACCGATTGCGCCAACAAGG
CDC26_LS1	CACAAAAGTAGAGGAATAATGGATGGATCTAGGATGTACGTATATATGATATTAGCGGTCTGAAGAGAAAAAAAAAACAGCAACAATAACATCGCACTTGcgtacgctgcaggtcgac
CDC26_LS2	AATACAACGTATATAAAACTAGAGAGAAGAAATTTTATAAGTGAAAGTGAATGTGGATGCGTGCGCGTGTGCGTGTGCGTGTGCGTATGCGGATATGCTAatcgatgaattcgagctcg
CPA1_+420_R	TTCTTGGTATCACTTCGTTGCTCC
CPA1_1002_F	AGGCATGATACACCTTCAAAGACC
CPA1_363_R	AGCAACACCTTCTCTCTGACACC
CPA1_-498_F	CCGTGGAAGGGTGTTTGACTC
CPA1_F_-479	TCATCATCGCATCGCATTACCTC
CPA1_R_234	ATTGTATTCATCGCGGGCTTCG
CPA1-116_F	TGGTTGGTTACCCAGAGTCCATG
CPA1-700_F	GGCAACCCAGAACTATGCCAAG
CPA1-CUb_F	CCAAGGAAAGAGTGTTGTTCacgctgcaggtcgacg
CPA1-CUb_R	ataccgtcgacctgcagcgtGAACAACACTCTTTCCTTGGCCAAC
CPA1-pKBJ001-R	tcctcctcgcccttgctcaccatagcaccgtcgacggtatcgatGAACAACACTCTTTCCTTGGCCAAC
CPA1pr_CPA1S2T_R	tttgttgcagcggaggtcattgtaatccatca
CPA1pr-480_R	TCATCATCGCATCGCATTACCTC
CPA1pr-96_F	GTCTTGGCAGGTGTATTGAGAGTTC
CPA1pr-CPA1S2T_F	taggggggtgatggattacaatgacctccgct

CPA1-S1	ATTGCTTAATAATCAGAAATTCTATCACAAACCACTCCTAAAAATATTTCAAATGcgtacgctgcaggtcgac
CPA1-S2	TTGAATCGTATTTAGATGTACGTATGTGTTACGTAATGTATAAATTTTGTTTTTAatcgatgaattcgagctcg
CPA1-S3	ATCGAGATTGCAGAGTATAAATGTTACTAAGTTGGCCAAGGAAAGAGTGTTGTTCcgtacgctgcaggtcgac
CPA1ter-313_R	CCTCACTAAAGGGAACAAAAGCTGGGTACCGGGCCCCCCCTCGAGtattatcatcat
CPA1ter-68_F	TTTGCGCTACTCGTCGTTGC
CPA2_-225_F	TTGTGTCACCTTGAGTAAGCATCG
CPA2_285_R	GATGTATTCTGGTGTAACGGGCAAG
CPA2_T2A_COREswap	AGGAAGAGCAATACAGTACATAGACAGGAAGAAAAGAATGGCTTCGATTTATACATCAACAGAGCCTACGAATTCTGCTTTTA
CPA2+193_R	GGCCCATGCGTTACTCACTTC
CPA2-234_F	TCGTAACGATTGTGTCACCTTGAG
CPA2-CUb_F	TTATTGGTTTCAAAGCATATacgctgcaggtcgacg
CPA2-CUb_R	ataccgtcgacctgcagcgtATATGCTTTGAAACCAATAAATTCATCCCAGG
CPA2-CYCter_R	GAGGGCGTGAATGTAAGCGTGACATAACTAATTACATGACTCGAGTCAATATGCTTTGAAACCAATAAATTCATCCCAGG
CPA2-pKBJ001_R	gagggcgtgaatgtaagcgtgacataactaattacatgactcgagTCAATATGCTTTGAAACCAATAAATTCATCCCAGG
CPA2pr_CPA2T2A_F	ACATAGACAGGAAGAAAAGAATGGCATCGATT
CPA2pr_CPA2T2A_R	GATGTATAAATCGATGCCATTCTTTTCTTCCTGT
CPA2pr-CPA2T2A_F	TAGACAGGAAGAAAAGAATGGCATCGATTTATACAT
CPA2pr-CPA2T2A_R	GTTGATGTATAAATCGATGCCATTCTTTTCTTCCT
CPA2pr-CPA2T2G_F	TAGACAGGAAGAAAAGAATGGGATCGATTTATACAT
CPA2pr-CPA2T2G_R	GTTGATGTATAAATCGATCCCATTCTTTTCTTCCT
CPA2pr-CPA2T2P_F	TAGACAGGAAGAAAAGAATGCCATCGATTTATACAT
CPA2pr-CPA2T2P_R	GTTGATGTATAAATCGATGGCATTCTTTTCTTCCT
CPA2pr-CPA2T2S_F	TAGACAGGAAGAAAAGAATGTCATCGATTTATACAT
CPA2pr-CPA2T2S_R	GTTGATGTATAAATCGATGACATTCTTTTCTTCCT
CPA2-S1	AAATTAGTTCTATAAAGGAAGAGCAATACAGTACATAGACAGGAAGAAAAGAATGcgtacgctgcaggtcgac
CPA2-S2	CATTATATAATATACAGTAATACAATTAGAGGCAGGTTTTTCTTTTGCACAATCAatcgatgaattcgagctcg
CPA2-S2-CdelTGA	ATCTCATGACGTTATAGTTCCACCAGAAGTCCGTTCCTGGGATGAATTTATTGGTTGAcgtacgctgcaggtcgac
CPA2-S3	TATAGTTCCACCAGAAGTCCGTTCCTGGGATGAATTTATTGGTTTCAAAGCATATcgtacgctgcaggtcgac
CPA2ter_313_R	CCTCACTAAAGGGAACAAAAGCTGGGTACCGGGCCCCCCCTCGAGGCGGATTCTCTCCGTAGCG
CPA2ter-313_R	CCTCACTAAAGGGAACAAAAGCTGGGTACCGGGCCCCCCCTCGAGGCGGATTCTCTCCGTAGCG
CUE1_UBC8_SalI_R	CTTCTTTTAGAGCTACTCATgtcgacgttaattaaagtcagcaaactttgcaaatct

CUE1-SalI-GID11_F	agtgataaagatttgcaaagtttgctgactttaattaacgtcgacATGACCATTGATGGCACGGG
CUE1-SalI-GID4_F	agtgataaagatttgcaaagtttgctgactttaattaacgtcgacATGATCAATAATCCTAAGGTAGACAGTGTAGC
CUE1-SalI-GID5_F	agtgataaagatttgcaaagtttgctgactttaattaacgtcgacATGACGGTGGCTTATTCCCTAGAG
CUE1-SalI-UBC6_F	agtgataaagatttgcaaagtttgctgactttaattaacgtcgacATGGCTACAAAGCAGGCTCAC
CYCter_316_R	CCTCACTAAAGGGAACAAAAGCTGGGTACCGGGCCCCCCCTCGAGGGCCGCAAATTAAAGCCTTCGAGCGTCC
CYCter_SpeI_PRS426_R	caaaagctggagctccaccgcggtggcggccgctctagaactagtgcaaattaaagccttcgagcgt
CYCter-247bp_R	CAAATTAAAGCCTTCGAGCGTCC
CYCter-416-R	AGCGCGCGTAATACGACTCACTATAGGGCGAATTGGGTACCGGCCGCAAATTA
D.radMetAP_BamHI_pRS315_R	GGTATCGATAAGCTTGATATCGAATTCCTGCAGCCCGGGGttatagcgtcaggatgtcgtagccc
D.radMetAP_F_128	TGACGCTCAAAGAACTCGACC
DBP3_-230_F	CCTCAGGCTTTGCGCTCTTG
DBP3_S1	AGCCTTTTAACGAAAGCATAAGTATTAACAGTTTGATATATAGGGGATTAAAATGcgtacgctgcaggtcgac
DBP3_S2	ATTGGCTATTATTAGAGAAGAAAATCCAAGATTGAAGTAAACGAAAAAACCCCTAatcgatgaattcgagctcg
DBP3pr-DBP3K3V_F	tataggggattaaaATGACAgttGAAGAAATCGCAGACAAGAAGAG
DBP3pr-DBP3K3V_R	TTCTTGTCTGCGATTTCTTCaacTGTCATtttaatcccctatatatcaaac
DBP3pr-DBP3WT_F	tataggggattaaaATGACAaagGAAGAAATCGCAGACAAGAAGAG
DBP3pr-DBP3WT_R	TTCTTGTCTGCGATTTCTTCcttTGTCATtttaatcccctatatatcaaac
DBP3ter-pRS313_R	CCTCACTAAAGGGAACAAAAGCTGGGTACCGGGCCCCCCCTCGAGtcgatttcccca
DLD3_-184_F	CGGATGACACCACTTGCCAC
DLD3_S1	AATATTTTATTCATTTGAGATTCAAGGCTTAAAGACAGCATATATAAGAATTATGcgtacgctgcaggtcgac
DLD3_S2	AATACTGTAAAGAAAAAGGGTTTGCTCTTTGAAAGTTAAAAATTAACAAAGTTCAatcgatgaattcgagctcg
DLD3pr-DLD3A3V_F	catatataagaattATGACGgttGCACATCCTGTTGCTCAGTTAACT
DLD3pr-DLD3A3V_R	AACTGAGCAACAGGATGTGCaacCGTCATaattctt
DLD3ter_pRS313_R	CCTCACTAAAGGGAACAAAAGCTGGGTACCGGGCCCCCCCTCGAGggacgaacactt
DOA1_F_+194	TAAAACAATAGGAGCGAGGCTTGG
DOA1_LS1	ATTTTAGTACGCTGATAATAAGGGAAGGCCACTGTCTTGGCTTATTTTATATATATATATTCATGTGTGATAGTAAGGTGTAGAGCAGCAGATTTGGAGTcgtacgctgcaggtcgac
DOA1_LS2	GACCGTGATAGTTTGTCATAATTTTCAATAGGGCAGAAAGAATTTTAAAGATTATTTGCTATCTAGACATTATGTGTTTTATATGATTGCTGTAAAAGTAatcgatgaattcgagctcg
DUR1,2_-198_F	TCGCTCACTTCTGAATATCAGGCTC
DUR1,2_S1	AAATAGAAATATCTTTTTTATAGTCACAATAAATTTCAGTTTTGATTAAAAAATGcgtacgctgcaggtcgac
DUR1,2_S2	TATAAAGACTAAATGAGTGCTCCTTTGATTTTAGATGCCAACAAAAGGTAATTCAatcgatgaattcgagctcg

DUR1,2_S3	CAATGGTGATATGGTTGATTCTGGTGACATAGTGGCCGTCATAGAGACATTGGCAcgtacgctgcaggtcgac
FLC1_-249_F	TGCTATGCGAATCTGAACCGATC
FLC1_S1	AGAGATTATTTTCATTATTGACACACATACCCGACCAAAAACGGCGTTAAGAATGcgtacgctgcaggtcgac
FLC1_S2	TCGTAATGATTTAATTACGTTGTTCTTTTTACCTTTATCCCATCGACAAAGCTTAatcgatgaattcgagctcg
FLC1_S3	TGCAAACGCCCAAGATGTTACTAAAAAAGCAAACATCCTGGATCCTGATTATTTGcgtacgctgcaggtcgac
GAL.E	CTAAGATAATGGGGCTCTTT
GDH1_-240_F	AGCGTAAGAAGTAGCAGCAAAGG
GDH1_S1	GTACTATCGCATTATTCTAATATAACAGTTAGGAGACCAAAAAGAAAAAGAAATGcgtacgctgcaggtcgac
GDH1_S2	AAAAAAGAAAGAACTTTTTATGAACTTTCCTCTTTTCTTTCTTTTAGACTATTTAatcgatgaattcgagctcg
GDH1_S3	TATCGCAAGTTTCATCAAGGTCTCTGATGCTATGTTTGACCAAGGTGATGTATTTcgtacgctgcaggtcgac
GID10_102_R	GGGTAGAGAGACATAGGCCGAAG
GID10_CYCter_F	GTGGATTTGAAATTGCCTAAtcatgtaattagttatgtcacgcttacattcac
GID10_CYCter_R	tgacataactaattacatgaTTAGGCAATTTCAAATCCACTTGAGTAGGT
GID10_F_703	CATCATCTGGAAGGCGCGTC
GID10_F_80	CTTCGGCCTATGTCTCTCTACC
Gid10_LS2	TACTAGTTTACTTATTGATGTAATATCAAGAACAATGTGCTTTTAAAAGAGACATGGTTGACGAGTAAACAAACATACATTGGTAATTCTATAAGGGTCTatcgatgaattcgagctcg
GID10_R_127	GAGGCAAACGTGTATCAGTTGAGG
GID10-S1	TTATCCTTTCGTATTGTGTTATGAGACTTTTCATTTAAAATATACTGTAGGTATGcgtacgctgcaggtcgac
GID11_+305_R	GAGAAATGTGGATTGTGCAGTG
GID11_-150_F	GATCAGAAAGTGAGGAGGAGGAGAC
GID11_-218_F	GTGTCACGTGACATTGAACG
GID11_50_R	CGTTCATCTTGCAGCGCCTC
GID11_CYCter_F	CTAGTTATGACTTATGTTGAtcatgtaattagttatgtcacgcttacattcac
GID11_CYCter_R	tgacataactaattacatgaTCAACATAAGTCATAACTAGAGAAACTTCTTCTTGC
GID11_CYCter_R	GAGGGCGTGAATGTAAGCGTGACATAACTAATTACATGACTCGAGTCAACATAAGTCATAACTAGAGAAACTTCTTCTTGCC
GID11_F_1237	CAGGGCAGAGTACACGTTGTAG
GID11_F_1882	GACTATCATGGTGTTTCCGCAAG
GID11_F_20	GGCAATCTAAGGAGGCGCTG
GID11_F_643	TTTACGTTGGGCCAGTTCATC
GID11_GID11ter_R	acgggtgaattaaaatcacaatatatgtatggctgaagtGTCGACTCAACATAAGTC
GID11_H305_Y333_F	CCAACCAATTCTCCTTACATTATATCGAAAACATATATGAAGCTCCAAATTCAGACC
GID11_H305_Y333_R	TCATATATGTTTTCGATATAATGTAAGGAGAATTGGTTGGTTAATTCATTTTGAT
GID11_L304_AflII_R	ATGcttaagTAAGGAGAATTGGTTGGTTAATTCATTTTGATTGTAAAC
GID11_N334_AflII_F	ATGcttaagAACATATATGAAGCTCCAAATTCAGACCAT
GID11_P84_S116_F	CTTCCGTATTGAGGTCTCCATCCAAAAATTTACATGTTCCTTCCGAGAAAC

GID11_P84_S116_R	GGAACATGTAAATTTTTGGATGGAGACCTCAATACGGAAGAATCC
GID11_R_128	ATGGAGACCTTGGCATCGTAGAG
GID11_S1	AATAAAGTGGTAGAAAAACAGCAATAAGTTACAAAAGTATACGTGTTAAAGAATGcgtacgctgcaggtcgac
GID11_S525_Q678_F	ATAAAATTAGTAACGAATCGCAGGAAAGTAACGAATTCTCAGAAGAAAACA
GID11_S525_Q678_R	GAGAATTCGTTACTTTCCTGCGATTCGTTACTAATTTTATCCATAACTTTCGGAAAAG
GID11_T454_S486_F	CAAATCATAATTTCACCACATCTATGCCAAATGTAACCACAGAACCA
GID11_T454_S486_R	GTGGTTACATTTGGCATAGATGTGGTGAAATTATGATTTGTATTATGCTTCCG
GID11pr-HA-GID11_F	tgttaaagaATGTACCCATACGATGTTCCAGATTACGCTGTCGACATGACCATTGATGGCACGGG
GID11-SalI-CYC_R	gagggcgtgaatgtaagcgtgacataactaattacatgagtcgacTCAACATAAGTCATAACTAGAGAAACTTCTTCTTGCC
GID4_95_R	GGTGTTGGTTCTGGCGAAGC
GID4_CYCter_F	GTTCTTTTGAGTTTGCTTGAtcatgtaattagttatgtcacgcttacattcac
GID4_CYCter_R	tgacataactaattacatgaTCAAGCAAACTCAAAAGAACAATCACTGG
GID4_CYCter_R	GAGGGCGTGAATGTAAGCGTGACATAACTAATTACATGACTCGAGTCAAGCAAACTCAAAAGAACAATCACTGGAC
GID4_F_19	GTAGACAGTGTAGCGGAGAAACC
GID4_F_625	TTCAAAGCCACAGACCAAACAGAC
GID4_KO	GGGGCAGGCGGGTTTTAAT
GID4_R_157	AGGGTGCGGTTGAAGTCAAG
GID4_S1	ATCATTTGTGGCGTCTTGTGCATGACACCAACACATATCGCAAGCTTGAGTCATGcgtacgctgcaggtcgac
GID4-SalI-CYC_R	gagggcgtgaatgtaagcgtgacataactaattacatgagtcgacTCAAGCAAACTCAAAAGAACAATCACTGGAC
GID5-CUb_F	ACCTGCTTTTGAAAGTTAAAacgctgcaggtcgacg
GID5-CUb_R	ataccgtcgacctgcagcgtTTTAACTTTCAAAAGCAGGTCCATGTGATATAG
GID5-SalI-CYC_R	gagggcgtgaatgtaagcgtgacataactaattacatgagtcgacTCATTTAACTTTCAAAAGCAGGTCCATGTGA
GID7_KO	CGCCTTGTGTGCGCTTGTAG
GID7-S1	AAGTCAAATATGAAAAACACTTCCAAGGGGGCGTACTACTTCAACTAATAAAATGcgtacgctgcaggtcgac
GID7-S2	TTTTTTTTTGTTACATAAAACTTTGCTTACGTATATATATAAGGTGGAGTATTAatcgatgaattcgagctcg
Gid9(Fyv10)_KO	TGTTGATGTTCTCATGCGAGTC
GID9_1212_F	AAATCAAGAGACGGAAACTGCCAC
GID9_194_F	AGCACGACGAGTTGGCACTAG
GID9_380_R	TTTCCATTGTGCGATGTTCCTG
GID9_843_F	AAAGCCAACTTCTTCTACCAGCTC
GID9-S1	TCATACATAAAACAGAGAAAATGATTATAAATTATAGGAAAGTAGGTAAGCCATGcgtacgctgcaggtcgac
GID9-S2	TGAAAGTTGGACAAATCTTTATATAAAAAAATGCATATAGCTTGAAACTATTTCAatcgatgaattcgagctcg
GIS1_-209_F	CTTACAGAAACTCTTTGCCCACCAC
GIS1_S1	CGTTGTAATTTTTTTTTTTTAATTTGAAGAATAGCTACAAAAACAGACTACAATGcgtacgctgcaggtcgac

GIS1_S2	AATATTCGATAAAAATTTTTTTTGAACCCATTTTGTATATCATTTTCTTGACCTAatcgatgaattcgagctcg
GIS1_S3	AAATAAAAAAATTCCATGCACTCAAGAAATGGAAAATACTAAATTAGCTGAATCAcgtacgctgcaggtcgac
GPD_349_F	AACGGGCACAACCTCAATGG
GPD-306_R	TGCGCTAAGAGAATGGACCTATG
GPD-CPA1_F	aaacaccagaacttagtttcgacggattctagaactagtggatccATGTCCTCCGCTGCAACAA
GPD-CPA2_F	aaacaccagaacttagtttcgacggattctagaactagtggatccATGACATCGATTTATACATCAACAGAGCC
GPD-GID5_F	aaacaccagaacttagtttcgacggattctagaactagtggatccATGACGGTGGCTTATTCCCTAGAG
GPD-GPM3_F	aaacaccagaacttagtttcgacggattctagaactagtggatccATGACTGTTACTGACACTTTTAAACTGTTTATTTTAAGG
GPD-MDH2_F	aaacaccagaacttagtttcgacggattctagaactagtggatccATGATTCTCCTTCTGATTCTTTTTCCCTG
GPD-NUb_F	AAACACCAGAACTTAGTTTCGACGGATTCTAGAACTAGTGGATCCatgcagattttcgtcaagactttgacc
GPD-NUb_F	aaacaccagaacttagtttcgacggattctagaactagtggatccatgcagattttcgtcaagactttgaccggt
GPD-PHM8_F	aaacaccagaacttagtttcgacggattctagaactagtggatccATGACTATCGCTAAAGATTACAGAACAATTTATAGAAAC
GPDpr_ATE1iso1_F	acaccagaacttagtttcgaATGGCTTTCTGGGCGGG
GPDpr_ATE1iso1_R	CCCCCCGCCCAGAAAGCCATtcgaaactaagttctggtgttttaaaactaaaaaaaagac
GPDpr_ATE1iso2_F	acaccagaacttagtttcgaATGGCTTTCTGGGCGGG
GPDpr_ATE1iso2_R	CCCCCCGCCCAGAAAGCCATtcgaaactaagttctggtgttttaaaactaaaaaaaagac
GPDpr_CYCter_F	acaccagaacttagtttcgatcatgtaattagttatgtcacgcttacattcac
GPDpr_CYCter_R	tgacataactaattacatgatcgaaactaagttctggtgttttaaaactaaaaaaaagac
GPDpr_F_91	AATTCTGCTGTAACCCGTACATGC
GPDpr_NTAN1_F	acaccagaacttagtttcgaatgccgctgctcgt
GPDpr_NTAN1_R	ccctcgacgagcagcggcattcgaaactaagttctggtgttttaaaactaaaaaaaagac
GPDpr_NTAQ1_F	acaccagaacttagtttcgaAtggaaggtaatggccccg
GPDpr_NTAQ1_R	gcggggccattaccttccaTtcgaaactaagttctggtgttttaaaactaaaaaaaagac
GPDpr_R_305	TTGCGCTAAGAGAATGGACCTATG
GPDpr_scATE1_F	acaccagaacttagtttcgaATGTCCGATAGATTCGTTATTTGGGC
GPDpr_scATE1_R	ATAACGAATCTATCGGACATtcgaaactaagttctggtgttttaaaactaaaaaaaagac
GPDpr_scNTA1_F	acaccagaacttagtttcgaATGCTAATAGACGCAATTCATGGTGC
GPDpr_scNTA1_R	TGAATTGCGTCTATTAGCATtcgaaactaagttctggtgttttaaaactaaaaaaaagac
GPDpr-200bp_F	ACCTTCTGCTCTCTCTGATTTGG
GPDpr-GID10-fw	acaccagaacttagtttcgaATGACATCACTGAATATCATGGGAAGAAAGT
GPDpr-GID10-rv	ATGATATTCAGTGATGTCATtcgaaactaagttctggtgttttaaaactaaaaaaaagac
GPDpr-GID11-fw	acaccagaacttagtttcgaATGACCATTGATGGCACGGG
GPDpr-GID11-rv	CCCGTGCCATCAATGGTCATtcgaaactaagttctggtgttttaaaactaaaaaaaagac
GPDpr-GID4-fw	acaccagaacttagtttcgaATGATCAATAATCCTAAGGTAGACAGTGTAGC
GPDpr-GID4-rv	ACCTTAGGATTATTGATCATtcgaaactaagttctggtgttttaaaactaaaaaaaagac
GPDpr-IPF1-fw	acaccagaacttagtttcgaATGGCTACTGGCAGGATTCAATTTG
GPDpr-IPF1-rv	TGAATCCTGCCAGTAGCCATtcgaaactaagttctggtgttttaaaactaaaaaaaagac
GPDpr-YDR222W-fw	acaccagaacttagtttcgaATGCTTGAATCGAGCAGTGATAAGATAAAG

GPDpr-YDR222W-rv	TCACTGCTCGATTCAAGCATtcgaaactaagttctggtgttttaaaactaaaaaaaagac
GPDpr-YOR283WK3V_F	aaacaccagaacttagtttcgacggattctagaactagtggatccATGACTGTTGAAGTACCATAT
GPD-UBC7_F	AAACACCAGAACTTAGTTTCGACGGATTCTAGAACTAGTGGATCCATGTCGAAAACCGCTCAGAAACG
GPM3_-271_F	TGACAGGATACGACAGCACTAAC
GPM3_333_R	CTTCCTTCAAATCTTGTGTCCTGC
GPM3_F_-255	TGTAAGTGTGACAGGATACGACAGC
GPM3_IRO_T2A	GAAATAGTGCAAAAAGATCTACTAATAACGAATAGTTATGGCTGTTACTGACACTTTTAAACTGTTTATTTTAAGGCATGGTC
GPM3_IRO_T2A_3	AGAGGATTGAGAAATAGTGCAAAAAGATCTACTAATAACGAATAGTTATGGCTGTTACTGACACTTTTAAACTGTTTATTTTAAGGCATGGTCAAAGTGAA
GPM3_IRO_WT	GAAATAGTGCAAAAAGATCTACTAATAACGAATAGTTATGACTGTTACTGACACTTTTAAACTGTTTATTTTAAGGCATGGTC
GPM3_R_381	TTGCCATGCGCCGTAATGAC
GPM3_S1	CTTTGAGAGGATTGAGAAATAGTGCAAAAAGATCTACTAATAACGAATAGTTATGcgtacgctgcaggtcgac
GPM3_T2A_IRO_2	AGAGGATTGAGAAATAGTGCAAAAAGATCTACTAATAACGAATAGTTATGAGTGTTACTGACACTTTTAAACTGTTTATTTTAAGGCATGGTCAAAGTGAA
GPM3_WT_IRO_2	AGAGGATTGAGAAATAGTGCAAAAAGATCTACTAATAACGAATAGTTATGACTGTTACTGACACTTTTAAACTGTTTATTTTAAGGCATGGTCAAAGTGAA
GPM3-CUb_F	AGGGTTTCGAAAAGAATCCAacgctgcaggtcgacg
GPM3-CUb_R	ataccgtcgacctgcagcgtTGGATTCTTTTCGAAACCCTCATCAC
GPM3-S2	TAAAAGGAAACCATGAAAAAAATGGCGCTAATTTTTTATTTTTAAAAACTATTCAatcgatgaattcgagctcg
GPM3-S3	ATCAGCTAAAGTTAATGCTCAAATGGTTCGTGATGAGGGTTTCGAAAAGAATCCAcgtacgctgcaggtcgac
GPM3-S4	TTAATTCACTTTGACCATGCCTTAAAATAAACAGTTTAAAAGTGTCAGTAACAGTcatcgatgaattctctgtcg
GPM3-WT	TCGACGGATTCTAGAACTAGTGGATCCATGACTGTTACTGACACTTTTAAACTGTTTATTTTA
HA-GID11_V25_F	tgttaaagaATGTACCCATACGATGTTCCAGATTACGCTGTCGACGTTTACCAAAACTATATGATGCCTGCTTTAGAAC
HA-GID11ter_F	ATTACGCTGCTCAGTGCTAGGCATAAAACAAGCACCTTCAAACAACAAAG
HA-GID11ter_R	TGAAGGTGCTTGTTTTATGCCTAGCACTGAGCAGCGTAATC
hGid4_F_362	TGCTCTACAGCGGCTCCAAG
hGid4_F_pKBJ001_BamHI	gacggattctagaactagtgATGTGTGCGCGAGGGCAA
hGid4_opt_F_579	GGACGAAGATGTAGACAGAAAGC
hGid4_opt_F_7	GCACGAGGTCAAGTCGGAAG
hGid4_opt_F_pKBJ001_BamHI	gacggattctagaactagtgATGTGTGCACGAGGTCAAG
hGid4_opt_R_106	GCCGTCTTAATAACCTTTCTGGTC
hGid4_opt_R_330	GATAGGTGGTGGCGGAATCAG
hGid4_opt_R_pKBJ001_XhoI	gacataactaattacatgacTCATCGGAACTCGTAGATTG
hGid4_R_383	AACTTGGAGCCGCTGTAGAG
hGid4_R_pKBJ001_XhoI	gacataactaattacatgacTCACCGGAATTCATAGATGGGTG
hGID8_231_R	ACCTTTCAGTATCATCTCCCGGATC
hGID8_59_F	ATAACTTGCATGTCCAGAGAGCAG

hGID8_XhoI_pKBJ001_R	gagggcgtgaatgtaagcgtgacataactaattacatgactcgagTTACTTGGGCTCCTCAATCACACC
His&Kan_Tag2	GCTGCGCACGTCAAGACTG
hphNT_F_alt	AGGAAGGAGTTAGACAACCTGAAG
IDI1_-276_F	CCAGTCAACAGTTTCGCAATGACG
IDI1_S1	GTATTTGGAATACAGGAAGAGTAAAAATAAGCCAAAAATTCATTACACCTCAATGcgtacgctgcaggtcgac
IDI1_S2	ATGATAACAAAGTTATTATGATTTTTATGTAGCCTATATTATTGACGCGTTGTTAatcgatgaattcgagctcg
IDI1_S3	GCAATTAGATGACCTTTCTGAAGTGGAAAATGACAGGCAAATTCATAGAATGCTAcgtacgctgcaggtcgac
IPF1_CYCter_F	AAAAGGTAAAAAGAGACTAAtcatgtaattagttatgtcacgcttacattcac
IPF1_CYCter_R	tgacataactaattacatgaTTAGTCTCTTTTTACCTTTTTCACAATGAATGTATAAAGGT
Ipf1_F_1217	TTCAAGCCTTAACTAGAGACGC
Ipf1_F_15	GATTCAATTTGCTGTTTCTACTCCCTGC
Ipf1_F_1798	ATAATACCCCATGATTTCGG
Ipf1_F_615	GCATATCTGCTACTTCCTTTTGCC
Ipf1_F_BamHI_pKBJ001	gacggattctagaactagtgatggctactggcaggattc
Ipf1_R_325	AAGAGGGCGCTAATCGCAGG
Ipf1_R_XhoI_pKBJ001	gacataactaattacatgacttagtctcttttttacctttttcacaatg
IRC13_F+202	AAGTCATAGAAGGAAAAGCACATGG
IRC13_LS1	CCGTCTACCGGTAAAGCTTTCTCACAATATACCGTACGTTTCAAAAAAAATATTGATTCTTTTTTTATAAAAATATCAGTAGTATGTATGGGCTGATTGTcgtacgctgcaggtcgac
IRC13_LS2	GATCCTACTGTAGAATGTGTTAGTCAAAAGCTGCTGCAATGGTTGAATTAAATTTTTCAAAAAGCCTGCTCCGAAATGAAAACTCTAGTACCTAAGACTTatcgatgaattcgagctcg
KlURA_F_413	AAGAGGTCACCAAAGAACCAAGG
LYS20_-217_F	GTTCTTGCTGACGATGATGCGTG
LYS20_S1	TTTCTTATCTACATAACAAACAAAGGAAGGACCCTGTATTGTTTTCCTAAAGATGcgtacgctgcaggtcgac
LYS20_S2	CTATATATCGTATGTAATAAGTGAAAGAACATAATGTAATGGTTTGGGAACGTTAatcgatgaattcgagctcg
LYS20pr-LYS20A3V_F	ttgttttcctaaagATGACTgttGCTAAACCAAATCCATATGC
LYS20pr-LYS20A3V_R	GCATATGGATTTGGTTTAGCaacAGTCATctttaggaaaacaataca
LYS20ter-pRS313_R	CCTCACTAAAGGGAACAAAAGCTGGGTACCGGGCCCCCCCTCGAGttgttaacgcct
MAEA_292_R	GCTCTTTGAGGTGCTCGATCC
MAEA_32_F	TCAAGGTGCCCTACGAGACG
MAEA_630_F	AAGAAAGCACTTCAGCCAAGCAG
MAEA_XhoI_pKBJ001_R	gagggcgtgaatgtaagcgtgacataactaattacatgactcgagTTACATGATGTACACCTTCTCGGCTTG
MAP1_196_F	CACAATGCTAAGGACGGCTTGG
MAP1_-254_F	GCTTAATTCCACAGGTTCTCGTTC
MAP1_616_R	CGGGCACACCGTGACAAATAAC
MAP1_BamHI_pRS315_R	GGTATCGATAAGCTTGATATCGAATTCCTGCAGCCCGGGGTCTGCTATGTCTGCGATGATTCTATTGGAAC
MAP1_BamHI_pRS316_F	TTGGAGCTCCACCGCGGTGGCGGCCGCTCTAGAACTAGTGGTCGGTTGTTCCATATTAACAAATAACGATGT

MAP1_D.radMetAP_F	ATAAGCAAAAAAATTGTATAgtgttaggctcggatgttatgagc
MAP1_D.radMetAP_R	ataacatccgagcctaacacTATACAATTTTTTTGCTTATTTTTTTCTTGCTAGGAATATACACAATAGC
MAP1_F_1127	GAAATCACCAGGTGGCCCAAG
MAP1_F_144	TTCTGCGACACAAGCTGTTATG
MAP1_F_202	GCTAAGGACGGCTTGGAAGG
MAP1_F_591	GAAGTTATTTGTCACGGTGTGC
MAP1_MAP1ter_F	CAAGACAGAGAATTAAATAGATCTAGGTATTTTTATCTTATACATATAGAAACCAATAAAAAACTTGAAC
MAP1_MAP1ter_R	TAAGATAAAAATACCTAGATCTATTTAATTCTCTGTCTTGGGCCACCT
MAP1_R_+302	CTCGTCGATGATTTCGGTATGGTTC
MAP1_R_621	TTTATCGGGCACACCGTGAC
MAP1_S1	ACGCTATTGTGTATATTCCTAGCAAGAAAAAAATAAGCAAAAAAATTGTATAATGcgtacgctgcaggtcgac
MAP1_S2	AAGTTCAAGTTTTTTATTGGTTTCTATATGTATAAGATAAAAATACCTAGATCTAatcgatgaattcgagctcg
MAP1_SpeI_pRS315_F	GGCGAATTGGAGCTCCACCGCGGTGGCGGCCGCTCTAGAAGTCGGTTGTTCCATATTAACAAATAACGATGT
MAP1_XhoI_pRS316_R	CCTCACTAAAGGGAACAAAAGCTGGGTACCGGGCCCCCCCTCTGCTATGTCTGCGATGATTCTATTGGA
MAP1pr_F_40	ACTGGTGCTAATGTCGAGAATGC
MAP1pr_MAP1_F	ATAAGCAAAAAAATTGTATAATGAGCACTGCAACTACAACAGT
MAP1pr_MAP1_R	GTTGTAGTTGCAGTGCTCATTATACAATTTTTTTGCTTATTTTTTTCTTGCTAGGAATATACACAATAG
MAP1pr_R_277	TGACTTTAGAACGAGAACCTGTGG
MAP2_F_287	TGGAAAGGGCCGAACATTGG
MAP2_F_-309	GCTGTTGCTTCCCTGAGCTAATTTG
MAP2_R_+290	ATTAGTAACCTGTTGCATCGCACC
MAP2_R_677	GCGTCCTTTACAGCGGCTAG
MAP2_S1	TAAGTGGGCTTTTACATCAACAAGTACTGTAGAAGCTCTACCGTATTGAAAAATGcgtacgctgcaggtcgac
MAP2_S2	ACAACAGTATTCATATACCTAGTGAGGAGGCCATTTGAAAGCGCATTTTACCTCAatcgatgaattcgagctcg
mCherry_30_R	CATGTTATCCTCCTCGCCCTTG
mCherry_415_F	CCCGTAATGCAGAAGAAGACCATG
mCherry-7_F	AGCAAGGGCGAGGAGGATAAC
MD-GPM3	TCGACGGATTCTAGAACTAGTGGATCCATGGATATGACTGTTACTGACACTTTTAAACTGTTTATTTTA
MDH2_761_F	AGGCCAAGAACGGTAAAGGTAG
MDH2-CUb_F	CATCGAGATCTGCATCATCTacgctgcaggtcgacgg
MDH2-CUb_R	ataccgtcgacctgcagcgtAGATGATGCAGATCTCGATGCAAC
MDMT_GPM3_IRO	AGAGGATTGAGAAATAGTGCAAAAAGATCTACTAATAACGAATAGTTATGGATATGACTGTTACTGACACTTTTAAACTGTTTATTTTAAGGCATGGTCAAAGTGAA
MDMT_PHM8_IRO	ATGTAGATAAAAAACACATAAGTTTTATACGCACGTAATCATGGATATGACTATCGCTAAAGATTACAGAACAATTTATAGAAACCAAATCA
MD-PHM8	TCGACGGATTCTAGAACTAGTGGATCCATGGATATGACTATCGCTAAAGATTACAGAACAATTTATAGA
MDT_GPM3_IRO	AGAGGATTGAGAAATAGTGCAAAAAGATCTACTAATAACGAATAGTTATGGATACTGTTACTGACACTTTTAAACTGTTTATTTTAAGGCATGGTCAAAGTGAA

MDT_PHM8_IRO	ATGTAGATAAAAAACACATAAGTTTTATACGCACGTAATCATGGATACTATCGCTAAAGATTACA GAACAATTTATAGAAACCAAATCA
MHO1_+319_R	TCAAGTTGGTTTCCTGGTACGAC
MHO1_F_+208	TGCTGTAATAATATGAGGCTCCC
MHO1_LS1	CTGATATATTTTCAAAGGAAAGTCTGACTGATACTTAAGTGAAGTGGTCCTAGTCGGTGGCTTAG GTGGACTACAGTGCAAAGAATAGAATTTTTCAAACcgtacgctgcaggtcgac
MHO1_LS2	GGAAGTTTTTGTTTTTTTTTCCTTGAGATGCTGTAGTATTTGGGAACAATTATACAATCGAAAGATA TATGCTTACATTCGACCGTTTTAGCCGTGATCAatcgatgaattcgagctcg
MHO1_P.I	gctctattggaataccatgagcctgcatgtgttgctggacgtattgacatTTCGTACGCTGCAGGTCGAC
MHO1_P.IIS	tagtcggtggcttaggtggactacagtgcaaagaatagaatttttcaaac**TAGGGATAACAGGGTAAT**CCGCGC GTTGGCCGATTCAT
MHO1_S2	ATTATACAATCGAAAGATATATGCTTACATTCGACCGTTTTAGCCGTGATCATTAatcgatgaattcga gctcg
ML-GPM3	TCGACGGATTCTAGAACTAGTGGATCCATGTTGATGACTGTTACTGACACTTTTAAACTGTTTATT TTA
MLMT_GPM3_IRO	AGAGGATTGAGAAATAGTGCAAAAAGATCTACTAATAACGAATAGTTATGTTGATGACTGTTACT GACACTTTTAAACTGTTTATTTTAAGGCATGGTCAAAGTGAA
MLMT_PHM8_IRO	ATGTAGATAAAAAACACATAAGTTTTATACGCACGTAATCATGTTGATGACTATCGCTAAAGATTA CAGAACAATTTATAGAAACCAAATCA
ML-PHM8	TCGACGGATTCTAGAACTAGTGGATCCATGTTGATGACTATCGCTAAAGATTACAGAACAATTTA TAGA
MLT_GPM3_IRO	AGAGGATTGAGAAATAGTGCAAAAAGATCTACTAATAACGAATAGTTATGTTGACTGTTACTGAC ACTTTTAAACTGTTTATTTTAAGGCATGGTCAAAGTGAA
MLT_PHM8_IRO	ATGTAGATAAAAAACACATAAGTTTTATACGCACGTAATCATGTTGACTATCGCTAAAGATTACAG AACAATTTATAGAAACCAAATCA
Moh1_F_35	CGTTATCTTCCCCATCATCATCG
Moh1_F_BamHI_pKBJ001	gacggattctagaactagtgatgggattgcgttactcc
Moh1_R_379	ACTTTCCTTCCTTATACTGC
Moh1_R_XhoI_pKBJ001	gacataactaattacatgactcaagtacatttacaaatgtttttc
MT-GPM3	TCGACGGATTCTAGAACTAGTGGATCCATGACTATGACTGTTACTGACACTTTTAAACTGTTTATT TTA
MTMT_GPM3_IRO	AGAGGATTGAGAAATAGTGCAAAAAGATCTACTAATAACGAATAGTTATGACTATGACTGTTACT GACACTTTTAAACTGTTTATTTTAAGGCATGGTCAAAGTGAA
MTMT_PHM_IRO	ATGTAGATAAAAAACACATAAGTTTTATACGCACGTAATCATGACTATGACT**ATCGCTAAAGATTA CAGAACAATTTATAGAAACCAAATCA**
MT-PHM8	TCGACGGATTCTAGAACTAGTGGATCCATGACTATGACTATCGCTAAAGATTACAGAACAATTTA TAGA
MTT_GPM3_IRO	AGAGGATTGAGAAATAGTGCAAAAAGATCTACTAATAACGAATAGTTATGACTACTGTTACTGAC ACTTTTAAACTGTTTATTTTAAGGCATGGTCAAAGTGAA
MTT_PHM8_IRO	ATGTAGATAAAAAACACATAAGTTTTATACGCACGTAATCATGACTACTATCGCTAAAGATTACA GAACAATTTATAGAAACCAAATCA
MX-GPM3	TCGACGGATTCTAGAACTAGTGGATCCATGNNKATGACTGTTACTGACACTTTTAAACTGTTTAT TTTA
MX-PHM8	TCGACGGATTCTAGAACTAGTGGATCCATGNNKATGACTATCGCTAAAGATTACAGAACAATTT ATAGA
NIT3_F_+188	TGACATGCAAAGCACAAGGC
NIT3_F_370bp	GACAAGCATCGGAAGGTCCATC
NIT3_LS1	TTAAAATTATCAATAATGTTGTATGATATCTTGCTAACTTAATTTGATTCTTGTAAAAACACAGCTTTT GTAGTAGCAGGAGGGCGTGAAGATCGCCAGTcgtacgctgcaggtcgac
NIT3_LS2	GCCTATACGCATATATGTATATATATATATATATATATGTATGTATGTGTATATGTATATGTACGTATA CCTTACATCATCATCTTTCTTTATATTCTCTatcgatgaattcgagctcg
NIT3_R_573bp	GTAGATCATGGCAAACGCACC

NTA1_F_-373	GGAGATCACCACAGTCCAAGC
NTA1_S1	AATGCTAAAAAGTGCTAGTTTACAGCGATAACTCTATCGTGACATTCAGTGAATGcgtacgctgcaggtcgac
NTA1_S2	ATATGCGTGTAACCTTATTAATTTATAATGTCTAATTTATTATAATATTCCTTCAatcgatgaattcgagctcg
NTA1pr_NTAN1_F	TCTATCGTGACATTCAGTGAatgccgctgctcgt
NTA1pr_NTAN1_R	ccctcgacgagcagcggcatTCACTGAATGTCACGATAGAGTTATCG
NTA1pr_NTAQ1_F	TCTATCGTGACATTCAGTGAAtggaaggtaatggccccg
NTA1pr_NTAQ1_R	gcggggccattaccttccaTTCACTGAATGTCACGATAGAGTTATCG
NTAN1_619_F	CGAACTTTAGCAGGAGGACCAATG
NTAN1_69_F	CCCGCCTTTGGAGGAAAGAG
NTAN1_CYC1ter_F	agatctcttctccaggaagttcatgtaattagttatgtcacgcttacattcacg
NTAN1_CYC1ter_R	tgacataactaattacatgaacttcctggagaagagatcttttccc
NTAN1_NTA1ter_F	agatctcttctccaggaagttaaAGGAATATTATAATAAATTAGACATTATAAATTAATAAGGTTACACGCA
NTAN1_NTA1ter_R	TAATTTATTATAATATTCCTTTAacttcctggagaagagatcttttcccacaag
NTAQ1_185_F	TACCTATCTGGAAACAACAGGCGAG
NTAQ1_563_F	GCGCCGTCTACACACTATCC
NTAQ1_CYCter_F	ggtttggcagtaaaaactgctcatgtaattagttatgtcacgcttacattcacg
NTAQ1_CYCter_R	tgacataactaattacatgagcagtttttactgccaaaccga
NTAQ1_NTA1ter_F	ttggcagtaaaaactgcTGAAGGAATATTATAATAAATTAGACATTATAAATTAATAAGGTTACACGC
NTAQ1_NTA1ter_R	TAATTTATTATAATATTCCTTCAgcagtttttactgccaaaccg
NUb-CPA2_F	cgacgacagagaattcatcgATGACATCGATTTATACATCAACAGAGCC
NUb-CPA2-R	GATGTATAAATCGATGTCATcgatgaattctctgtcgtcgg
NUb-CUE1_F	ggatccctgggtctggggctactagtgaattgcaaagtaatcagcatcc
NUb-CUE1_R	ttactttgcaattcactagtagccccagacccaggg
NUb-GID11_F	cgacgacagagaattcatcgATGACCATTGATGGCACGGG
NUb-GID11_R	CCCGTGCCATCAATGGTCATcgatgaattctctgtcgtcgg
NUb-GID4_F	cgacgacagagaattcatcgATGATCAATAATCCTAAGGTAGACAGTGTAGC
NUb-GID4_R	ACCTTAGGATTATTGATCATcgatgaattctctgtcgtcg
P.I _Gpm3_T2A	GTTACTGACACTTTTAAACTGTTTATTTTAAGGCATGGTCAAAGTGAATTTTCGTACGCTGCAGGTCGAC
P.I _Pfk2_T2A	GTTACTACTCCTTTTGTGAATGGTACTTCTTATTGTACCGTCACTGCATATTCGTACGCTGCAGGTCGAC
P.I Cpa1 TtoS_2	CCAATCAAGGGTTGCGTGAAGACTAATATCTGACCACGGTAGGAAGGATCTTCGTACGCTGCAGGTCGAC
P.I Gpm3 T2A_2	AATTCACTTTGACCATGCCTTAAAATAAACAGTTTAAAAGTGTCAGTAACTTCGTACGCTGCAGGTCGAC
P.I Pfk2 T2A_2	TATGCAGTGACGGTACAATAAGAAGTACCATTCACAAAAGGAGTAGTAACTTCGTACGCTGCAGGTCGAC
P.I_Cpa1_TtoS	GATCCTTCCTACCGTGGTCAGATATTAGTCTTCACGCAACCCTTGATTGGTTCGTACGCTGCAGGTCGAC
P.I_CPA2_T2A	TCCTCGGTAGTAAAAGCAGAATTCGTAGGCTCTGTTGATGTATAAATCGATTCGTACGCTGCAGGTCGAC
P.I-GID11	AATAAAGTGGTAGAAAAACAGCAATAAGTTACAAAAGTATACGTGTTAAAGAATGTTCGTACGCTGCAGGTCGAC
P.II Cpa1 TtoS_2	AATTCTATCACAAACCACTCCTAAAAATATTTCAAATGTCCTCCGCTGCATAGGGATAACAGGGTAAT CCGCGCGTTGGCCGATTCAT
P.II Gpm3 T2A_2	AGAGGATTGAGAAATAGTGCAAAAAGATCTACTAATAACGAATAGTTATGTAGGGATAACAGGGTAAT CCGCGCGTTGGCCGATTCAT

P.II Pfk2 T2A_2	TAGATTTAGAGACTAGTTTAGCATTGGCCAAGAACTAACCATACGCAATGTAGGGATAACAGGG TAAT CCGCGCGTTGGCCGATTCAT
P.IIS _Gpm3_T2A	CATAACTATTCGTTATTAGTAGATCTTTTTGCACTATTTCTCAATCCTCTTAGGGATAACAGGGTAA TCCGCGCGTTGGCCGATTCAT
P.IIS _Pfk2_T2A	CATTGCGTATGGTTAGTTCTTGGCCAATGCTAAACTAGTCTCTAAATCTATAGGGATAACAGGGT AATCCGCGCGTTGGCCGATTCAT
P.IIS CPA2 T2A	AGTTCTATAAAGGAAGAGCAATACAGTACATAGACAGGAAGAAAAGAATGTAGGGATAACAGG GTAATCCGCGCGTTGGCCGATTCAT
P.IIS_Cpa1_TtoS	TGCAGCGGAGGACATTTGAAATATTTTTAGGAGTGGTTTGTGATAGAATTTAGGGATAACAGGGT AATCCGCGCGTTGGCCGATTCAT
P.IIS-GID11	AAAGAGTAATAAAACGGGTGAATTAAAATCACAATATATGTATGGCTGAAGTTCATAGGGATAAC AGGGTAATCCGCGCGTTGGCCGATTCAT
pAnB19-DC_14	CCTTACATCTTGTGCTAAGGCTAAGAGGTGGTGATTGTGGATCCGGAGCTTGGCTGTTGCCCG TCTCAC
pAnB19-DD_15	CCTTACATCTTGTGCTAAGGCTAAGAGGTGGTGATGATGGATCCGGAGCTTGGCTGTTGCCCG TCTCAC
pAnB19-DI_16	CCTTACATCTTGTGCTAAGGCTAAGAGGTGGTGATATTGGATCCGGAGCTTGGCTGTTGCCCG TCTCAC
pAnB19-DT_17	CCTTACATCTTGTGCTAAGGCTAAGAGGTGGTGATACTGGATCCGGAGCTTGGCTGTTGCCCG TCTCAC
pAnB19-ED_18	CCTTACATCTTGTGCTAAGGCTAAGAGGTGGTGAAGATGGATCCGGAGCTTGGCTGTTGCCC GTCTCAC
pAnB19-EN_19	CCTTACATCTTGTGCTAAGGCTAAGAGGTGGTGAAAATGGATCCGGAGCTTGGCTGTTGCCCG TCTCAC
pAnB19-EQ_20	CCTTACATCTTGTGCTAAGGCTAAGAGGTGGTGAACAAGGATCCGGAGCTTGGCTGTTGCCC GTCTCAC
pAnB19-NC_01	CCTTACATCTTGTGCTAAGGCTAAGAGGTGGTAATTGTGGATCCGGAGCTTGGCTGTTGCCCG TCTCAC
pAnB19-ND_02	CCTTACATCTTGTGCTAAGGCTAAGAGGTGGTAATGATGGATCCGGAGCTTGGCTGTTGCCCG TCTCAC
pAnB19-NI_03	CCTTACATCTTGTGCTAAGGCTAAGAGGTGGTAATATTGGATCCGGAGCTTGGCTGTTGCCCG TCTCAC
pAnB19-NK_04	CCTTACATCTTGTGCTAAGGCTAAGAGGTGGTAATAAAGGATCCGGAGCTTGGCTGTTGCCCG TCTCAC
pAnB19-NN_05	CCTTACATCTTGTGCTAAGGCTAAGAGGTGGTAATAATGGATCCGGAGCTTGGCTGTTGCCCG TCTCAC
pAnB19-NS_06	CCTTACATCTTGTGCTAAGGCTAAGAGGTGGTAATTCTGGATCCGGAGCTTGGCTGTTGCCCG TCTCAC
pAnB19-NT_07	CCTTACATCTTGTGCTAAGGCTAAGAGGTGGTAATACTGGATCCGGAGCTTGGCTGTTGCCCG TCTCAC
pAnB19-NY_08	CCTTACATCTTGTGCTAAGGCTAAGAGGTGGTAATTATGGATCCGGAGCTTGGCTGTTGCCCG TCTCAC
pAnB19-QD_09	CCTTACATCTTGTGCTAAGGCTAAGAGGTGGTCAAGATGGATCCGGAGCTTGGCTGTTGCCC GTCTCAC
pAnB19-QN_10	CCTTACATCTTGTGCTAAGGCTAAGAGGTGGTCAAAATGGATCCGGAGCTTGGCTGTTGCCCG TCTCAC
pAnB19-QS_11	CCTTACATCTTGTGCTAAGGCTAAGAGGTGGTCAATCTGGATCCGGAGCTTGGCTGTTGCCCG TCTCAC
pAnB19-QW_12	CCTTACATCTTGTGCTAAGGCTAAGAGGTGGTCAATGGGGATCCGGAGCTTGGCTGTTGCCC GTCTCAC
pAnB19-QY_13	CCTTACATCTTGTGCTAAGGCTAAGAGGTGGTCAATATGGATCCGGAGCTTGGCTGTTGCCCG TCTCAC
PDC2_-202_F	GCTGCTGCATATTTCCGTTCTGAG
PDC2_S1	TGAATTTTGTGGTAACACCAAGCAGTAAAGAGACAGCTTTATTATAACCAGCATGcgtacgctgcag gtcgac

PDC2_S2	GGCAAAACTACAAAAAAGAGCAATGAATATCGAGATCTTATTAAGTTTATATCTAatcgatgaattcgagctcg
PDC2_S3	TTCAAACCTCCCAGACTCTAATAACTTACACTTACCTGGTAACACAGGCTTTTTTcgtacgctgcaggtcgac
PFK2_-291_F	GAAGTCTCTCGCTTCATGTTGTTG
PFK2_F_-471	TAGTGGAAGCCACGGTTACG
PFK2_IRO_T2A	GACTAGTTTAGCATTGGCCAAGAACTAACCATACGCAATGGCTGTTACTACTCCTTTTGTGAATGGTACTTCTTATTGTACCG
PFK2_IRO_WT	GACTAGTTTAGCATTGGCCAAGAACTAACCATACGCAATGACTGTTACTACTCCTTTTGTGAATGGTACTTCTTATTGTACCG
PFK2_R_268	ACCAAGGATTGGGTGGCATG
PFK2_S1	AGAACTAGATTTAGAGACTAGTTTAGCATTGGCCAAGAACTAACCATACGCAATGcgtacgctgcaggtcgac
PFK2_S2	TTAACATTAATTGACATTAATAATAGAAAGTGTAATAAAAGGTCATTTTCTTTTAatcgatgaattcgagctcg
PGK1_F_1029	CGAAAAGTTCGCTGCTGGTACTAAGG
PGK1_LS2	TAAAAAATATTCAAAAAATAAAATAAACTATTATTTTAGCGTAAAGGATGGGGAAAGAGAAAAGAAAAAAATTGATCTATCGATTTCAATTCAATTCAATatcgatgaattcgagctcg
PGK1_LS3	CACTGACAAGATCTCCCATGTCTCTACTGGTGGTGGTGCTTCTTTGGAATTATTGGAAGGTAAGGAATTGCCAGGTGTTGCTTTCTTATCCGAAAAGAAAcgtacgctgcaggtcgac
PHM8_-276_F	GCAACGTGCTTCACATACAAACC
PHM8_-277_F	AGCAACGTGCTTCACATACAAACC
PHM8_291_R	CGTTCTGCCTCATCGTCGTC
PHM8_-296_R	GATTCGATTAGGCGTTCTGCCTC
PHM8_692_F	ACGAAAGCAATGTGCGGAGC
PHM8_896_F	TGGAAGAGTTGGAAGAGGAAGG
PHM8_IRO_WT	ATGTAGATAAAAAACACATAAGTTTTATACGCACGTAATCATGACTATCGCTAAAGATTACAGAACAATTTATAGAAACCAAATCA
PHM8_P.I	ATCTGCTTTTTGATTTGGTTTCTATAAATTGTTCTGTAATCTTTAGCGATTTCGTACGCTGCAGGTCGAC
PHM8_P.IIS	AAAAGATTTAATGTAGATAAAAAACACATAAGTTTTATACGCACGTAATCTAGGGATAACAGGGTAATCCGCGCGTTGGCCGATTCAT
PHM8_R_+255	CAAGGTCGGACTGAAACTATACAGC
PHM8_S1	GTAAAAGATTTAATGTAGATAAAAAACACATAAGTTTTATACGCACGTAATCATGcgtacgctgcaggtcgac
PHM8_S2	AATTTCTATCCTGAAGGGAATATTAAATTTGTTTTCTAAAATCAGGTAACAGTCAatcgatgaattcgagctcg
PHM8-CUb_F	AGATCAATGTTCAGTCATCAacgctgcaggtcgacg
PHM8-CUb_R	ataccgtcgacctgcagcgtTGATGACTGAACATTGATCTGTTGATTTGAC
PHM8-WT	TCGACGGATTCTAGAACTAGTGGATCCATGACTATCGCTAAAGATTACAGAACAATTTATAGA
pKBJ001_BamHI_ARMC8_F	aaacaccagaacttagtttcgacggattctagaactagtggatccATGGAAGTAACAGCTAGCAGTCG
pKBJ001_BamHI_hGID8_F	aaacaccagaacttagtttcgacggattctagaactagtggatccATGAGTTATGCAGAAAAACCCGATGAAA
pKBJ001_BamHI_MAEA_F	aaacaccagaacttagtttcgacggattctagaactagtggatccATGACCCTGAAGGTCCAGGAG
pKBJ001_BamHI_RANBP10_F	aaacaccagaacttagtttcgacggattctagaactagtggatccATGGCGGCAGCGACG
pKBJ001_BamHI_RANBP9_F	aaacaccagaacttagtttcgacggattctagaactagtggatccATGCGGGAGTGGAGAACC
pKBJ001_BamHI_RMND5A_F	aaacaccagaacttagtttcgacggattctagaactagtggatccATGGATCAGTGCGTGACGG

pKBJ001_BamHI_RMND5B_F	aaacaccagaacttagtttcgacggattctagaactagtggatccATGGAGCAGTGTGCGTGC
pKBJ001_BamHI_scGID2_F	aaacaccagaacttagtttcgacggattctagaactagtggatccATGTCTGAATTACTAGATAGCTTTGAGACAGAG
pKBJ001_BamHI_scGID8_F	aaacaccagaacttagtttcgacggattctagaactagtggatccATGACTATATCTACTCTTAGTAACGAGACCACG
pKBJ001_BamHI_SSD1_F	aaacaccagaacttagtttcgacggattctagaactagtggatccATGTCTAAAAATAGCAACGTTAACAACAATAGATCC
pKBJ001_BamHI_WDR26_F	aaacaccagaacttagtttcgacggattctagaactagtggatccATGCAGGCAAATGGTGCAG
pKBJ001_Hind3_SSD1_R	gagggcgtgaatgtaagcgtgacataactaattacatgactcgagTTATACCCTCTTCATGAATGGATTTAATGCACGG
pKBJ001_SSD1_F	aaacaccagaacttagtttcgacggattctagaactagtggatccATGTCTAAAAATAGCAACGTTAACAACAATAGATCC
pKBJ001_XhoI_GID5R-2	gagggcgtgaatgtaagcgtgacataactaattacatgactcgagTCATTTAACTTTCAAAAGCAGGTCCATGTGATATAGTAACG
pKBJ001_XhoI_scGID8_R	gagggcgtgaatgtaagcgtgacataactaattacatgactcgagTCAGTTTTCGACCCTAGGAACCCC
pKBJ001_XhoI-scGID5_R	gagggcgtgaatgtaagcgtgacataactaattacatgactcgagTCATTTAACTTTCAAAAGCAGGTCCATGTGATATAGT
pKBJ001-BamHI-scGID5_F	aaacaccagaacttagtttcgacggattctagaactagtggatccATGACGGTGGCTTATTCCCTAGAG
pKBJ001-CAN1-F	aaacaccagaacttagtttcgacggattctagaactagtggatccATGACAAATTCAAAAGAAGACGCCGAC
pKBJ001-CPA1pr-F	tcactaaagggaacaaaagctggagctccaccgcggtggcggccgcGTGTATGATGTAATCCATCACC
pKBJ001-CPA2_F	aaacaccagaacttagtttcgacggattctagaactagtggatccATGACATCGATTTATACATCAACAGAGCCT
pKBJ1_3xHA_XhoI_R	gagggcgtgaatgtaagcgtgacataactaattacatgactcgagCTAGCACTGAGCAGCGTAATCT
pkBJ1_Bam_GID1_F	aaacaccagaacttagtttcgacggattctagaactagtggatccATGTCTGAATATATGGATGACGTAGACCG
pKBJ1_Bam_GID1_F	aaacaccagaacttagtttcgacggattctagaactagtggatccATGGCAGAGAAATCAATATTTAATGAGCCTG
pKBJ1_Bam_GID7_F	aaacaccagaacttagtttcgacggattctagaactagtggatccATGTCACACACTAATAAGATCGCATACGT
pKBJ1_Bam_RANBP10optF	aaacaccagaacttagtttcgacggattctagaactagtggatccATGGCTGCAGCGACTGC
pKBJ1_Bam_WDR26optF	aaacaccagaacttagtttcgacggattctagaactagtggatccATGCAAGCCAATGGCGC
pKBJ1_HA_BamHI_F	aaacaccagaacttagtttcgacggattctagaactagtggatccATGTACCCATACGATGTTCCTGACTATG
pKBJ1_Xho_GID7_R	gagggcgtgaatgtaagcgtgacataactaattacatgactcgagTTAATTTCTTGAAATTTTCCAGATTTTTATCTTACCGTCATCAC
pKBJ1_Xho_RANBP10optR	gagggcgtgaatgtaagcgtgacataactaattacatgactcgagTTAGTGAAGGTAGTCATCGACTCTGGC
pKBJ1_Xho_WDR26optR	gagggcgtgaatgtaagcgtgacataactaattacatgactcgagTTAACTATCCATACTAGAGCATTCCTCTTCGA
pRS313-DBP3pr_F	TTGGAGCTCCACCGCGGTGGCGGCCGCTCTAGAACTAGTGGATCCgggactaagata
pRS313-DLD3pr_F	TTGGAGCTCCACCGCGGTGGCGGCCGCTCTAGAACTAGTGGATCCgtgcgtgatcat
pRS313-LYS20pr_F	TTGGAGCTCCACCGCGGTGGCGGCCGCTCTAGAACTAGTGGATCCcaaaattgctgg
pRS313-STF2pr_F	TTGGAGCTCCACCGCGGTGGCGGCCGCTCTAGAACTAGTGGATCCgtaagcaatgaa
pRS426_BamHI_GPDpr_F	ggtatcgataagcttgatatcgaattcctgcagcccgggggatcctcattatcaatactcgccatttcaaagaatacgtaaataat
RANBP10_1273_F	TCCGTCAATTACTCCGAGTCCAAC

RANBP10_135_F	GGTCAACCAGCAAGAGACTCC
RANBP10_310_R	AATAAATGCCACAGGCAGCAGG
RANBP10_660_F	GCCCTTCCCGTTTGACATTGAG
RANBP10_XhoI_pKBJ001_R	gagggcgtgaatgtaagcgtgacataactaattacatgactcgagTTAGTGCAAGTAGTCATCAACTCTGGCA
RANBP10opt_1221_F	CCCATCCAGCTCATCCAGTAGTTC
RANBP10opt_32_F	GAAATCCGCAACCTGGCGAC
RANBP10opt_321_R	GACCTCAAAGTAGTAAATGCCGCAG
RANBP10opt_627_F	GGGCGAGATAGTAGACGCAAAC
RANBP9_372_R	GCCTCCCAAACATCGTACTTCAC
RANBP9_48_F	TATCGGAGATCGAGAAGGAGAATGG
RANBP9_749_F	TGGAAGATTGTGACACCGAAATGG
RANBP9_XhoI_pKBJ001_R	gagggcgtgaatgtaagcgtgacataactaattacatgactcgagTTAATGTAGGTAGTCTTCCACTGTGGC
RCR1_F_+201	TATTCCGCCTCCTCTCTCGAAGC
RCR1_LS1	TTTAAATGACCGACAGGAAGCTCATGCAGAAAAGGCACCTGTAATAGCTTATTGATCATTCCAATAAATAGGAAAGTATAACTCGAATTAAGAATAAGGAcgtacgctgcaggtcgac
RCR1_LS2	TTAAAATAATTATTATAGAGATTGGGTAAAAAAATGTAAATATTTCTGGCAAAATATTGTAACTCAACTGTAAGAGGACAGCCGGAAAAAAAGATTCAGTatcgatgaattcgagctcg
RMND5A_326_R	CAGCCATCTATTCCCACACTGC
RMND5A_39_F	GGTGCTGCACAAGTTCTCAGG
RMND5A_620_F	CCACAAATCAGCGAGAGGCATTAC
RMND5A_XhoI_pKBJ001_R	gagggcgtgaatgtaagcgtgacataactaattacatgactcgagTTAGAAAAATATCTGTTTGGCATCTCCTGGAC
RMND5B_19_F	GTGGAGAGAGAGCTGGACAAGG
RMND5B_254_R	CTGCTGTGAATGTCCTTATGGTCC
RMND5B_600_F	CTTCATCCGCCTCTTGGCAG
RMND5B_XhoI_pKBJ001_R	gagggcgtgaatgtaagcgtgacataactaattacatgactcgagTTAGAATATGATGCGTTTCCCATCT
S2-GID4	TAAAGTTAGTGAAGAGAAAAGGGTATGCAGGTAAAAACGAATATATCACACATCAatcgatgaattcgagctcg
S2-YLR149C	AAAGAGTAATAAAACGGGTGAATTAAAATCACAATATATGTATGGCTGAAGTTCAATCGATGAATTCGAGCTCG
scATE_1252_F	GGCCATGCTCCAAATGGTATTCC
scATE_654_F	GAAGCCAGGCGAGAAACTGAAG
scATE1_11_F	GATTCGTTATTTGGGCTCCCTCG
scATE1_CYCter_F	TATATAGTGAGCAAATGTGAtcatgtaattagttatgtcacgcttacattcac
scATE1_CYCter_R	tgacataactaattacatgaTCACATTTGCTCACTATATAAAATGACGGC
scGID2_XhoI_pKBJ001_R	gagggcgtgaatgtaagcgtgacataactaattacatgactcgagTCAAAGCATAACAAAACGAACCTTTTTTGTACT
scGID5_1163_F	CGCAGTGTCTTTCTCTACCACAAC
scGID5_1844_F	GCCAGAATGAAGAGAAGTTTCAGC
scGID5_2432_F	TCGGGTATAATGAATCAGTGGCTGG
scGID5_36_F	GATTAGTAATTCCCTGGTGGGAGAC
scGID5_366_R	GTCTGGGAATCCGCAATTTGG
scGID5_660_F	AGTATCCAGGCCAGCGTCAC
scGID8_292_R	CAAAGTAGTTCAACAGAAGCCGTGG

scGID8_51_F	CGGCCAAGGCAAGAATGGTG
scGID8_619_F	AGAAGTCACCATCAACAGGAGAAC
scNTA1_1256_F	AGGATGATGATGAGAGTTCGCTTG
scNTA1_644_F	TGATTCTATGTCCAATGGCGTG
scNTA1_9_F	AGACGCAATTCATGGTGCTAAG
scNTA1_CYCter_F	AATTTGAAGTGTTTAGGTGAtcatgtaattagttatgtcacgcttacattcac
scNTA1_CYCter_R	tgacataactaattacatgaTCACCTAAACACTTCAAATTGGACCTCAC
sfGFP_270_F	AGGCTACGTGCAAGAGAGAACTATC
sfGFP_F_659	TATTGGAATTTGTCACCGCTGC
sfGFP_pKBJ001_R	gagggcgtgaatgtaagcgtgacataactaattacatgactcgagttacttataaagctcgtccattccgtgagt
sfGFP-50_F	AACTGGACGGAGATGTAAACGGAC
sfGFP-CYCter_R	gagggcgtgaatgtaagcgtgacataactaattacatgactcgagTCACTTATAAAG
SNO1_-218_F	ACCCTTACCCTTGTCGGCTG
SNO1_S1	TTTTCTTATTATTTCATTTCGTTAAATAGAAAGAAAAACCATATCTTAAAGTATGcgtacgctgcaggtcgac
SNO1_S2	AAAAAATCTCTCAGGTTTTGGTAATATAAAAATGTGGAAAACCGGCGGTATTTTAatcgatgaattcgagctcg
SNO1_S3	TGCTGACAGTGATACAAGATTTCATGATTGGTTTATCAGACAGTTTGTTTCTAATcgtacgctgcaggtcgac
SSD1_1230_F	GGACGATGTTTGGGAGTCCAAG
SSD1_1871_F	GGCCAATCACATCTTTGCATCC
SSD1_2546_F	AAGCTACATTACTTCCCACCCTGTC
SSD1_3040_F	ATCCACGATACTCCATACACCGAAG
SSD1_3560_F	CATCTGCAAGCGACAACAAGC
SSD1_677_F	CAACTTCAAACCTATCACCTCCCTC
SSD1_87_F	CCCAAAGCAGATTCATGTTGCAC
STF2_-178_F	GAGCGCAGAAGCGAACACTTG
STF2_S1	AACGAACAATCAACAGTAACAAACCGCTCAAGTGTACAACCAATCAGAAAAAATGcgtacgctgcaggtcgac
STF2_S2	AGGCCACTATCCTTCAGAGATCAAAAAACCTTTTTTTATCTTGAAAACGCCCTCAatcgatgaattcgagctcg
STF2pr-STF2 R3V_F	accaatcagaaaaaATGACGgttACAAACAAGTGGACC
STF2pr-STF2 R3V_R	CGTTCGGTCCACTTGTTTGTaacCGTCATtttttctga
STF2ter-pRS313-R	CCTCACTAAAGGGAACAAAAGCTGGGTACCGGGCCCCCCCTCGAGgaatacttgact
SYF1_-380_F	AACCTCCATTACCTCATTCTCTCC
SYF1_S1	TTGGACTCAACTATCCTTCAGTACCGCAAAACTTATTGTGTCCATATATCCTATGcgtacgctgcaggtcgac
SYF1_S2	CAAAAAAGAACTTATGGTTTCGAAAATGATGCATGATTTTACATAGCTTATATCAatcgatgaattcgagctcg
SYF1_S3	TACCCAATCAACCTCTTCATATTCGATTAATCCAGATGAAATAGAACTAGATATTcgtacgctgcaggtcgac
TAF1_-203_F	AGTAATGAGCGTCTGTGGGTCC
TAF1_S1	TAGCATTTTAAACACAGAGAGAAAAAGAAGTACAACAGGAGTATAAGGCGATATGcgtacgctgcaggtcgac
TAF1_S2	ATACAAAACCTTTACAAAAGTTTTATTCGATCAATACATCGTTATACTGAATCTAatcgatgaattcgagctcg
TAF1_S3	AACAAATAAATCTTGTCCAATGTATAGCAGTAAAGATAACCCTGCTTCACCAAAGcgtacgctgcaggtcgac

TMA10_-162_F	GTTCTGGCAGGTAGATTTGTACTCC
TMA10_F_+201	GTATGGATATGGTATGGCTTGAGGTAGG
TMA10_LS1	TTTATTATAAGCACAGCAAAAACGTTAAATAAATCTAATAAGATTTCATTATAACATAACATTAAAG CACACAAATTTCTAACACAAACACAATTCAAACcgtacgctgcaggtcgac
TMA10_LS2	TTTATATATGCATACACGTTATTGAAGTTATATGGTCGTTAAATCATTAAAAGGCCCGTTTCTTTGA AATATGCTAACGGAATCAAACCGGTCGGGTCGGatcgatgaattcgagctcg
TMA10_S1	TTATAACATAACATTAAAGCACACAAATTTCTAACACAAACACAATTCAAACATGcgtacgctgcaggt cgac
TMA10_S2	AAAAGGCCCGTTTCTTTGAAATATGCTAACGGAATCAAACCGGTCGGGTCGGTTAatcgatgaatt cgagctcg
TOP1_-43_F	AAATCTAAAGGGAGGGCAGAGC
TOP1_S1	AATAAAAAAAATCTAAAGGGAGGGCAGAGCTCGAAACTTGAAACGCGTAAAAATGcgtacgctgc aggtcgac
TOP1_S2	GAACTTGATGCGTGAATGTATTTGCTTCTCCCCTATGCTGCGTTTCTTTGCGTTAatcgatgaattcg agctcg
UBC12_F_+258	AACGAGTGGCGTTTTCGATTGC
UBC12_LS1	TCAGCCAAAAGGTAAAATGAGATGAAAAAGGCCAATCATTCATAAATGTACTTAGAGACATTAAA GAATCAGTTAGAGAATATAAAACAAGATAATAAAAcgtacgctgcaggtcgac
UBC12_LS2	AGATGTTACCAAGGCGACAACTCGCCTAGTATGTCACAATTATCTATAATTTTATTGTTTATATATA ATCAAATCAACCGAAAATTACTCTGAACTTGACatcgatgaattcgagctcg
UBC7-CYCter_R	GAGGGCGTGAATGTAAGCGTGACATAACTAATTACATGACTCGAGTCAGAATCCTAATGATTTC AAAATGGATAACTTTACCTGT
UBC7-CYCter_R	GAGGGCGTGAATGTAAGCGTGACATAACTAATTACATGACTCGAGTCAGAATCCTAATGATTTC AAAATGGATAACTTTACCTGT
UBP15_F_+208	GAATGGTGATTAGAAAGGCAGG
UBP15_LS1	GTTTGTTTGCCCCTACGTTTTGCCCCTTTGATCAAACTATCAGTTAAGATATTAATTTTTTTGAGAA AACGATTCTTTGATTAGTCTCTTCAAACAAACAcgtacgctgcaggtcgac
UBP15_LS2	AGCATTGCCTGTGTGGAAGTGATGGCGGCTGAGAGATTATCATAAAAAAACATAAAAAAAATGG AGAAAACATCAAAGCTAAACATAGTCGTAAGACGTAatcgatgaattcgagctcg
URA3.1	TTCAATAGCTCATCAGTCGA
URA3-CYC1ter_R	gagggcgtgaatgtaagcgtgacataactaattacatgactcgagttagttttgctggccgcatcttct
VPS9_F_+191	CTCATAGTAATGCCAGATGCTCAAGG
VPS9_LS1	TGCCGGTACTTGATGTAATGACACATAACATTGAAAAGTTCTACATCCAACGGGCTTGAGTTTCT CTTCATCAAACAACAAAGAACAGGAATCAACAGCCcgtacgctgcaggtcgac
VPS9_LS2	CAGTAAAAAATGTCTCCTGCGGTAAGTTATTTTTACTATTATATTTTTACAAATACATATTGCTAGG CTACTCTATACATGAAATATGTGCATGAGATCAatcgatgaattcgagctcg
WDR26_1270_F	TGCTCTGAGCTTTGGCTTTGG
WDR26_1825_F	CTGACAGGGCACACACGTAC
WDR26_276_R	AACGGTTGCTGAGGATGCTG
WDR26_674_F	AGGATGGCAAGGTCCTGGAG
WDR26_73_F	GGACAGGGACAGACACCAGAAC
WDR26_XhoI_pKBJ001_R	gagggcgtgaatgtaagcgtgacataactaattacatgactcgagTTAACTATCCATGCTACTGCATTCCT
WDR26opt_115_F	AATGGAGAGAGCAGCCCGTC
WDR26opt_1239_F	CAACTACTTGGTGGCGTGTGG
WDR26opt_1877_F	CCAGTATGATGGCTTCCGCTTC
WDR26opt_276_R	CACAGTTGCGGAAGACGCAG
WDR26opt_706_F	TTGAGATGCGAATTGACGCCATTG
YDR222W_CYCter_F	AGAGCACCTTCATTAGTTGAtcatgtaattagttatgtcacgcttacattcac

YDR222W_CYCter_R	tgacataactaattacatgaTCAACTAATGAAGGTGCTCTCAACGA
YDR222W_F_128	ACAATGATAGTGAAACGGGCTACC
YDR222W_F_768	TGATGTTCCTGTCGTTTATCTGGACGC
YDR222W_F_BamHI_pKBJ001	gacggattctagaactagtgatgcttgaatcgagcagtg
YDR222W_R_165	ACTTATGGTGTGTTGGTAGCC
YDR222W_R_XhoI_pKBJ001	gacataactaattacatgactcaactaatgaaggtgctc
YDR344C_F_+182	TTTGTTATACCCACGAAGAAGTGCG
YDR344C_LS1	TGGATTTCGTTTGAAATCCGGACGGAAAACTCAAAAGAAGTCCAACCACCAACCATTTTCGAGCCTCAAGAATCTCTAAGCAGGTTTCTTTACTAAGGGGcgtacgctgcaggtcgac
YDR344C_LS2	ATTTGTCTTGGCGCCGCACACAGGAACTGCGCACTTCTTTTTGTCCTAGGTTGCTTATCACACCATATGGTGCACCCGTGCTCGTTGTCACTGCCTTTTTatcgatgaattcgagctcg
YGL149W_F_+199	TTCCAGTCCTGATAAAGTTGC
YGL149W_LS1	AACTCTCTCTCTGCTATTCTTCTTAGCAGACTTGCCTGCGGTAGTCTTTGAAAAATCAGATATATCCTTGTCCTCCTTATTGAGTAGAACTGCCAGTGACcgtacgctgcaggtcgac
YGL149W_LS2	TGATGTATGTGTATGTAGATGTAAGTATAAGTTACGGTTGCAAGAGCTTGGCCCCTTAGACGTGCCCAACGTAGTTTCTTGCTGGACGCCAAAGAAGAAGatcgatgaattcgagctcg
YGR045C_F_-273	AGAGAGTCTGGTACAGCATTGG
YGR045C_S1	TTCTTTCTGTTGTAAGGGATGCTTCGTCACGTAAAATGGCCGCCGGAGTGAGATGcgtacgctgcaggtcgac
YGR045C_S2	CACGGTGACATAAGTGCTGAAAATCCCAACTTCTAGTAAAGAATTAACAAATTCAatcgatgaattcgagctcg
YLR149C_KO	GTGTCACGTGACATTGAACG
YLR365W_F_+245	ATGCACATTTACCTCCCACTTCG
YLR365W_LS1	TGCATACTTAAAAGTAATCAGACCGAATGAACATGTGCCTTTGCATTACTTCTTTTCAAAGGACATCTCTTTGCAAGCTAACCATCTGAAAGGCCGATGAcgtacgctgcaggtcgac
YLR365W_LS2	CATTGGAAGTCTTCCAATGCTGGACTTGAAAAATAGGGTGTCGTCTTACTGGCACTTCTCGAGCACTCCGGTTGCGAGAAGAATAACGGATCATACTTGTatcgatgaattcgagctcg
YLR407W_F_+141	ACAGGGAATACTCTAACAACAAACG
YLR407W_LS1	TTGTCACATATTTTTGTCCATTAAGGTCGTTAAAACCCGAATAATTTTGTACGATCAGTTTAGTAAAAGAAATACAGTATTCAAAAGCTAACGGTTTATTcgtacgctgcaggtcgac
YLR407W_LS2	TAAATGACGAAGTTCTTTAACTGAGTTAAAGTTGTGTAATGCAAATTTGAAGAAAGGAAAAGATGCTATAAGGCAAAACAAAAAGGACGTCGACACTCAGatcgatgaattcgagctcg
YMR114C_F_+196	GATCTTCCTGCTTGTGTTTACACC
YMR114C_LS1	AATGAAAGGGATCAAAAAAGGGAACAAAGCAATGAACAGTTGAACCAAGAGACTTAATTAAAGTATACCTGATGCTAATACCAGACTTTCATAACCCAAGcgtacgctgcaggtcgac
YMR114C_LS2	TGAATTATTACGGATTCACAATAGTCACTTGAGAAACTAAATAAAATAAGTAACAACGAACATTATATAGACTATCGATGATAAACAAACTAAAAAAATGatcgatgaattcgagctcg
YMR141C_F_+203	TCAGAGGTATCAGAGAAAAGAGGG
YMR141C_LS1	TATGTACACTGTATAATGGGAAGCCATCACTCATAACAAAATATTCTGTTATCACTGAATTGTGACGCTCAGATAAGATAAACATCCAAAGCGCATACTGcgtacgctgcaggtcgac
YMR141C_LS2	GAGAGACTGTTAAAAACGACCTTCCGTTCGACCACTCAAACTGTAGTAGGAGTTCTTTTCTCTATTTATATGCTTGCAATGTTCGCAGAAAAAGCACCATatcgatgaattcgagctcg
YOR283W_-282_F	TCGAAGGCGTTATCTTGTACTGC
YOR283W_-282_F	TCGAAGGCGTTATCTTGTACTGC
YOR283W_319_R	CACCCATATAACGCTCCCTTAACC
YOR283W_S1	GCAACGAAGCTCGAAGCTATACAAGCACCCAAAAATATATTTATACCCAAGAATGcgtacgctgcaggtcgac
YOR283W_S2	GCATTTCTAATACAAAATGAGAAAAACCCAACAGTGAATAACCATATAGTGTCTAatcgatgaattcgagctcg

YOR283W-P.I	AATCTGATGATGTTGTTATCGTCATTATCGCAATAATATGGTACTTCCTTTTCGTACGCTGCAGGTCGAC
YOR283W-P.IIS	GAAGCTCGAAGCTATACAAGCACCCAAAAATATATTTATACCCAAGAATGTAGGGATAACAGGGTAATCCGCGCGTTGGCCGATTCAT
YOR283W-S2	GCATTTCTAATACAAAATGAGAAAAACCCAACAGTGAATAACCATATAGTGTCTAatcgatgaattcgagctcg
YOR283W-S3	AAACACCCAACATCTTGGTGATGGCGAATTTGTCGTCAGTGACTTAAGATTACGTcgtacgctgcaggtcgac
YOR283W-T2A-IRO	GCTATACAAGCACCCAAAAATATATTTATACCCAAGAATGGCTAAGGAAGTACCATATTATTGCGATAATGACGATAACAACA
YOR302W_-345_F	TCATCATCGCATCGCATTACCTC
YOR302W_S1	ATCGACTCTTCTACATACCCTTTTTGCAGATTTGAAATAAAAAAAACATTATATGcgtacgctgcaggtcgac
YOR302W_S2	AATATTTTTAGGAGTGGTTTGTGATAGAATTTCTGATTATTAAGCAATGAAATTAatcgatgaattcgagctcg
ZPS1_-173_F	TATAGACGCCGCACATGCTTTC
ZPS1_S1	GGATTGAGCAATTAAGATAGAAAACCAAATCCACACACAACTACTAAACATTATGcgtacgctgcaggtcgac
ZPS1_S2	ACTAATATTTACGGTATAGAAAACATATTCTGTGGAAGTAATGATGTGGTTATTAatcgatgaattcgagctcg
ZPS1_S3	TCTCGCTGACGTTTACAGTGCTTCTGTTATACCTGGTGGCTGTCTAGGTAACTTGcgtacgctgcaggtcgac

Table S 4: List of instruments used in this study

Instrument	**Supplier**
ROTOR pinning robot	Singer Instruments
PhenoBooth	Singer Instruments
Spark 20M plate reader with monochromator	TECAN
Chemidoc imaging system	Bio-Rad
Liquidator 96	Steinbrenner
BioShakeXP microtiter plate shaker	Analytik Jena
EASY HPLC 1000	Thermo Fisher Scientific
Q Exactive Plus mass spectrometer	Thermo Fisher Scientific
EASY HPLC 1200	Thermo Fisher Scientific
Exploris 480 mass spectrometer	Thermo Fisher Scientific
Orbitrap Astral mass spectrometer	Thermo Fisher Scientific

Table S 5: List of software used

Software	**Source/Reference**
Microsoft Office 2016 / Microsoft Office 365	Microsoft
Adobe Illustrator 25.4.8	Adobe
RStudio 2024.12.1	https://posit.co/products/open-source/rstudio
R (version 4.2.3)	(R Core Team 2023)
ImageLab 6.1.0	BioRad
Clustal Omega	(Sievers and Higgins 2021; Madeira et al. 2024)

Jalview 2.11.4.1	(Waterhouse et al. 2009) https://www.jalview.org/
MaxQuant suite 1.6.5.0, 1.6.10.43, and 2.1.3.0	(Cox and Mann 2008)
Andromeda search engine	(Cox et al. 2011)
SnapGene 4.0.8	https://www.snapgene.com
AlphaFold 2	(Jumper et al. 2021; Varadi et al. 2022)
AlphaFold 3	(Abramson et al. 2024)
UCSF ChimeraX 1.8	(Goddard et al. 2018; Pettersen et al. 2021; Meng et al. 2023) https://www.cgl.ucsf.edu/chimerax/

Table S 6: List of R packages used.

Package	**Reference**
biomaRt	(Durinck et al. 2005; Durinck et al. 2009)
tidyverse	(Wickham et al. 2019)
EBImage	(Pau et al. 2010)
gdata	(Warnes et al. 2024)
lazyeval	(Wickham 2022)
data.table	(Dowle and Srinivasan 2023)
gitter	(Wagih and Parts 2021)
openxlsx	(Schauberger and Walker 2023)
gridExtra	(Auguie 2017)
locfit	(Loader 2024)
xlsx	(Dragulescu and Arendt 2020)
writexl	(Ooms 2024)
ggrepel	(Slowikowski 2024)

List of abbreviations

5-FOA	5-fluoroorotic acid
Ac	Acetyl-
AMP	Adenosine monophosphate
Arg	Arginine
ATP	Adenosine triphosphate
cloNAT	Nourseothricin
CORE	Counter selectable reporter
CRL	Cullin RING ligase
CTLH	C-terminal to LisH
CUb	C-terminal ubiquitin fragment
DNA	Deoxyribonucleic acid
DTT	Dithiothreitol
DUB	Deubiquitinase
E1	E1 ubiquitin-activating enzyme
E2	E2 ubiquitin-conjugating enzyme
E3	E3 ubiquitin ligase

EDTA	Ethylenediaminetetraacetic acid
ER	Endoplasmic reticulum
ERAD	Endoplasmic-reticulum-associated protein degradation
EtOH	Ethanol
e.v.	Empty vector
FDR	False discovery rate
G418	Geneticin
GFP	Green fluorescent protein
GID	Glucose induced degradation deficient
GOI	Gene of interest
HA	Hemagglutinin
HCl	Hydrochloric acid
HECT	Homologous to the E6AP carboxyl terminus
HF	High-fidelity
His	Histidine
HPLC	High-performance liquid chromatography
HRP	Horseradish peroxidase
IDR	Intrinsically disordered region
IMB	Institute of Molecular Biology
ipTM	Interface predicted template modelling
LFQ	Label-free quantitation
Lys	Lysine
MES	2-(*N*-morpholino)ethanesulfonic acid
MetAP	Methionine aminopeptidase
MPS	Multiplexed protein stability
MOPS	3-(*N*-morpholino)propanesulfonic acid
MS	Mass spectrometry
MSG	Monosodium glutamate
mTOR	Mechanistic target of rapamycin
NAT	Nourseothricin
NUb	N-terminal ubiquitin fragment
OD	Optical density
OE	Overexpression
ORF	Open reading frame
PAE	Predicted alignment error
PAS	Phagosome assembly site
PBS	Phosphate buffered saline
PCR	Polymerase chain reaction
PE	Phosphatidylethanolamine
PPi	Pyrophosphate
Pro	Proline
pTM	Predicted template modelling
RBR	RING-IBR-RING
RING	Really interesting new gene
RNA	Ribonucleic acid
SC	Synthetic complete
SDS	Sodium dodecyl sulfate
SDS-PAGE	Sodium dodecyl sulfate polyacrylamide gel electrophoresis

sfGFP	Superfolder green fluorescent protein
SGA	Synthetic genetic array
SPO	Sporulation
tFT	Tandem-fluorescent protein timer
UPS	Ubiquitin proteasome system
Ura	Uracil
WT	Wild type
YP	Yeast extract peptone
YPD	Yeast extract peptone dextrose

Amino acids

A	Alanine
C	Cysteine
D	Aspartic acid/ Aspartate
E	Glutamic acid/ Glutamate
F	Phenylalanine
G	Glycine
H	Histidine
I	Isoleucine
K	Lysine
L	Leucine
M	Methionine
N	Asparagine
P	Proline
Q	Glutamine
R	Arginine
S	Serine
T	Threonine
V	Valine
W	Tryptophane
Y	Tyrosine

List of figures

References

Abramson, Josh; Adler, Jonas; Dunger, Jack; Evans, Richard; Green, Tim; Pritzel, Alexander et al. (2024): Accurate structure prediction of biomolecular interactions with AlphaFold 3. In *Nature* 630 (8016), pp. 493–500. DOI: 10.1038/s41586-024-07487-w.

Adams, Benjamin M.; Oster, Michela E.; Hebert, Daniel N. (2019): Protein Quality Control in the Endoplasmic Reticulum. In *The protein journal* 38 (3), pp. 317–329. DOI: 10.1007/s10930-019-09831-w.

Aguilera, M.; Oliveros, M.; Martínez-Padrón, M.; Barbas, J. A.; Ferrús, A. (2000): Ariadne-1: a vital Drosophila gene is required in development and defines a new conserved family of ring-finger proteins. In *Genetics* 155 (3), pp. 1231–1244. DOI: 10.1093/genetics/155.3.1231.

Aiken, Charity T.; Kaake, Robyn M.; Wang, Xiaorong; Huang, Lan (2011): Oxidative stress-mediated regulation of proteasome complexes. In *Molecular & cellular proteomics : MCP* 10 (5), R110.006924. DOI: 10.1074/mcp.M110.006924.

Aksnes, Henriette; Drazic, Adrian; Marie, Michaël; Arnesen, Thomas (2016): First Things First: Vital Protein Marks by N-Terminal Acetyltransferases. In *Trends in Biochemical Sciences* 41 (9), pp. 746–760. DOI: 10.1016/j.tibs.2016.07.005.

Aksnes, Henriette; Ree, Rasmus; Arnesen, Thomas (2019): Co-translational, Post-translational, and Non-catalytic Roles of N-Terminal Acetyltransferases. In *Molecular cell* 73 (6), pp. 1097–1114. DOI: 10.1016/j.molcel.2019.02.007.

Aksnes, Henriette; van Damme, Petra; Goris, Marianne; Starheim, Kristian K.; Marie, Michaël; Støve, Svein Isungset et al. (2015): An organellar nα-acetyltransferase, naa60, acetylates cytosolic N termini of transmembrane proteins and maintains Golgi integrity. In *Cell reports* 10 (8), pp. 1362–1374. DOI: 10.1016/j.celrep.2015.01.053.

André, Bruno (2018): Tribute to Marcelle Grenson (1925-1996), A Pioneer in the Study of Amino Acid Transport in Yeast. In *International journal of molecular sciences* 19 (4). DOI: 10.3390/ijms19041207.

Arnesen, Thomas; van Damme, Petra; Polevoda, Bogdan; Helsens, Kenny; Evjenth, Rune; Colaert, Niklaas et al. (2009): Proteomics analyses reveal the evolutionary conservation and divergence of N-terminal acetyltransferases from yeast and humans. In *Proc. Natl. Acad. Sci. U.S.A.* 106 (20), pp. 8157–8162. DOI: 10.1073/pnas.0901931106.

Auguie, Baptiste (2017): gridExtra: Miscellaneous Functions for "Grid" Graphics. Available online at https://CRAN.R-project.org/package=gridExtra.

Bachmair, A.; Finley, D.; Varshavsky, A. (1986): In vivo half-life of a protein is a function of its amino-terminal residue. In *Science (New York, N.Y.)* 234 (4773), pp. 179–186. DOI: 10.1126/science.3018930.

Baker, R. T.; Varshavsky, A. (1995): Yeast N-terminal amidase. A new enzyme and component of the N-end rule pathway. In *Journal of Biological Chemistry* 270 (20), pp. 12065–12074. DOI: 10.1074/jbc.270.20.12065.

Bard, Jared A. M.; Goodall, Ellen A.; Greene, Eric R.; Jonsson, Erik; Dong, Ken C.; Martin, Andreas (2018): Structure and Function of the 26S Proteasome. In *Annual review of biochemistry* 87, pp. 697–724. DOI: 10.1146/annurev-biochem-062917-011931.

Barroso-Gomila, Orhi; Merino-Cacho, Laura; Muratore, Veronica; Perez, Coralia; Taibi, Vincenzo; Maspero, Elena et al. (2023): BioE3 identifies specific substrates of ubiquitin E3 ligases. In *Nat Commun* 14 (1), p. 7656. DOI: 10.1038/s41467-023-43326-8.

Bartel, B.; Wünning, I.; Varshavsky, A. (1990): The recognition component of the N-end rule pathway. In *The EMBO Journal* 9 (10), pp. 3179–3189. DOI: 10.1002/j.1460-2075.1990.tb07516.x.

Baryshnikova, Anastasia; Costanzo, Michael; Dixon, Scott; Vizeacoumar, Franco J.; Myers, Chad L.; Andrews, Brenda; Boone, Charles (2010): Synthetic genetic array (SGA) analysis in Saccharomyces cerevisiae and Schizosaccharomyces pombe. In *Methods in enzymology* 470, pp. 145–179. DOI: 10.1016/S0076-6879(10)70007-0.

Bayne, Rosemary A.; Jayachandran, Uma; Kasprowicz, Aleksandra; Bresson, Stefan; Tollervey, David; Wallace, Edward W. J.; Cook, Atlanta G. (2022): Yeast Ssd1 is a non-enzymatic member of the RNase II family with an alternative RNA recognition site. In *Nucleic acids research* 50 (5), pp. 2923–2937. DOI: 10.1093/nar/gkab615.

Blikstad, I.; Nelson, W. J.; Moon, R. T.; Lazarides, E. (1983): Synthesis and assembly of spectrin during avian erythropoiesis: stoichiometric assembly but unequal synthesis of alpha and beta spectrin. In *Cell* 32 (4), pp. 1081–1091. DOI: 10.1016/0092-8674(83)90292-1.

Bogenhagen, Daniel F.; Haley, John D. (2020): Pulse-chase SILAC-based analyses reveal selective oversynthesis and rapid turnover of mitochondrial protein components of respiratory complexes. In *The Journal of biological chemistry* 295 (9), pp. 2544–2554. DOI: 10.1074/jbc.RA119.011791.

Bonissone, Stefano; Gupta, Nitin; Romine, Margaret; Bradshaw, Ralph A.; Pevzner, Pavel A. (2013): N-terminal protein processing: a comparative proteogenomic analysis. In *Molecular & cellular proteomics : MCP* 12 (1), pp. 14–28. DOI: 10.1074/mcp.M112.019075.

Brachmann, C. B.; Davies, A.; Cost, G. J.; Caputo, E.; Li, J.; Hieter, P.; Boeke, J. D. (1998): Designer deletion strains derived from Saccharomyces cerevisiae S288C: a useful set of strains and plasmids for PCR-mediated gene disruption and other applications. In *Yeast* 14 (2), pp. 115–132. DOI: 10.1002/(SICI)1097-0061(19980130)14:2<115::AID-YEA204>3.0.CO;2-2.

Broach, J. R.; Strathern, J. N.; Hicks, J. B. (1979): Transformation in yeast: development of a hybrid cloning vector and isolation of the CAN1 gene. In *Gene* 8 (1), pp. 121–133. DOI: 10.1016/0378-1119(79)90012-X.

Buccitelli, Christopher; Selbach, Matthias (2020): mRNAs, proteins and the emerging principles of gene expression control. In *Nat Rev Genet* 21 (10), pp. 630–644. DOI: 10.1038/s41576-020-0258-4.

Buchberger, Alexander; Bukau, Bernd; Sommer, Thomas (2010): Protein quality control in the cytosol and the endoplasmic reticulum: brothers in arms. In *Molecular cell* 40 (2), pp. 238–252. DOI: 10.1016/j.molcel.2010.10.001.

Buetow, Lori; Huang, Danny T. (2016): Structural insights into the catalysis and regulation of E3 ubiquitin ligases. In *Nature reviews. Molecular cell biology* 17 (10), pp. 626–642. DOI: 10.1038/nrm.2016.91.

Bulatov, Emil; Ciulli, Alessio (2015): Targeting Cullin-RING E3 ubiquitin ligases for drug discovery: structure, assembly and small-molecule modulation. In *The Biochemical journal* 467 (3), pp. 365–386. DOI: 10.1042/BJ20141450.

Chakrabarti, Pinak; Chakravarty, Devlina (2022): Intrinsically disordered proteins/regions and insight into their biomolecular interactions. In *Biophysical chemistry* 283, p. 106769. DOI: 10.1016/j.bpc.2022.106769.

Chang, Y. H.; Teichert, U.; Smith, J. A. (1990): Purification and characterization of a methionine aminopeptidase from Saccharomyces cerevisiae. In *The Journal of biological chemistry* 265 (32), pp. 19892–19897.

Chen, Bryan; Retzlaff, Marco; Roos, Thomas; Frydman, Judith (2011): Cellular strategies of protein quality control. In *Cold Spring Harbor Perspectives in Biology* 3 (8), a004374. DOI: 10.1101/cshperspect.a004374.

Chen, Shun-Jia; Kim, Leehyeon; Song, Hyun Kyu; Varshavsky, Alexander (2021): Aminopeptidases trim Xaa-Pro proteins, initiating their degradation by the Pro/N-degron pathway. In *Proceedings of the National Academy of Sciences of the United States of America* 118 (43). DOI: 10.1073/pnas.2115430118.

Chen, Shun-Jia; Wu, Xia; Wadas, Brandon; Oh, Jang-Hyun; Varshavsky, Alexander (2017): An N-end rule pathway that recognizes proline and destroys gluconeogenic enzymes. In *Science (New York, N.Y.)* 355 (6323). DOI: 10.1126/science.aal3655.

Cheng, S. H.; Gregory, R. J.; Marshall, J.; Paul, S.; Souza, D. W.; White, G. A. et al. (1990): Defective intracellular transport and processing of CFTR is the molecular basis of most cystic fibrosis. In *Cell* 63 (4), pp. 827–834. DOI: 10.1016/0092-8674(90)90148-8.

Chiang, M. C.; Chiang, H. L. (1998): Vid24p, a novel protein localized to the fructose-1, 6-bisphosphatase-containing vesicles, regulates targeting of fructose-1,6-bisphosphatase from the vesicles to the vacuole for degradation. In *J Cell Biol* 140 (6), pp. 1347–1356. DOI: 10.1083/jcb.140.6.1347.

Christensen, Devin E.; Brzovic, Peter S.; Klevit, Rachel E. (2007): E2-BRCA1 RING interactions dictate synthesis of mono- or specific polyubiquitin chain linkages. In *Nat Struct Mol Biol* 14 (10), pp. 941–948. DOI: 10.1038/nsmb1295.

Chrustowicz, Jakub; Sherpa, Dawafuti; Li, Jerry; Langlois, Christine R.; Papadopoulou, Eleftheria C.; Vu, D. Tung et al. (2024): Multisite phosphorylation dictates selective E2-E3 pairing as revealed by Ubc8/UBE2H-GID/CTLH assemblies. In *Molecular cell* 84 (2), 293-308.e14. DOI: 10.1016/j.molcel.2023.11.027.

Ciehanover, A.; Hod, Y.; Hershko, A. (1978): A heat-stable polypeptide component of an ATP-dependent proteolytic system from reticulocytes. In *Biochemical and biophysical research communications* 81 (4), pp. 1100–1105. DOI: 10.1016/0006-291x(78)91249-4.

Coti, Andrea (2024): Dissecting Specificity of the Human Arg/N-degron Pathway. Doctoral Thesis. Johannes Gutenberg-Universität Mainz, Mainz.

Cox, Jürgen; Mann, Matthias (2008): MaxQuant enables high peptide identification rates, individualized p.p.b.-range mass accuracies and proteome-wide protein quantification. In *Nat Biotechnol* 26 (12), pp. 1367–1372. DOI: 10.1038/nbt.1511.

Cox, Jürgen; Neuhauser, Nadin; Michalski, Annette; Scheltema, Richard A.; Olsen, Jesper V.; Mann, Matthias (2011): Andromeda: a peptide search engine integrated into the MaxQuant environment. In *Journal of proteome research* 10 (4), pp. 1794–1805. DOI: 10.1021/pr101065j.

Cronan, J. E. (1989): The E. coli bio operon: transcriptional repression by an essential protein modification enzyme. In *Cell* 58 (3), pp. 427–429. DOI: 10.1016/0092-8674(89)90421-2.

Da Jeong, Eun; Lee, Hye Seon; Ku, Bonsu; Kim, Cheol-Hee; Kim, Seung Jun; Shin, Ho-Chul (2023): Insights into the recognition mechanism in the UBR box of UBR4 for its specific substrates. In *Commun Biol* 6 (1), p. 1214. DOI: 10.1038/s42003-023-05602-7.

Dammer, Eric B.; Na, Chan Hyun; Xu, Ping; Seyfried, Nicholas T.; Duong, Duc M.; Cheng, Dongmei et al. (2011): Polyubiquitin linkage profiles in three models of proteolytic stress suggest the etiology of Alzheimer disease. In *The Journal of biological chemistry* 286 (12), pp. 10457–10465. DOI: 10.1074/jbc.M110.149633.

Deter, R. L.; Baudhuin, P.; DUVE, C. de (1967): Participation of lysosomes in cellular autophagy induced in rat liver by glucagon. In *The Journal of cell biology* 35 (2), C11-6. DOI: 10.1083/jcb.35.2.C11.

Deutschbauer, Adam M.; Jaramillo, Daniel F.; Proctor, Michael; Kumm, Jochen; Hillenmeyer, Maureen E.; Davis, Ronald W. et al. (2005): Mechanisms of haploinsufficiency revealed by genome-wide profiling in yeast. In *Genetics* 169 (4), pp. 1915–1925. DOI: 10.1534/genetics.104.036871.

Diao, Jiajie; Liu, Rong; Rong, Yueguang; Zhao, Minglei; Zhang, Jing; Lai, Ying et al. (2015): ATG14 promotes membrane tethering and fusion of autophagosomes to endolysosomes. In *Nature* 520 (7548), pp. 563–566. DOI: 10.1038/nature14147.

Dikic, Ivan (2017): Proteasomal and Autophagic Degradation Systems. In *Annual review of biochemistry* 86, pp. 193–224. DOI: 10.1146/annurev-biochem-061516-044908.

Dikic, Ivan; Elazar, Zvulun (2018): Mechanism and medical implications of mammalian autophagy. In *Nat Rev Mol Cell Biol* 19 (6), pp. 349–364. DOI: 10.1038/s41580-018-0003-4.

Dinh, Trinh V.; Bienvenut, Willy V.; Linster, Eric; Feldman-Salit, Anna; Jung, Vincent A.; Meinnel, Thierry et al. (2015): Molecular identification and functional characterization of the first Nα-acetyltransferase in plastids by global acetylome profiling. In *Proteomics* 15 (14), pp. 2426–2435. DOI: 10.1002/pmic.201500025.

Dobson, Christopher M. (2003): Protein folding and misfolding. In *Nature* 426 (6968), pp. 884–890. DOI: 10.1038/nature02261.

Dong, Cheng; Zhang, Heng; Li, Li; Tempel, Wolfram; Loppnau, Peter; Min, Jinrong (2018): Molecular basis of GID4-mediated recognition of degrons for the Pro/N-end rule pathway. In *Nat Chem Biol* 14 (5), pp. 466–473. DOI: 10.1038/s41589-018-0036-1.

Dowle, Matt; Srinivasan, Arun (2023): data.table: Extension of 'data.frame'. Available online at https://CRAN.R-project.org/package=data.table.

Dragulescu, Adrian; Arendt, Cole (2020): xlsx: Read, Write, Format Excel 2007 and Excel 97/2000/XP/2003 Files. Available online at https://CRAN.R-project.org/package=xlsx.

Drazic, Adrian; Aksnes, Henriette; Marie, Michaël; Boczkowska, Malgorzata; Varland, Sylvia; Timmerman, Evy et al. (2018): NAA80 is actin's N-terminal acetyltransferase and regulates cytoskeleton assembly and cell motility. In *Proc. Natl. Acad. Sci. U.S.A.* 115 (17), pp. 4399–4404. DOI: 10.1073/pnas.1718336115.

Durinck, Steffen; Moreau, Yves; Kasprzyk, Arek; Davis, Sean; Moor, Bart de; Brazma, Alvis; Huber, Wolfgang (2005): BioMart and Bioconductor: a powerful link between biological databases and microarray data analysis. In *Bioinformatics* 21 (16), pp. 3439–3440. DOI: 10.1093/bioinformatics/bti525.

Durinck, Steffen; Spellman, Paul T.; Birney, Ewan; Huber, Wolfgang (2009): Mapping identifiers for the integration of genomic datasets with the R/Bioconductor package biomaRt. In *Nat Protoc* 4 (8), pp. 1184–1191. DOI: 10.1038/nprot.2009.97.

Duttler, Stefanie; Pechmann, Sebastian; Frydman, Judith (2013): Principles of cotranslational ubiquitination and quality control at the ribosome. In *Molecular cell* 50 (3), pp. 379–393. DOI: 10.1016/j.molcel.2013.03.010.

DUVE, C. de; PRESSMAN, B. C.; GIANETTO, R.; WATTIAUX, R.; APPELMANS, F. (1955): Tissue fractionation studies. 6. Intracellular distribution patterns of enzymes in rat-liver tissue. In *The Biochemical journal* 60 (4), pp. 604–617. DOI: 10.1042/bj0600604.

Engel, Stacia R.; Aleksander, Suzi; Nash, Robert S.; Wong, Edith D.; Weng, Shuai; Miyasato, Stuart R. et al. (2025): Saccharomyces Genome Database: advances in genome annotation, expanded biochemical pathways, and other key enhancements. In *Genetics* 229 (3). DOI: 10.1093/genetics/iyae185.

Ferber, S.; Ciechanover, A. (1987): Role of arginine-tRNA in protein degradation by the ubiquitin pathway. In *Nature* 326 (6115), pp. 808–811. DOI: 10.1038/326808a0.

Finley, Daniel; Ulrich, Helle D.; Sommer, Thomas; Kaiser, Peter (2012): The Ubiquitin–Proteasome System of Saccharomyces cerevisiae. In *Genetics* 192 (2), pp. 319–360. DOI: 10.1534/genetics.112.140467.

Forster, Duncan T.; Li, Sheena C.; Yashiroda, Yoko; Yoshimura, Mami; Li, Zhijian; Isuhuaylas, Luis Alberto Vega et al. (2022): BIONIC: biological network integration using convolutions. In *Nat Methods* 19 (10), pp. 1250–1261. DOI: 10.1038/s41592-022-01616-x.

Freemont, P. S.; Hanson, I. M.; Trowsdale, J. (1991): A novel cysteine-rich sequence motif. In *Cell* 64 (3), pp. 483–484. DOI: 10.1016/0092-8674(91)90229-r.

Fridy, Peter C.; Li, Yinyin; Keegan, Sarah; Thompson, Mary K.; Nudelman, Ilona; Scheid, Johannes F. et al. (2014): A robust pipeline for rapid production of versatile nanobody repertoires. In *Nat Methods* 11 (12), pp. 1253–1260. DOI: 10.1038/nmeth.3170.

Gameiro, Eduardo; Juárez-Núñez, Karla A.; Fung, Jia Jun; Shankar, Susmitha; Luke, Brian; Khmelinskii, Anton (2025): Genome-wide conditional degron libraries for functional genomics. In *The Journal of cell biology* 224 (2). DOI: 10.1083/jcb.202409007.

Gautschi, Matthias; Just, Sören; Mun, Andrej; Ross, Suzanne; Rücknagel, Peter; Dubaquié, Yves et al. (2003): The yeast N(alpha)-acetyltransferase NatA is quantitatively anchored to the ribosome and interacts with nascent polypeptides. In *Molecular and cellular biology* 23 (20), pp. 7403–7414. DOI: 10.1128/MCB.23.20.7403-7414.2003.

Gelperin, Daniel M.; White, Michael A.; Wilkinson, Martha L.; Kon, Yoshiko; Kung, Li A.; Wise, Kevin J. et al. (2005): Biochemical and genetic analysis of the yeast proteome with a movable ORF collection. In *Genes & development* 19 (23), pp. 2816–2826. DOI: 10.1101/gad.1362105.

George, Arlene J.; Hoffiz, Yarely C.; Charles, Antoinette J.; Zhu, Ying; Mabb, Angela M. (2018): A Comprehensive Atlas of E3 Ubiquitin Ligase Mutations in Neurological Disorders. In *Frontiers in genetics* 9, p. 29. DOI: 10.3389/fgene.2018.00029.

Goddard, Thomas D.; Huang, Conrad C.; Meng, Elaine C.; Pettersen, Eric F.; Couch, Gregory S.; Morris, John H.; Ferrin, Thomas E. (2018): UCSF ChimeraX: Meeting modern challenges in visualization and analysis. In *Protein science : a publication of the Protein Society* 27 (1), pp. 14–25. DOI: 10.1002/pro.3235.

Goldberg, A. L. (1972): Degradation of abnormal proteins in Escherichia coli (protein breakdown-protein structure-mistranslation-amino acid analogs-puromycin). In *Proceedings of the National Academy of Sciences of the United States of America* 69 (2), pp. 422–426. DOI: 10.1073/pnas.69.2.422.

Gottemukkala, Karthik V.; Chrustowicz, Jakub; Sherpa, Dawafuti; Sepic, Sara; Vu, Duc Tung; Karayel, Özge et al. (2024): Non-canonical substrate recognition by the human WDR26-CTLH E3 ligase regulates prodrug metabolism. In *Molecular cell* 84 (10), 1948-1963.e11. DOI: 10.1016/j.molcel.2024.04.014.

Gunjan, Akash; Verreault, Alain (2003): A Rad53 kinase-dependent surveillance mechanism that regulates histone protein levels in S. cerevisiae. In *Cell* 115 (5), pp. 537–549. DOI: 10.1016/s0092-8674(03)00896-1.

Gurumurthy, Sushma; Xie, Stephanie Z.; Alagesan, Brinda; Kim, Judith; Yusuf, Rushdia Z.; Saez, Borja et al. (2010): The Lkb1 metabolic sensor maintains haematopoietic stem cell survival. In *Nature* 468 (7324), pp. 659–663. DOI: 10.1038/nature09572.

Hamasaki, Maho; Furuta, Nobumichi; Matsuda, Atsushi; Nezu, Akiko; Yamamoto, Akitsugu; Fujita, Naonobu et al. (2013): Autophagosomes form at ER-mitochondria contact sites. In *Nature* 495 (7441), pp. 389–393. DOI: 10.1038/nature11910.

Hara, K.; Yonezawa, K.; Weng, Q. P.; Kozlowski, M. T.; Belham, C.; Avruch, J. (1998): Amino acid sufficiency and mTOR regulate p70 S6 kinase and eIF-4E BP1 through a common effector

mechanism. In *Journal of Biological Chemistry* 273 (23), pp. 14484–14494. DOI: 10.1074/jbc.273.23.14484.

Harding, T. M.; Morano, K. A.; Scott, S. V.; Klionsky, D. J. (1995): Isolation and characterization of yeast mutants in the cytoplasm to vacuole protein targeting pathway. In *J Cell Biol* 131 (3), pp. 591–602. DOI: 10.1083/jcb.131.3.591.

Harkness, Troy A. A.; Davies, Gerald F.; Ramaswamy, Vijay; Arnason, Terra G. (2002): The ubiquitin-dependent targeting pathway in Saccharomyces cerevisiae plays a critical role in multiple chromatin assembly regulatory steps. In *Genetics* 162 (2), pp. 615–632. DOI: 10.1093/genetics/162.2.615.

Harper, J. Wade; Bennett, Eric J. (2016): Proteome complexity and the forces that drive proteome imbalance. In *Nature* 537 (7620), pp. 328–338. DOI: 10.1038/nature19947.

Haschke, Anika (2023): Functional Conservation of the GID Ubiquitin Ligase. Bachelor Thesis. Johannes Gutenberg-Universität Mainz, Mainz. Institute for Molecular Biology.

Hatakeyama, Shigetsugu; Nakayama, Kei-ichi I. (2003): U-box proteins as a new family of ubiquitin ligases. In *Biochemical and biophysical research communications* 302 (4), pp. 635–645. DOI: 10.1016/s0006-291x(03)00245-6.

Heathcote, Karen C.; Keeley, Thomas P.; Myllykoski, Matti; Lundekvam, Malin; McTiernan, Nina; Akter, Salma et al. (2024): N-terminal cysteine acetylation and oxidation patterns may define protein stability. In *Nat Commun* 15 (1), p. 5360. DOI: 10.1038/s41467-024-49489-2.

Hehl, Laura A.; Horn-Ghetko, Daniel; Prabu, J. Rajan; Vollrath, Ronnald; Vu, D. Tung; Pérez Berrocal, David A. et al. (2024): Structural snapshots along K48-linked ubiquitin chain formation by the HECT E3 UBR5. In *Nat Chem Biol* 20 (2), pp. 190–200. DOI: 10.1038/s41589-023-01414-2.

Hershko, A.; Ciechanover, A.; Rose, I. A. (1979): Resolution of the ATP-dependent proteolytic system from reticulocytes: a component that interacts with ATP. In *Proceedings of the National Academy of Sciences of the United States of America* 76 (7), pp. 3107–3110. DOI: 10.1073/pnas.76.7.3107.

Ho, Cheuk Hei (2011): Molecular Barcoded Plasmid Yeast ORF Library: Linking Bioactive Compounds to their Cellular Targets and Mapping Dosage Suppressor Networks. Doctoral thesis. University of Toronto, Toronto.

Ho, Cheuk Hei; Magtanong, Leslie; Barker, Sarah L.; Gresham, David; Nishimura, Shinichi; Natarajan, Paramasivam et al. (2009): A molecular barcoded yeast ORF library enables mode-of-action analysis of bioactive compounds. In *Nat Biotechnol* 27 (4), pp. 369–377. DOI: 10.1038/nbt.1534.

Honda, R.; Tanaka, H.; Yasuda, H. (1997): Oncoprotein MDM2 is a ubiquitin ligase E3 for tumor suppressor p53. In *FEBS letters* 420 (1), pp. 25–27. DOI: 10.1016/S0014-5793(97)01480-4.

Hosokawa, Nao; Hara, Taichi; Kaizuka, Takeshi; Kishi, Chieko; Takamura, Akito; Miura, Yutaka et al. (2009): Nutrient-dependent mTORC1 association with the ULK1-Atg13-FIP200 complex required for autophagy. In *Molecular biology of the cell* 20 (7), pp. 1981–1991. DOI: 10.1091/mbc.e08-12-1248.

Hou, Chao; Li, Yuxuan; Wang, Mengyao; Wu, Hong; Li, Tingting (2022): Systematic prediction of degrons and E3 ubiquitin ligase binding via deep learning. In *BMC Biology* 20 (1), p. 162. DOI: 10.1186/s12915-022-01364-6.

Hu, Rong-Gui; Sheng, Jun; Qi, Xin; Xu, Zhenming; Takahashi, Terry T.; Varshavsky, Alexander (2005): The N-end rule pathway as a nitric oxide sensor controlling the levels of multiple regulators. In *Nature* 437 (7061), pp. 981–986. DOI: 10.1038/nature04027.

Huang, Hai-Tsang; Lumpkin, Ryan J.; Tsai, Ryan W.; Su, Shuyao; Zhao, Xu; Xiong, Yuan et al. (2024): Ubiquitin-specific proximity labeling for the identification of E3 ligase substrates. In *Nat Chem Biol* 20 (9), pp. 1227–1236. DOI: 10.1038/s41589-024-01590-9.

Hughes, Christopher S.; Moggridge, Sophie; Müller, Torsten; Sorensen, Poul H.; Morin, Gregg B.; Krijgsveld, Jeroen (2019): Single-pot, solid-phase-enhanced sample preparation for proteomics experiments. In *Nat Protoc* 14 (1), pp. 68–85. DOI: 10.1038/s41596-018-0082-x.

Huibregtse, J. M.; Scheffner, M.; Beaudenon, S.; Howley, P. M. (1995): A family of proteins structurally and functionally related to the E6-AP ubiquitin-protein ligase. In *Proceedings of the National Academy of Sciences of the United States of America* 92 (7), pp. 2563–2567. DOI: 10.1073/pnas.92.7.2563.

Hwang, Cheol-Sang; Shemorry, Anna; Varshavsky, Alexander (2010): N-Terminal Acetylation of Cellular Proteins Creates Specific Degradation Signals. In *American Association for the Advancement of Science*, 1/28/2010. Available online at https://www.science.org/doi/10.1126/science.1183147, checked on 7/19/2025.

Iconomou, Mary; Saunders, Darren N. (2016): Systematic approaches to identify E3 ligase substrates. In *The Biochemical journal* 473 (22), pp. 4083–4101. DOI: 10.1042/BCJ20160719.

Itakura, Eisuke; Kishi-Itakura, Chieko; Mizushima, Noboru (2012): The hairpin-type tail-anchored SNARE syntaxin 17 targets to autophagosomes for fusion with endosomes/lysosomes. In *Cell* 151 (6), pp. 1256–1269. DOI: 10.1016/j.cell.2012.11.001.

Ivan, M.; Kaelin, W. G. (2001): The von Hippel-Lindau tumor suppressor protein. In *Current opinion in genetics & development* 11 (1), pp. 27–34. DOI: 10.1016/s0959-437x(00)00152-0.

Janke, Carsten; Magiera, Maria M.; Rathfelder, Nicole; Taxis, Christof; Reber, Simone; Maekawa, Hiromi et al. (2004): A versatile toolbox for PCR-based tagging of yeast genes: new fluorescent proteins, more markers and promoter substitution cassettes. In *Yeast (Chichester, England)* 21 (11), pp. 947–962. DOI: 10.1002/yea.1142.

Ji, Chang Hoon; Kim, Hee Yeon; Heo, Ah Jung; Lee, Su Hyun; Lee, Min Ju; Kim, Su Bin et al. (2019): The N-Degron Pathway Mediates ER-phagy. In *Molecular cell* 75 (5), 1058-1072.e9. DOI: 10.1016/j.molcel.2019.06.028.

Joazeiro, Claudio A. P. (2019): Mechanisms and functions of ribosome-associated protein quality control. In *Nat Rev Mol Cell Biol* 20 (6), pp. 368–383. DOI: 10.1038/s41580-019-0118-2.

Johnson, E. S.; Gonda, D. K.; Varshavsky, A. (1990): cis-trans recognition and subunit-specific degradation of short-lived proteins. In *Nature* 346 (6281), pp. 287–291. DOI: 10.1038/346287a0.

Jumper, John; Evans, Richard; Pritzel, Alexander; Green, Tim; Figurnov, Michael; Ronneberger, Olaf et al. (2021): Highly accurate protein structure prediction with AlphaFold. In *Nature* 596 (7873), pp. 583–589. DOI: 10.1038/s41586-021-03819-2.

Jung, Chang Hwa; Jun, Chang Bong; Ro, Seung-Hyun; Kim, Young-Mi; Otto, Neil Michael; Cao, Jing et al. (2009): ULK-Atg13-FIP200 complexes mediate mTOR signaling to the autophagy machinery. In *Molecular biology of the cell* 20 (7), pp. 1992–2003. DOI: 10.1091/mbc.e08-12-1249.

Kaneko, Masayuki; Ishiguro, Masataro; Niinuma, Yoshifumi; Uesugi, Mai; Nomura, Yasuyuki (2002): Human HRD1 protects against ER stress-induced apoptosis through ER-associated degradation. In *FEBS letters* 532 (1-2), pp. 147–152. DOI: 10.1016/s0014-5793(02)03660-8.

Karanasios, Eleftherios; Stapleton, Eloise; Manifava, Maria; Kaizuka, Takeshi; Mizushima, Noboru; Walker, Simon A.; Ktistakis, Nicholas T. (2013): Dynamic association of the ULK1 complex with omegasomes during autophagy induction. In *J Cell Sci* 126 (Pt 22), pp. 5224–5238. DOI: 10.1242/jcs.132415.

Karim, Ashty S.; Curran, Kathleen A.; Alper, Hal S. (2013): Characterization of plasmid burden and copy number in Saccharomyces cerevisiae for optimization of metabolic engineering applications. In *FEMS yeast research* 13 (1), pp. 107–116. DOI: 10.1111/1567-1364.12016.

Kats, Ilia; Khmelinskii, Anton; Kschonsak, Marc; Huber, Florian; Knieß, Robert A.; Bartosik, Anna; Knop, Michael (2018): Mapping Degradation Signals and Pathways in a Eukaryotic N-terminome. In *Molecular cell* 70 (3), 488-501.e5. DOI: 10.1016/j.molcel.2018.03.033.

Kats, Ilia; Reinbold, Christian; Kschonsak, Marc; Khmelinskii, Anton; Armbruster, Laura; Ruppert, Thomas; Knop, Michael (2022): Up-regulation of ubiquitin-proteasome activity upon loss of NatA-dependent N-terminal acetylation. In *Life science alliance* 5 (2). DOI: 10.26508/lsa.202000730.

Khmelinskii, Anton; Keller, Philipp J.; Bartosik, Anna; Meurer, Matthias; Barry, Joseph D.; Mardin, Balca R. et al. (2012): Tandem fluorescent protein timers for in vivo analysis of protein dynamics. In *Nature biotechnology* 30 (7), pp. 708–714. DOI: 10.1038/nbt.2281.

Khmelinskii, Anton; Knop, Michael (2014): Analysis of protein dynamics with tandem fluorescent protein timers. In *Methods in molecular biology (Clifton, N.J.)* 1174, pp. 195–210. DOI: 10.1007/978-1-4939-0944-5_13.

Kim, Bong Heon; Kim, Min Kyung; Oh, Sun Joo; Nguyen, Kha The; Kim, Jun Hoe; Varshavsky, Alexander et al. (2022): Crystal structure of the Ate1 arginyl-tRNA-protein transferase and arginylation of N-degron substrates. In *Proceedings of the National Academy of Sciences of the United States of America* 119 (31), e2209597119. DOI: 10.1073/pnas.2209597119.

Kim, Heon-Ki; Kim, Ryu-Ryun; Oh, Jang-Hyun; Cho, Hanna; Varshavsky, Alexander; Hwang, Cheol-Sang (2014): The N-terminal methionine of cellular proteins as a degradation signal. In *Cell* 156 (1-2), pp. 158–169. DOI: 10.1016/j.cell.2013.11.031.

Kim, Min Kyung; Oh, Sun Joo; Lee, Byung-Gil; Song, Hyun Kyu (2016): Structural basis for dual specificity of yeast N-terminal amidase in the N-end rule pathway. In *Proceedings of the*

National Academy of Sciences of the United States of America 113 (44), pp. 12438–12443. DOI: 10.1073/pnas.1612620113.

Knop, Michael; Siegers, Katja; Pereira, Gislene; Zachariae, Wolfgang; Winsor, Barbara; Nasmyth, Kim; Schiebel, Elmar (1999): Epitope tagging of yeast genes using a PCR-based strategy: more tags and improved practical routines. In *Yeast* 15 (10B), pp. 963–972. DOI: 10.1002/(SICI)1097-0061(199907)15:10B<963::AID-YEA399>3.0.CO;2-W.

Komander, David; Rape, Michael (2012): The ubiquitin code. In *Annual review of biochemistry* 81, pp. 203–229. DOI: 10.1146/annurev-biochem-060310-170328.

Kong, Ka-Yiu Edwin; Fischer, Bernd; Meurer, Matthias; Kats, Ilia; Li, Zhaoyan; Rühle, Frank et al. (2021): Timer-based proteomic profiling of the ubiquitin-proteasome system reveals a substrate receptor of the GID ubiquitin ligase. In *Molecular cell* 81 (11), 2460-2476.e11. DOI: 10.1016/j.molcel.2021.04.018.

Kong, Ka-Yiu Edwin; Ochs, Christian; Debarnot, Cécile; Myllykoski, Matti; Blanco, Denís Arribas; Shankar, Susmitha et al. (2025): Bidirectional control of a metabolic transition by the GID ubiquitin ligase. In *bioRxiv*, 2025.07.15.664932. DOI: 10.1101/2025.07.15.664932.

Kong, Ka-Yiu Edwin; Shankar, Susmitha; Rühle, Frank; Khmelinskii, Anton (2023): Orphan quality control by an SCF ubiquitin ligase directed to pervasive C-degrons. In *Nat Commun* 14 (1), p. 8363. DOI: 10.1038/s41467-023-44096-z.

Koren, Itay; Timms, Richard T.; Kula, Tomasz; Xu, Qikai; Li, Mamie Z.; Elledge, Stephen J. (2018): The Eukaryotic Proteome Is Shaped by E3 Ubiquitin Ligases Targeting C-Terminal Degrons. In *Cell* 173 (7), 1622-1635.e14. DOI: 10.1016/j.cell.2018.04.028.

Kwon, Yong Tae; Kashina, Anna S.; Davydov, Ilia V.; Hu, Rong-Gui; An, Jee Young; Seo, Jai Wha et al. (2002): An Essential Role of N-Terminal Arginylation in Cardiovascular Development. In *American Association for the Advancement of Science*, 5/7/2002. Available online at https://www.science.org/doi/10.1126/science.1069531, checked on 7/19/2025.

LAEMMLI, U. K. (1970): Cleavage of structural proteins during the assembly of the head of bacteriophage T4. In *Nature* 227 (5259), pp. 680–685. DOI: 10.1038/227680a0.

Lam, Yun Wah; Lamond, Angus I.; Mann, Matthias; Andersen, Jens S. (2007): Analysis of nucleolar protein dynamics reveals the nuclear degradation of ribosomal proteins. In *Current biology : CB* 17 (9), pp. 749–760. DOI: 10.1016/j.cub.2007.03.064.

Lange, Sven M.; Armstrong, Lee A.; Kulathu, Yogesh (2022): Deubiquitinases: From mechanisms to their inhibition by small molecules. In *Molecular cell* 82 (1), pp. 15–29. DOI: 10.1016/j.molcel.2021.10.027.

Langlois, Christine R.; Beier, Viola; Karayel, Ozge; Chrustowicz, Jakub; Sherpa, Dawafuti; Mann, Matthias; Schulman, Brenda A. (2022): A GID E3 ligase assembly ubiquitinates an Rsp5 E3 adaptor and regulates plasma membrane transporters. In *EMBO reports* 23 (6), e53835. DOI: 10.15252/embr.202153835.

Lee, Min Jae; Tasaki, Takafumi; Moroi, Kayoko; An, Jee Young; Kimura, Sadao; Davydov, Ilia V.; Kwon, Yong Tae (2005): RGS4 and RGS5 are in vivo substrates of the N-end rule pathway. In

Proceedings of the National Academy of Sciences of the United States of America 102 (42), pp. 15030–15035. DOI: 10.1073/pnas.0507533102.

Levine, Arnold J. (2020): p53: 800 million years of evolution and 40 years of discovery. In *Nat Rev Cancer* 20 (8), pp. 471–480. DOI: 10.1038/s41568-020-0262-1.

Li, X.; Chang, Y. H. (1995): Amino-terminal protein processing in Saccharomyces cerevisiae is an essential function that requires two distinct methionine aminopeptidases. In *Proceedings of the National Academy of Sciences of the United States of America* 92 (26), pp. 12357–12361. DOI: 10.1073/pnas.92.26.12357.

Li, Zhijian; Vizeacoumar, Franco J.; Bahr, Sondra; Li, Jingjing; Warringer, Jonas; Vizeacoumar, Frederick S. et al. (2011): Systematic exploration of essential yeast gene function with temperature-sensitive mutants. In *Nat Biotechnol* 29 (4), pp. 361–367. DOI: 10.1038/nbt.1832.

Lin, Hsiu-Chuan; Yeh, Chi-Wei; Chen, Yen-Fu; Lee, Ting-Ting; Hsieh, Pei-Yun; Rusnac, Domnita V. et al. (2018): C-Terminal End-Directed Protein Elimination by CRL2 Ubiquitin Ligases. In *Molecular cell* 70 (4), 602-613.e3. DOI: 10.1016/j.molcel.2018.04.006.

Linster, Eric; Forero Ruiz, Francy L.; Miklankova, Pavlina; Ruppert, Thomas; Mueller, Johannes; Armbruster, Laura et al. (2022): Cotranslational N-degron masking by acetylation promotes proteome stability in plants. In *Nat Commun* 13 (1), p. 810. DOI: 10.1038/s41467-022-28414-5.

Loader, Catherine (2024): locfit: Local Regression, Likelihood and Density Estimation. Available online at https://CRAN.R-project.org/package=locfit.

Lobanov, Michail Yu; Furletova, Eugeniya I.; Bogatyreva, Natalya S.; Roytberg, Michail A.; Galzitskaya, Oxana V. (2010): Library of disordered patterns in 3D protein structures. In *PLOS Computational Biology* 6 (10), e1000958. DOI: 10.1371/journal.pcbi.1000958.

Madeira, Fábio; Madhusoodanan, Nandana; Lee, Joonheung; Eusebi, Alberto; Niewielska, Ania; Tivey, Adrian R. N. et al. (2024): The EMBL-EBI Job Dispatcher sequence analysis tools framework in 2024. In *Nucleic acids research* 52 (W1), W521-W525. DOI: 10.1093/nar/gkae241.

Maitland, Matthew E. R.; Lajoie, Gilles A.; Shaw, Gary S.; Schild-Poulter, Caroline (2022): Structural and Functional Insights into GID/CTLH E3 Ligase Complexes. In *International journal of molecular sciences* 23 (11). DOI: 10.3390/ijms23115863.

Manifava, Maria; Smith, Matthew; Rotondo, Sergio; Walker, Simon; Niewczas, Izabella; Zoncu, Roberto et al. (2016): Dynamics of mTORC1 activation in response to amino acids. In *eLife Sciences Publications, Ltd*, 11/10/2016. Available online at https://elifesciences.org/articles/19960, checked on 7/18/2025.

Maspero, Elena; Mari, Sara; Valentini, Eleonora; Musacchio, Andrea; Fish, Alexander; Pasqualato, Sebastiano; Polo, Simona (2011): Structure of the HECT:ubiquitin complex and its role in ubiquitin chain elongation. In *EMBO reports* 12 (4), pp. 342–349. DOI: 10.1038/embor.2011.21.

Matta-Camacho, Edna; Kozlov, Guennadi; Li, Flora F.; Gehring, Kalle (2010): Structural basis of substrate recognition and specificity in the N-end rule pathway. In *Nat Struct Mol Biol* 17 (10), pp. 1182–1187. DOI: 10.1038/nsmb.1894.

McShane, Erik; Selbach, Matthias (2022): Physiological Functions of Intracellular Protein Degradation. In *Annual review of cell and developmental biology* 38, pp. 241–262. DOI: 10.1146/annurev-cellbio-120420-091943.

Melnykov, Artem; Chen, Shun-Jia; Varshavsky, Alexander (2019): Gid10 as an alternative N-recognin of the Pro/N-degron pathway. In *Proceedings of the National Academy of Sciences of the United States of America* 116 (32), pp. 15914–15923. DOI: 10.1073/pnas.1908304116.

Meng, Elaine C.; Goddard, Thomas D.; Pettersen, Eric F.; Couch, Greg S.; Pearson, Zach J.; Morris, John H.; Ferrin, Thomas E. (2023): UCSF ChimeraX: Tools for structure building and analysis. In *Protein science : a publication of the Protein Society* 32 (11), e4792. DOI: 10.1002/pro.4792.

Menssen, Ruth; Schweiggert, Jörg; Schreiner, Jens; Kusevic, Denis; Reuther, Julia; Braun, Bernhard; Wolf, Dieter H. (2012): Exploring the topology of the Gid complex, the E3 ubiquitin ligase involved in catabolite-induced degradation of gluconeogenic enzymes. In *The Journal of biological chemistry* 287 (30), pp. 25602–25614. DOI: 10.1074/jbc.M112.363762.

Merzlyak, Ekaterina M.; Goedhart, Joachim; Shcherbo, Dmitry; Bulina, Mariya E.; Shcheglov, Aleksandr S.; Fradkov, Arkady F. et al. (2007): Bright monomeric red fluorescent protein with an extended fluorescence lifetime. In *Nat Methods* 4 (7), pp. 555–557. DOI: 10.1038/nmeth1062.

Mészáros, Bálint; Kumar, Manjeet; Gibson, Toby J.; Uyar, Bora; Dosztányi, Zsuzsanna (2017): Degrons in cancer. In *Science signaling* 10 (470). DOI: 10.1126/scisignal.aak9982.

Miles, Shawna; Li, Li Hong; Melville, Zephan; Breeden, Linda L. (2019): Ssd1 and the cell wall integrity pathway promote entry, maintenance, and recovery from quiescence in budding yeast. In *Molecular biology of the cell* 30 (17), pp. 2205–2217. DOI: 10.1091/mbc.E19-04-0190.

Minami, Y.; Weissman, A. M.; Samelson, L. E.; Klausner, R. D. (1987): Building a multichain receptor: synthesis, degradation, and assembly of the T-cell antigen receptor. In *Proceedings of the National Academy of Sciences of the United States of America* 84 (9), pp. 2688–2692. DOI: 10.1073/pnas.84.9.2688.

Mueller, Franziska; Friese, Alexandra; Pathe, Claudio; Da Silva, Richard Cardoso; Rodriguez, Kenny Bravo; Musacchio, Andrea; Bange, Tanja (2021): Overlap of NatA and IAP substrates implicates N-terminal acetylation in protein stabilization. In *Science advances* 7 (3). DOI: 10.1126/sciadv.abc8590.

Muhar, Matthias F.; Farnung, Jakob; Cernakova, Martina; Hofmann, Raphael; Henneberg, Lukas T.; Pfleiderer, Moritz M. et al. (2025): C-terminal amides mark proteins for degradation via SCF-FBXO31. In *Nature* 638 (8050), pp. 519–527. DOI: 10.1038/s41586-024-08475-w.

Mukhopadhyay, Urbi; Levantovsky, Sophie; Carusone, Teresa Maria; Gharbi, Sarah; Stein, Frank; Behrends, Christian; Bhogaraju, Sagar (2024): A ubiquitin-specific, proximity-based

labeling approach for the identification of ubiquitin ligase substrates. In *Science advances* 10 (32), eadp3000. DOI: 10.1126/sciadv.adp3000.

Nascimbeni, Anna Chiara; Giordano, Francesca; Dupont, Nicolas; Grasso, Daniel; Vaccaro, Maria I.; Codogno, Patrice; Morel, Etienne (2017): ER-plasma membrane contact sites contribute to autophagosome biogenesis by regulation of local PI3P synthesis. In *The EMBO Journal* 36 (14), pp. 2018–2033. DOI: 10.15252/embj.201797006.

Nguyen, Henry C.; Wang, Wei; Xiong, Yong (2017): Cullin-RING E3 Ubiquitin Ligases: Bridges to Destruction. In *Sub-cellular biochemistry* 83, pp. 323–347. DOI: 10.1007/978-3-319-46503-6_12.

Nguyen, Kha The; Lee, Chang-Seok; Mun, Sang-Hyeon; Truong, Nhung Thimy; Park, Sang Ki; Hwang, Cheol-Sang (2019): N-terminal acetylation and the N-end rule pathway control degradation of the lipid droplet protein PLIN2. In *The Journal of biological chemistry* 294 (1), pp. 379–388. DOI: 10.1074/jbc.RA118.005556.

Nishimura, Taki; Tamura, Norito; Kono, Nozomu; Shimanaka, Yuta; Arai, Hiroyuki; Yamamoto, Hayashi; Mizushima, Noboru (2017): Autophagosome formation is initiated at phosphatidylinositol synthase-enriched ER subdomains. In *The EMBO Journal* 36 (12), pp. 1719–1735. DOI: 10.15252/embj.201695189.

Ooms, Jeroen (2024): writexl: Export Data Frames to Excel 'xlsx' Format. Available online at https://CRAN.R-project.org/package=writexl.

Pan, Man; Zheng, Qingyun; Wang, Tian; Liang, Lujun; Mao, Junxiong; Zuo, Chong et al. (2021): Structural insights into Ubr1-mediated N-degron polyubiquitination. In *Nature* 600 (7888), pp. 334–338. DOI: 10.1038/s41586-021-04097-8.

Pandey, Udai Bhan; Nie, Zhiping; Batlevi, Yakup; McCray, Brett A.; Ritson, Gillian P.; Nedelsky, Natalia B. et al. (2007): HDAC6 rescues neurodegeneration and provides an essential link between autophagy and the UPS. In *Nature* 447 (7146), pp. 859–863. DOI: 10.1038/nature05853.

Park, Joon Sung; Lee, Jae-Young; Nguyen, Yen Thi Kim; Kang, Nae-Won; Oh, Eun Kyung; Jang, Dong Man et al. (2020): Structural Analyses on the Deamidation of N-Terminal Asn in the Human N-Degron Pathway. In *Biomolecules* 10 (1). DOI: 10.3390/biom10010163.

Park, Mi Seul; Bitto, Eduard; Kim, Kyung Rok; Bingman, Craig A.; Miller, Mitchell D.; Kim, Hyun-Jung et al. (2014): Crystal structure of human protein N-terminal glutamine amidohydrolase, an initial component of the N-end rule pathway. In *PLOS ONE* 9 (10), e111142. DOI: 10.1371/journal.pone.0111142.

Pau, Grégoire; Fuchs, Florian; Sklyar, Oleg; Boutros, Michael; Huber, Wolfgang (2010): EBImage--an R package for image processing with applications to cellular phenotypes. In *Bioinformatics* 26 (7), pp. 979–981. DOI: 10.1093/bioinformatics/btq046.

Pédelacq, Jean-Denis; Cabantous, Stéphanie; Tran, Timothy; Terwilliger, Thomas C.; Waldo, Geoffrey S. (2006): Engineering and characterization of a superfolder green fluorescent protein. In *Nat Biotechnol* 24 (1), pp. 79–88. DOI: 10.1038/nbt1172.

Peng, Bingyin; Williams, Thomas C.; Henry, Matthew; Nielsen, Lars K.; Vickers, Claudia E. (2015): Controlling heterologous gene expression in yeast cell factories on different carbon substrates and across the diauxic shift: a comparison of yeast promoter activities. In *Microb Cell Fact* 14 (1), p. 91. DOI: 10.1186/s12934-015-0278-5.

Pettersen, Eric F.; Goddard, Thomas D.; Huang, Conrad C.; Meng, Elaine C.; Couch, Gregory S.; Croll, Tristan I. et al. (2021): UCSF ChimeraX: Structure visualization for researchers, educators, and developers. In *Protein science : a publication of the Protein Society* 30 (1), pp. 70–82. DOI: 10.1002/pro.3943.

Piatkov, Konstantin I.; Brower, Christopher S.; Varshavsky, Alexander (2012a): The N-end rule pathway counteracts cell death by destroying proapoptotic protein fragments. In *Proceedings of the National Academy of Sciences of the United States of America* 109 (27), E1839-47. DOI: 10.1073/pnas.1207786109.

Piatkov, Konstantin I.; Colnaghi, Luca; Békés, Miklos; Varshavsky, Alexander; Huang, Tony T. (2012b): The auto-generated fragment of the Usp1 deubiquitylase is a physiological substrate of the N-end rule pathway. In *Molecular cell* 48 (6), pp. 926–933. DOI: 10.1016/j.molcel.2012.10.012.

Piatkov, Konstantin I.; Oh, Jang-Hyun; Liu, Yuan; Varshavsky, Alexander (2014): Calpain-generated natural protein fragments as short-lived substrates of the N-end rule pathway. In *Proceedings of the National Academy of Sciences of the United States of America* 111 (9), E817-26. DOI: 10.1073/pnas.1401639111.

Piersimoni, Lolita; Kastritis, Panagiotis L.; Arlt, Christian; Sinz, Andrea (2022): Cross-Linking Mass Spectrometry for Investigating Protein Conformations and Protein-Protein Interactions–A Method for All Seasons. In *Chemical reviews* 122 (8), pp. 7500–7531. DOI: 10.1021/acs.chemrev.1c00786.

Polevoda, B.; Norbeck, J.; Takakura, H.; Blomberg, A.; Sherman, F. (1999): Identification and specificities of N-terminal acetyltransferases from Saccharomyces cerevisiae. In *The EMBO Journal* 18 (21), pp. 6155–6168. DOI: 10.1093/emboj/18.21.6155.

Polevoda, B.; Sherman, F. (2001): NatC Nalpha-terminal acetyltransferase of yeast contains three subunits, Mak3p, Mak10p, and Mak31p. In *The Journal of biological chemistry* 276 (23), pp. 20154–20159. DOI: 10.1074/jbc.M011440200.

Price, C. W.; Holwell, J. H.; Abdelal, A. T. (1978): Purification and properties of the arginine-specific carbamoyl-phosphate synthase from Saccharomyces cerevisiae. In *Journal of general microbiology* 106 (1), pp. 145–151. DOI: 10.1099/00221287-106-1-145.

Qiao, Shuai; Langlois, Christine R.; Chrustowicz, Jakub; Sherpa, Dawafuti; Karayel, Ozge; Hansen, Fynn M. et al. (2020): Interconversion between Anticipatory and Active GID E3 Ubiquitin Ligase Conformations via Metabolically Driven Substrate Receptor Assembly. In *Molecular cell* 77 (1), 150-163.e9. DOI: 10.1016/j.molcel.2019.10.009.

Qiao, Shuai; Lee, Chia-Wei; Sherpa, Dawafuti; Chrustowicz, Jakub; Cheng, Jingdong; Duennebacke, Maximilian et al. (2022): Cryo-EM structures of Gid12-bound GID E3 reveal

steric blockade as a mechanism inhibiting substrate ubiquitylation. In *Nature communications* 13 (1), p. 3041. DOI: 10.1038/s41467-022-30803-9.

R Core Team (2023): R: A language and environment for statistical computing. R Foundation for Statistical. Vienna, Austria. Available online at https://www.R-project.org/, checked on 07/21/2025.

Rao, H.; Uhlmann, F.; Nasmyth, K.; Varshavsky, A. (2001): Degradation of a cohesin subunit by the N-end rule pathway is essential for chromosome stability. In *Nature* 410 (6831), pp. 955–959. DOI: 10.1038/35073627.

Rappsilber, Juri; Ishihama, Yasushi; Mann, Matthias (2003): Stop and go extraction tips for matrix-assisted laser desorption/ionization, nanoelectrospray, and LC/MS sample pretreatment in proteomics. In *Analytical chemistry* 75 (3), pp. 663–670. DOI: 10.1021/ac026117i.

Ravid, Tommer; Hochstrasser, Mark (2008): Diversity of degradation signals in the ubiquitin-proteasome system. In *Nat Rev Mol Cell Biol* 9 (9), pp. 679–690. DOI: 10.1038/nrm2468.

Reinbold, Christian; Kong, Ka-Yiu Edwin; Kats, Ilia; Khmelinskii, Anton; Knop, Michael (2023): Multiplexed protein stability (MPS) profiling of terminal degrons using fluorescent timer libraries in Saccharomyces cerevisiae. In *Methods in enzymology* 686, pp. 321–344. DOI: 10.1016/bs.mie.2023.02.017.

Renart, J.; Reiser, J.; Stark, G. R. (1979): Transfer of proteins from gels to diazobenzyloxymethyl-paper and detection with antisera: a method for studying antibody specificity and antigen structure. In *Proceedings of the National Academy of Sciences of the United States of America* 76 (7), pp. 3116–3120. DOI: 10.1073/pnas.76.7.3116.

Renz, Christian; Asimaki, Evrydiki; Meister, Cindy; Albanèse, Véronique; Petriukov, Kirill; Krapoth, Nils C. et al. (2024): Ubiquiton-An inducible, linkage-specific polyubiquitylation tool. In *Molecular cell* 84 (2), 386-400.e11. DOI: 10.1016/j.molcel.2023.11.016.

Rock, K. L.; Gramm, C.; Rothstein, L.; Clark, K.; Stein, R.; Dick, L. et al. (1994): Inhibitors of the proteasome block the degradation of most cell proteins and the generation of peptides presented on MHC class I molecules. In *Cell* 78 (5), pp. 761–771. DOI: 10.1016/s0092-8674(94)90462-6.

Rual, Jean-François; Venkatesan, Kavitha; Hao, Tong; Hirozane-Kishikawa, Tomoko; Dricot, Amélie; Li, Ning et al. (2005): Towards a proteome-scale map of the human protein-protein interaction network. In *Nature* 437 (7062), pp. 1173–1178. DOI: 10.1038/nature04209.

Ruan, Hao; Yu, Chen; Niu, Xiaogang; Zhang, Weilin; Liu, Hanzhong; Chen, Limin et al. (2020): Computational strategy for intrinsically disordered protein ligand design leads to the discovery of p53 transactivation domain I binding compounds that activate the p53 pathway. In *Chem. Sci.* 12 (8), pp. 3004–3016. DOI: 10.1039/D0SC04670A.

Santt, Olivier; Pfirrmann, Thorsten; Braun, Bernhard; Juretschke, Jeannette; Kimmig, Philipp; Scheel, Hartmut et al. (2008): The yeast GID complex, a novel ubiquitin ligase (E3) involved in the regulation of carbohydrate metabolism. In *Molecular biology of the cell* 19 (8), pp. 3323–3333. DOI: 10.1091/mbc.e08-03-0328.

Schauberger, Philipp; Walker, Alexander (2023): openxlsx: Read, Write and Edit xlsx Files. Available online at https://CRAN.R-project.org/package=openxlsx.

Schlatter, Ivan D.; Meira, Maria; Ueberschlag, Vanessa; Hoepfner, Dominic; Movva, Rao; Hynes, Nancy E. (2012): MHO1, an evolutionarily conserved gene, is synthetic lethal with PLC1; Mho1p has a role in invasive growth. In *PloS one* 7 (3), e32501. DOI: 10.1371/journal.pone.0032501.

Schmidt, Marion; Haas, Wilhelm; Crosas, Bernat; Santamaria, Patricia G.; Gygi, Steven P.; Walz, Thomas; Finley, Daniel (2005): The HEAT repeat protein Blm10 regulates the yeast proteasome by capping the core particle. In *Nature structural & molecular biology* 12 (4), pp. 294–303. DOI: 10.1038/nsmb914.

Semenza, G. L.; Wang, G. L. (1992): A nuclear factor induced by hypoxia via de novo protein synthesis binds to the human erythropoietin gene enhancer at a site required for transcriptional activation. In *Molecular and cellular biology* 12 (12), pp. 5447–5454. DOI: 10.1128/mcb.12.12.5447-5454.1992.

Shemorry, Anna; Hwang, Cheol-Sang; Varshavsky, Alexander (2013): Control of protein quality and stoichiometries by N-terminal acetylation and the N-end rule pathway. In *Molecular cell* 50 (4), pp. 540–551. DOI: 10.1016/j.molcel.2013.03.018.

Sherpa, Dawafuti; Chrustowicz, Jakub; Qiao, Shuai; Langlois, Christine R.; Hehl, Laura A.; Gottemukkala, Karthik Varma et al. (2021): GID E3 ligase supramolecular chelate assembly configures multipronged ubiquitin targeting of an oligomeric metabolic enzyme. In *Molecular cell* 81 (11), 2445-2459.e13. DOI: 10.1016/j.molcel.2021.03.025.

Shin, Jin Seok; Park, Si Hoon; Kim, Leehyeon; Heo, Jiwon; Song, Hyun Kyu (2021): Crystal structure of yeast Gid10 in complex with Pro/N-degron. In *Biochemical and biophysical research communications* 582, pp. 86–92. DOI: 10.1016/j.bbrc.2021.10.007.

Sievers, Fabian; Higgins, Desmond G. (2021): The Clustal Omega Multiple Alignment Package. In *Methods in molecular biology (Clifton, N.J.)* 2231, pp. 3–16. DOI: 10.1007/978-1-0716-1036-7_1.

Sikorski, R. S.; Hieter, P. (1989): A system of shuttle vectors and yeast host strains designed for efficient manipulation of DNA in Saccharomyces cerevisiae. In *Genetics* 122 (1), pp. 19–27. DOI: 10.1093/genetics/122.1.19.

Siloto, Rodrigo M.P.; Weselake, Randall J. (2012): Site saturation mutagenesis: Methods and applications in protein engineering. In *Biocatalysis and Agricultural Biotechnology* 1 (3), pp. 181–189. DOI: 10.1016/j.bcab.2012.03.010.

Simwela, Nelson V.; Johnston, Luana; Bitar, Paulina Pavinski; Jaecklein, Eleni; Altier, Craig; Sassetti, Christopher M.; Russell, David G. (2024): Genome-wide screen of Mycobacterium tuberculosis-infected macrophages revealed GID/CTLH complex-mediated modulation of bacterial growth. In *Nat Commun* 15 (1), p. 9322. DOI: 10.1038/s41467-024-53637-z.

Skraban, Cara M.; Wells, Constance F.; Markose, Preetha; Cho, Megan T.; Nesbitt, Addie I.; Au, P. Y. Billie et al. (2017): WDR26 Haploinsufficiency Causes a Recognizable Syndrome of

Intellectual Disability, Seizures, Abnormal Gait, and Distinctive Facial Features. In *American journal of human genetics* 101 (1), pp. 139–148. DOI: 10.1016/j.ajhg.2017.06.002.

Slobodkin, Moran Rawet; Elazar, Zvulun (2013): The Atg8 family: multifunctional ubiquitin-like key regulators of autophagy. In *Essays Biochem* 55, pp. 51–64. DOI: 10.1042/bse0550051.

Slowikowski, Kamil (2024): ggrepel: Automatically Position Non-Overlapping Text Labels with 'ggplot2'. Available online at https://CRAN.R-project.org/package=ggrepel.

Sluimer, Jasper; Distel, Ben (2018): Regulating the human HECT E3 ligases. In *Cellular and molecular life sciences : CMLS* 75 (17), pp. 3121–3141. DOI: 10.1007/s00018-018-2848-2.

Smit, Judith J.; Sixma, Titia K. (2014): RBR E3-ligases at work. In *EMBO reports* 15 (2), pp. 142–154. DOI: 10.1002/embr.201338166.

Snyder, Nathan A.; Silva, Gustavo M. (2021): Deubiquitinating enzymes (DUBs): Regulation, homeostasis, and oxidative stress response. In *The Journal of biological chemistry* 297 (3), p. 101077. DOI: 10.1016/j.jbc.2021.101077.

Song, Ok-kyu; Wang, Xiaorong; Waterborg, Jakob H.; Sternglanz, Rolf (2003): An Nalpha-acetyltransferase responsible for acetylation of the N-terminal residues of histones H4 and H2A. In *Journal of Biological Chemistry* 278 (40), pp. 38109–38112. DOI: 10.1074/jbc.C300355200.

Soto, Iliana; Couvillion, Mary; Hansen, Katja G.; McShane, Erik; Moran, J. Conor; Barrientos, Antoni; Churchman, L. Stirling (2022): Balanced mitochondrial and cytosolic translatomes underlie the biogenesis of human respiratory complexes. In *Genome Biol* 23 (1), p. 170. DOI: 10.1186/s13059-022-02732-9.

Stiburek, Lukas; Cesnekova, Jana; Kostkova, Olga; Fornuskova, Daniela; Vinsova, Kamila; Wenchich, Laszlo et al. (2012): YME1L controls the accumulation of respiratory chain subunits and is required for apoptotic resistance, cristae morphogenesis, and cell proliferation. In *Molecular biology of the cell* 23 (6), pp. 1010–1023. DOI: 10.1091/mbc.E11-08-0674.

Stirling, Peter C.; Bloom, Michelle S.; Solanki-Patil, Tejomayee; Smith, Stephanie; Sipahimalani, Payal; Li, Zhijian et al. (2011): The complete spectrum of yeast chromosome instability genes identifies candidate CIN cancer genes and functional roles for ASTRA complex components. In *PLoS genetics* 7 (4), e1002057. DOI: 10.1371/journal.pgen.1002057.

Stochaj, Wayne R.; Berkelman, Tom; Laird, Nancy (2006): Staining membrane-bound proteins with ponceau s. In *CSH protocols* 2006 (5), pdb.prot4543. DOI: 10.1101/pdb.prot4543.

Storici, Francesca; Resnick, Michael A. (2006): The delitto perfetto approach to in vivo site-directed mutagenesis and chromosome rearrangements with synthetic oligonucleotides in yeast. In *Methods in enzymology* 409, pp. 329–345. DOI: 10.1016/S0076-6879(05)09019-1.

Stuckey, Samantha; Mukherjee, Kuntal; Storici, Francesca (2011): In Vivo Site-Specific Mutagenesis and Gene Collage Using the Delitto Perfetto System in Yeast Saccharomyces cerevisiae. In Hideo Tsubouchi (Ed.): DNA Recombination, vol. 745. Totowa, NJ: Humana Press (Methods in Molecular Biology), pp. 173–191.

Sung, Min-kyung; Porras-yakushi, Tanya R.; Reitsma, Justin M.; Huber, Ferdinand M.; Sweredoski, Michael J.; Hoelz, André et al. (2016): A conserved quality-control pathway that mediates degradation of unassembled ribosomal proteins. In *eLife Sciences Publications, Ltd*, 8/23/2016. Available online at https://elifesciences.org/articles/19105, checked on 7/18/2025.

Suraweera, Amila; Münch, Christian; Hanssum, Ariane; Bertolotti, Anne (2012): Failure of amino acid homeostasis causes cell death following proteasome inhibition. In *Molecular cell* 48 (2), pp. 242–253. DOI: 10.1016/j.molcel.2012.08.003.

Taggart, James Christopher; Zauber, Henrik; Selbach, Matthias; Li, Gene-Wei; McShane, Erik (2020): Keeping the Proportions of Protein Complex Components in Check. In *Cell systems* 10 (2), pp. 125–132. DOI: 10.1016/j.cels.2020.01.004.

Tasaki, Takafumi; Zakrzewska, Adriana; Dudgeon, Drew D.; Jiang, Yonghua; Lazo, John S.; Kwon, Yong Tae (2009): The substrate recognition domains of the N-end rule pathway. In *Journal of Biological Chemistry* 284 (3), pp. 1884–1895. DOI: 10.1074/jbc.M803641200.

Thoden, J. B.; Raushel, F. M.; Benning, M. M.; Rayment, I.; Holden, H. M. (1999): The structure of carbamoyl phosphate synthetase determined to 2.1 A resolution. In *Acta crystallographica. Section D, Biological crystallography* 55 (Pt 1), pp. 8–24. DOI: 10.1107/S0907444998006234.

Thumm, M.; Egner, R.; Koch, B.; Schlumpberger, M.; Straub, M.; Veenhuis, M.; Wolf, D. H. (1994): Isolation of autophagocytosis mutants of Saccharomyces cerevisiae. In *FEBS letters* 349 (2), pp. 275–280. DOI: 10.1016/0014-5793(94)00672-5.

Toyama, Brandon H.; Hetzer, Martin W. (2013): Protein homeostasis: live long, won't prosper. In *Nat Rev Mol Cell Biol* 14 (1), pp. 55–61. DOI: 10.1038/nrm3496.

Tsukada, M.; Ohsumi, Y. (1993): Isolation and characterization of autophagy-defective mutants of Saccharomyces cerevisiae. In *FEBS letters* 333 (1-2), pp. 169–174. DOI: 10.1016/0014-5793(93)80398-E.

van Damme, Petra; Evjenth, Rune; Foyn, Håvard; Demeyer, Kimberly; Bock, Pieter-Jan de; Lillehaug, Johan R. et al. (2011a): Proteome-derived peptide libraries allow detailed analysis of the substrate specificities of N(alpha)-acetyltransferases and point to hNaa10p as the post-translational actin N(alpha)-acetyltransferase. In *Molecular & cellular proteomics : MCP* 10 (5), M110.004580. DOI: 10.1074/mcp.M110.004580.

van Damme, Petra; Hole, Kristine; Gevaert, Kris; Arnesen, Thomas (2015): N-terminal acetylome analysis reveals the specificity of Naa50 (Nat5) and suggests a kinetic competition between N-terminal acetyltransferases and methionine aminopeptidases. In *Proteomics* 15 (14), pp. 2436–2446. DOI: 10.1002/pmic.201400575.

van Damme, Petra; Hole, Kristine; Pimenta-Marques, Ana; Helsens, Kenny; Vandekerckhove, Joël; Martinho, Rui G. et al. (2011b): NatF contributes to an evolutionary shift in protein N-terminal acetylation and is important for normal chromosome segregation. In *PLOS Genetics* 7 (7), e1002169. DOI: 10.1371/journal.pgen.1002169.

van Damme, Petra; Kalvik, Thomas V.; Starheim, Kristian K.; Jonckheere, Veronique; Myklebust, Line M.; Menschaert, Gerben et al. (2016): A Role for Human N-alpha

Acetyltransferase 30 (Naa30) in Maintaining Mitochondrial Integrity. In *Molecular & cellular proteomics : MCP* 15 (11), pp. 3361–3372. DOI: 10.1074/mcp.M116.061010.

van Damme, Petra; Lasa, Marta; Polevoda, Bogdan; Gazquez, Cristina; Elosegui-Artola, Alberto; Kim, Duk Soo et al. (2012): N-terminal acetylome analyses and functional insights of the N-terminal acetyltransferase NatB. In *Proc. Natl. Acad. Sci. U.S.A.* 109 (31), pp. 12449–12454. DOI: 10.1073/pnas.1210303109.

Varadi, Mihaly; Anyango, Stephen; Deshpande, Mandar; Nair, Sreenath; Natassia, Cindy; Yordanova, Galabina et al. (2022): AlphaFold Protein Structure Database: massively expanding the structural coverage of protein-sequence space with high-accuracy models. In *Nucleic acids research* 50 (D1), D439-D444. DOI: 10.1093/nar/gkab1061.

Varadi, Mihaly; Bertoni, Damian; Magana, Paulyna; Paramval, Urmila; Pidruchna, Ivanna; Radhakrishnan, Malarvizhi et al. (2024): AlphaFold Protein Structure Database in 2024: providing structure coverage for over 214 million protein sequences. In *Nucleic acids research* 52 (D1), D368-D375. DOI: 10.1093/nar/gkad1011.

Varland, Sylvia; Silva, Rui Duarte; Kjosås, Ine; Faustino, Alexandra; Bogaert, Annelies; Billmann, Maximilian et al. (2023): N-terminal acetylation shields proteins from degradation and promotes age-dependent motility and longevity. In *Nat Commun* 14 (1), p. 6774. DOI: 10.1038/s41467-023-42342-y.

Varshavsky, Alexander (2005): Ubiquitin fusion technique and related methods. In *Methods in enzymology* 399, pp. 777–799. DOI: 10.1016/S0076-6879(05)99051-4.

Varshavsky, Alexander (2019): N-degron and C-degron pathways of protein degradation. In *Proceedings of the National Academy of Sciences of the United States of America* 116 (2), pp. 358–366. DOI: 10.1073/pnas.1816596116.

Varshavsky, Alexander (2024): N-degron pathways. In *Proceedings of the National Academy of Sciences of the United States of America* 121 (39), e2408697121. DOI: 10.1073/pnas.2408697121.

Wagih, Omar; Parts, Leopold (2021): gitter: Quantification of Pinned Microbial Cultures.

Walker, K. W.; Bradshaw, R. A. (1999): Yeast methionine aminopeptidase I. Alteration of substrate specificity by site-directed mutagenesis. In *The Journal of biological chemistry* 274 (19), pp. 13403–13409. DOI: 10.1074/jbc.274.19.13403.

Wang, Hengbin; Wang, Liangjun; Erdjument-Bromage, Hediye; Vidal, Miguel; Tempst, Paul; Jones, Richard S.; Zhang, Yi (2004): Role of histone H2A ubiquitination in Polycomb silencing. In *Nature* 431 (7010), pp. 873–878. DOI: 10.1038/nature02985.

Wanless, Antony G.; Lin, Yuan; Weiss, Eric L. (2014): Cell morphogenesis proteins are translationally controlled through UTRs by the Ndr/LATS target Ssd1. In *PloS one* 9 (1), e85212. DOI: 10.1371/journal.pone.0085212.

Ward, C. L.; Kopito, R. R. (1994): Intracellular turnover of cystic fibrosis transmembrane conductance regulator. Inefficient processing and rapid degradation of wild-type and mutant proteins. In *Journal of Biological Chemistry* 269 (41), pp. 25710–25718. Available online at https://pubmed.ncbi.nlm.nih.gov/7523390/.

Warnes, Gregory R.; Gorjanc, Gregor; Magnusson, Arni; Andronic, Liviu; Rogers, Jim; MacQueen, Don; Korosec, Ales (2024): gdata: Various R Programming Tools for Data Manipulation. Available online at https://cran.r-project.org/web/packages/gdata/gdata.pdf, checked on 07/22/2025.

Waterhouse, Andrew M.; Procter, James B.; Martin, David M. A.; Clamp, Michèle; Barton, Geoffrey J. (2009): Jalview Version 2--a multiple sequence alignment editor and analysis workbench. In *Bioinformatics* 25 (9), pp. 1189–1191. DOI: 10.1093/bioinformatics/btp033.

Weber, P. C.; Ohlendorf, D. H.; Wendoloski, J. J.; Salemme, F. R. (1989): Structural origins of high-affinity biotin binding to streptavidin. In *Science (New York, N.Y.)* 243 (4887), pp. 85–88. DOI: 10.1126/science.2911722.

Weidberg, Hilla; Shpilka, Tomer; Shvets, Elena; Abada, Adi; Shimron, Frida; Elazar, Zvulun (2011): LC3 and GATE-16 N termini mediate membrane fusion processes required for autophagosome biogenesis. In *Developmental Cell* 20 (4), pp. 444–454. DOI: 10.1016/j.devcel.2011.02.006.

Weidemann, A.; Johnson, R. S. (2008): Biology of HIF-1alpha. In *Cell Death Differ* 15 (4), pp. 621–627. DOI: 10.1038/cdd.2008.12.

Weissman, A. M. (2001): Themes and variations on ubiquitylation. In *Nature reviews. Molecular cell biology* 2 (3), pp. 169–178. DOI: 10.1038/35056563.

Whiteway, M.; Szostak, J. W. (1985): The ARD1 gene of yeast functions in the switch between the mitotic cell cycle and alternative developmental pathways. In *Cell* 43 (2 Pt 1), pp. 483–492. DOI: 10.1016/0092-8674(85)90178-3.

Wickham, Hadley (2022): lazyeval: Lazy (Non-Standard) Evaluation. Available online at https://cran.r-project.org/web/packages/lazyeval/lazyeval.pdf, checked on 07/22/2025.

Wickham, Hadley; Averick, Mara; Bryan, Jennifer; Chang, Winston; McGowan, Lucy; François, Romain et al. (2019): Welcome to the Tidyverse. In *JOSS* 4 (43), p. 1686. DOI: 10.21105/joss.01686.

Winzeler, E. A.; Shoemaker, D. D.; Astromoff, A.; Liang, H.; Anderson, K.; Andre, B. et al. (1999): Functional characterization of the S. cerevisiae genome by gene deletion and parallel analysis. In *Science (New York, N.Y.)* 285 (5429), pp. 901–906. DOI: 10.1126/science.285.5429.901.

Xu, Ping; Duong, Duc M.; Seyfried, Nicholas T.; Cheng, Dongmei; Xie, Yang; Robert, Jessica et al. (2009): Quantitative proteomics reveals the function of unconventional ubiquitin chains in proteasomal degradation. In *Cell* 137 (1), pp. 133–145. DOI: 10.1016/j.cell.2009.01.041.

Yanagitani, Kota; Juszkiewicz, Szymon; Hegde, Ramanujan S. (2017): UBE2O is a quality control factor for orphans of multiprotein complexes. In *Science (New York, N.Y.)* 357 (6350), pp. 472–475. DOI: 10.1126/science.aan0178.

Yang, Qi; Zhou, Xunzhao; Yi, Sheng; Li, XiaoLing; Zhang, Qiang; Zhang, Shujie et al. (2024): Novel loss-of-function variants in WDR26 cause Skraban-Deardorff syndrome in two Chinese patients. In *Front. Pediatr.* 12, p. 1429586. DOI: 10.3389/fped.2024.1429586.

Yang, Quan; Zhao, Jinyao; Chen, Dan; Wang, Yang (2021): E3 ubiquitin ligases: styles, structures and functions. In *Mol Biomed* 2 (1), p. 23. DOI: 10.1186/s43556-021-00043-2.

Yofe, Ido; Weill, Uri; Meurer, Matthias; Chuartzman, Silvia; Zalckvar, Einat; Goldman, Omer et al. (2016): One library to make them all: streamlining the creation of yeast libraries via a SWAp-Tag strategy. In *Nature methods* 13 (4), pp. 371–378. DOI: 10.1038/nmeth.3795.

Zavortink, Michael; Rutt, Lauren N.; Dzitoyeva, Svetlana; Henriksen, Jesslyn C.; Barrington, Chloe; Bilodeau, Danielle Y. et al. (2020): The E2 Marie Kondo and the CTLH E3 ligase clear deposited RNA binding proteins during the maternal-to-zygotic transition. In *eLife Sciences Publications, Ltd*, 6/23/2020. Available online at https://elifesciences.org/articles/53889, checked on 7/19/2025.

Zhang, Zhiqian; Mena, Elijah L.; Timms, Richard T.; Koren, Itay; Elledge, Stephen J. (2025): Degrons: defining the rules of protein degradation. In *Nat Rev Mol Cell Biol*, pp. 1–16. DOI: 10.1038/s41580-025-00870-z.

Zhang, Zhiqian; Sie, Brandon; Chang, Aiquan; Leng, Yumei; Nardone, Christopher; Timms, Richard T.; Elledge, Stephen J. (2023): Elucidation of E3 ubiquitin ligase specificity through proteome-wide internal degron mapping. In *Molecular cell* 83 (18), 3377-3392.e6. DOI: 10.1016/j.molcel.2023.08.022.

Appendix II

Acknowledgements

First and foremost, I would like to thank XXXXXXXXXXX for the opportunity to work on this project, his supervision over my experiments, scientific input, and the funding to conduct these experiments. Without his guidance, patience, and sometimes a couple of nudges back onto the right path, this would not have been possible. Secondly, I would like to express my gratitude to XXXXXXXXXXXXX, who took on a crucial role in supervising me during my introduction time in the lab, teaching me the yeast techniques needed for my experiments, and always being there for advice when needed.

Next, I would like to thank the members of my thesis advisory committee, who, besides XXXXXXXXXX, are XXXXXXXXXXXXX and XXXXXXXXXXXXX. The TAC meetings with them, even though stressful to prepare, were always highly productive and their input helped see things from a different perspective at times.

Of course, my thanks also must go out to all members of the Khmelinskii lab, both current and former, for creating an atmosphere in which it was always a joy to work. One would be hard-pressed to find another group full of people like this who are always there for scientific discussion or advice. Particular thanks must go to XXXXXXXXXXXX in this context, who makes sure in the background that the lab does not fall into chaos, who handles orders, work orders, and almost anything organizational.

Additional thanks go to the IMB Core Facilities, particularly the IMB Media lab for preparing and autoclaving media for us, saving us countless hours, the Protein Production Facility for providing affordable and reliable enzymes and antibodies, and the Proteomics Core facility for conducting whole proteome analysis, as well as the acetylation mass spectrometry experiments.

Last, but certainly not least, my heartfelt thanks go to my family and friends who supported me throughout my academic journey and without whom I might not have persevered to this point. At this point I would particularly like to thank my late grandmother, who sadly passed away just shortly before I finished this thesis.

Curriculum vitae

Personal details:

Name:	Christian Peter Ochs
Date of birth:	05.04.1996
Place of birth:	Frankfurt am Main
Address:	Am Gonsenheimer Spieß 16, 55122 Mainz
Phone number (mobile):	+49 151 75048772
Email address:	C.ochs1996@gmx.de
Nationality:	German

Education:

Institute of Molecular Biology, Mainz 09/2021-08/2025
PhD candidate under supervision of XXXXXXXXXXX
Dissecting substrate recognition by GID Ubiquitin ligases

Reorientation and application to PhD programs 04/2021-08/2021

Goethe Universität Frankfurt am Main 10/2018-03/2021
Master of Science under supervision of XXXXXXXXXXX
Analysis of TonB-dependent transporters *in Anabaena sp.* PCC 7120

Provadis School of International Management and Technology 09/2014-06/2017
Bachelor of Science Biopharmaceutical Science under Supervision of XXXXXXXXXXX
Purification of two-chain-insulin-Fc fusion proteins

Work experience:

Bayer Crop Science in collaboration with Tempo-Team AG 01/2018-09/2018
Laboratory technician
Screening of herbicide candidates

Sanofi-Aventis Deutschland GmbH 06/2017-12/2017
Internship R&D
Cell culture and purification of proteins

Sanofi-Aventis Deutschland GmbH 09/2014-06/2017
Vocational training
Biology laboratory technician

Publications:

Kong, Ka-Yiu Edwin; Ochs, Christian; Debarnot, Cécile; Myllykoski, Matti; Blanco, Denís Arribas; Shankar, Susmitha et al. (2025): Bidirectional control of a metabolic transition by the GID ubiquitin ligase. In *bioRxiv*, 2025.07.15.664932. DOI: 10.1101/2025.07.15.664932. (Pre-print)

Faust, Christine; Ochs, Christian; Korn, Marcus; Werner, Ulrich; Jung, Jennifer; Dittrich, Werner et al. (2020): Production of a novel heterodimeric two-chain insulin-Fc fusion protein. In *Protein engineering, design & selection : PEDS* 33. DOI: 10.1093/protein/gzaa026.